CATALYTIC BLEACHING OF COTTON: MOLECULAR AND MACROSCOPIC ASPECTS

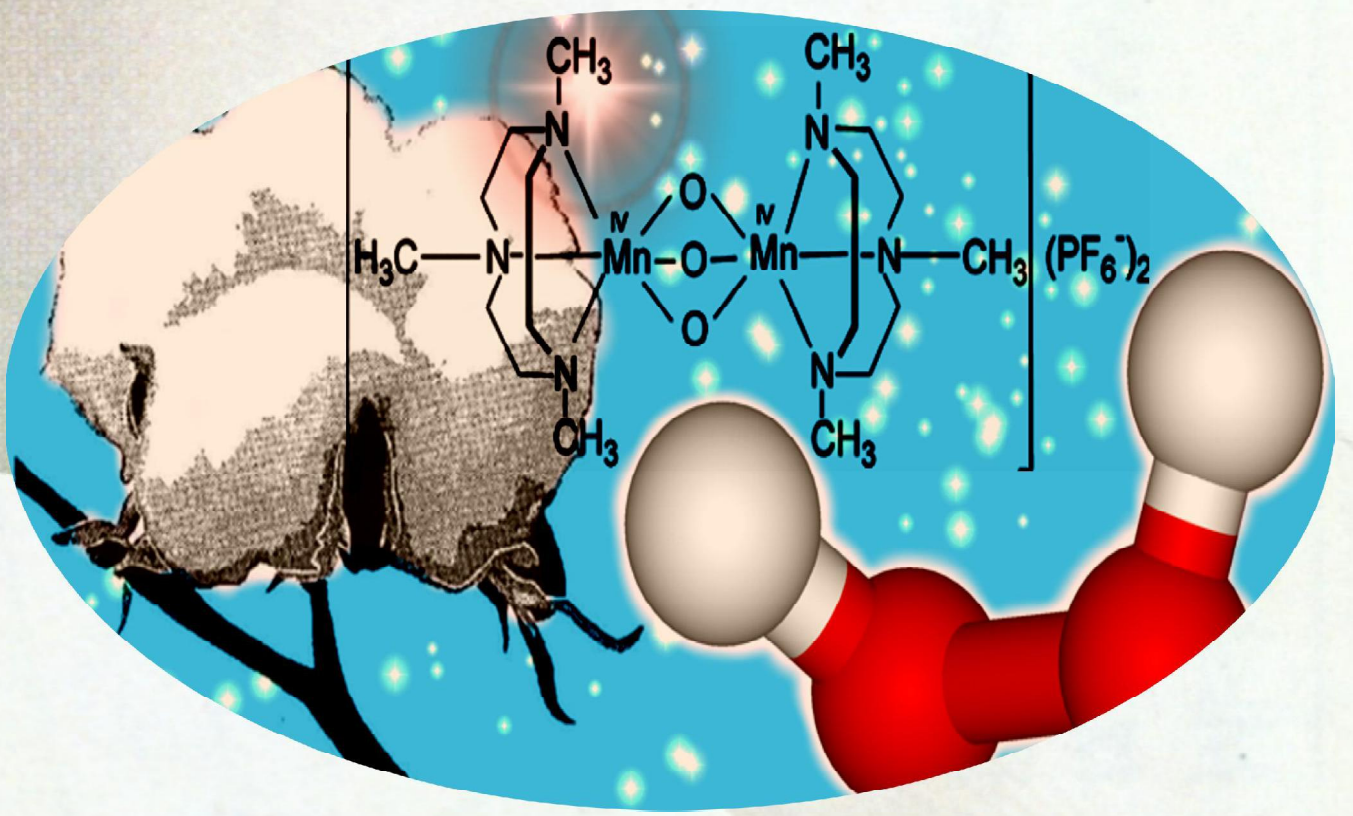

TATJANA TOPALOVIĆ

CATALYTIC BLEACHING OF COTTON: MOLECULAR AND MACROSCOPIC ASPECTS

Dissertation committee

Chairman:
Prof. Dr. ir. A. Bliek, University of Twente, the Netherlands

Promotor:
Prof. Dr. ir. M.M.C.G. Warmoeskerken, University of Twente, the Netherlands

Assistant-promotor:
Dr. ir. V.A. Nierstrasz, University of Twente, the Netherlands

Members:
Prof. Dr. ir. J.A.M. Kuipers, University of Twente, the Netherlands
Prof. Dr. ir. W.P.M. van Swaaij, University of Twente, the Netherlands
Prof. Dr. P.J. Hauser, North Carolina State University, NC, USA
Dr. R. Hage, Unilever R&D, the Netherlands
Dr. W. Coerver, Vlisco B.V., the Netherlands

This work has been financially supported by the E.E.T. program (Project Nr. EET01108).

T. Topalović
Catalytic Bleaching of Cotton: Molecular and Macroscopic Aspects
Thesis, University of Twente, the Netherlands
ISBN 90-365-2454-7

Print: Wöhrmann Print Service, the Netherlands

Cover design: Dragan Jocić & Tatjana Topalović

CATALYTIC BLEACHING OF COTTON: MOLECULAR AND MACROSCOPIC ASPECTS

DISSERTATION

to obtain
the doctor's degree at the University of Twente,
on the authority of the rector magnificus,
Prof. Dr. W.H.M. Zijm,
on account of the decision of the graduation committee,
to be publicly defended
on Friday 26 January 2007 at 15.00 hrs.

by

Tatjana Topalović
born on 23 March 1972
in Sjenica, Serbia

Dit proefschrift is goedgekeurd door de promotor
Prof.dr.ir. M.M.C.G. Warmoeskerken

en de assistent-promotor
Dr.ir. V.A. Nierstrasz

Mami za njenu ljubav

Contents

GENERAL INTRODUCTION

Textiles occupy a truly unique position in terms of man's relationship with matter. Being close to the body, unbreakably linked to our well-being, a means of expressing our personality and present in a thousand ways in our day-to-day activities, textiles are inevitable feature of the human society.

From the artisan production of the distant past to the advent of modern industry, textiles have remained a field in which a flair for creativity and the search for innovation have been a constant source of inspiration and inventiveness. One would never suspect simply from looking at them just how much know-how goes into making modern textiles. It takes state-of-the-art chemistry and technology to turn natural and synthetic raw materials into attractive products. Chemistry has always been a major factor in different areas of textiles and great deal of the chemical industry was originally motivated by the textile industry. This trend still continues and chemistry nowadays attracts enormous attention in the textile industry, mostly since it is being unbreakably involved in wet processing of textiles.

The mission of scientists and engineers is to take advantage of the possibilities of modern chemistry in order to break out traditional safe haven of textiles. Exploring other areas of knowledge could lead to finding new and unexpected applications and more efficient processing methods, which will allow bringing creative products at competitive prices on the market. In this ever-changing world of textile innovation, Europe has always been a key player. Throughout the 20th century, it was the number one producer of textiles and trader at each of the many stages of fabric production, as well as in garment making and in the fashion industry.

In view of the challenges that the textile industry is facing and will continue to face over the coming years, it should continue to be encouraged to invest in research and development which will lead to new intelligent materials, as well as to new and more efficient processing methods. An important aspect in achieving efficient wet processing methods is that they should be cost effective, environmentally friendly and gentle to the textile material. Innovative efficient strategies to achieve these goals are needed. Innovation is in particular concerning the traditional pre-treatment and processing of natural fibres since these operations are financially and environmentally costly. Hence, in the next few years we can expect to see significant changes in bleaching techniques to help maintained bleached fabric quality under more demanding conditions presented by shorter and "cleaner" bleaching procedures.

Aim and scope of the present thesis

The bleaching of cotton prior to dyeing is a science in itself – very exciting and complex. Since natural colorants in the cotton fibre are basically unaffected by scouring processes, bleaching is essential for a good level of whiteness. Of the importance of bleaching and whiteness in textile manufacturing and exploitation there can be no doubt. Currently, the most common industrial bleaching agent is hydrogen peroxide. It does not have side-effects that impact the environment. However the conditions during bleaching pose a serious problem due to possible radical reactions of the bleaching compounds with the fibre. Additionally, alkaline conditions negatively influence the effluent treatment, and the temperatures needed for the process (typically higher than 80^{o}C) impact the cost. Since stabilisers are also included in the bleach bath, their deposits could cause abrasion and distortion of the fabric imparting a harsh handle and, due to poor rinsability, their removal from the fabric requires large volumes of water.

The focus of this thesis is on finding possible strategy to achieve an innovative solution for cotton bleaching, based on the introduction of the catalyst in the hydrogen peroxide bleaching system. This approach could lead to the benefits of lower temperature and less alkaline bleaching, giving rise to an environmentally friendly bleaching system, mainly in terms of energy conservation, by maintaining the high product quality (whiteness) and minimised fibre damage as the major targets. In the last two decades, a wide variety of transition-metal complexes have been patented for bleaching applications in laundry cleaning and paper/pulp bleaching. The vast knowledge generated in these areas can surely serve as a solid basis for the application of the catalysts in industrial cotton bleaching. Various approaches have led to more stable/robust bleaching catalysts, such as the use of 1,4,7-trimethyl-1,4,7-triazacyclononane ligands (TACN) for manganese. This family of the catalysts, especially the dinuclear manganese(IV) tri-μ-oxo bridged complex of the ligand TACN (MnTACN), are today the most promising catalysts for the application in industrial bleaching of cotton.

Taking into account the current status of research in this field, the primary research objectives of this thesis are: (1) to establish the mechanism (both chemical and physical) of low-temperature cotton bleaching with hydrogen peroxide catalysed by the MnTACN complex; (2) to disclose important facts with regard possible application of the catalyst MnTACN in the industrial bleaching of cotton; and (3) to identify the physicochemical effects of catalytic bleaching on cotton fibre (surface). With these objectives in mind, the fundamental aspects of catalytic bleaching are studied at molecular and macroscopic level. This is important in order to develop and realise the application of catalytic bleaching on industrial scale.

To achieve these objectives six chapters are being integrated in the thesis. The outline of the thesis is as follows:

- In Chapter 1, after the introduction on the origin of colour in native cotton and the importance of obtaining white cotton, various aspects of conventional cotton bleaching are presented. Special emphasis is given to hydrogen peroxide based processes and the development of catalytic bleaching processes in the area of the laundry cleaning is considered versus industrial bleaching of cotton. Finally, a brief overview of potential bleaching catalysts is presented with an emphasis on the dinuclear manganese compound (MnTACN) containing 1,4,7-trimethyl-1,4,7-triazacyclononane ligands as the most promising catalyst for cotton bleaching.

- Chapter 2 reports on an unprecedented catalytic activation of molecular oxygen with the MnTACN catalyst towards the oxidation of cotton pigment morin at ambient temperatures in alkaline aqueous solution. The involvement of superoxide O_2^- and/or H_2O_2 is investigated employing a novel method based on the analysis of reaction kinetics in the presence of acceleratory and/or inhibitory enzymes. The design of this method is inspired by the principle of important physiological pathways in human body, which include the generation and consumption of reactive oxygen species by means of different enzymes.

- In Chapter 3 the chemical mechanism of catalytic bleaching of cotton pigment morin under homogeneous conditions is studied in detail. Here we assume that the mechanism of oxidation of coloured matter present in cotton fibre during bleaching is similar to that in a homogeneous system to the exclusion of transport phenomena. Both the substrate scope (coloured matter) and the catalyst scope (activation) are studied. On the basis of the chemical, spectroscopic and kinetic data, as well as the results of inhibition/acceleration enzymatic tests obtained in previous chapter, we propose the mechanism of the reaction.

- Chapter 4 discusses the performance of the catalyst MnTACN in the bleaching of cotton with hydrogen peroxide. Bleaching of cotton takes place in a heterogeneous system, which is naturally more complex than a homogeneous model system. The most important bleaching parameters, pH and temperature, as well as kinetics of hydrogen peroxide decomposition during bleaching process, are investigated. The use of this macroscopic approach provides more insight into possible application of the catalyst in hydrogen peroxide based bleaching of cotton in practical conditions.

- Surface chemistry and wetting properties of cotton fibres as affected by catalytic bleaching are investigated in Chapter 5 by using both regular and model fabric. The model cotton fabric, previously freed of most removable impurities, was stained for the purpose of this study with one pigment only, i.e. morin. This approach has provided the tool to explore and to quantify the chemical and physical effects on cotton fibre after catalytic bleaching and to distinguish between the three types of catalytic action: pigment bleaching, removal of non-cellulosic compounds and oxidation of cellulose.

- In Chapter 6 a kinetic model is established for a homogeneous model system and, based on that, an attempt is made to explain a more complex kinetics of catalytic bleaching of cotton. A general strategy for the study of the mechanism and kinetics of catalytic bleaching is presented followed by the relevant theory to enable a discriminatory assessment of the experimental data obtained.

1

The search for whiter cotton

"White ... is not a mere absence of colour; it is a shining and affirmative thing, as fierce as red, as definite as black.... God paints in many colours; but He never paints so gorgeously, I had almost said so gaudily, as when He paints in white."

G.K. Chesterton (1874-1936)
"A Piece of Chalk" Tremendous Trifles (1909).

1.1 Colour white

1.1.1 The magic of white

The colours we see on a surface are the wavelengths of the light it reflects. The rest of the wavelengths (i.e. colours) are absorbed (slightly warming the surface) - so a red surface is one that absorbs light in the green/blue part of the visible spectrum (subtractive versus additive colour). The white is a colour but not as simple as it appears to be. It is basically a colour containing all the colours of the spectrum and is sometimes described as an achromatic colour. While black absorbs the sunlight, white reflects it, the fact being well known from our everyday life.

White is often used with positive connotation in the Western world. It is recognised as a colour of purity, freshness, neutrality and cleanliness. It has been universally used as an indicator of quality such as free from contamination. White also has a Biblical meaning for holiness and is the Christian colour for all high Holy Days and festival days of the Church Year, especially the seasons of Christmas and Easter. The colour white is used for baptism, marriage, ordination and dedications. Nevertheless, there is substantial evidence of cultural differences in using white. For example, the association between black and mourning, commonly found in Western society, is not found in Chinese society and parts of Africa, where white is associated with funerals. However, both Western and Eastern cultures use white to signify purity and righteousness, as in the modern Western tradition (as well as Japan) of white apparel for women being married, particularly for the first time. In classic Indian thought, it stands for repose and understanding; in Western society it tends to mean shy, sociable, tender and soothing; black people in South Africa associate it with purity [1].

The pure (i.e. pristine) white colour should not be confused with the natural, cheap, off-white natural colour of wool, which was cheap to produce as was white linen. The colour and material of the clothing that people wore in the past was extremely important. In the past not everyone was allowed to wear white clothes. Citizens of Ancient Rome were wearing toga: a plain white toga was worn by all adult male citizens, whereas a bleached toga was worn by politicians [2]. During the Elizabethan Era, the period associated with the reign of Queen Elizabeth I (1558-1603) which is often considered to be a golden age in English history, people who could wear the colour white were dictated by the so called the Sumptuary Laws. The colours of Elizabethan clothes, including the colour white, provided information about the status of the man or woman wearing them. This was not just dictated by the wealth of the person, it also reflected their social standing. The pristine white colour was difficult and expensive to produce and therefore worn by the wealthy. Only those who could keep their clothes clean (they had servants) would wear the pristine white colour [3].

The ultimate classic, the colour white has been associated with class and style for very long time. Nowadays, white is interesting in its own as a fashion theme. If our environment makes it difficult to maintain whites, it does not make it impossible, and the colour white continues to be associated with maturity, simplicity and honour.

1.1.2 The measurement of white

Colour is a sensation and, as such, is not measurable. However, colour systems comprising three parameters have been developed whereby colours can be clearly determined and compared one with another. This objective colour specification is called colorimetry, established in 1931 by the International Commission on Illumination (CIE) [4].

The term “whiteness measurement” is often given to those colorimetric methods which are used in connection with white samples. In principle, whiteness can be measured by the degree of departure from the “perfect white” position in a three dimensional colour space. Therefore, whiteness is associated with a region in colour space where objects are accepted as white inside the chromaticity diagram. Although the white region appears fairly narrow, there are about 5,000 distinguishable white colours, and 30,000 so called “ish” whites, such as bluish white, yellowish white, greenish white etc [5]. Therefore, there are apparent differences between different samples within the class described white. The term “white” used in the description of textile (as well as paper), is thus not an absolute term. There are degrees of whiteness, and it is meaningful to claim that one textile material is whiter than another.

An equation has long been sought which would provide a single scale whiteness so that, from the equation, a whiteness index for a sample could be calculated. To this end, many equations have been proposed, with different industries, for example paper, paint, textiles, each having their own preferences. The difficulty in devising an equation has been in establishing the weightings of lightness and chromaticities to yield a scale which relates to perceived whiteness [6-7].

White samples are often more difficult to assess than coloured ones because white, besides being objectively quantifiable, is also a subjective connotation of quality which is greatly influenced by personal taste. The agreement on “perfect white” has not been reached yet, since a strong preference for the concept of whiteness is governed by trade, nationality, habit and product. As a result, no single formula for whiteness is universally accepted [8].

1.2 The colour and structure of native cotton

1.2.1 The origin of colour in cotton

Natural products are usually not white. A natural cotton cloth is ivory colour, the bleaching makes it white. Cotton is by far the most popular fibre in use today, at least in terms of volume of production. When the waxes and other impurities have been removed (after scouring) the cotton still has a yellowish or brown discolouration. This is caused by the natural colouring matter, which can only be removed effectively by oxidative bleaching agents. The natural colouring matter is present only in traces and its composition has not been still established with certainty.

Many events impact cotton fibres, with the most highly valued cotton white and homogenous in colour. Since cotton is a natural fibre, it is influenced by growing conditions, microorganisms, weathering, trash, dust, oil, and other extraneous materials. It remains difficult to measure and understand all the aspects of colour and trash. Cotton fibre colour values are understood to change and age over the years. Generally, the colour of cotton fibres is primarily determined by conditions of temperature and/or humidity, cotton lint exposure to sunlight, and cotton varieties. Action by parasites or micro-organism, as well as technical defects in harvesting and subsequent storage and transport, may all affect the colour of cotton. The colour of cotton ranges from white to yellowish and is classed into the groups “White”, “Light Spotted”, “Spotted Tinged” and “Yellow Stained”, in descending order of quality. HVI (instrument measurement) classing has been available on an optional basis to all cotton growers since 1981. The colour of cotton is measured by the degree of reflectance (Rd) and yellowness (+b). Reflectance indicates how bright or dull a sample is, and yellowness indicates the degree of colour pigment. A three-digit colour code is used to indicate the colour grade. This colour grade is determined by locating the quadrant of the colour chart in which the Rd and +b values intersect [9].

Knowledge of the origin and development of the cotton fibre is an aid in understanding its composition and the origin of its natural colour. Cotton is a hair attached to the seed of several species of the botanical genus *Gossypium* which belongs to the order Malvaceae. The cotton plant grows to a height which may be up to 1-1.5 m and its cultivation varies depending on climate, soil etc. Before the plant reaches its full height, it throws of flower stalks at the extremity of which the blossom pods subsequently appear. These expand until they reach about the size of a bean when they burst and display the blossom which lasts for only 24 hours. When the blossom falls, a small dark green triangular pod forms, which then increases to the size of a walnut. This is termed a boll and may contain 20 or more seeds. The epidermal cells on the young seeds begin to grow and elongate, forming long tube-like cells with an ultimate length over 1000 to

4000 times the cross-sectional diameter. In about 18 days the cell wall starts to thicken and elongation practically stops. When maturity is reached (50 to 60 days after flowering) the boll bursts to display the cotton seeds covered in a “downy” mass of cotton (Figure 1.1) [10-11].

In many varieties of cotton, the seed has not only the long fibres (lint) used for the spinning into yarn but also there grow, from the seed, an undergrowth of short coarser fibres (fuzz) which may be coloured whereas the lint fibres are near white (Figure 1.1). After harvesting the cotton bolls are allowed to mature and dry for around thirty days. To obtain the cotton fibres, the hairs are then cut from the seed by means of knives, the process being called ginning.

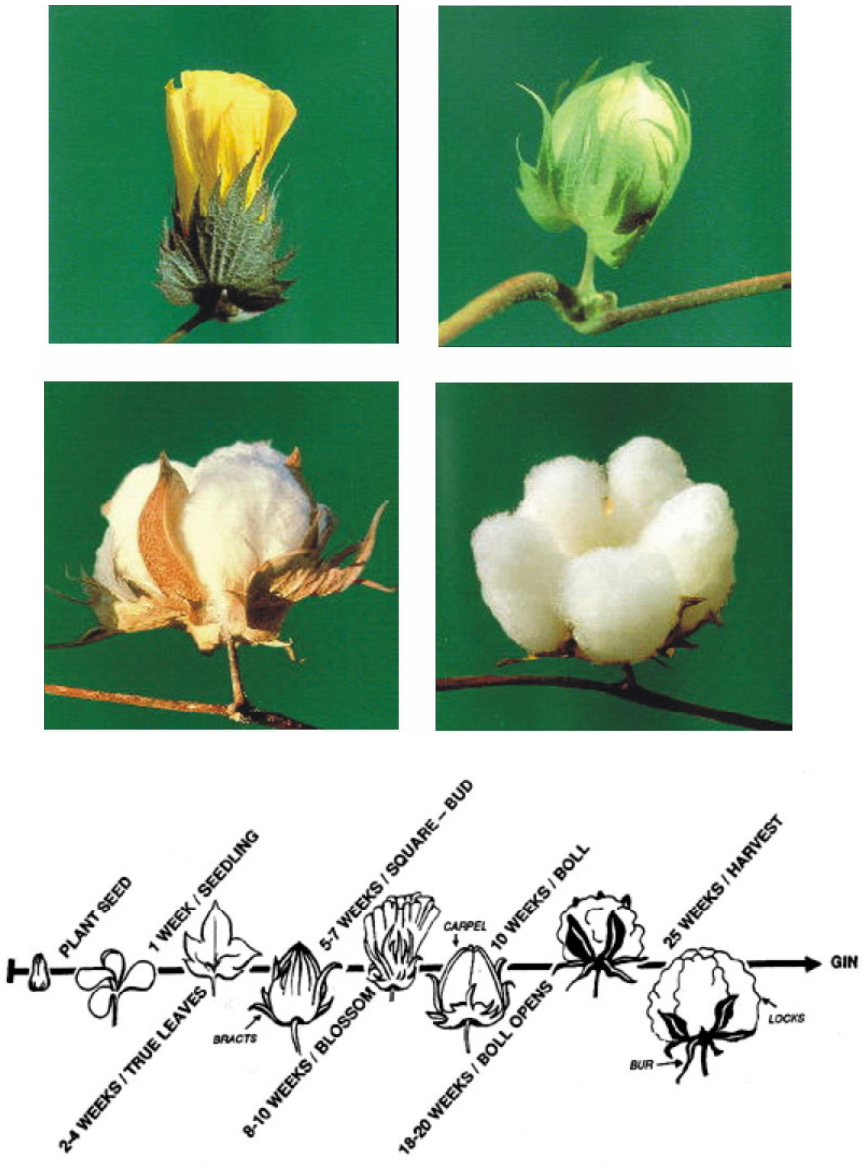

Figure 1.1 The growth and maturation of cotton [12-13].

Raw cotton in the trade is classified by fibre length (staple), uniformity, fineness, colour, cleanliness, handle, strength and elasticity. Principal defects are impurities, short staple and high content of immature and badly developed or "dead" fibres. Some grades are of harsh rough handle whilst others are silky soft.

The composition of the fibre reflects its cellular nature. Although cellulose is the major constituent, any of the substances commonly found in plant cells may be expected to be present in at least small amounts. The nature of the pigment which is responsible for the faint creamy colour of raw cotton is still not known for certain. It is possible that cotton fibres contain some of the flavonoid pigments found in the cotton flowers and cotton seeds [14-16].

The pigment of brown cotton has been more thoroughly studied than the other pigments. It has been established that it consists of flavones such as morin and gossypetin (Figure 1.2a-b). Cotton fibres contain a considerable amount of polyphenols such as gossypol (Figure 1.2c), flavone and tanning substances, whereas the content of these substances depends on the maturity of the fibre. The chromatographic analysis of the colouring matter contained in naturally-coloured cotton fibres has shown the presence of substances containing groups of phloroglucinol, resorcinol and pyrocatechol in the molecule [17]. According to other scientists, the natural colour of cotton is at least genetically related to chlorogenic acid (Figure 1.2d), a condensation product of caffeic acid and quinic acid [18].

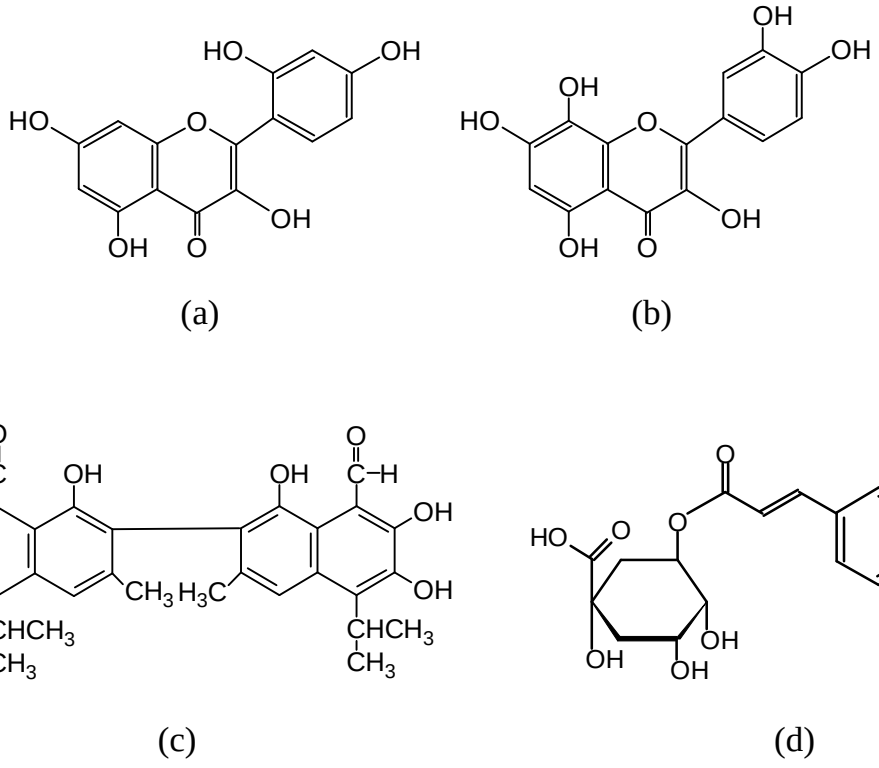

Figure 1.2 Structure of morin (a), gossypetin (b), gossypol (c) and chlorogenic acid (d).

1.2.2 Cotton structure

Since the chemical composition of the material is determining factor in its behaviour toward any chemical treatment, a presentation of this composition should precede any discussion of the bleaching technology. Detailed information on the structure of cotton fibres has been conveniently summarised in the literature and only a brief digest is made here.

The morphology of the cotton fibre is complex. It consists largely of cellulose but with some residual protoplasm in the lumen, and fats, waxes and pectins confined mainly to the outer layers of the fibre. The removal of the latter impurities to obtain absorbent fabrics of good whiteness is essential for further processing.

The fibre is considered to be built up in layers from substantially crystalline fibrils of cellulose, the ordered regions being the bulk of the fibrils and the disordered regions being confined to the surfaces (and to very short regions along the length) of the fibrils. Chemical reactions take place on the surfaces of the fibrils of different sizes and, in certain circumstances, at imperfections within the crystalline lattice of the fibrils [19].

The cellulose chain molecules are believed to form into flat ribbons which can aggregate in stacks with the aid of van der Waals forces which act perpendicularly to the main planes of the glucopyranose rings [20]. These stacks are considered to be held together laterally by hydrogen bonding between equatorial hydroxyl groups protruding from the edges of the ribbons.

Both swelling and drying profoundly modify the fibrillar aggregation, the distribution of void spaces within the fibres and hence the internal volume accessible to reagents, i.e. the fibre accessibility. Fibre accessibility is dependent upon the fine structure and this influences the rate, extent and uniformity of wet processing (bleaching, dyeing, etc.). Thus accessibility is dependent upon the microporosity and the internal surface area of the fibre. The implied effect of the accessibility is to allow transport of reagents or dyes inward to reaction sites or the movement of reaction products out from the reaction sites, or both.

Although cotton fibre is considered to be a single cell, it consists of four characteristic regions: cuticle; primary wall; secondary wall; and lumen (Figure 1.3) [10].

Cuticle consists of a very thin outer layer of tightly moulded material. It consists of a deposit of cotton wax and pectic material. The cotton wax is a complex mixture of waxes, fats and resins. One of the functions of cuticle is to protect the fibre from atmospheric oxidation which possibly arises from the action of the ultra-violet component of strong sunlight. The *primary wall* consists mainly of

cellulose, having thickness of only 0.1-0.2 nm as compared to the overall width of the fibre of 20 nm. The cellulose within the primary wall has been laid down in the form of fine threads or fibrils, and within this network of fibrils the impurities are found. These are mainly pectic substances and some fatty ones.

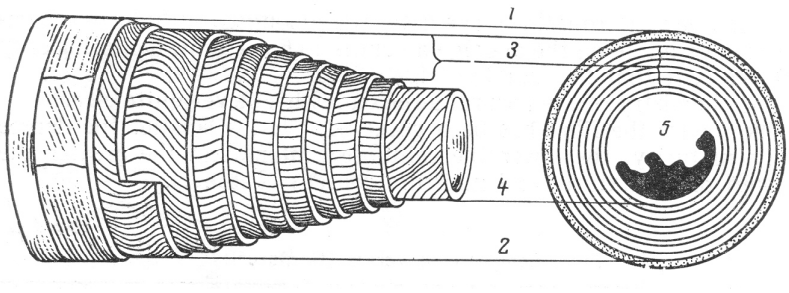

Figure 1.3 The structure of cotton fibre: (1) cuticle, (2) primary wall, (3) secondary wall, (4) lumen, (5) protoplasmic material [10].

The molecular chain of cellulose, as the basic substance of cotton, is stretched. The cellulose molecules stabilise themselves, lying parallel, through intermolecular and intramolecular hydroxyl bonds (Figure 1.4) which, in spatial construction, leads to a unit cell in X-ray terms.

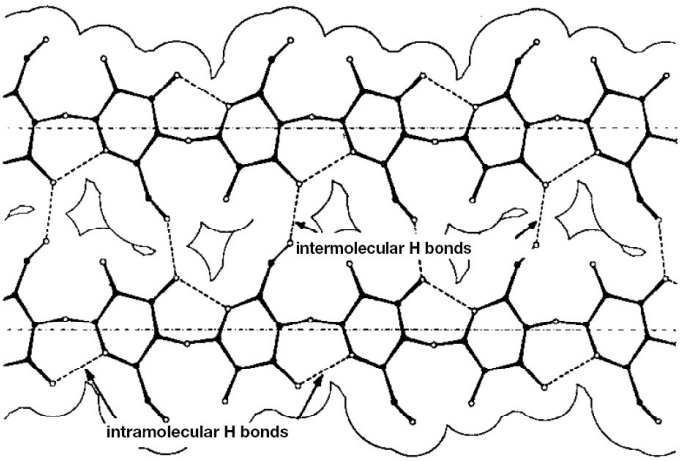

Figure 1.4 Intermolecular and intramolecular hydrogen bonds in cotton cellulose [10].

The *secondary wall* forms roughly 90% of the total weight of the fibre. It is composed of successive layers of cellulose deposited on the inner side of the primary wall. The fibrils in the secondary wall are aligned in layers or lamellae and follow a spiral path around the fibre axis. *Lumen* is canal that stretches from the base of the fibre to the tip where it is closed. It contains protoplasmic material essential for cell growth so that when the fibre dries out a residue is left in the lumen after evaporation.

The internal structure of the fibrils has not yet been fully described, and various models have been discussed in literature. The various models could be summarised stating the following: (i) 1 cotton fibre = 15,000 microfibrils; (ii) 1 microfibril = 400 elementary fibrils (aggregated crystallographically); (iii) 1 elementary fibril = 100 cellulose chains arranged in 6-8 packages; (iv) diameter of macrofibril = 400 nm; (v) diameter of microfibril = 200-300 nm; (vi) diameter of elementary fibrils = 3.5 nm.

In the inter-fibrillary spaces of 5-10 nm width, lignin - amongst other things - fills in as a "cement". The intermicellar spaces of 1 nm located between the elementary fibrils are accessible to H_2O, $ZnCl_2$ or I_2, but not for dyes (unless the pores are expanded through boiling off with alkali). Macroscopically, this structure peaks in the texture of the secondary wall, which is surrounded by the thin primary wall.

1.3 Current bleaching processes

Cotton fabrics cannot be processed into apparel and other finished goods until the fabrics have passed through several water-intensive wet processing stages. Wet processing enhances the appearance, durability, and serviceability of fabrics by converting undyed and unfinished goods, known as "grey" goods, into finished consumers' goods. Also collectively known as finishing, wet processing has been broken down into four stages: fabric preparation, dyeing, printing, and finishing.

The cotton fabric preparation steps are shown in Figure 1.5. Preparation, also known as pre-treatment, consists of a series of various treatment and rinsing steps critical to obtaining good results in subsequent textile finishing processes. Typical preparation treatments include desizing, scouring and bleaching. Preparation steps can also include processes, such as singeing and mercerizing, designed to chemically or physically alter the fabric. In certain cases, some processes may be omitted and the order of the processes in a particular plant may vary, as shown in flow diagram, depending on the particular end product that is desired.

Bleaching of cotton, in the original sense of the term, means the whole sequence of purification processes for making the goods whiter regardless of whether it is carried out in preparation for dyeing and printing or in the processing of undyed goods [21]. The definition of bleaching by the Textile Terms and Definitions Committee of the Textile Institute is: "The procedure, other than by scouring only, of improving the whiteness of textile material by decolourising it from the grey state, with or without the removal of natural colouring and/or extraneous substances" [22].

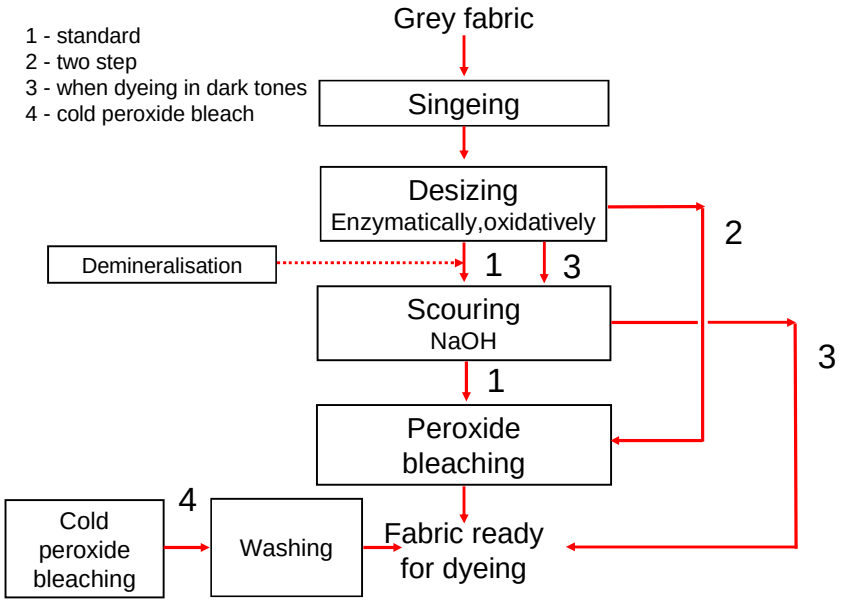

Figure 1.5 Cotton fabric preparation process flow diagram.

As already described, cotton fibres possess inherent pigment colouring matter which accounts for the "grey" textile's characteristic yellow/brown appearance. Although scouring and subsequent washing may produce a clean absorbent substrate, small amount of pigment colorant still remains; so bleaching is necessary for a large percentage of goods intended for dyeing. In the case of fabrics to be printed or for white end-uses bleaching is essential. Coloured impurities have to be removed in order to prevent their optical interference with the colour to be developed by the dyes. If bleaching is done in preparation for dyeing and printing, apart from the removal of coloured impurities its purpose is to facilitate ready absorption and even, uniform distribution of the dye. Therefore, the actual purpose of bleaching varies with the end use of the goods and this variation is partly responsible for the variety of bleaching methods used. In current bleaching processes the most successful way of removing the pigment colorant from natural fibres is by oxidative means using three principle oxidants - sodium hypochlorite (NaOCl); sodium chlorite ($NaClO_2$) and hydrogen peroxide (H_2O_2).

1.3.1 History of bleaching with hydrogen peroxide

Hydrogen peroxide is by far the most commonly used bleaching agent for cotton and cotton blends, accounting for more than 90% of the bleaching agents used in textile operations [23], and is typically used with caustic solutions.

Hydrogen peroxide was suggested for bleaching in 1818, first applied for bleaching in 1882, but the method attained commercial significance only since about 1930. Some hydrogen peroxide was made by electrolytic methods in

Europe as early as 1912 and in the late 1920s this manufacturing method was established in the USA by E.I. Du Pont de Nemours. The commercial availability of increased quantities of hydrogen peroxide led these companies to develop its use for bleaching cellulose. By 1940 in the USA, peroxide accounted for over 60% of cotton bleaching, but the transition from hypochlorite and chlorite bleaching only made significant headway from the mid-1950s in Europe [24].

The peroxide route offered savings of over 50% in labour, water and energy costs. This better overall economics and process versatility caused chlorite use to almost disappear by the late 1970s. In comparison to the use of hydrogen peroxide itself, there has been a small use of chemicals which, when dissolved provide a solution of hydrogen peroxide, for example sodium percarbonate and sodium perborate. In Europe, these two mild bleaches have for many years provided the solid bleach component of domestic laundry powders.

Hydrogen peroxide bleaching, particularly of cotton, has gained in importance in view of the effluent problems (AOX - absorbable organic halogens) caused by hypochlorite bleaching. Although specific process conditions are needed for its application to cotton, there is some degree of variation tolerated without the problems of excessive fibre damage. High temperatures accelerate the bleaching process. Therefore, temperatures close to the boil (or even above) are frequently used. Since low pH values retard the hydrogen peroxide effectiveness, sodium hydroxide is included in the bleaching bath to give a pH of 10.5 to 11.5. With further increasing of pH hydrogen peroxide rapidly decomposes to give oxygen and bleaching is suppressed again.

The inclusion of sodium hydroxide into the bath and the use of modern bleach bath additive “cocktails” containing wetting agents, detergents and emulsifiers enable simultaneous scouring and bleaching to be carried out. One further essential additive to the bleach bath is a stabiliser. Stabilising hydrogen peroxide in the bleaching liquor is of fundamental importance to a uniform bleaching result and largely gentle treatment of the textile raw fibre material. The most important, very frequently used stabiliser systems are organic stabilisers based on phosphoric acids, aminocarboxylates and sodium silicate (waterglass) in combination with alkaline earth metal ions, particularly magnesium ions [25-26]. In the bleaching liquor, sodium silicate and magnesium ions form colloids, which act as buffers, and keep liquor alkalinity constant. The anticatalytic effect of this classic stabiliser is based on the fact that H_2O_2 decomposition catalysts are incorporated in the waterglass colloids, and are chemically inactivated. Therefore, sodium silicate not only helps to buffer the pH, but also inactivates metallic impurities (i.e. Fe, Cu) which could cause extensive fibre damage by catalytic decomposition of hydrogen peroxide. The disadvantages of silicate stabilisers include difficulty in removal during washing, formation of deposits on the fibre and on processing machinery, harsh handle etc. This is the reason

that nowadays organic stabilisers are mostly employed, such as aminocarboxylates (e.g. ethylenediaminotetraacetic acid - EDTA).

1.3.2 The hydrogen peroxide bleaching process

The hydrogen peroxide bleaching process, as well as other bleaching processes, generally involves three steps: (1) the material is saturated with the bleaching agent, activator, stabiliser, and other necessary chemicals; (2) the temperature is raised to the recommended level and held for the amount of time needed to complete the bleaching action; and (3) the material is thoroughly washed and dried.

The treatment time and bleach-bath concentration depend upon the temperatures and process equipment used. Batch bleaching on a winch at 80-90^{o}C may take 1-2 hours with 3-5 mL/L of hydrogen peroxide (35% by weight). Cold batch bleaching takes at least 6 hours after impregnation in a 40-50 mL/L hydrogen peroxide solution. However, a rapid 20-30 minute bleach is possible using continuous low-liquor ratio or pad-steam techniques and with hydrogen peroxide concentration of 1.0 to 1.75% o.w.f.

Cotton can be bleached in various forms, i.e. also in different processing stages. The bleaching of cotton in loose stock and card sliver form is of subordinate importance. The bleaching of cotton yarns is mainly done in cross-wound packages or warp beams in circulation-type equipment, mainly in two stages for full white, first with hypochlorite and then hydrogen peroxide. Nevertheless, the great majority of cotton is bleached in woven or knitted fabric form. The processes are based closely on those of scouring; bleaching is effected either in rope or open-width form, in batches or continuously, and in the same equipment. Production quantities and fabric quality determine the choice.

Only lightweight qualities with no tendency to crease are suitable for fabric bleaching in rope form. Small batches can be bleached in the winch, and liquor circulation vessels are employed for large batches. This bleaching process is called “kier bleaching”. The equipment used for continuous rope bleaching is the J-box with upstream impregnating section. Bleaching fabrics in open-width form is suitable for all woven fabric qualities. Usually, batches scoured in a jigger are subsequently bleached in the jigger. The second possibility of batch bleaching is offered by the “pad-roll”, pad mangle-dwell or batch bleaching process. A batch bleaching line comprises a pad mangle - or better, an impregnating section - a heating unit (steam, air, infrared) and a dwell chamber. Cold dwell processes are of interest from the energy saving standpoint. All temperature variants are suggested for hydrogen peroxide. The lower the temperature the longer the dwell time.

Continuous processes for bleaching in open-width form are of great importance.

The equipment used is the same as for the alkali stage in scouring. The processes comprise impregnating the fabric with the bleaching liquor, heating by steam and dwelling in a steam atmosphere with subsequent washing off. Less room is taken up by HT (high temperature) or pressure steamers, in which the bleaching process is carried out within 45 to 120 s at 130-140^{o}C. Medium term bleaching processes with steaming times of 10-20 minutes are more usual. Short bleaching times of 1-3 minutes can be achieved with hydrogen peroxide in open steamers with the use of superheated steam. Scouring and bleaching each take 2 minutes.

1.4 Routes to low-temperature bleaching: Catalysis vs. activation

Current technologies have their restrictions, being under increasing pressure to be environmentally safe, cost-effective and energetically efficient. Decreasing the temperature of the bleaching process is an important challenge that will undoubtedly lead to general savings in energy consumption. Unfortunately, at ambient temperature, hydrogen peroxide provides poor bleaching and is used inefficiently. Hence, processes on the basis of oxidative catalysts are a promising alternative for cotton bleaching at low temperatures ($\leq$ 40°C) and short treatment times.

In general, the hydrogen peroxide bleaching systems are used for pulp/paper bleaching, laundry cleaning and raw cotton bleaching. It is noteworthy that the research that has been ongoing in laundry bleaching has been the most dynamic and progressive with regard development and testing potential catalysts for low-temperature bleaching. The extraordinary interest of the detergent industry in oxidation catalysts can be seen in a large number of patents and publications related to catalytic bleaching aimed at laundry bleaching [27]. The knowledge generated in this research area can be used in the development of a catalytic approach in the field of bleaching of raw cotton. However, to reach this objective, it is essential to identify the principal differences between current technologies applied in raw cotton bleaching and laundry cleaning, which could lead to different constraints for the application of a catalyst.

In contrast to raw cotton bleaching, where hydrogen peroxide is used in its generic form, in laundry bleaching sodium percarbonate (or perborate) is used as a “solid” hydrogen peroxide delivering agent. Upon dissolution of sodium percarbonate in water the carbonate buffer and hydrogen peroxide are released quickly, but still high washing temperatures (70-90^{o}C) are required to obtain good bleaching [28-29]. In 1978 a bleach activator tetraacetylethylenediamine (TAED) was introduced in detergent formulations that “boosted” perborate performance, thereby opening the door to a reduction in wash temperatures between 40 and 60^{o}C. Today, TAED and nonanoyloxybenzene sulphonate (NOBS) are amongst the most commonly applied precursors for peracids (see Figure 1.6), as the peracids themselves are often not sufficiently stable.

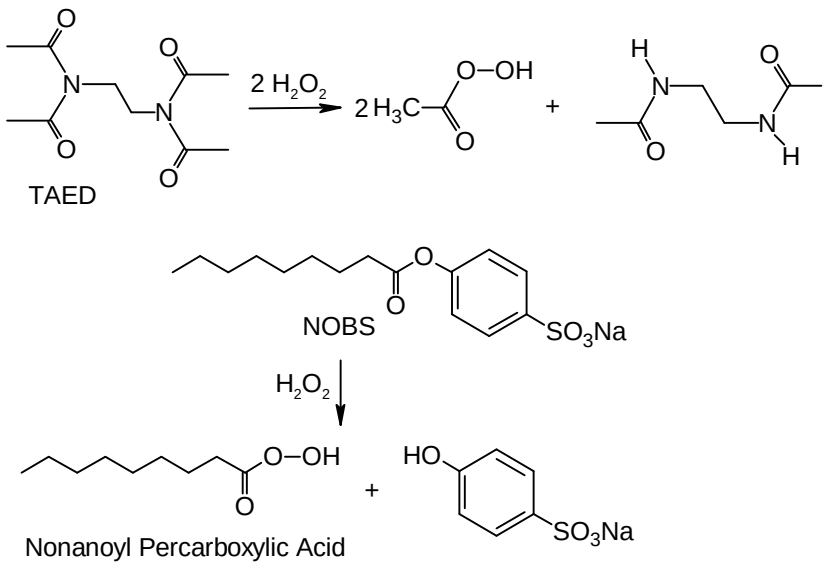

Figure 1.6 Bleach precursors applied in detergents: TAED and NOBS.

The above described use of bleaching activators has been one of the ways to improve laundry bleaching, but they have never been used in raw cotton bleaching. The addition of bleaching activators improves the process (bleaching at lower temperatures and lower concentrations of bleaching agents required). However, the bleach activators are not catalytically active as they react in stoichiometric amounts. Besides this general shortcoming that one molecule of activator is required per molecule of substrate to be bleached (Figure 1.7), in most of cases activators also contain a large leaving group (L), which contributes nothing to the bleaching action and pollutes the waste water unnecessarily.

In catalytic systems, a metal complex is converted by H_2O_2 in an intermediate stage into an active bleaching species. This species then reverts to its original form at the end of bleaching process and is available for another H_2O_2 molecule (Figure 1.7). If the turnover rate is high enough, it should be possible to achieve the same bleaching performance with the catalyst concentrations in the ppm range as with 5% of a conventional activator [30].

The application of catalysts is therefore an economic as well as an environmental solution. Using catalysts in bleaching process can lead to lower process temperature and shorter bleaching time, with probably less use of bleaching agent, i.e. H_2O_2. In laundry cleaning, the application of the catalysts would also lead to less or no addition of activators. In raw cotton bleaching the application of the catalysts would possibly lead to the reduction in the amount of chemicals (e.g. stabilisers, sodium hydroxide). In general, the ideal catalyst should be effective at temperatures between 20 and 60^{o}C and have adequate

chemical stability in the pH range 8-11 throughout the bleaching or cleaning process. Ready availability of the required raw materials coupled with low-cost industrial-scale catalyst production is also a prerequisite.

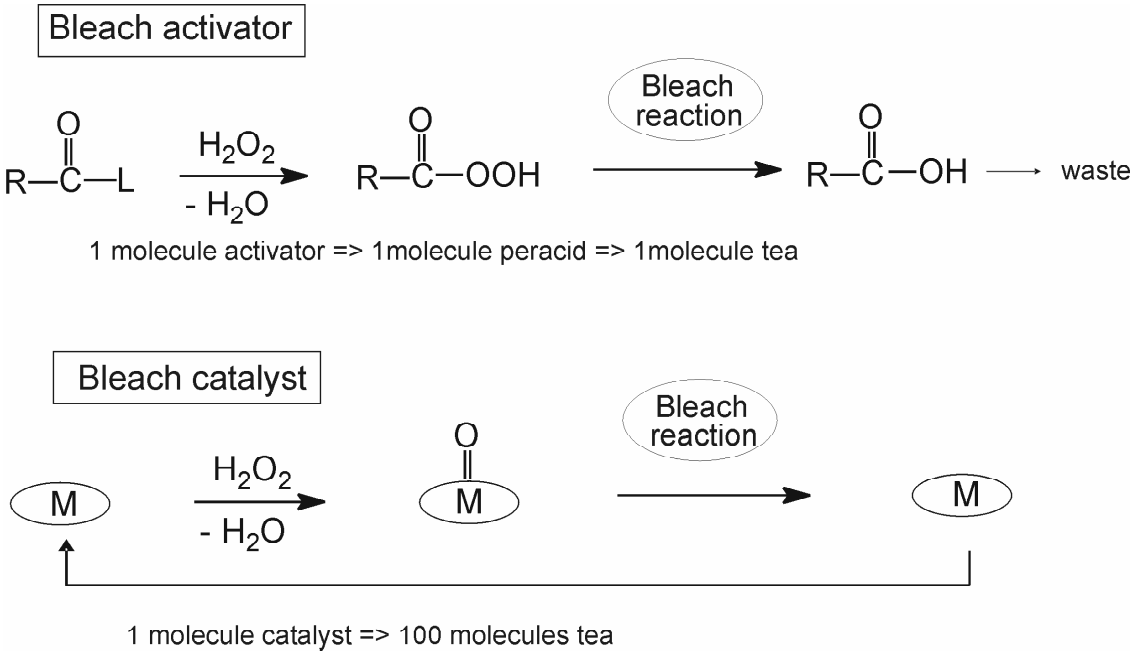

Figure 1.7 Bleach mechanism of activators and catalysts.

General requirements for application of a bleach catalyst in both laundry cleaning and raw cotton bleaching are good bleaching activity combined with negligible fibre damage. Additional requirements for the application of the catalyst in laundry bleaching are: (i) no interactions with dye molecules on cotton and (ii) the inhibition of dye transfer (staining of white textiles by dye molecules coming off the coloured fabrics) by bleaching the migrating dyes in the wash liquor. Therefore, the potential application of catalytic oxidation in laundry bleaching involves two types of action: a homogeneous reaction of dye transfer inhibition and a heterogeneous bleaching with a wide variety of stains (hydrophilic as well as oily), without fibre or colour damage after a number of repeated washing cycles [31]. Moreover, the detergent producers should always anticipate a possible overdosing done often by consumers in household laundry cleaning. These all pose relatively difficult requirements with regard application of bleaching catalysts in laundry cleaning entailing rather high catalyst selectivity. The first and the only commercial application of a catalyst in the detergent formulation was in 1994 [32], but soon after it had to be withdrawn from the market being alleged for causing severe fabric and dye damage (see Section 1.5.2) [33]. At the present no catalyst is employed in the detergent formulations used for laundry cleaning, despite an active research that has been ongoing in this field.

One of the main common aspects of laundry cleaning and raw cotton bleaching should be a similarity in the chemical mechanism of bleaching of certain stains in laundry and bleaching of coloured matter present in native cotton fibre. Structural features of common stains relevant for laundry cleaning (e.g. wine-, fruit- and tea-stains) (Figure 1.8) are comparable to coloured matter present in native cotton fibre (Section 1.2.1).

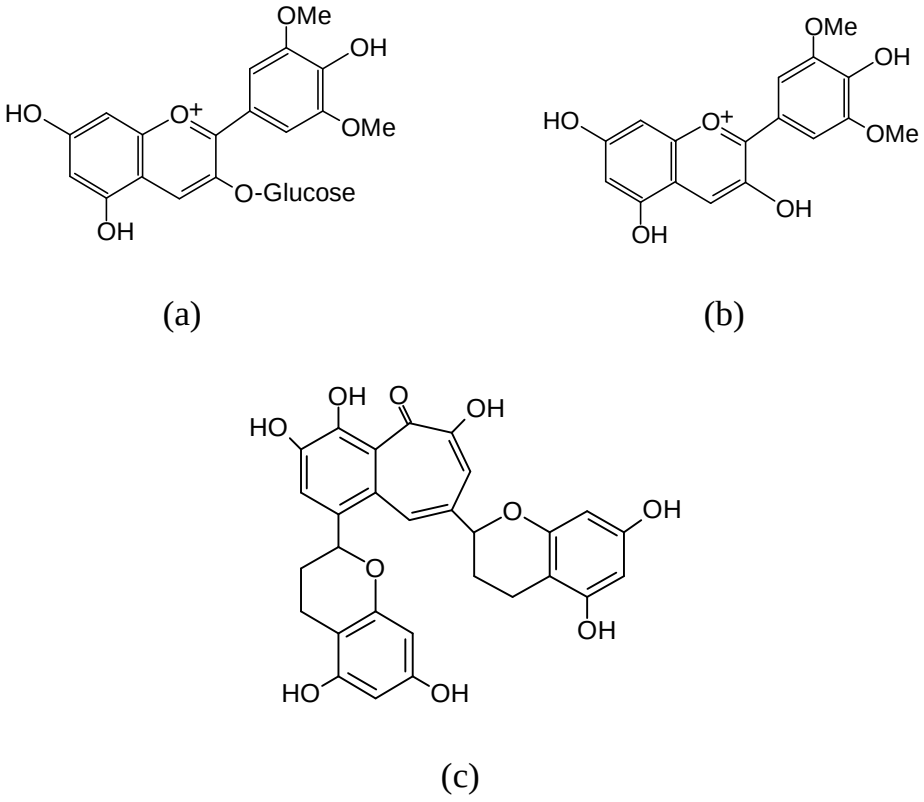

Figure 1.8 Structures of anthocyanin present in red wine (a), malvidin as a model for anthocyanins present in fruit (b) and theaflavin present in tea (c).

However, the application of catalysts in these processes is very different due to the different processing conditions (e.g. process speed, dosage and number of repeating processing steps). For example, the overdosing of catalytic bleach system that can lead to fibre damage in laundry cleaning can easily be avoided during bleaching of raw cotton in industrial conditions where the process is performed under strictly controlled conditions. Furthermore, important limitations related towards application of catalysts in detergent formulations such as, for example, dye transfer inhibition and colour damage, are not an issue in catalytic bleaching of raw cotton. Finally, raw cotton is subjected only once to a bleaching process, different from laundry bleaching where the goods are repeatedly washed thus increasing the chance of fibre damage.

Based on these considerations, the application of the catalysts in industrial bleaching of raw cotton seems to be promising, i.e. relatively easier to overcome the existing barriers. Nevertheless, the most difficult would certainly be to psychologically leave the harbour of "safe" traditional bleaching approach and to sail into an open sea of smart oxidation catalysis. This is especially since the term "catalytic" has been for decades associated with an undesired fibre damage phenomenon occurring in textile practice, but not for an alternative process which can lead to significant savings in energy.

It is noteworthy that, different from a dynamic competition between the leading detergents producers that continues with a large number of patents and publications on the use of bleaching catalysts, the research directed to catalytic bleaching of raw cotton is hardly found in open literature. Anyhow, the vast knowledge generated on the bleaching catalysts for possible detergent application can surely serve as a solid basis for textile practice, especially with regard the choice of the catalyst.

1.5 Bleaching catalysts

1.5.1 An overview of available solutions

It has been known since 19th century that the oxidative power of hydrogen peroxide is greatly enhanced by transition metal ions, when Fenton invented his analytical reagent Fe(II) + H_2O_2, and textile bleachers recognised the tendency of rust particles to make pinholes in cloth. The active species here is the hydroxyl radical:

$$Fe^{2+} + H_2O_2 \rightarrow Fe^{3+} + OH^- + OH^\bullet$$

The hydroxyl radical is extremely strong oxidant that Fenton's reagent is now used commercially to destroy organic pollutants in industrial effluents [34-35]. However, this reagent was too strong and too unselective to be used in either organic synthesis or textile bleaching.

In general, interactions between hydrogen peroxide, and transition metal ions, and organic compounds started to be studied soon after hydrogen peroxide was discovered in 1818, and the literature on them is very extensive. Seeking for systems or compounds that act as selective oxidants towards bleaching of cotton fibre and also satisfy a number of practical requirements, one would have to comb all this literature. Despite the fact that literature related to bleach catalysts grows rapidly, the lack of complete and systematic data (sometimes even on stain-bleaching) that would allow a proper analysis and to pinpoint the most appropriate catalyst for the bleaching of cotton is apparent.

Generally, the bleaching catalyst should meet the following requirements: oxidative and hydrolytic stability, sufficient bleaching efficiency and cause no or low fibre damage, low processing temperature ($T \leq 40°C$) and alkaline conditions ($pH \geq 7$), environmentally acceptable, easy production and low cost. In the past there have been a number of attempts to develop catalytic bleaching systems. In the mid-sixties, the use of cobalt salts in combination with picolinic acid was proposed [36]. The aim was to achieve a balanced ratio of complexed (non-bleaching) metal ions in the detergent liquor to free (reactive) metal ions on the fibre being bleached. Metal ions, however, give only a slight increase in performance of hydrogen peroxide, though they do promote its catalytic decomposition in non-bleaching oxygen and water and the formation of the highly reactive hydroxyl radicals, which have marked fibre-damaging properties. When manganese salts are used, deposits of manganese dioxide can also form on the fabric, marring its appearance. To avoid free metal ions in the wash liquor it is therefore necessary for the metal to be used in the form of a relatively stable complex. It must be ensured that at least one coordination point of the metal is not occupied because otherwise no reaction with hydrogen peroxide can take place. Thus, for example, EDTA complexes of the transition metals have no bleaching properties. By contrast, certain porphyrin complexes of manganese or iron are in principle suitable as bleaching catalysts [30]. From an environmental acceptance aspect, the transition metals complexes based on manganese and iron are of particular interest.

Hage and Lienke [27] have recently reviewed the transition-metal bleach catalysts for pulp bleaching and laundry cleaning applications. The authors have discussed several manganese and iron compounds patented as bleaching catalysts in more detail since mechanistic investigations were published previously. Special emphasis has been given to manganese-triazacylononane complexes, Schiff-base, cross-bridged macrocyclic and complexes with 2,2':6,2''-terpyridine. As the most relevant iron complexes, the authors discussed the iron complexes with tris(pyridine-2ylmethyl)amine, pentadentate nitrogen-donor and macrocyclic tetraamidate ligands. Besides, they have reviewed other transition-metal compounds, including cobalt catalysts that activate hydrogen peroxide for laundry and hard surface cleaning applications and vanadium-based polyoxometalates to enhance delignification by dioxygen. An overview of paper-pulp bleach catalysts research has also been recently published [37].

1.5.2 Manganese-triazacyclononane complexes

A crucial breakthrough in terms of bleaching activity came with manganese complexes with 1,4,7-trimethyl-1,4,7-triazacyclononane ligands (TACN) [38]. These are probably the most effective catalysts for hydrogen peroxide low-temperature bleaching. Manganese-TACN complexes are claimed to be efficient, selective oxidation catalysts at room temperature i.e. in cold water and at pH's

greater than 9 where most of detergents are buffered. The alkaline conditions are also characteristic for the industrial bleaching of grey cotton fabrics. As already discussed, free manganese ions cannot be used as the manganese would precipitate out as brown MnO_2 and cause stains. Manganese-TACN complexes form homogeneous and stable solutions, so there is no danger of precipitation. The oxidation state of the metal seems to be stabilised by complexation to nitrogen containing ligands. In addition to triazamacrocycles, larger azamacrocyclic rings, Schiff bases, multidentate ligands and pyridine systems have been employed ([27] and references therein) as stabilisation ligands for the manganese and cobalt ion.

The manganese is in a similar environment in triazacyclononane complexes to that found in some Mn metalloenzymes, where the complexed manganese can change the oxidation state reversibly without being lost from the complex. Figure 1.9 and Figure 1.10 show a typical ligand and the type of manganaese complexes used as the catalysts, respectively.

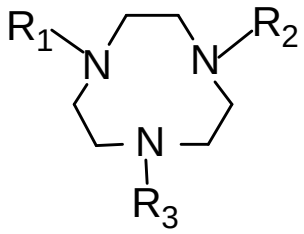

L^1 $R_1 = R_2 = R_3 = CH_3$
L^2 $R_1 = R_2 = R_3 = CH_2\ CH_2OH$

Figure 1.9 Typical ligand: triazacyclononane.

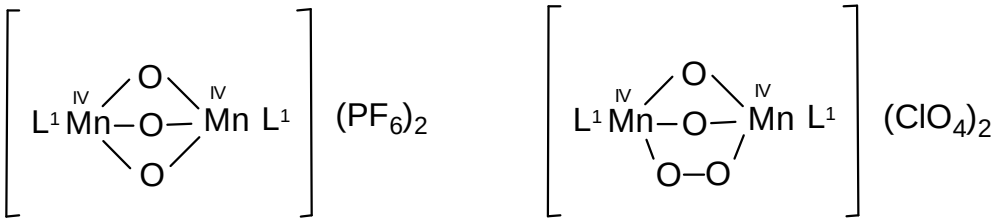

(a) (b)

Figure 1.10 Typical manganese-triazacyclononane complexes which catalyse hydrogen peroxide bleaching.

The first bleach catalyst employed in commercial detergent products was a dinuclear manganese compound containing 1,4,7-trimethyl-1,4,7-triazacyclononane ligands (MnTACN) (Figure 1.10a) [32]. The compound was first published in 1988 as a model for manganese-containing enzymes by Wieghardt and co-workers [39]. According to the examples given in the original patent, the bleaching activity at 40^{o}C on tea-model stains is very high [32].

Other stains such as wine, fruit, and curry stains were also bleached efficiently, in all cases using hydrogen peroxide. The efficiency of tea stain bleaching is optimal between pH 9 and 11. However, the detergent product containing this catalyst was withdrawn from the market [33] after it was alleged that the product yields increased fabric- and dye-damage after several washing cycles. The catalyst is still applied in various machine-dishwashing products and is responsible for superior removal of tea residues. The mechanism of the oxidation process with this catalyst was investigated by using phenolic compounds and catechol as models for tea stains [38, 40-41] and will be discussed in more detail in Chapter 3.

Based on the literature available, we can conclude that MnTACN catalyst is one of (if not) the most active catalysts for hydrogen peroxide activation in bleaching of stains. It can be hardly found a recent publication on new bleach catalysts, whose activity is not compared with that of MnTACN [31, 42-43]. The efforts with new catalysts for the application in laundry cleaning have been made to overcome the problems with fibre damage and to prevent dye oxidation, but not to outperform the activity of MnTACN which still serves as a benchmark. Nevertheless, the drawbacks of the catalyst when applied in detergents for laundry cleaning, such as fibre damage, did not seem to us as equally relevant as for bleaching in industrial conditions since it is one-step process. The second drawback, the oxidation of dye on cloth, is not an issue at all in bleaching of grey cotton fabric. We have also recognised that various stains (tea, wine, fruits) are polyphenolic in nature and based on the flavonoid structure, similar to the pigments found in native cotton fibre (Section 1.2.1). Moreover, morin (Figure 1.2a) that is one of the pigments found in cotton fibre has often been used as a model compound for tea-stains [31, 42, 44]. Based on these considerations, the MnTACN catalyst has been chosen to study catalytic bleaching of grey cotton fabric described in this thesis.

1.6 Outlook

In the last two decades a wide variety of transition-metal complexes have been patented for bleaching applications. Many more have been tested and not found to be active. Various approaches have led to more stable/robust bleaching catalysts, such as the use of 1,4,7-triazacyclononane ligands for manganese, the cross-bridged macrocyclic ligands with manganese or pentadentate ligands with iron. This research has mainly been directed towards laundry cleaning and paper/pulp bleaching processes. Up to now, the research related to the industrial bleaching of “grey” cotton does not leave up this competition.

Nevertheless, much more must and can be done. To achieve sustainable chemistry a sea of change in the chemical community is required. The principles of green and sustainable chemistry must become an integral part of textile

chemical education and practice. If chemists increasingly direct their strengths to contribute to sustainable textile industry, chemistry will become more interesting and compelling for textile industrial applications, and may lose its "toxic" and "high-energy" consuming image. It will become more worthy of public support and spawn exciting economic enterprises that nurture sustainability. This thesis is an attempt towards achieving that goal. It will be shown that, although 'white is not as simple as it seems to be', bleaching does not have to be high energy consuming and/or long-time acquiring process. The work presented here will show that by using environmentally benign oxidant H_2O_2 in combination with the proven high-performing dinuclear manganese catalyst MnTACN both short-time and low-temperature bleaching process can be accomplished. It is a fundamental and comprehensive study that includes an integrated approach of both molecular and macroscopic aspects of catalyst based cotton bleaching bringing up together chemistry, material and engineering phenomena.

Literature cited

[1] Crozier, W.R., The psychology of colour preferences, Rev. Prog. Coloration, **26** (1996) 63-72.

[2] History on the Net, The Romans Clothing, http://www.historyonthenet.com/Romans/clothing.htm, 15.11.2006

[3] The Color White, http://www.elizabethan-era.org.uk/color-white.htm, 15.11.2006

[4] International Commission on Illumination, http://www.cie.co.at/ciecb/, 20.11.2006

[5] Aksoy, B., Fleming, P.D., Joyce, M.K., Whitenes evaluations on tinted and FWA added papers, http://www.wmich.edu/ppse/staff/publications/fleming, 17.11.2006

[6] Wardman, R.H., An update on numerical problems in colour physics, Rev. Prog. Coloration, **24** (1994) 55-75.

[7] Griesser, R., Instrumental measurement of fluorescence and determination of whiteness: Review and advances, Rev. Prog. Coloration, **11** (1981) 25-36.

[8] Chong, T.F., Instrumental measurement and control of colour, Rev. Prog. Coloration, **18** (1988) 47-55.

[9] UNCTAD commodities, Market information in the commodities area, Cotton, http://r0.unctad.org/infocomm/anglais/cotton/quality.htm, 20.11.2006

[10] Peters, R.H., Textile chemistry. Volume 1. The chemistry of fibres, Elsevier Publishing Company, Amsterdam/London/New York (1963) pp. 159.

[11] Guthrie, J.D., The chemistry of lint cotton. A. Composition. In Chemistry and Chemical Technology of Cotton, Ed. by Ward K. Jr., Interscience Publishers, Inc., New York (1955) pp. 1-14.

[12] Swicofil AG Textile Services, Cotton, http://www.swicofil.com/products/001cotton.html, 27.10.2006

[13] Cottons Journey, Story of cotton, http://www.cottonsjourney.com/Storyofcotton/print.asp, 17.11.2006

[14] Trotman, E.R., Textile scouring and bleaching, Charles Griffin and Company Ltd., London (1968) p. 21.

[15] Ryser, U., Holloway, P.J., Ultrastructure and chemistry of soluble and polymeric lipids in cell walls from seed coats and fibres of *Gossypium* species, Planta, **163** (1985) 151-163.

[16] Hedin P.A., Jenkis J.N., Parrot W.L., Evaluation of flavonoids in *Gossypium arboreum*

(L.) cottons as potential source of resistance to tobacco budworm., J. Chem. Ecol., **18** (1992) 105-114.
[17] Sadov, F., Korchagin, M., Matetsky, A., Natural admixtures of cotton fibre. In "Chemical technology of fibrous materials", Mir Publishers, Moscow (1973) pp. 45-56.
[18] Oparin, A.I., Rogowin, S.A., Zur Kenntnis der Natur der Baumwollpigmente, Melliand Textilber., **11** (1930) 944-946.
[19] Holme, I., Fibre physics and chemistry in relation to coloration, Rev. Prog. Coloration, **7** (1976) 1-22.
[20] Warwicker, J.O., Wright, A.C., Function of sheets of cellulose chains in swelling reactions on cellulose, J. Appl. Polym. Sci., **11** (1967) 659-671.
[21] Valko, E.I., Bleaching. In Chemistry and Chemical Technology of Cotton, K.Ward Jr., Ed., Interscience Publishers, Inc., New York (1955) p. 117-215.
[22] Farnfield, C.A., Alvey, P.J., (Eds.), Textile Terms and Definitions, Seventh Edition, The Textile Institute, Manchester (1975) p. 16.
[23] Cardamone, J.M., Marmer, W.N., in "Chemistry of the Textiles Industry", Ed. C.M. Carr, Chapman & Hall, London (1995) pp. 46-101.
[24] Dickinson, K., Preparation and bleaching, Rev. Prog. Coloration, **14** (1984) 1-8.
[25] Rouette, H.K., Encyclopedia of textile finishing, Springer-Verlag (1998) pp. 173-176, 289.
[26] Rucker, J.W., Smith, C.B., Troubleshooting in preparation: A systematic approach, www.p2pays.org/ref/03/02332.pdf, 06.10.2006.
[27] Hage, R., Lienke, A., Applications of Transition-Metal Catalysts to Textile and Wood-Pulp Bleaching, Angew. Chem. Int. Ed., **45** (2006) 206-222.
[28] Ho, L.T.T., Formulating Detergents and Personal Care Products. A Guide to Product Development., AOCS Press, New York, 2000.
[29] Milne, N.J., Oxygen bleaching systems in domestic laundry, J. Surfactants Deterg., **1** (1998) 253-261.
[30] Reinhardt, G., Nestler, B., Seebach, M., Bleach Activation by Metal Complexes, Jorn. Com. Esp. Deterg., **28** (1998) 105-114.
[31] Dannacher, J.J., Catalytic bleach: Most valuable applications for smart oxidation chemistry, J. Mol. Catal. A - Chemical, **251** (2006) 159-176.
[32] Favre, F., Hage, R., van der Helm-Rademaker, K., Koek, J.H., Martens, R.J., Swarthoff, T., van Vliet M.R.P., Bleach activation, EP 0458397 (Unilever) 1991.
[33] Verrall, M., Unilever consigns manganese catalyst to the back-burner, Nature **373** (1995) 181.
[34] Santina, P.F., Method for removing toxic substances in water, US Patent 5575919 (Solvay Interox) 1996.
[35] Solvay Interox, Houston, Fenton's Reagent (Company report).
[36] Conecny, J.O., Meeker, R.E., Bleaching, US Patent 3156654 (Shell) 1964.
[37] Suchy, M., Argyropoulos, D.S., Catalysis and activation of oxygen and peroxide delignification of chemical pulps: A review, Tappi, **1** (2002) 9-26.
[38] Hage, R., Iburg, J.E., Kerschner, J., Koek, J.H., Lempers, E.L.M., Martens, R.J., Racherla, U.S., Russell, S.W., Swarthoff, T., van Vliet, M.R.P., Warnaar, J. B., van der Wolf, L., Krijnen, L.B.**,** Efficient manganese catalysts for low-temperature bleaching, Nature, **369** (1994) 637.
[39] Wieghardt, K., Bossek, U., Nuber, B., Weiss, J., Bonvoisin, J., Corbella, M., Vitols, S.E., Girerd, J.J., Synthesis, Crystal Structures, Reactivity, and Magnetochemistry of a Series of Binuclear Complexes of Manganese(II), -(III), and -(IV) of Biological Relevance. The Crystal Structure of $[L'M^{IV}(\mu\text{-}O)_3\ M^{IV}L'](PF_6)_2{\cdot}H_2O$ Containing an Unprecedented Short Mn···Mn Distance of 2.296 Å, J. Am. Chem. Soc., **110** (1988) 7398-7411.
[40] Gilbert, B.C., Kamp, N.W.J., Lindsay Smith, J.R., Oakes, J., EPR evidence for one-electron oxidation of phenols by a dimeric manganese(IV)/(IV) triazacyclononane

complex in the presence and absence of hydrogen peroxide, J. Chem. Soc., Perkin Trans. (1997) 2161-2165.

[41] Gilbert, B.C., Kamp, N.W.J., Lindsay Smith, J.R., Oakes, J., Electrospray mass spectrometry evidence for an oxo-manganese(V) species generated during the reaction of manganese triazacyclononane complexes with H_2O_2 and 4-methoxyphenol in aqueous solution, J. Chem. Soc., Perkin Trans. (1998) 1841-1843.

[42] Wieprecht, T., Xia J., Heinz, U., Dannacher, J., Schlingloff, G., Novel terpyridine-manganese(II) complexes and their potential to activate hydrogen peroxide, Journal of Molecular Catalysis A - Chemical, **203** (2003) 113-128.

[43] Bösing, M., Krebs, B., Nestler, B., Seebach, M., Reinhardt, G., Wohlers, M., Dingerdissen, U., Low-temperature bleaching with manganese-containing heteropolytungstates, Appl. Catal. A, **184** (1999) 273-278.

[44] Pulvirenti, A.L., Epoxidation and bleaching catalyses by homo- and heterogeneous manganese, cobalt, and iron azamacrocyclic complexes, PhD thesis, Purdue University, 2000.

2

Oxygen activation catalysed by a dinuclear manganese(IV)complex and bleaching of cotton pigment morin

The purpose of bleaching of cotton is to oxidise natural pigments and to confer pure white appearance to the fibres. The colour of native cotton fibre is mainly due to the presence of flavonoids. This chapter reports on an unprecedented catalytic activation of molecular oxygen with the dinuclear manganese(IV) 1,4,7-trimethyl-1,4,7-triazacyclononane complex via stepwise formation of hydrogen peroxide towards the oxidation of flavonoids at ambient temperatures in an alkaline aqueous solution. The involvement of superoxide O_2^- and/or H_2O_2 has been investigated employing a novel method based on the analysis of reaction kinetics in the presence of acceleratory and/or inhibitory enzymes.

2.1 Introduction

The design and development of soluble transition metal complexes, which are able to effectively catalyse substrate oxidation by hydrogen peroxide or molecular oxygen, has been attracting the scientific community for decades [1-6]. The enthusiasm about finding effective catalysts originates in the existence of numerous enzymes in nature, which are able to activate these oxidants [7]. Whilst a variety of transition metal complexes are known to activate H_2O_2 for substrate oxidation [3-4, 8-9], activation of O_2 to yield a selective oxidation reaction is more scarce. Most examples deal with systems that initiate radical based reactions [10] and some give dioxygenation type of reactions with specific substrates [11-12]. Only a few examples of ruthenium based complexes that catalyse the oxygen transfer to alkenes are known, such as ruthenium porphyrin catalysts [13] and ruthenium based polyoxomatallates [14].

Similarly, a number of dinuclear manganese complexes have been prepared as models for the enzymes, since dinuclear μ-oxo manganese centres appear as subunits in a number of biologically important metalloenzymes, e.g. in the oxygen evolving centre (OEC) of photosystem II [15-16] and in catalases [17]. Wieghardt *et al.* [18-24] have prepared a number of structural models using dinuclear manganese complexes of the ligand 1,4,7-trimethyl-1,4,7-triazacyclononane (TACN) including the μ-oxo, peroxo and acetate bridged complexes. These models have received increasing attention in recent years as potential oxidation catalysts. Mono- and, in particular, di-nuclear manganese complexes of TACN were identified as highly active bleach catalysts [4]. As explained in Chapter 1, the dinuclear tri-μ-oxo bridged manganese(IV) complex of the ligand 1,4,7-trimethyl-1,4,7-triazacyclononane (MnTACN, Figure 2.1a) was further developed and used in a commercial detergent for domestic use. At 40°C a small amount (0.05%) of this metal complex, i.e. a hundredth of the typical dosage of commonly used bleach activator tetraacetylethylenediamine (TAED) [25-26] that is used in stoichiometric amounts, can provide as much bleaching power as the formulations activated by TAED. Although the detergent was withdrawn from the market, this was the beginning of a surge of interest in this and related complexes as catalysts for organic oxidation using the environmentally acceptable oxidant H_2O_2.

Apart from stain bleaching [4, 27] the MnTACN has been proven to be a potential catalyst for a number of oxidative processes such as epoxidation of alkenes [28], oxidation of DNA [29], phenols [30], alcohols [31], sulphides [32], alkanes [33] azo-dyes [34] and, most recently, cis-dihydroxylation of alkenes [35]. MnTACN can be used in organic solvents and in aqueous solution at pH<11.

The scope of this thesis is to investigate the possibility of low-temperature bleaching of grey cotton employing MnTACN as the catalyst and to understand the fundamental aspects of catalytic bleaching, both at a molecular and at a macroscopic scale. This knowledge is essential when introducing an efficient, stable and reproducible catalytic bleaching process into industrial applications. To the best of our knowledge, molecular aspects of cotton fibre bleaching, such as the mechanism of the reaction between the pigments responsible for the colour of cotton fibre and active bleaching species, has scarcely been investigated. A reason for the lack of publications related to this topic lays probably in the fact that cotton catalytic bleaching takes place in a heterogeneous system, which presents difficulties to study chemical phenomena independently. Moreover, the detailed information on the nature of cotton fibre pigments is hardly found in open literature.

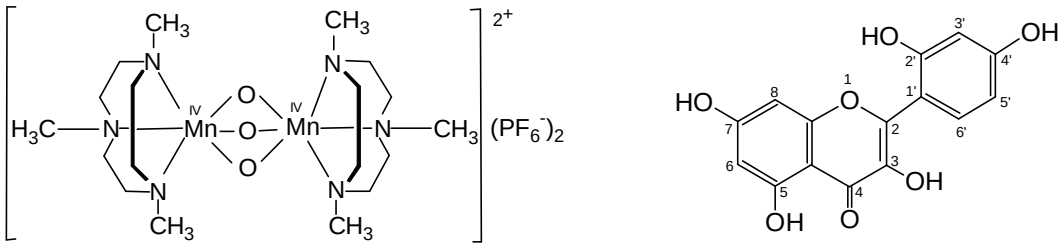

(a) (b)

Figure 2.1 Chemical structure of the MnTACN catalyst (a) and morin (b).

To study chemical mechanism involved, it is necessary to exclude the influence of transport phenomena that exist in such a heterogeneous reaction system. Since this thesis is partially devoted to molecular aspects of cotton bleaching, the nature of colouring matter (pigments present in cotton fibre) is introduced as an important aspect. From the literature [36] (see also Chapter 1) we know that mainly flavonoids are responsible for the colour of cotton fibres. Assuming that the mechanism of oxidation of coloured matter present in cotton fibre during bleaching is similar to that in a homogeneous system to the exclusion of transport phenomena, we have developed a homogeneous model system based on flavonoids as model compounds. The primary flavonoid examined is morin - 3,5,7,2',4'-pentahydroxyflavone [37] (Figure 2.1b) due to its presence in native cotton fibre. Bleaching in this context involves oxidising of flavonoids, i.e. morin.

In contrast to the MnTACN catalysis reported in studies published up until now, where hydrogen peroxide was employed together with MnTACN, the present chapter reports an unprecedented ability of MnTACN to utilise dioxygen as oxidant in the bleaching of cotton pigment at ambient temperatures in an alkaline aqueous solution. This finding is a novel reaction, not only in the field of textile chemistry but in chemistry in general. It is worthwhile to mention that

catalytic oxidations of flavonoids with molecular oxygen have received enormous attention in the research that has been ongoing in fields of medicine, biochemistry, pharmacy, nutrition, etc., due to their large array of biological activities such as antioxidant [38-39], anti-inflammatory [40], anticarcinogenic [41-42] behaviour, etc. For that reason, the references cited in this chapter originate mostly from scientific fields other than textiles.

2.2 The chemistry of dioxygen

Molecular oxygen is the most abundant and inexpensive oxygenating/oxidising agent, which can effect in the presence of an appropriate catalyst a variety of useful oxidation reactions in biological systems. These range from so-called di- or monooxygenase systems where two or one O-atoms of the O_2 are incorporated into the organic substrate (Eqs. 2.1 and 2.2, respectively) to oxidative-dehydrogenation systems, where H-atoms are removed from organics as H_2O_2 or H_2O (Eqs. 2.3 and 2.4, respectively). In terms of strict, modern nomenclature, "oxygenase activity" (or O-atom incorporation) is effected by enzymatic di- or monoxygenases, and it is represented by Eqs. 2.1 and 2.2, while "oxidase activity" (reduction of O_2 via electron transfer reactions) is effected by oxidases, and is represented by Eqs. 2.3 and 2.4.

Many studies with models (i.e. non-protein systems) aim to mimic the enzyme systems, particularly their high selectivity (formation of a single product) and operation under ambient conditions, whereas their activity is nominated as "oxygenase" or "oxidase" activity [43].

$$\text{substrate } S + O_2 \longrightarrow S(2\ O) \qquad (2.1)$$

$$S + O_2 + 2\ H^+ + 2\ e \longrightarrow S(O) + H_2O \qquad (2.2)$$

$$(SH)_2 + O_2 \longrightarrow S + H_2O_2 \qquad (2.3)$$

$$2\ (SH)_2 + O_2 \longrightarrow 2\ S + 2\ H_2O \qquad (2.4)$$

Whether as an oxygenation or oxidising agent, O_2 is clearly an attractive and highly desirable oxidant when environmental requirements are considered as any inorganic co-product is typically water (Eqs. 2.2 and 2.4). However, because of its biradical nature, non-coordinated O_2 reacts with organic substrates preferably according to a radical-chain mechanism, which generally operates with low selectivity. Much more selective oxidation processes can be realised by activation of the O_2 through a coordination to a metal centre; the coordination is generally followed by transfer of electrons from the metal to the oxygen moiety.

Despite its powerful oxidising character, reactions of oxygen with reducing

substrates are usually slow at ambient temperatures [44]. Oxygen is a stable biradical with two unpaired electrons generating the electronic triplet ground state of the O_2 molecule (Figure 2.2). Triplet dioxygen has a very sluggish kinetic reactivity but is capable of reacting with a strong thermodynamic driving force. The higher energy and greater reactivity of singlet than triplet O_2 is a major contributing factor in maintaining the present level of triplet dioxygen in the atmosphere. A concerted insertion of the ground state dioxygen into organic (diamagnetic) molecules (such as flavonoids) is a spin-forbidden process. Biological systems activate triplet dioxygen for controlled chemical synthesis via electron transfer and proton transfer reduction. When dioxygen oxidises organic molecules, it itself is reduced. It generally undergoes reactions in a stepwise manner via formation of free radical intermediates with one unpaired electron [45]. By adding electrons one at a time to the molecular orbitals of ground state dioxygen, the step-wise reduction products of oxygen takes place (Eqs. 2.5 - 2.7, Figure 2.2).

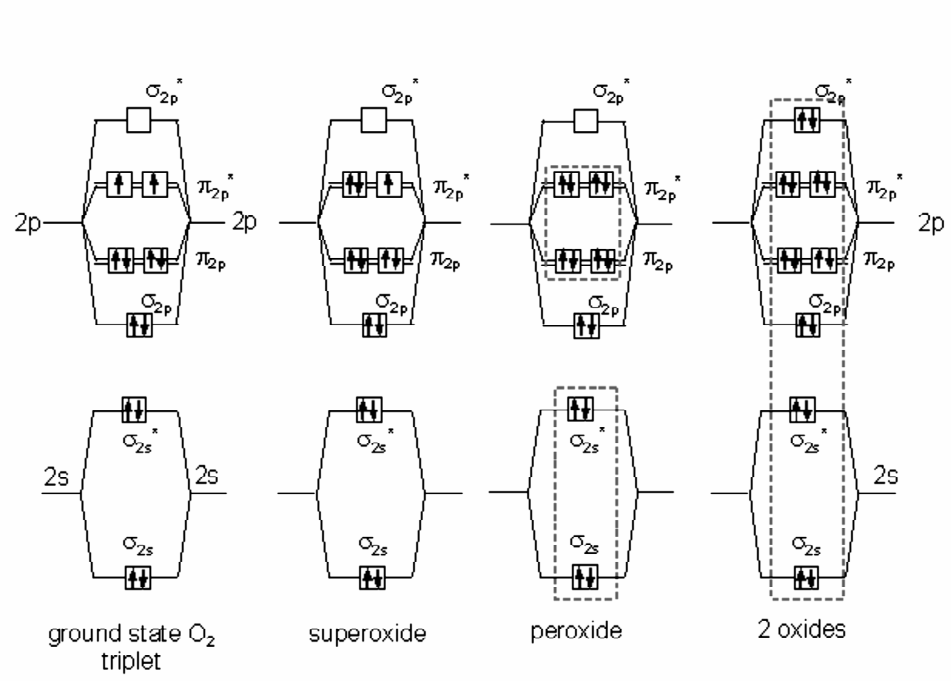

Figure 2.2 Dioxygen reduction products [46].

On the addition of one electron, superoxide is formed. Upon reduction of superoxide by the second electron, peroxide is formed. Two more electrons produce 2 separated oxides since no bonds connect the atoms (the number of electrons in antibonding and bonding orbitals are identical). Each of these species can react with protons to produce species such as HO_2, H_2O_2 (hydrogen peroxide) and H_2O. It are the first two reactive reduction products (O_2^- and H_2O_2) of dioxygen that make it potentially toxic in biological systems, but highly desirable in textile bleaching systems.

$$O_2 + e^- \longrightarrow O_2^- \quad (2.5)$$

$$O_2^- + H^+ \longrightarrow HO_2 \quad (2.6)$$

$$HO_2 + H^+ + e^- \longrightarrow H_2O_2 \quad (2.7)$$

After the production of the first diamagnetic species (Eq. 2.7 and Figure 2.2), the following steps do not depend on spin correlation in the radicals:

$$H_2O_2 + H^+ + e^- \longrightarrow H_2O + OH^- \quad (2.8)$$

$$OH^- + H^+ \longrightarrow H_2O \quad (2.9)$$

Although dioxygen is a strong oxidant at pH 7 (when it is a concerted four-electron transfer agent), it is a weak single-electron oxidant [45]. In terms of the reduction potential, the limiting step is the first electron transfer to O_2. Electron sources in the enzyme adequate for the reduction of dioxygen will produce all the other reduced forms via reduction (Eq. 2.5), hydrolysis and disproportionation steps (Eqs. 2.6 - 2.9).

Enzymes that utilise dioxygen must activate it in some way, which decreases the activation energy. These are typically metalloenzymes, and often heme-containing proteins. Since metals such as Fe(II) and Cu(II) are themselves free radicals (i.e. they have unpaired electrons), they react readily with ground state oxygen which itself is a radical. The molecular orbitals of the metal and oxygen combine to produce new orbitals which for oxygen are more singlet-like in nature. Likewise, dioxygen reacts more readily with organic molecules which can themselves form reasonably stable free radicals.

2.3 Interaction of manganese with dioxygen in biological systems

The subject of activation of dioxygen, as a molecule of intrinsic importance in a wide range of biological and industrial processes, and homogeneous catalytic oxidation by metal complexes has been in the focus of attention over the last 20 years [43]. The number of original and review papers devoted to various aspects of dioxygen activation increase rapidly. This trend is obviously to the importance of catalytic oxidation in biological processes, such as dioxygen transport, and the action of oxygenase and oxidase enzymes related to metabolism.

In nature, aerobic life forms actively transport O_2 from the atmosphere to the appropriate cellular systems where the oxidative power of the O-O linkage is acquired for metabolism. The first and apparently the simplest step in this process of respiration involves the reversible coordination of the O_2 molecule to the iron- or copper-containing active sites of the metalloproteins hemoglobin,

hemerythrin, and hemocyanin (Hc) [47]. This binding step involves electron transfer from the reduced metal site to the O_2 molecule with a concomitant decrease in O-O bond order, as exemplified by the 2-electron reduction of dioxygen to peroxide effected reversibly by the dicopper active site in Hc.

The structural and functional modeling of metalloenzymes, particularly of those containing iron, copper, cobalt, manganese, etc., have provided a wealth of indirect information helping to understand how the active centres of metalloenzymes may operate. The knowledge gained from the study of metalloenzyme models is also applicable in the design of transition metal complexes as catalysts for specific reactions. This approach has become known as biomimetic or bioinspired catalysis and continues to be a fruitful and expanding area of research.

Recognition of the involvement of manganese in biological redox chemistry started in 1970 with the discovery of Mn-superoxide dismutase [11]. The importance of manganese in dioxygen metabolism was further confirmed with the discovery that the oxygen-evolving complex in photosystem II, which provides the reducing equivalents for photosynthesis, requires manganese as part of the active site [12]. While Mn(II) had been established in structural roles and as a component of metal ATP (adenosine triphosphate) complexes, these findings of redox activity ushered in the modern era of bioinorganic manganese coordination chemistry. The discovery in the early 1980s that some bacterial catalases required Mn [48], and the subsequent discovery of other Mn-containing redox enzymes such as Mn-ribonucleotide reductase (RR) [49] have fuelled interest in this field and accelerated the progress of understanding during the past 10 years. It is now recognised that manganese interacts with dioxygen [50-52] as well as with its reduced derivatives in biological systems in numerous ways, making use of a variety of different Mn structures. The nuclearity of Mn sites that interact with O_2^{n-} (n = 0, 1, 2) in biology range from mononuclear (Mn-oxalate oxidase, Mn-superoxide dismutase) and dinuclear (Mn-catalase, Mn-RR) to tetranuclear (OEC), making use of the Mn(II), Mn(III), Mn(IV), and possibly, Mn(V) oxidation states.

The synthesis and characterisation of manganese coordination complexes to model the structure, reactivity, and spectroscopy of manganese in its various oxidation states, with various ligand types and nuclearities, has contributed substantially to the understanding of the role and mechanism of manganese interaction in biological dioxygen chemistry. Initially, much of the work in this field involved the oxygenation of Mn-porphyrin complexes, building on studies of manganese-substituted hemoglobin [53]. Once it was understood that the Mn sites in Mn-SOD and the OEC were “non-heme” sites, however, model studies expanded to use Schiff base and other N- and O-donor ligand sets. An extensive research effort has produced structural models for the higher oxidation state sites often by reaction of lower oxidation state precursors with dioxygen. The many

Mn-coordination complexes which resulted have allowed the effects of various geometric and electronic modifications to the metal coordination sphere to be probed in order to elucidate the rich spectroscopy of the biological Mn sites. Additionally, increased mechanistic understanding of the interaction of dioxygen and its reduced derivatives with the various oxidation states of Mn, primarily through functional models of the Mn-catalase and Mn-SOD, has proven to be essential to understanding the enzymatic systems at a more chemical level.

2.4 Catalytic oxygenation of flavonoids

Flavonoids, particularly flavones and isoflavones, are common natural products which are widely distributed among different plants providing the colour (from pale yellow to orange) in flowers, trees and fruits. Similarly, these compounds are mainly responsible for the colour of cotton fibre (Section 2.1). Flavonoids are very important natural dietary compounds exhibiting a large array of biological activities such as with antioxidant [38-39] and anticarcinogenic [42]. This is owing to their ability to bind metal ions and/or undergo oxidation by O_2 [54].

The ability of simple transition metal salts (e.g. Mn(II) and Cu(II) to catalyse oxidation of morin by O_2 under alkaline conditions was stated by López-Benet *et al.* [55-56]. The reaction was used to develop kinetic procedures for the determination of manganese with no attention given to the mechanistic aspects. Although a free metal ion is effective as a bleach activator, it cannot be used, because under the alkaline reaction conditions the metal is unstable, and tends to stain fabric with metal oxide deposits [4]. The oxidation state of the metal seems to be stabilised by complexation to nitrogen containing ligands. More recently, Wieprecht *et al*. have demonstrated that Mn(II)-terpyridine based catalysts have been shown to be effective in the oxidation of morin under alkaline aqueous conditions at 40^{o}C [57]. The exact role of manganese in the bleach activation, that is, which step of the activation is facilitated by the presence of Mn, is still unclear.

Nevertheless, more detailed studies have been published on the oxygenation of flavonoids by O_2 catalysed by quercetinase and model complexes. Quercitinase is a copper-containing enzyme produced by *Aspergillus flavus* and belongs to the dioxygenases. This reaction has been the subject of both theoretical [58] and mechanistic [59] investigations since 1960 [60-62]. The mechanism of this reaction has been delineated as an oxidative cleavage of the heterocyclic ring of 3-hydroxyflavones to give the corresponding depsides with oxygen atoms incorporated in atom-economic fashion and the elimination of carbon monoxide (Figure 2.3). Photosensitised [63], base-catalysed [64] and Co(salen)-catalysed [65-66] [salenethylenebis(salicylideneaminato)] oxygenation of 3-hydroxy-flavones causes a similar type of degradation.

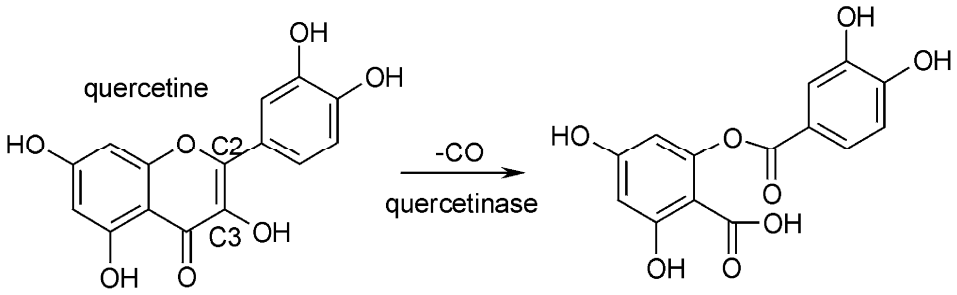

Figure 2.3 Proposed mode of action of quercetinase [59].

The oxygenolysis reaction catalysed by quercetinase is a spin-forbidden process, since the triplet ground state of O_2 should react with the singlet ground state of quercetin to produce the singlet ground state of the phenolic carboxylic ester. The most widely accepted hypothesis is that the reaction occurs via a tautomerisation process, deprotonated Cu(II)-bound quercetin becomes the Cu(I) flavonoxy-associated complex, which gives molecular oxygen the possibility to react with the substrate [67]. Several mechanisms have been proposed for both this addition and the following steps of the oxygenolysis reaction [68-69]. One is based on the hypothesis that the copper atom attracts one electron and, by polarising the remaining oxidised substrate, allows it to react with molecular oxygen. The alternative possibility arises from the hypothesis that O_2 could be added and then activated on the metal centre before being metabolised by the flavonoid. In both cases, quercetin is coordinated to the copper atom. A theoretical study [67] indicates that the copper cation acts as an oxidant towards the substrate and that the reaction proceeds through a 1,3-cycloaddition.

2.5 Experimental section

2.5.1 Experimental strategy

The activation of molecular oxygen by MnTACN in the oxidation of morin and the involvement of superoxide O_2^- and/or H_2O_2 was investigated employing a novel method developed for the purpose of this study. The design of this method was inspired by the principle of important physiological pathways in human body, which include the generation and consumption of reactive oxygen species by means of different enzymes. Superoxide dismutase and catalase were used as inhibitory enzymes (superoxide dismutase catalyses dismutation of O_2^- anion into O_2 and H_2O_2; catalase catalyses decomposition of H_2O_2 into O_2 and H_2O); xanthine oxidase and alcohol oxidase were used as acceleratory enzymes (xanthine oxidase catalyses reduction of O_2 to O_2^-; alcohol oxidase catalyses reduction of O_2 to H_2O_2). A more detailed discussion on these enzymes and explanations of mode of their action are given in Section 2.5.4. The reaction kinetics was monitored in the presence and absence of acceleratory and/or inhibitory enzymes. Both qualitative data (UV-Vis reaction profiles) and

quantitative data (rate constants and maximum reaction rates) served to demonstrate the different performance of the reaction system in the tests with enzymes. This approach was used to prove the nature of active species derived from dioxygen as well as the bi-phasic nature of the reaction when carried out below pH 10.2.

2.5.2 Chemicals

The catalyst MnTACN (Figure 2.1a) [20] was provided by Unilever R&D (Vlaardingen, The Netherlands). Manganese chloride and manganese sulphate were obtained from Fluka. Morin, xanthine and methanol were purchased from Sigma. Hydrogen peroxide (30%), potassium superoxide, sodium hydroxide (extra pure), sodium hydrogencarbonate were obtained from Merck.

The enzymes used in this study were as follows: superoxide dismutase (SOD) from bovine erythrocytes (Fluka - C.A.S. No. 9054-89-1), catalase from bovine liver (Sigma - C.A.S. No. 9001-05-2), xanthine oxidase (XOD) fom bovine milk (Sigma - C.A.S. No. 9002-17-9) and alcohol oxidase (AOX) from *Candida boidinii* (Sigma-Aldrich - C.A.S. No. 9073-63-6).

All reactants were used as obtained without further purification. Demineralised water was used throughout the study.

2.5.3 Catalysis experiments

The absorption spectra of alkaline aqueous solution of morin under aerobic conditions and their change upon the addition of MnTACN (and H_2O_2 or KO_2 when required) were measured in a thermostated Hewlett Packard 8453 spectrophotometer and the data were analysed with a PC using UV-Vis ChemStation software Rev.A.08.01 (Agilent Technologies, CA USA). Fluorimeter 17F type quartz cuvettes with quartz B24 joint neck (Chandos Intercontinental, UK) - lightpath 2 and 10 mm, were used in the experiments.

The required amount of a freshly prepared buffered stock solution of MnTACN (and H_2O_2 or KO_2 when required) was added as quickly as possible in a cuvette containing an appropriate amount of buffered stock solution of morin. The absorbance change at 410 nm (maximum absorbance of morin in visible part of spectrum) in time was determined. The experiments were carried out under the following conditions: [morin], 160 μM; [MnTACN], 2.5 μM; [H_2O_2] or [KO_2], 160 μM, 10 mM $NaHCO_3$ buffer. In the experiments that required the absence of O_2 in the reaction mixture, anaerobic conditions were obtained by purging the buffered stock solution of morin in the cuvette with N_2 for 20 minutes prior to the injection of a N_2 purged MnTACN stock solution.

In the experiments where MnTACN was replaced with Mn(II) salts ($MnCl_2$ or

$MnSO_4$), the conditions were kept identical (pH, temperature and concentrations of other reactants) as for MnTACN catalysis, whereas the Mn(II) salts were used at equivalents of [Mn], i.e. [$MnCl_2$] or [$MnSO_4$], 5 μM.

2.5.4 Effect of enzymes

In the experiments done with the enzymes (catalase, SOD, AOX and XOD), 1 U (unit) of an enzyme was used per 1 μmole of morin. 1 U corresponds to the amount of enzyme (other than SOD) which converts 1 μmole of substrate per minute at pH 7.0 and 25°C. This was further decreased with a factor 10, 10^2 or 10^3, until no more effect of enzyme addition is observed when compared to the reaction performed in the absence of enzyme. On the basis of these experiments the activity of the enzymes was proven and the most appropriate concentrations for the following acceleratory and/or inhibitory experiments were chosen. The reactions with enzymes were performed at pH 10.0 and 25°C where the lag-phase of the reaction (in the absence of enzyme) was still present, whilst the maximum reaction rate was sufficiently fast (see Figure 2.4 in Section 2.5.5). The preincubation time was 2.5 min (reaction with enzymes prior to addition of the catalyst MnTACN). Methanol and xanthine were used as substrates for the enzymes AOX and XOD, respectively, at the concentration equivalent to concentration of morin, i.e. 160 μM.

Experiments designated as *inhibitory* were done using SOD and/or catalase enzymes, whereas, experiments designated as *acceleratory* were done by means of XOD or AOD enzymes. UV-Vis spectrophotometry was used to follow reaction kinetics as explained in Section 2.5.3.

SOD [70] is known as an enzyme which can catalyse the dismutation of univalently reduced oxygen - superoxide (Eq. 2.10)

$$2\ O_2^- + 2\ H^+ \xrightarrow{\text{SOD}} O_2 + H_2O_2 \qquad (2.10)$$

It has been demonstrated to be useful in detecting the role of O_2^- in certain enzyme reactions [71]. Some enzymes such as milk xanthine oxidase are capable of univalent reduction of dioxygen with the release of superoxide anion, O_2^-. In this case, for example, the addition of SOD can be used as scavenger to remove superoxide anion and to competitively inhibit the reaction.

Catalases are enzymes which catalyse the decomposition of hydrogen peroxide into water and dioxygen (Eq. 2.11).

$$2\ H_2O_2 \xrightarrow{\text{catalase}} H_2O + O_2 \qquad (2.11)$$

The reaction is very fast and maintaining the optimal conditions of pH and temperature ensures the hydrogen peroxide decomposition.

Catalase is produced naturally within the human body and acts, like SOD, as an antioxidant enzyme. It helps the body to convert hydrogen peroxide into water and oxygen, thus preventing the formation of carbon dioxide bubbles in the blood. Catalase also uses hydrogen peroxide to break down potentially harmful toxins in the body, including alcohol, phenol, and formaldehyde. This enzyme works closely (in synergism) with SOD to prevent free radical damage to the body in a way that SOD converts the dangerous superoxide radical to hydrogen peroxide, which catalase converts to harmless water and dioxygen [72]. Catalases are amongst the most efficient enzymes found in cells; each catalase molecule can convert millions of hydrogen peroxide molecules every second.

Xanthine oxidase (XOD) is a member of the xanthine oxidoreductase group, found in mammals at highest concentration within the liver and intestine [73]. XOD is the prototypical member of the molybdenum hydroxylase family of enzymes. It can catalyse the hydroxylation of various aromatic heterocycles by formal insertion of an oxygen atom into a C-H bond, e.g. the hydyroxylation of purines in the 2, 6, and 8 ring positions (e.g. purine to hypoxanthine to xanthine to uric acid), as well as the oxidation of a wide range of aldehydes and other substrates, although its physiological role is thought to be in purine oxidation [74]. Mammalian XOD is a homodimer containing one molybdenum, one flavin, and two different $[Fe_2S_2]$ centres per subunit [74].

In contrast to SOD and catalase systems, XOD generates rather than consumes reducing equivalents during catalysis and utilises water as opposed to O_2 as the source of oxygen for substrate hydroxylation [74]. Substrate oxidation occurs at the molybdenum site, which becomes reduced from Mo(VI) to Mo(IV) in the process. The catalytic cycle is completed by electron transfer from molybdenum to the $[Fe_2S_2]$ clusters and then the flavin, where the electrons are donated to an acceptor such as O_2 [75-76].

The univalent reduction of molecular oxygen to superoxide anion by XOD is an important physiological pathway in human body [77], where this enzyme is involved in the metabolism of xanthine to uric acid (Eq. 2.12). Hence, XOD is a source of oxygen free radicals since it reacts with molecular oxygen, thereby releasing superoxide free radicals.

$$\text{Xanthine} + O_2 + H_2O \xrightarrow{\text{XOD}} \text{Uric acid} + H^+ + O_2^- \qquad (2.12)$$

However, an excess of superoxide anions are capable of damaging biomacromolecules by both directly and indirectly forming hydrogen peroxide or highly reactive hydroxyl radicals [78]. As explained above, the organism

possesses defence mechanisms to reduce the oxidative damage utilising enzymes such as SOD and catalase.

XOD can be used to generate superoxide radicals for use in the enzymatic assay of activity of SOD [71]. O_2^- generated by the xanthine/XOD reaction (Eq. 2.12) is spontaneously converted to dioxygen and hydrogen peroxide (Eq. 2.13). This spontaneous dismutation reaction occurs rapidly in acidic conditions.

$$2\ O_2^- + 2\ H^+ \longrightarrow O_2 + H_2O_2 \qquad (2.13)$$

The introduction of alcohol oxidase (AOX) is associated to its capability of reduction of dioxygen to hydrogen peroxide (Eq. 2.14).

$$\text{Alcohol} + O_2 \xrightarrow{\text{AOX}} \text{Aldehyde} + H_2O_2 \qquad (2.14)$$

AOX, which was first found in a basidiomycete by Janssen *et al*. [79-80], is specific for short-chain, linear aliphatic alcohols and catalyses their oxidation by O_2 where the reaction products are an aldehyde and H_2O_2 (Eq. 2.14). AOX has found its application in the field of enzyme-mediated colorimetric analysis of methanol [81] and ethanol [82]. One of its most interesting applications is the determination of low concentrations of ethanol in aqueous media, particularly in human body fluids [82].

2.5.5 Kinetics assessment

Time traces, i.e. absorbance vs. time plots recorded at 410 nm were used for the determination of the length of lag-phase (initial reaction induction period), the maximum reaction rate and the rate constant of catalytic oxidation of morin (Figure 2.4).

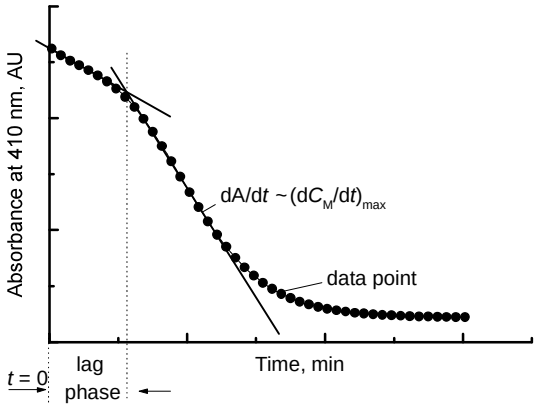

Figure 2.4 The determination of lag-phase and maximum reaction rate from UV-Vis time traces.

The lag-phase length (min) was determined by extrapolation as the time that corresponds to the point of slope change from a slow reaction phase (lag-phase) to a fast reaction phase (Figure 2.4). The maximum reaction rate was calculated as the slope of concentration vs. time profiles (dC_M/dt, mol L^{-1} s^{-1}) of the fast reaction phase, where C_M is the concentration of morin. C_M at the different reaction times was calculated on the basis of the linear calibration diagram obtained by measuring the absorbance at 410 nm for the different morin concentrations. The plots of ln C_M against time showed good linearity (R=0.9997), indicating first order kinetics with respect to morin, this being the base for the calculation of the rate constant k (s^{-1}).

2.6 Results and discussion

2.6.1 Dioxygen activation by MnTACN

As explained in Section 2.1 and references therein, MnTACN and related complexes have proven to be very active, and often selective, in the catalysed oxidation of organic substrates with H_2O_2 in non-aqueous systems and provide stain bleaching activity in detergent formulations under alkaline conditions. In contrast to these studies, where H_2O_2 was employed together with MnTACN, this chapter reveals the ability of MnTACN to use O_2 as terminal oxidant in bleaching of cotton pigment morin.

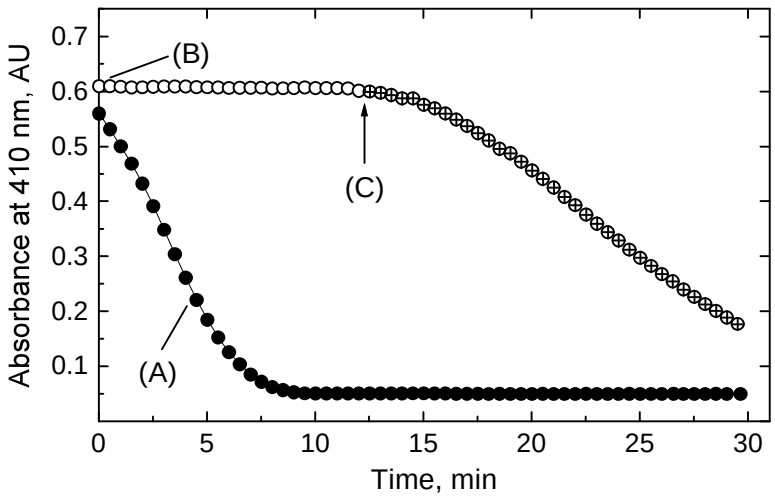

Figure 2.5 O_2 concentration dependence of MnTACN catalysed oxidation of morin by O_2: (A) air equilibrated; (B) N_2 purged; (C) O_2 bubbled through a N_2 purged solution. [MnTACN], 2.5 μM; [morin], 160 μM; 10 mM $NaHCO_3$ buffer, pH 10.2 at 25°C.

The rapid oxidation of morin by O_2 catalysed by MnTACN at room temperature and pH 10.2 is demonstrated in Figure 2.5 (curve A), $k = 6.27 \times 10^{-3}$ s^{-1}. Curve B represents the reaction performed under the same conditions in the absence of

O_2 (in a N_2 purged solution), after which O_2 is bubled through (curve C). Figure 2.5 shows that no acitivity is observed, over 10 minutes, upon addition of MnTACN to morin in N_2 purged solution (curve B). Subsequent gassing with O_2 of the N_2 purged solution results in a very rapid oxidation of morin (curve C). As it can be seen from curve A, over the same period under air equilibrated conditions complete oxidation of morin is observed.

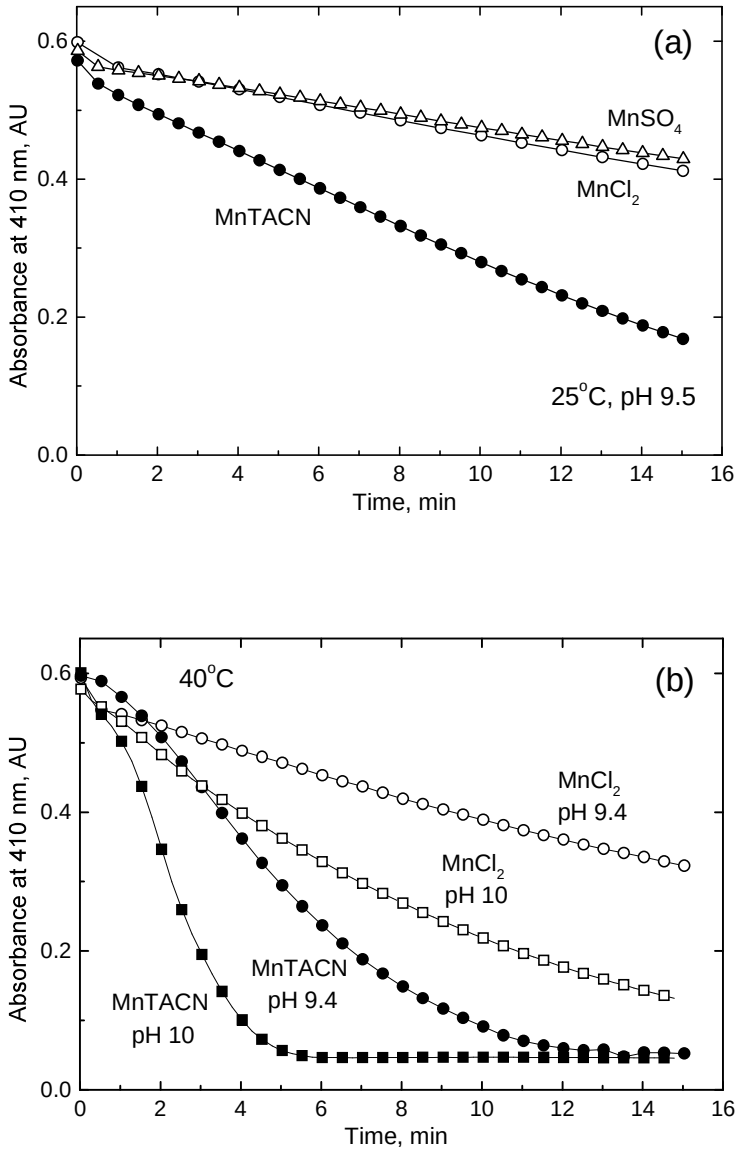

Figure 2.6 Absorbance vs. time plots for the oxidation of morin with O_2 catalysed by MnTACN or Mn(II) salts at the different temperatures and pHs; [MnTACN], 2.5 μM; [$MnCl_2$] and [$MnSO_4$], 5μM; [morin], 160 μM; 10 mM $NaHCO_3$ buffer.

If MnTACN is replaced with Mn(II) salts ($MnCl_2$ or $MnSO_4$) and experiments are done under identical conditions (pH and temperature), Mn(II) has been expected to be a catalyst in the oxidation of morin [55-56] (Section 2.4). The reaction

profiles obtained for the different temperatures and pHs are presented in Figure 2.6. The reactions performed in the presence of MnTACN are considerably faster compared to corresponding reactions catalysed by Mn(II) salts. For example, at 40^{o}C the rate constant k is 1.07×10^{-2} s^{-1} (at pH 10) or 3.95×10^{-3} s^{-1} (at pH 9.5) for the MnTACN catalysed reaction. The corresponding values for $MnCl_2$ catalysed reaction are 1.64×10^{-3} s^{-1} and 6.34×10^{-4} s^{-1}, respectively. Hence, the first order rate constant increases with a factor ~6.5 by replacing Mn(II) salts with MnTACN. The relatively high activity of MnTACN compared with Mn(II) salts (at equivalent [Mn]), precludes the possibility that the catalytic action observed is as a result of ligand dissociation.

2.6.2 pH dependence

An investigation of the pH dependence of the oxidation of morin by O_2/MnTACN shows that the rate of the reaction rises with increasing pH, especially in the pH range 9.6-10.0 (Figure 2.7). A strong pH dependence of the reaction kinetics in this range suggests that the basic forms of reactants are most active.

The first order rate constant reaches a maximum value $k = 6.32 \times 10^{-3}$ s^{-1} at pH 10.4. A decrease in the rate constant at pH > 10.4 can be attributed to the deactivation of the catalyst (dissociation to MnO_2) [4, 34]. The experiments carried out in the absence of MnTACN serve as blank. For example, the fist order rate constant of the blank at pH 10.4 is $k = 0.11 \times 10^{-3}$ s^{-1}.

The slower reaction kinetics below pH 10.2 are associated with the presence of an initial lag-phase (Figures 2.7b and 2.8). Both parameters (the rate constant and the length of lag-phase) show a comparable pH dependence. A retardation of the fast phase of the catalytic oxidation reaction at lower pH values (Figure 2.7a) corresponds to an increase in the length of lag phase (Figure 2.7b). Thus, the lag-phase, which is 9 minutes long at pH 9.6, shortens significantly over relatively narrow pH range (pH 9.6-10.2). No discernible lag-phase is present at pH $\geq$ 10.2.

To reveal the origin of the lag-phase is an important issue. It is unlikely that it can be attributed to the deprotonation of morin as the 3-OH and 5-OH hydroxyl groups of morin (see Figure 2.1b) are deprotonated at lower pH (pKa 3.5 and 8.1, respectively) [39]. Furthermore, the fact that the $MnCl_2$ (or $MnSO_4$) catalysed oxidation shows a similar pH dependence to that observed for MnTACN (see Figure 2.6) indicates that the pH dependence is not due to the rapid decomplexation of MnTACN above pH 10. Hence, it can be hypothesised that the increase in reaction rate and the decrease in the lag-phase observed between pH 9.6 and pH 10.2 can essentially be the consequence of a slow reaction step that involves O_2 and/or ionisation of active species derived from O_2.

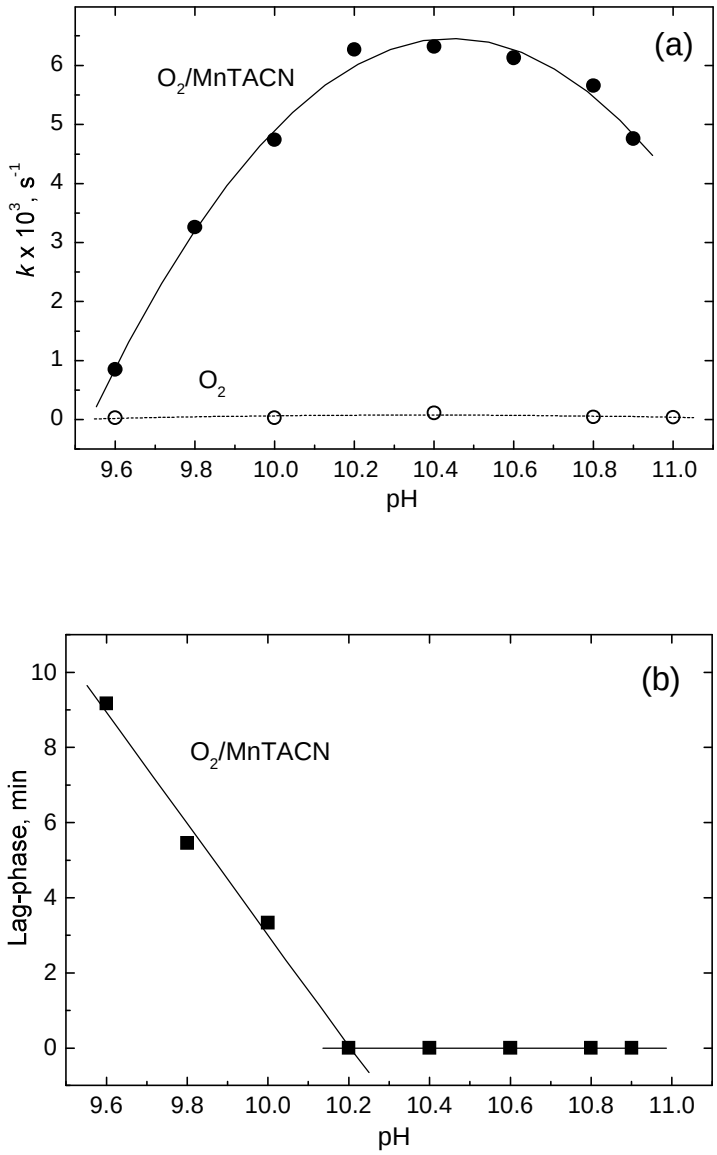

Figure 2.7 pH dependence of the rate constant *k* (a) and the lag-phase (b) of oxidation of morin with MnTACN/O_2 in 10 mM $NaHCO_3$ buffer; [MnTACN], 2.5 μM; [morin], 160 μM; 25°C.

The addition of stoichiometric quantities of either KO_2 or H_2O_2 at pH 10 where the corresponding reaction with O_2 begins with the lag-phase (curve A in Figure 2.8, $k_A = 4.49 \times 10^{-3}$ s^{-1}), results in rapid oxidation of morin ($k_B = 8.62 \times 10^{-3}$ s^{-1}; $k_C = 10.68 \times 10^{-3}$ s^{-1}) with no lag-phase present at the beginning of the reaction (curves B and C, respectively). This additionally supports the hypothesis that the presence of lag-phase is attributable to the activation of O_2. It remains unclear in what manner MnTACN and morin are involved in the formation of reactive oxygen species that are responsible for the oxidation of morin in the fast phase.

The latter question, together with other relevant mechanistic details, will be discussed in Chapter 3.

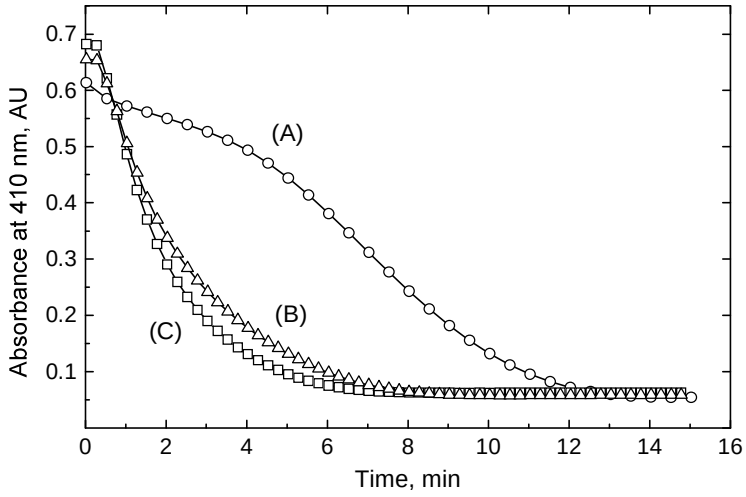

Figure 2.8. MnTACN catalysed oxidation of morin by O_2 (curve A), KO_2 (curve B) and H_2O_2 (curve C). [MnTACN], 2.5 μM; [morin], 160 μM; [KO_2] or [H_2O_2], 160 μM; 10 mM $NaHCO_3$ buffer, pH 10 at 25^{o}C.

2.6.3 Effect of enzymes: Inhibitory and/or acceleratory experiments

The present chapter is being dedicated to the detailed study of the involvement of O_2^- and/or H_2O_2 in the oxidation of morin. This has been investigated through the use of the enzymes superoxide dismutase (SOD) catalase, xanthine oxidase (XOD) and alcohol oxidase (AOX) as described in following sections.

2.6.3.1 Effect of SOD and catalase: Inhibitory experiments

The observation of a bi-phasic (lag-phase and fast phase) oxidation process below pH 10.2, each phase showing a similar pH dependence indicates that during the oxidation of cotton pigment morin by the O_2/MnTACN system various pathways are operative: a relatively slow pathway involving O_2 and a faster pathway involving superoxide and/or H_2O_2, both being activated by MnTACN.

Being inspired by the “self-defence” mechanism that operates in the human body on the basis of synergism of SOD and catalase (see Section 2.5.4), we have designed the inhibitory experiments to utilise these enzymes in the dioxygen activation by MnTACN - so to remove free dioxygen reduction products from the reaction system (superoxide and/or hydrogen peroxide).

SOD from bovine erythrocytes, scavenger of superoxide anion (Section 2.5.4), is used to test for the formation and release of the superoxide anion. The reaction profiles at the different concentrations of SOD are compared to the reference reaction performed in the absence of SOD in Figure 2.9. The results show that the maximum reaction rate is sensitive to the presence of SOD when 10^{-1} or 1 U of SOD is used relative to 1 μmole morin, i.e. relatively slow reaction kinetics is observed compared to the reaction performed in the absence of this enzyme. Further lowering of concentration of SOD with a factor 10 leads to a faster kinetics of the fast reaction phase, which is close or equal to the kinetics obtained in the absence of enzyme.

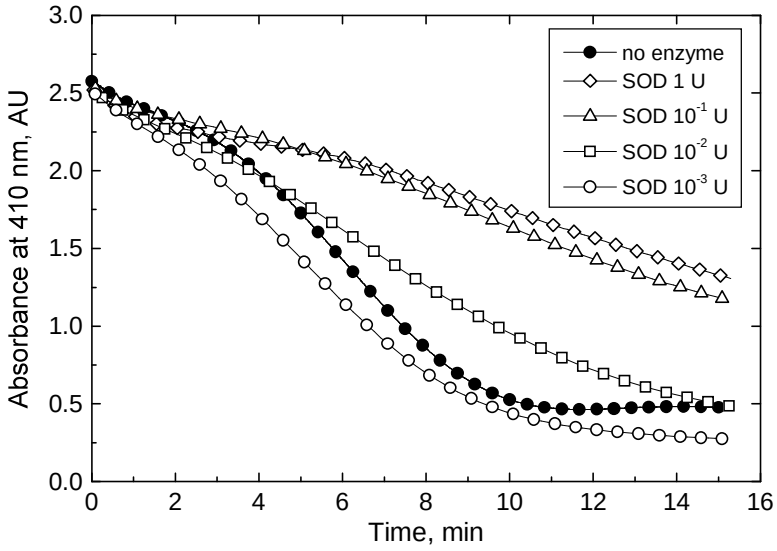

Figure 2.9 Effect of SOD: Kinetics of oxidation of morin by MnTACN using O_2 in the absence and presence of SOD. [MnTACN], 2.5 μM; [morin], 160 μM; [SOD], 10^{-3}, 10^{-2}, 10^{-1} or 1 U of SOD / 1 μmole morin; 10 mM $NaHCO_3$ buffer, pH 10 at 25°C.

Catalase from bovine liver is used to prove the formation of hydrogen peroxide. The reaction dependence on the catalase concentration is presented in Figure 2.10. Catalase shows a similar effect as SOD, i.e. the retardation of reaction fast phase when 1 or 10^{-1} U of this enzyme is used per 1 μmole of morin. The concentrations of 10^{-2} and 10^{-3} U of catalase per 1 μmole of morin are rather low to produce any effect on the reaction kinetics.

However, the results obtained by testing the reaction with SOD and catalase do not unambiguously clarify the involvement of either H_2O_2 or O_2^- to be the species derived from O_2 in the oxidation of morin catalysed by the MnTACN catalyst. The presence of either of these two enzymes causes a significant retardation of the reaction (Table 2.1). Furthermore, we have been concerned that the retardation of the reaction in the presence of SOD can be due to the catalase activity of SOD under the reaction conditions applied. Therefore, it is not possible to differentiate whether H_2O_2 and/or O_2^- are formed from O_2. To

answer these questions, a more systematic and detailed study was required and for that we elaborated the acceleration/inhibitory experiments using enzymes alcohol oxidase (AOX) or xanthine oxidase (XOD) in addition to the catalase and/or SOD. Before the combined enzymatic effect is discussed, the effect of acceleratory enzymes AOX or XOD alone will be described.

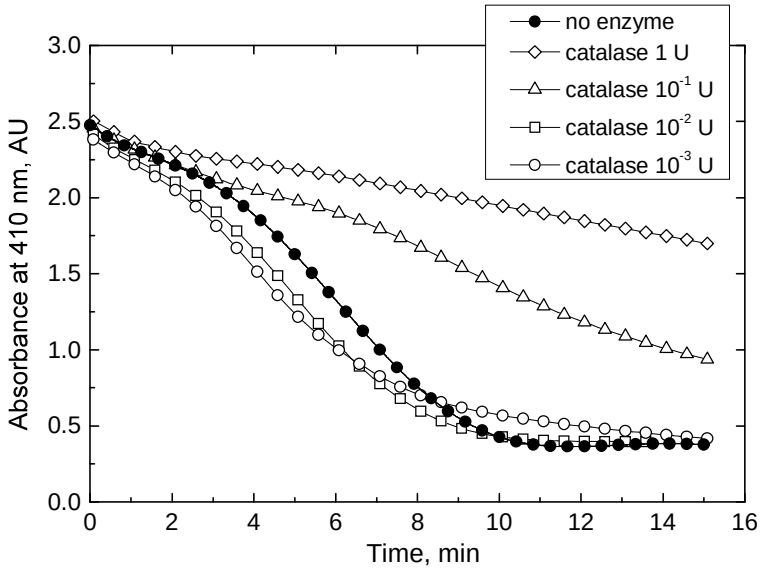

Figure 2.10 Effect of catalase: Kinetics of oxidation of morin by MnTACN using O_2 in the absence and presence of catalase. [MnTACN], 2.5 μM; [morin], 160 μM; [catalase], 10^{-3}, 10^{-2}, 10^{-1} or 1 U of catalase / 1 μmole morin; 10 mM $NaHCO_3$ buffer, pH 10 at 25°C.

2.6.3.2 Effect of XOD and AOX: Acceleratory experiments

The purpose of using of XOD in this study is based on the ability of XOD to generate superoxide radicals from dioxygen (see Section 2.5.4) that is present in an aqueous solution of morin prior to addition of catalyst MnTACN. This is to assure that the dioxygen dissolved in an aqueous solution under airequilibrated conditions is converted into superoxide (Eq. 2.12) and, partially, into hydrogen peroxide (Eq. 2.13).

The reaction performed in the presence of 1 U of XOD from bovine milk relative to 1 μmole of morin using xanthine as substrate is remarkably faster compared to the reaction performed in the absence of this enzyme (Figure 2.11). More importantly, there is no lag-phase present in case of the XOD accelerated oxidation of morin. Similarly to the SOD and catalase systems (Section 2.6.3.1), there is a clear dependence of the reaction kinetics on the enzyme concentration. When the enzyme concentration is decreased with factor 10, the reaction is visibly slower where a distinct, albeit short, lag-phase is observed. A further tenfold decrease of the concentration of XOD brings the reaction kinetics back to approximately the same kinetics observed when no XOD is present in the reaction mixture.

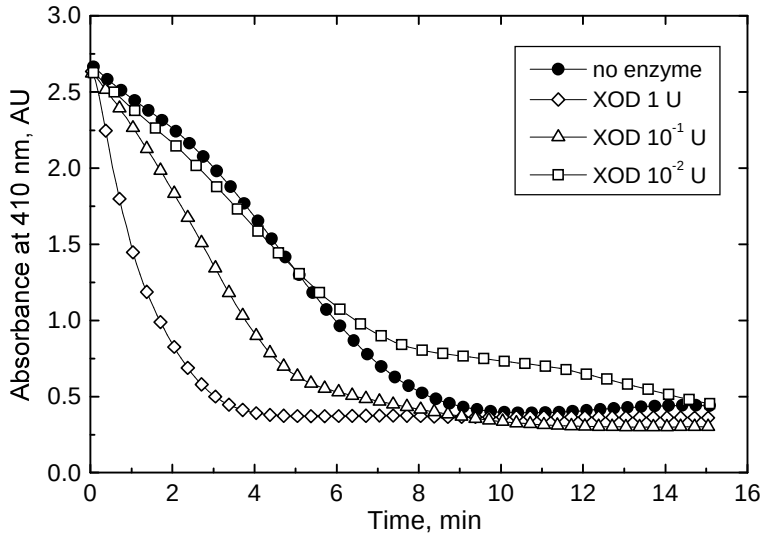

Figure 2.11 Effect of XOD: Kinetics of oxidation of morin by MnTACN using O_2 in the absence and presence of XOD. [MnTACN], 2.5 μM; [morin], 160 μM; [XOD], 10^{-2}, 10^{-1} or 1 U of XOD / 1 μmole morin; [xanthine], 160 μM; 10 mM $NaHCO_3$ buffer, pH 10 at 25°C.

The elimination of lag-phase and faster reaction kinetics by "pre-activation" of dioxygen by XOD is in accordance with the results obtained on the addition of stoichiometric quantities of KO_2 instead of O_2 (Section 2.6.3), thus confirming a straightforward activity of XOD.

Similarly to XOD, we have used AOX, as an acceleratory enzyme, to generate an equivalent amount of H_2O_2 from aqueous dioxygen prior to the addition of MnTACN by using methanol as a substrate.

The dose response curves obtained for AOX from *Candida boidinii* are presented in Figure 2.12. The presence of AOX results in a rapid reaction and complete removal of the lag-phase due to the formation of H_2O_2 when used at concentration of 1 or 10^{-1} U relative to 1 μmole of morin. This is to be expected taking into consideration the results obtained by adding the equivalent amounts of H_2O_2 (Section 2.6.3) to MnTACN catalyst. The reaction in these cases proceeds via a fast mechanism without the presence of an initial lag-phase. When AOX is present at lower concentrations, e.g. 10^{-2} or 10^{-3} U relative to 1 μmole of morin, a low or no effect of AOX on reaction kinetics can be observed. So we can conclude that the performance of AOX is as anticipated i.e. the enzyme is capable of converting dissolved O_2 into hydrogen peroxide effectively within pre-treatment time at concentration of 1 or 10^{-1} U relative to 1 μmole of morin.

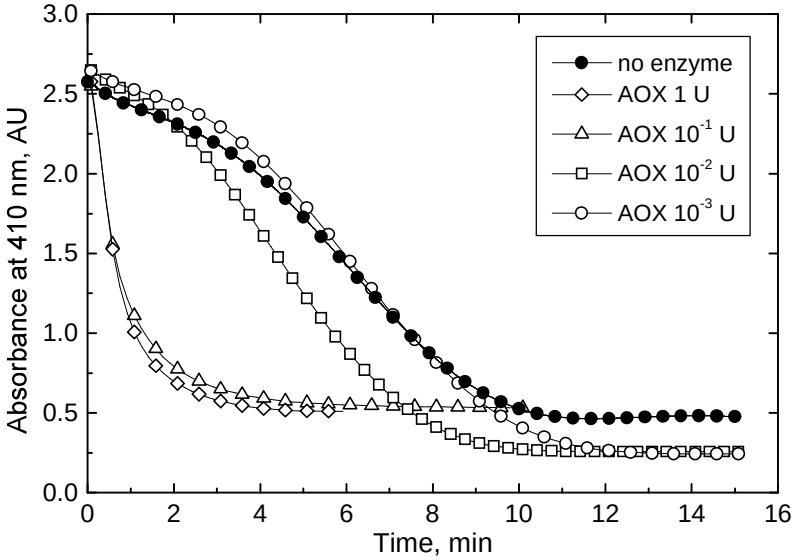

Figure 2.12 Effect of AOX: Kinetics of oxidation of morin by MnTACN using O_2 in the absence and presence of AOX. [MnTACN], 2.5 μM; [morin], 160 μM; [AOX], 10^{-3}, 10^{-2}, 10^{-1} or 1 U of AOX / 1 μmole morin; [methanol], 160 μM; 10 mM $NaHCO_3$ buffer, pH 10 at 25°C.

2.6.3.3 Combined enzymatic effect: The evidence for stepwise formation of H_2O_2

The purpose of using combined enzymatic systems, AOX or XOD in the presence of catalase and/or SOD is to answer open questions left in Section 2.6.3.1 by providing additional evidences of the H_2O_2 and O_2^- involvement in the MnTACN catalysed oxidation of morin using dioxygen as terminal oxidant.

Table 2.1 summarises the kinetic data for the oxidation of morin with O_2/MnTACN in the presence of inhibitory and/or acceleratory enzymes. In all cases, plots of ln C_M against time were linear with a gradient k confirming that the reaction is fist order with respect to morin. In addition, values calculated for the maximum reaction rate are given in the same table.

The data in Table 2.1 give a quantitative illustration of the different performance of the system morin/O_2/MnTACN in the presence of different reactive oxygen species whose derivation from molecular oxygen is tuned through the employment of inhibitory and/or acceleratory enzymes.

It is important to underline, as shown in Section 2.6.3.2, that both XOD and AOX are active under the reaction conditions applied. The kinetic data in Table 2.1 (Entry 5 and 6) are in accordance with the qualitative examination (Figures 2.11 and 2.12). Both the maximum reaction rate and rate constants of the oxidation of morin are considerably higher in the presence of either XOD or

AOX than in case when no enzyme is present in the system (Entry 1). Based on this, the effect of AOX and XOD has further been used to prove the activity of catalase and SOD, and thus their inhibitory effect on the reaction of oxidation of morin with O_2/MnTACN. For these experiments, the concentration of 1 U of enzyme relative to 1 μmole of morin is chosen as the optimal concentration for all enzymes.

Table 2.1. Kinetic data for the oxidation of cotton pigment morin in the presence and absence of enzymes SOD, catalase, XOD and AOX. [(i)]

Entry	Enzyme	$(-dC_M/dt)_{max} \cdot 10^7$ mol L^{-1} s^{-1}	$k \cdot 10^3$ s^{-1}	R [(ii)]
1	no enzyme	2.95	4.49	0.9997
	Inhibitory experiments			
2	SOD	0.90	0.88	0.9999
3	catalase	0.51	0.43	0.9995
4	SOD + catalase	0.29	0.23	0.9997
	Acceleratory experiments			
5	XOD	13.42	10.83	0.9998
6	AOX	21.10	15.35	0.9933
	Acceleratory/Inhibitory experiments			
7a [(iii)]	XOD + SOD	12.38	9.66	0.9976
7b [(iv)]		1.45	3.13	0.9994
8	XOD + catalase	2.78	3.32	0.9996
9	XOD + SOD + catalase	0.27	0.23	0.9996
10	AOX + SOD	17.73	15.46	0.9912
11	AOX + catalase	0.18	0.04	0.9991
12	AOX + SOD + catalase	0.01	0.05	0.9992

[(i)] Reaction conditions: [MnTACN], 2.5 μM; [morin], 160 μM; [enzyme], 1 U / 1 μmole morin; 10 mM $NaHCO_3$ buffer, pH 10 at 25°C.
[(ii)] Correlation coefficients of least-squares regressions.
[(iii)] The first (fast) reaction phase considered (Figure 2.14).
[(iv)] The second (slow) reaction phase considered (Figure 2.14).

Figure 2.13 illustrates the effect of AOX on the reaction profiles in the presence of catalase and/or SOD. As already discussed in Section 2.6.3.2, AOX leads to the complete removal of the initial lag-phase together with an increase of the maximum reaction rate, which is in accordance with Eq. 2.14. Pre-incubation of the reaction mixture with AOX/catalase results in a tremendous (three orders of magnitude) retardation of the reaction (Entry 6 and 11 in Table 2.1). This proves that H_2O_2 generated from aqueous O_2 by AOX can successfully be converted back to O_2 by catalase (Eq. 2.11) under the reaction conditions applied.

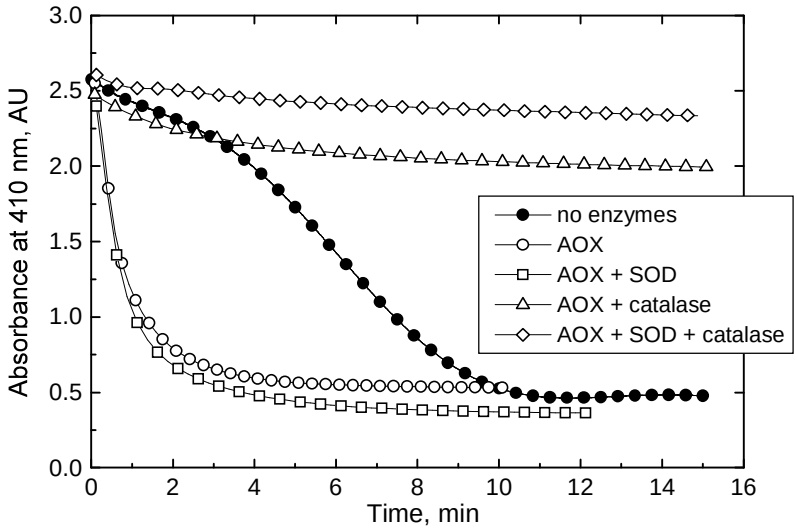

Figure 2.13 The effect of AOX in the absence and presence of catalase and/or SOD. [MnTACN], 2.5 μM; [morin], 160 μM; [CH_3OH], 160 μM; [AOX] = [SOD] = [catalase], 1 U / 1 μmole morin; 10 mM $NaHCO_3$ buffer, pH 10.2 at 25°C.

When catalase is replaced with SOD in the system with AOX, the kinetics of this reaction shows the same pattern as in the case of AOX used alone (Figure 2.13, Entry 10 in Table 2.1). This is the direct evidence that, under the reaction conditions applied, the possibility of catalase activity assigned to SOD should be excluded. In case of preincubation of the reaction system with the triple enzymatic system: acceleratory (AOX) and inhibitory (catalase and SOD), both the lag-phase and the fast reaction phase are inhibited, whereas the rate constant in this case is comparable to one obtained using the system with AOX and catalase (Entry 11 and 12 in Table 2.1). The difference in maximum reaction rate between these two is clearly due to the SOD effect on lag-phase.

Using the same principle, the experiments presented in Figure 2.13 are repeated replacing AOX with XOD (Figure 2.14). The system with XOD is in fact more complex than the system based on AOX, since the reaction of reduction of O_2 into O_2^- catalysed by XOD (Eq. 2.12) can further proceed via dismutation of O_2^- into O_2 and H_2O_2 (Eq. 2.13). Taking this into account, it seemed reasonable that an addition of either SOD or catalase to XOD would have to result in different reaction profiles than the one of the reaction mixture preincubated with XOD alone. Figure 2.14 confirms that this is in fact the case. The addition of catalase to XOD results in a significant retardation of the reaction when compared to the reaction performed in the presence of XOD alone (Entry 8 and 5, Table 2.1). Although the reaction slows down to approximately the same kinetics as for the reaction performed in the absence of enzymes (Entry 1), the reaction profile looks rather different since no lag-phase is present in this case (Figure 2.14). This indicates that although catalase is capable of decomposing H_2O_2 generated

under these conditions, the proportion of activated oxygen (O_2^-) resulted from the XOD activity is sufficient to initiate the reaction with no lag-phase and to bring the reaction kinetics about the kinetics of oxidation of morin by O_2/MnTACN in the absence of enzymes.

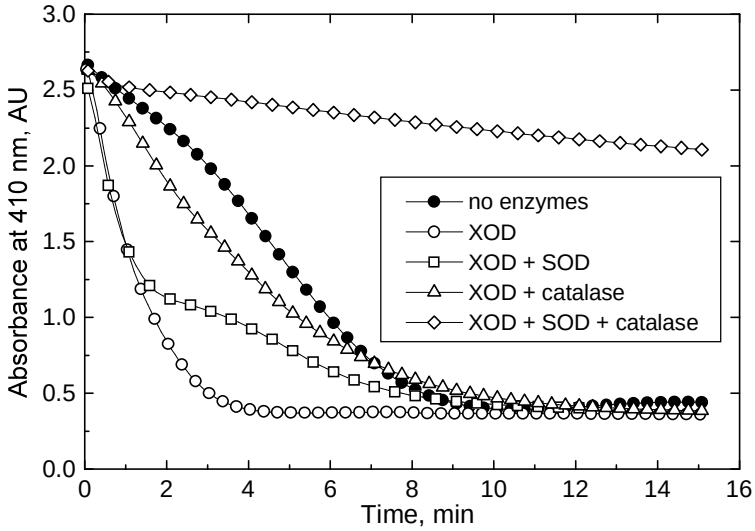

Figure 2.14 The effect of XOD in the absence and presence of SOD and/or catalase. [MnTACN], 2.5 μM; [morin], 160 μM; [xanthine], 160 μM; [XOD] = [SOD] = [catalase], 1 U / 1 μmole morin; 10 mM $NaHCO_3$ buffer, pH 10 at 25°C.

The addition of SOD to XOD causes no change in the first phase of reaction. This effect can be explained by the presence of H_2O_2 generated partially as a result of XOD catalysis followed by spontaneous dismutation of O_2^- (Eqs. 2.12 and 2.13, respectively) and partially by the SOD catalysis (Eq. 2.10). The nature of superoxide radical is such that it may act either as a reductant or as an oxidant. In the dismutation reaction, half is oxidised to O_2 by the other half, which is in turn reduced to H_2O_2. Thus, in a later phase of the reaction, the lack of H_2O_2 and reaction dependence on O_2 leads to the reaction retardation. The kinetic data for the first fast and second slow phase are given by Entries 7a and 7b, respectively, in Table 2.1. If the triple enzymatic system, acceleratory (XOD) and inhibitory (catalase and SOD), is used for the incubation of the reaction mixture prior to the addition of the catalyst, the reaction is remarkably decelerated (Entry 9). This proves that O_2^- and H_2O_2, both generated as a result of the XOD activity, can be ultimately converted into O_2 due to a double inhibitory effect of the coupled enzymatic system of catalase and SOD.

The results obtained on the use of both AOX and XOD in combination with SOD and/or catalase allow drawing final conclusions on the effect of catalase and/or SOD on the reaction of oxidation of morin with O_2 catalysed by MnTACN. We have seen that both catalase and SOD independently decelerate the fast reaction phase (Section 2.6.3.1). Based on the results discussed for the

XOD and AOX systems, we have proven that SOD and catalase are active under the reaction conditions and that no catalase activity can be assigned to SOD as a consequence of relatively high concentration used.

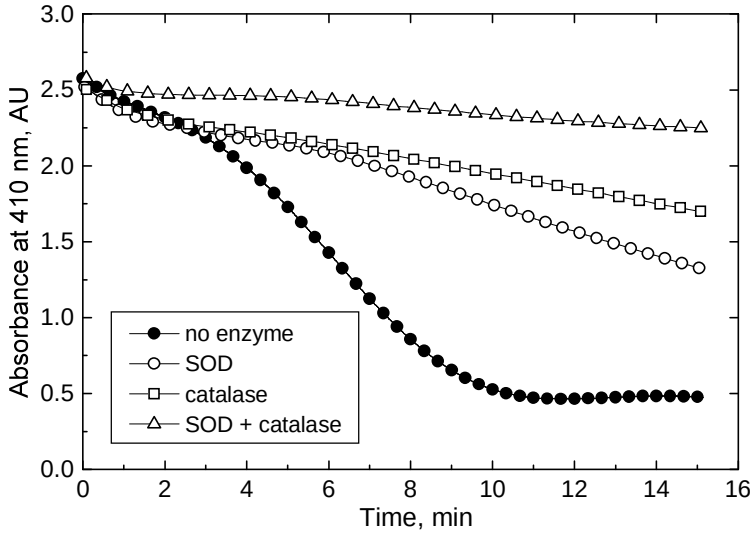

Figure 2.15 The effect of catalase and/or SOD. [MnTACN], 2.5 μM; [morin], 160 μM; [catalase] = [SOD], 1 U / 1 μmole morin; 10 mM $NaHCO_3$ buffer, pH 10 at 25°C.

Coupled system of catalase and SOD added to the reaction mixture prior to the addition of the catalyst (Figure 2.15), suppresses both fast and lag phase of the reaction noticeably (Entry 4 in Table 2.1). The kinetic data in this case are comparable with the corresponding data obtained when the pre-incubation is done with XOD, SOD and catalase (Entry 9 in Table 2.1.; see also Figures 2.14 and 2.15). These results unequivocally provide the evidence that the limiting step is the first electron transfer to O_2 to form superoxide (the presence of lag-phase), whereas both superoxide and hydrogen peroxide are operative in the fast reaction phase.

2.7 Conclusions

Catalytic oxidations and oxygenations with molecular oxygen are among the most important topics in recent years in the large fields of chemistry and biology, and great efforts have been made for understanding mechanisms and reactions and development of chemical model systems in both fields of industries and academic laboratories.

This chapter reports on the activation of molecular oxygen in the oxidation of cotton pigment morin catalysed by the dinuclear manganese(IV) complex of the ligand 1,4,7-trimethyl-1,4,7-triazacyclononane (MnTACN) in alkaline aqueous solutions under ambient conditions. In contrast to earlier studies where H_2O_2 was employed together with MnTACN, in the present study the ability of

MnTACN to use O_2 as terminal oxidant is reported for the first time. The activity of MnTACN is found to be superior to catalysed oxidation by free Mn(II) and proceeds rapidly even at ambient temperature indicating that MnTACN does not dissociate into free Mn(II) during catalytic activation reaction.

The catalytic activity is pH dependent, and a maximum in activity for MnTACN catalysed system is obtained at pH 10.6, whereas below pH 10.2 the presence of an initial lag-phase is observed.

The oxidation of morin is studied in the scope of oxygen activation, i.e. identification of active species derived from dioxygen. The involvement of superoxide O_2^- and/or H_2O_2 is investigated employing a novel method based on change in reaction kinetics in the presence of acceleratory and/or inhibitory enzymes. The design of this method is inspired by the principle of important physiological pathways in human body that include generation of reactive oxygen species as well as their consumption by means of different enzymes such as xanthine oxidase (XOD), superoxide dismutase (SOD) and catalase enzymes, which is extended to the use of alcohol oxidase (AOX).

The distinct differences in the kinetic data obtained when the reaction is performed in the presence or absence of acceleratory (XOD or AOX) and/or inhibitory (SOD and/or catalase) enzymes demonstrate straightforward activity of all enzymes used. Consequently, based on the acceleratory effect with a removal of lag-phase caused by both AOX and XOD, it is possible to conclude that the presence of a slow reaction phase is due to the O_2 involvement (rate-controlling step). Inhibitory effect of both SOD and catalase on the reaction fast phase implies stepwise formation of hydrogen peroxide, i.e. both H_2O_2 and O_2^- are operative in the oxidation of morin by O_2 catalysed by MnTACN. This is in agreement with the reaction kinetics observed for the MnTACN catalysis when using H_2O_2 (or KO_2) as oxidant.

The inhibitory and/or acceleratory enzymatic experimental approach designed in this study is recommended as a tool that can possibly be used to study generation of reactive oxygen species in the reaction systems other than the one studied in this chapter under similar reaction conditions (low-temperature alkaline aqueous solutions).

Literature cited

[1] Manchanda, R., Brudvig, G.W., Crabtree, R.H., High-valent oxomanganese clusters: Structural and mechanistic work relevant to the oxygen-evolving center in photosystem II, Coord. Chem. Rev., **144** (1995) 1-38.

[2] Yagi, M., Kaneko, M., Molecular catalysts for water oxidation, Chem. Rev., **101** (2001) 21-35.

[3] Collins, T.J., Designing ligands for oxidizing complexes, Acc. Chem. Res., **27** (1994) 279-285.

[4] Hage, R., Iburg, J.E., Kerschner, J., Koek, J.H., Lempers, E.L.M., Martens, R.J., Racherla, U.S., Russell, S.W., Swarthoff, T., van Vliet, M.R.P., Warnaar, J. B., van der Wolf, L., Krijnen, L.B., Efficient manganese catalysts for low-temperature bleaching, Nature, **369** (1994) 637.

[5] Weinstock, I.A., Barbuzzi, E.M.G., Wemple, M.W., Cowan, J.J., Reiner, R.S., Sonnen, D.M., Heintz, R.A., Bond, J.S., Hill, C.L., Equilibrating metal-oxide cluster ensembles for oxidation reactions using oxygen in water, Nature, **414** (2001) 191-195.

[6] Wieprecht, T., Xia J., Heinz, U., Dannacher, J., Schlingloff, G., Novel terpyridine-manganese(II) complexes and their potential to activate hydrogen peroxide, J. Mol. Catal. A: Chemical, **203** (2003) 113-128.

[7] Wieghardt, K., The Active Sites in Manganese-Containing Metalloproteins and Inorganic Model Complexes, Angew. Chem., Int. Ed. Engl., **28** (1989) 1153-1172.

[8] Delroisse, M., Verlhac, J.-P., Synthesis of di-μ-oxo manganese(III/IV) complexes as functional models of L. Plantarum pseudo-catalase: influence of electronic and steric factors; catalysis and kinetics of hydrogen peroxide disproportionation J. Chem. Soc. Chem. Comm. (1995) 949-950.

[9] Hage, R., Oxidation catalysis by biomimetic manganese complexes, Recl. Trav. Chim. Pays-Bas, **115** (1996) 385-395.

[10] Sheldon, R.A., Metalloporphyrins in Catalytic Oxidations, Marcel Dekker, Inc., New York, 1994.

[11] Que, L.,Jr., Ho, R.Y.N., Dioxygen Activation by Enzymes with Mononuclear Non-Heme Iron Active Sites, Chem. Rev., **96** (1996) 2607-2624.

[12] Costas, M., Mehn, M.P., Jensen, M.P., Que, L.,Jr., Dioxygen Activation at Mononuclear Nonheme Iron Active Sites: Enzymes, Models, and Intermediates, Chem. Rev., **94** (1994) 807-826.

[13] Groves, J.T., Quinn, R., Aerobic Epoxidation of Olefins with ruthenium Porphyrin Catalysts, J. Am. Chem. Soc., **107** (1985) 5790-5792.

[14] Neumann, R., Dahan, M., A ruthenium-substituted polyoxometalate as an inorganic dioxygenase for activation of molecular oxygen, Nature, **388** (1997) 353-355.

[15] Kok, B., Forbusch, B., McGloin, M., Cooperation of charges in photosynthetic O_2 evolution-I. A linear four step mechanism, Photochem. Photobiol., **11** (1970) 457-475.

[16] Liang, W., Latimer, M.J., Dau, H., Roelofs, T.A., Sauer, K., Klein, M.P., Correlation between structure and the magnetic spin state of the manganese cluster in the oxygen-evolving complex of Photosystem II in the S<SUB>2 state: Determination by X-ray spectroscopy, Biochem., **33** (1994) 4923-4932.

[17] Dismukes, G.C., Siderer, Y., Intermediates of a polynuclear manganese center involved in photosynthetic oxidation of water, Proc. Natl. Acad. Sci. USA, **78** (1981) 274-278.

[18] Wieghardt, K., Bossek, U., Gebert, W., Synthesis of a Tetranuclear Manganese(IV) Cluster with Adamantane Skeleton: $[(C_6H_{15}N_3)_4Mn_4O_6]^{4+}$, Angew. Chem., Int. Ed., Eng., **22** (1983) 328-329.

[19] Wieghardt, K., Bossek, U., Nuber, B., Weiss, J., The reactivity of the $\{Mn_2(\mu\text{-}O)(\mu\text{-}CH_3CO_2)_2\}^{2+}$ core. The crystal structures of $[LMn(N_3)_3]$ and $[L'Mn(S_4)(H_2O)]$ (L=1,4,7-triazacyclononane, L'= N,N',N''-trimethyl-1,4,7-triazacyclononane), Inorg. Chim. Acta,

126 (1987) 39-43.

[20] Wieghardt, K., Bossek, U., Nuber, B., Weiss, J., Bonvoisin, J., Corbella, M., Vitols, S.E., Girerd, J.J., Synthesis, Crystal Structures, Reactivity, and Magnetochemistry of a Series of Binuclear Complexes of Manganese(II), -(III), and -(IV) of Biological Relevance. The Crystal Structure of $[L'M^{IV}(\mu\text{-}O)_3\ M^{IV}L'](PF_6)_2\cdot H_2O$ Containing an Unprecedented Short Mn···Mn Distance of 2.296 Å, J. Am. Chem. Soc., **110** (1988) 7398-7411.

[21] Wieghardt, K., The Active Sites in Manganese-Containing Metalloproteins and Inorganic Model Complexes, Angew. Chem., Int. Ed. Eng., **28** (1989) 1153-1172.

[22] Bossek, U., Weyermuller, T., Nuber, B., Weiss, J., Wieghardt, K., $[L_2Mn_2(\mu\text{-}O)_2(\mu\text{-}O_2)](ClO_4)_2$. The First Binuclear (μ-Peroxo)dimanganese(IV) Complex (L = 1,4,7-trimethyl-1,4,7-triazacyclononane). A model for the $S_4 \rightarrow S_0$ Transformation in the Oxygen-Evolving Complex in Photosynthesis, J. Am. Chem. Soc., **112** (1990) 6387-6388.

[23] Wieghardt, K., Weiss, J., Bossek, U., Synthesis and Structural and Spectroscopic Studies of Manganese Complexes of Pendant-Arm Macrocycles Based on 1,4,7-Triazacyclononane: Crystal Structures of the Manganese(II) Complex $[MnLH_3][MnCl_4]$ and of the Mixed-Valence Manganese(II)-Manganese(IV) Hydrogen-Bridged Dimer $[MnLH_3LMn][PF_6]_3$ (LH_3=N,N',"-Tris[(2S)-2-hydroxypropyl]-1,4,7-triazacyclononane) and of the Manganese(IV) Monomer $[MnL'][ClO_4]$ ($L'H_3$=N,N',N''-Tris(2-hydroxyethyl)-1,4,7-triazacyclononane), Inorg. Chem., **30** (1991) 4397-4402.

[24] Hage, R., Gunnewegh, E.A., Niel, J., Tjon, F.S.B., Weymuller, T., Wieghardt, K., NMR spectra of dinuclear manganese and iron compounds containing 1,4,7-triazacyclononane and 1,4,7-trimethyl-1,4,7-triazacyclononane, Inorg. Chim. Acta, **268** (1998) 43-48.

[25] Phillips, D., Duncan, M., Graydon, A., Bevan, G., Loyd, J., Harbon, C., Hoffmeister, J., J. Soc. Dyers Colour., **113** (1997) 281.

[26] Bachmann, F., Dannacher, J.J., Freiermuth, B., Studer, M., Kelemen, J.,Vat dye sensitised fibre damage and dye fading by catalytic and activated peroxide bleaching, J. Soc. Dyers Colour., **116** (2000) 108-115.

[27] Hage, R., Lienke, A., Applications of Transition-Metal Catalysts to Textile and Wood-Pulp Bleaching, Angew. Chem. Int. Ed., **45** (2006) 206-222.

[28] De Vos, D.E., Bein, T., Highly selective olefin epoxidation with manganese triazacyclononane complexes: impact of ligand substitution, J. Organomet. Chem., **520** (1996) 195-200.

[29] Kobayashi, T., Tsuchiya, K., Nishida, Y., 8-Hydroxy-2-deoxyguanosine formation and DNA damage induced by a dinuclear manganese(IV) complex and hydrogen peroxide, J. Chem. Soc., Dalton Trans. (1996) 2391-2392.

[30] Gilbert, B.C., Kamp, N.W.J., Lindsay Smith, J.R., Oakes, J., EPR evidence for one-electron oxidation of phenols by a dimeric manganese(IV)/(IV) triazacyclononane complex in the presence and absence of hydrogen peroxide, J. Chem. Soc., Perkin Trans. (1997) 2161-2165.

[31] Zondervan, C., Hage, R., Feringa, B.L., Selective catalytic oxidation of benzyl alcohols to benzaldehydes with a dinuclear manganese(IV) complex, J. Chem. Soc., Chem. Commun. (1997) 419-420.

[32] Barton, D.H.R., Li, W., Smith., J.A., Binuclear manganese complexes as catalysts in the selective and efficient oxidation of sulfides to sulfones, Tetrahedron Lett., **39** (1998) 7055-7058.

[33] Lindsay Smith, J.R., Shul'pin, G.B., Efficient stereoselective oxygenation of alkanes by peroxyacetic acid or hydrogen peroxide and acetic acid catalysed by a manganese(IV) 1,4,7- trimethyl-1,4,7-triazacyclononane complex, Tetrahedron Lett., **39** (1998) 4909-4912.

[34] Gilbert, B.C., Lindsay Smith, J.R., Newton, M.S., Oakes, J., Pons i Prats, R., Azo dye oxidation with hydrogen peroxide catalysed by manganese 1,4,7-triazacyclononane

complexes in aqueous solution, Org. Biomol. Chem. (2003) 1568-1577.
[35] De Boer, J.W., Brinksma, J., Browne, W.R., Meetsma, A., Alsters, P.L., Hage, R., Feringa, B.L., $[Mn_2O(RCO_2)_2(tmtacn)_2]$: Tailoring the Selectivity of a Highly H_2O_2-Efficient Catalyst, J. Am. Chem. Soc., **127** (2005) 7990-7991.
[36] Sadov, F., Korchagin, M., Matetsky, A., Natural admixtures of cotton fibre. In "Chemical technology of fibrous materials", Mir Publishers, Moscow (1973) pp. 45-56.
[37] Wu, T.-W., Fung, K.-P., Zeng, L.-H., Wu, J., Hempel, A., Grey, A.A., Camerman, N. Molecular properties and myocardial salvage effects of morin hydrate, Biochem. Pharmacol., **49** (1995) 537-543.
[38] Wu, T.-W., Zeng, L.-H., Wu, J., Fung, K.-P., Morin: A wood pigment that protects three types of human cells in the cardiovascular system against oxyradical damage, Biochem. Pharmacol., **47** (1994) 1099-1103.
[39] Jovanovic, S.V., Steeden, S., Tosic, M., Marjanovic, B., Simic, M.G., Flavonoids as Antioxidants, J. Am. Chem. Soc., **116** (1994) 4846-4851.
[40] Middleton, E., Jr., Effect of plant flavonoids on immune and inflammatory cell function, Adv. Exp. Med. Biol., **439** (1998) 175-182.
[41] Mitcher, L.A., Tekkepalli, H., Waner, P.B.B., Kuo, S., Shanhel, D.M., Stewart, G., Naringenin, apigenin and genistein are weak estrogens, which bind to the estrogen receptor and elicit estrogen-induced responses. Antimutagenic and anticarcinogenic effects, Mutat. Res., **267** (1982) 229-241.
[42] Manach, C., Regerat, F., Texier, O., Agullo, G., Demigne, C., Remesy, C., Bioavailability, metabolism and physiological impact of 4-oxo-flavonoids, Nutr. Res., **16** (1996) 517-544.
[43] Simándi, L.I., Advances in Catalytic Activation of Dioxygen by Metal Complexes, Kluwer Academic Publishers, Dordrecht, 2003.
[44] Prabhakar, R., Siegbahn, P.E.M., Minaev, B.F., A theoretical study of the dioxygen activation by glucose oxidase and copper amine oxidase, Biochim. Biophys. Acta, **1647** (2003) 173-178.
[45] Klinman, J.P., Life as aerobes: are there simple rules for activation of dioxygen by enzymes?, J. Biol. Inorg. Chem., **6** (2001) 1-13.
[46] Jakubowski, H., The chemistry of dioxygen, http://employees.csbsju.edu/hjakubowski/classes/ch331/oxphos/oldioxygenchem.html, 17.05.2006
[47] Tolman, W.B., Making and Breaking the Dioxygen O-O Bond: New Insights from Studies of Synthetic Copper Complexes, Acc. Chem. Res., **30** (1997) 227-237.
[48] Bugg, T.D.H., Sanvoisin, J., Spence, E.L., Exploring the catalytic mechanism of the extradiol catechol dioxygenases, Biochem. Soc. Trans., **25** (1997) 81-85.
[49] Bugg, T.D.H., Winfield, C.J., Enzymatic cleavage of aromatic rings: Mechanistic aspects of the catechol dioxygenases and later enzymes of bacterial oxidative cleavage pathways, Nat. Prod. Rep., **5** (1998) 513-530.
[50] Requena, L., Bornemann, S., Barley (*Hordeum vulgare*) oxalate oxidase is a manganese-containing enzyme, Biochem. J., **343** (1999) 185-190.
[51] Tanner, A., Bowater, L., Fairhurst, S.A., Bornemann, S., Oxalate decarboxylase requires manganese and dioxygen for activity-overexpression and characterization of *Bacillus subtilis* YvrK and YoaN, J. Biol. Chem., **276** (2001) 43627-43634.
[52] Escutia, M.R., Bowater, L., Edwards, A., Bottrill, A.R., Burrell, M.R., Polanco, R., Vicuña, R., Bornemann, S., Cloning and Sequencing of Two *Ceriporiopsis subvermispora* Bicupin Oxalate Oxidase Allelic Isoforms: Implications for the Reaction Specificity of Oxalate Oxidases and Decarboxylases, Appl. Environ. Microbiol., **71** (2005) 3608-3616.
[53] Bugg, T.D.H., Lin, G., Solving the riddle of the intradiol and extradiol catechol dioxygenases: how do enzymes control hydroperoxide rearrangements?, Chem.

Commun., (2001) 941-952.
[54] Balogh-Hergovich, E., Speier, G., Kinetics and Mechanism of the Base-Catalyzed Oxygenation of Flavonol in DMSO-H_2O Solution, J. Org. Chem., **66** (2001) 7974-7978.
[55] López Benet, F.J., Hernández Hernández, F., Medina Escriche, J., Marín Saez, R., Kinetic-Fluorimetric Study of the Catalytic Effect of Manganese(II) on the Air Oxidation of Morin, Analyst, **111** (1986) 1325-1330.
[56] Medina Escriche, J., López Benet, F.J., F.J., Hernández Hernández, F., Kinetic-Fluorimetric Study of the Activator Effect of Zirconium(IV) on the Air Oxidation of Morin Catalysed by Manganese(II), Analyst, **113** (1988) 437-442.
[57] Wieprecht, T., Schlingloff, Xia J., Heinz, U., Schneider, A., Dubs, M.J., Bachmann, F., Hazenkamp, M.,G., Dannacher, J., Use of metal complex compounds as catalysts for oxidation using molecular oxygen or air, Patent No. WO2004039933, (Ciba SC) 2004.
[58] Siegbahn, P.E.M., Hybrid DFT Study of the Mechanism of Quercetin 2,3-Dioxygenase, Inorg. Chem., **43** (2004) 5944-5953.
[59] Steiner, R.A., Kalk, K.H., Dijkstra, B.W., Anaerobic enzyme·substrate structures provide insight into the reaction mechanism of the copper-dependent quercetin 2,3-dioxygenase, Proc. Natl. Acad. Sci., **99** (2002) 16625-16630.
[60] Westlake, D.W.S., Roxburgh, J.M., Talbot, G., Microbial production of Carbon Monoxide from Flavonoids, Nature (1961) 510-511.
[61] Simpson, F.J., Narasimhacgari, N., Westlake, D.W.S., Degradation of rutin by *Aspergillus flavus*. The carbon monoxide producing system, Can. J. Microbiol., **9** (1963) 15-25.
[62] Krishnamurty, H.G., Simpson, F.J., Degradation of rutin by *Aspergillus flavus*. Studies with oxygen 18 on the action of a dioxygenase on quercetin, J. Biol. Chem., **245** (1970) 1467-1471.
[63] Studer, S.L., Brewer, W.E., Martinez, M.L., Chou, P.T., Time-resolved study of the photooxygenation of 3-hydroxyflavone, J. Am. Chem. Soc., **111** (1989) 7643-7644.
[64] Nishinaga, A., Tojo, T., Tomita, H., Matsuura, T., Base-catalysed oxygenolysis of 3-hydroxyflavones, J. Chem. Soc., Perkin Trans., 1 (1979) 2511-2516.
[65] Nishinaga, A., Tojo, T., Matsuura, T., A model catalytic oxygenation for the reaction of quercetinase, J. Chem. Soc., Chem. Commun. (1974) 896-897.
[66] Nishinaga, A., Kuwashige, T., Tsutsui, T., Mashino, T., Maruyama, K., On the mechanism of a model quercetinase reaction using a cobalt Schiff-base complex, J. Chem. Soc., Dalton Trans. (1994) 805-810.
[67] Fiorucci, S., Golebiowski, J., Cabrol-Bass, D., Antonczak, S., Oxygenolysis of Flavonoid Compounds: DFT Description of the Mechanism for Quercetin, Chem. Phys. Chem., **5** (2004) 1726-1733.
[68] Russo, N., Toscano, M., Uccella, N., Semiempirical molecular modeling into quercetin reactive site: Structural, conformational, and electronic features, J. Agric. Food Chem., **48** (2000) 3232-3237.
[69] Krishnamachari, V., Levine, L.H., Par, P.W., Flavonoid oxidation by the radical generator AIBN: A unified mechanism for quercetin radical scavenging, J. Agric. Food Chem., **50** (2002) 4357-4363.
[70] Keele, B.B.,Jr., McCord, J.M., Fridovich, I., Superoxide Dismutase from *Escherichia coli* B. A new manganese-containing enzyme, J. Biol. Chem., **245** (1970) 6176-6181.
[71] McCord, J.M., Fridovich, I., Superoxide Dismutase - An Enzymic Function for Erythrocuprein (Hemocuprein), J. Biol. Chem., **244** (1969) 6049-6055.
[72] Ginsburg, I., Misgav, R., Pinson, A., Varani, J., Ward, P.A., Kohen, R., Synergism among oxidants, proteinases, phospholipases, microbial hemolysins, cationic proteins, and cytokines, Inflammation, **16** (1992) 520-538.
[73] Dew, T.P., Day, A.J., Morgan, M.R.A., Xanthine Oxidase Activity in Vitro: Effects of Food Extracts and Components, J. Agric. Food Chem., **53** (2005) 6510-6515.

[74] Hille, R., The Mononuclear Molybdenum Enzymes, Chem. Rev., **96** (1996) 2757-2816.
[75] Doonan, C.J., Stockert, A., Hille, R., George, G.N., Nature of the Catalytically Labile Oxygen at the Active Site of Xanthine Oxidase, J. Am. Chem. Soc., **127** (2005) 4518-4522.
[76] McNaughton, R.L., Helton, M.E., Cosper, M.M., Enemark, J.H., Kirk, M.L., Nature of the Oxomolybdenum-Thiolate π-Bond: Implications for Mo-S Bonding in Sulfite Oxidase and Xanthine Oxidase, Inorg. Chem., **43** (2004) 1625-1637.
[77] Nijveldt, R.J., van Nood, E., van Hoorn, D.E.C., Boelens, P.G., van Norren, K., van Leeuwen, P.A.M., Flavonoids: a review of probable mechanisms of action and potential applications, Am. J. Clin. Nutr., **74** (2001) 418-425.
[78] Kim, Y.-J., Chung, J.E., Kurisawa, M., Uyama, H., Kobayashi, S., Superoxide Anion Scavenging and Xanthine Oxidase Inhibition of (+)-Catechin-Aldehyde Polycondensates. Amplification of the Antioxidant Property of (+)-Catechin by Polycondensation with Aldehydes, Biomacromolecules, **5** (2004) 547-552.
[79] Janssen, F.W., Kerwin, R.M., Ruelius, H.W., Alcohol oxidase, a novel enzyme from a basidiomycete, Biochim. Biophys. Res. Commun., **20** (1965) 630-634.
[80] Janssen, F.W., Ruelius, H.W., Alcohol oxidase, a flavoprotein from several Basidiomycetes species. Crystallization by fractional precipitation with polyethylene glycol, Biochim. Biophys. Acta, **151** (1968) 303-342.
[81] Herzberg, G.R., Rogerson, M., Use of alcohol oxidase to measure the methanol produced during the hydrolysis of D- and L-methyl-3-hydroxybutyric acid, Anal. Biochem., **149** (1985) 354-357.
[82] Phillips; R.C., Colorimetric ethanol analysis method and test device, US patent No. 4 734 360 (1988).

3

Mechanism and kinetics of catalytic bleaching under homogeneous conditions

Understanding the chemical mechanism of bleaching under homogeneous conditions is the first step to help to emerge the application of the catalysts into industrial bleaching. The primary focus of this chapter is to reveal the mechanistic and kinetic details of catalytic bleaching under homogeneous conditions. To this end, we have studied both the substrate scope (coloured matter) and the catalyst scope (activation). A mechanistic proposal that resulted from this approach is given herein.

3.1 Introduction

In the last decade the area of catalytic bleaching has evolved to a dynamic industrial research field. A wide variety of transition-metal complexes have been patented as catalysts for bleaching applications. Many homogeneous oxidation systems, using hydrogen peroxide and catalysed by transition-metal ions and complexes, are developed at laboratory scale, but as yet there are no published examples of their commercial applications. Undoubtedly, many more catalysts have been tested and not found to be active.

To understand the exact chemical mechanism of bleaching under homogeneous conditions is the first step to help to emerge the application into the real industrial process. Despite the numerous patents, scientific publications and intense research in this area, the knowledge on the mechanism of catalytic bleaching is still limited. It is perhaps not entirely surprising when being aware of the problem complexity with regard to rather modest existing knowledge about the nature of coloured matter and its bonding to textile fibres together with a vague depiction of active forms of transition-metal complexes. From the literature that has been available so far, it is apparent that the mechanism has mostly been considered in two aspects separately: the substrate scope and the catalyst scope.

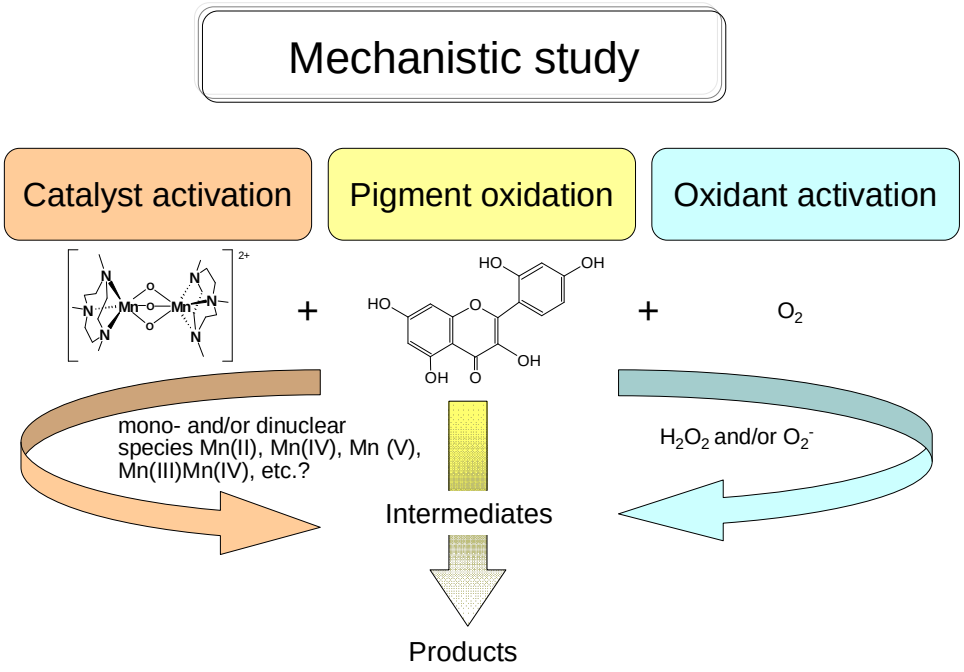

Figure 3.1 The strategy to study the mechanism of catalytic bleaching using a homogeneous model system.

The primary focus of this chapter is to reveal the mechanistic and kinetic details of catalytic bleaching under homogeneous conditions. Here we assume that the mechanism of oxidation of coloured matter present in cotton fibre during bleaching is similar to that in a homogeneous system to the exclusion of transport phenomena. To this end, we have studied both the substrate scope (coloured matter) and the catalyst scope (activation). A simplified scheme that helps to understand the questions posed and the strategy of the study performed is shown in Figure 3.1. It can be seen that the main substrate chosen to study the aspects of the MnTACN catalysed cotton pigment oxidation is morin. MnTACN stands for a dinuclear tri-μ-oxo bridged manganese(IV) complex of the ligand 1,4,7-trimethyl-1,4,7-triazacyclononane. The work presented here is in fact a continued mechanistic and kinetic study discussed in previous chapter. As the result of this approach, the present chapter ends with a mechanistic proposal, which also includes the mechanistic conclusions on the oxidant activation drawn in Chapter 2. Before the results are presented, we have considered it useful to give a short literature overview on up to date studies of mechanism of (i) oxidation of flavonoids and (ii) MnTACN catalysis.

3.2 Substrate scope: Mechanistic studies of oxidation of flavonoids

Although there are several studies where flavonoids and catechol derivatives were used in model bleaching experiments [1-5] as mimics for tea stains, the enormous scientific interest that flavonoids receive for a considerable time is owing to a positive impact they have on human health as a result of their antioxidant properties. Therefore, it is not surprising that the major progress in understanding the mechanism of oxidation of flavonoids has indeed been made in the scientific areas of medical, biochemical and food research. For a better insight into their fate during metabolism, emphasis has been put on studies of flavonoids interactions with prooxidative compounds found in living cell systems, i.e. enzymes and transition metal cations. Although we study the oxidation of flavonoids for the purpose of catalytic bleaching, the similarity in mechanistic pathways with well studied cell systems apparently exists as mentioned in Chapter 2. The efficiency of flavonoids as antioxidant compounds greatly depends on their chemical structure. Three structural features being the most important determinants are (structure **1** in Figure 3.2) [6-10]: (a) the *o*-dihydroxy (catechol) structure in the B ring, which is a radical target site; (b) the 2,3-double bond in conjugation with a 4-keto function, which are responsible for electron delocalisation from the B ring; and (c) the additional presence of both 3- and 5-hydroxyl groups for maximal radical-scavenging potential and strongest radical scavenging. Further, the *o*-dihydroxy structure, as well as the 4-keto and 3- or 5-hydroxyl groups are considered to be essential functions with respect to chelating metal ions.

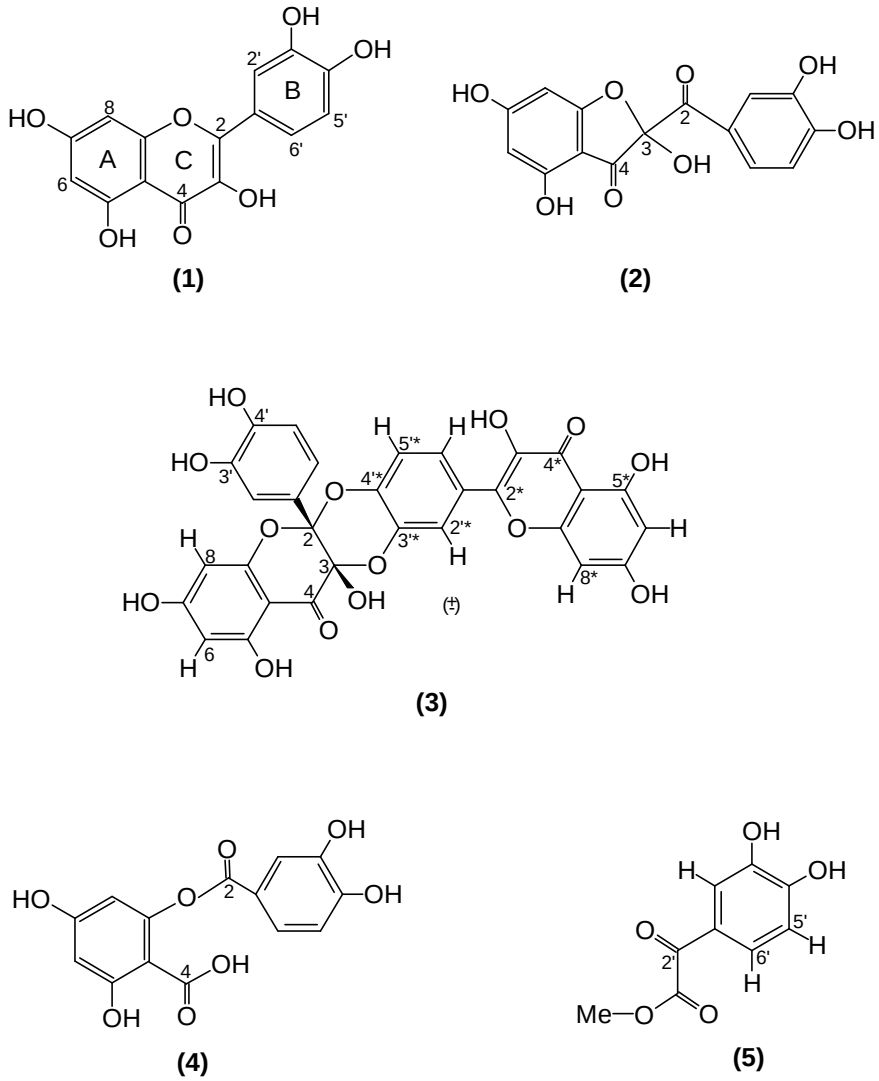

Figure 3.2 Quercetin and oxidised products generated from the radical generator AIBN [19].

Different enzymes have been reported to catalyse the oxidation of flavonoids, leading to a variety of reaction products. Attention was especially paid to the investigation of quercetinase [11], peroxidase [12-13] and polyphenoloxidase [14]. Several authors have reported the chelation of Cu(II) and Fe(III) by various polyhydroxy-compounds, proposing the 3',4'-dihydroxy moiety of the catechol rings, the 3-hydroxy-4-ketogroups and the 5-hydroxy-4-keto function as possible binding sites [15-17]. Although several reaction products resulted from chemical or enzymatic oxidation have been reported, providing direct evidence as to reactive site(s) of flavonoid antioxidant activity [18], the picture emerging from these studies is that the oxidation of flavonoids is complex, resulting in a wide variety of, in many cases, unidentified reaction products.

Recently Krishnamachari *et al.* [19] isolated four oxidised flavonoid derivatives (Figure 3.2) generated from reacting a pentahydroxylated flavone quercetin

(structure **1**) with the peroxyl radical generator 2,2'-azobis-isobutyronitrile (AIBN) by chromatographic methods and identified by NMR and MS analyses. Compounds included 2-(3,4-dihydroxybenzoyl)-2,4,6-trihydroxy-3(2*H*)-benzofuranone (structure **2**); 1,3,11a-trihydroxy-9-(3,5,7-trihydroxy-4 H-1-benzopyran-4-on-2-yl)-5a-(3,4-dihydroxyphenyl) - 5,6,11 - hexahydro-5,6,11-trioxanaphthacene-12-one (structure **3**); 2-(3,4-dihydroxybenzoyloxy)-4,6-dihydroxybenzoic acid (structure **4**); and methyl 3,4-dihydroxyphenylglyoxylate (structure **5**).

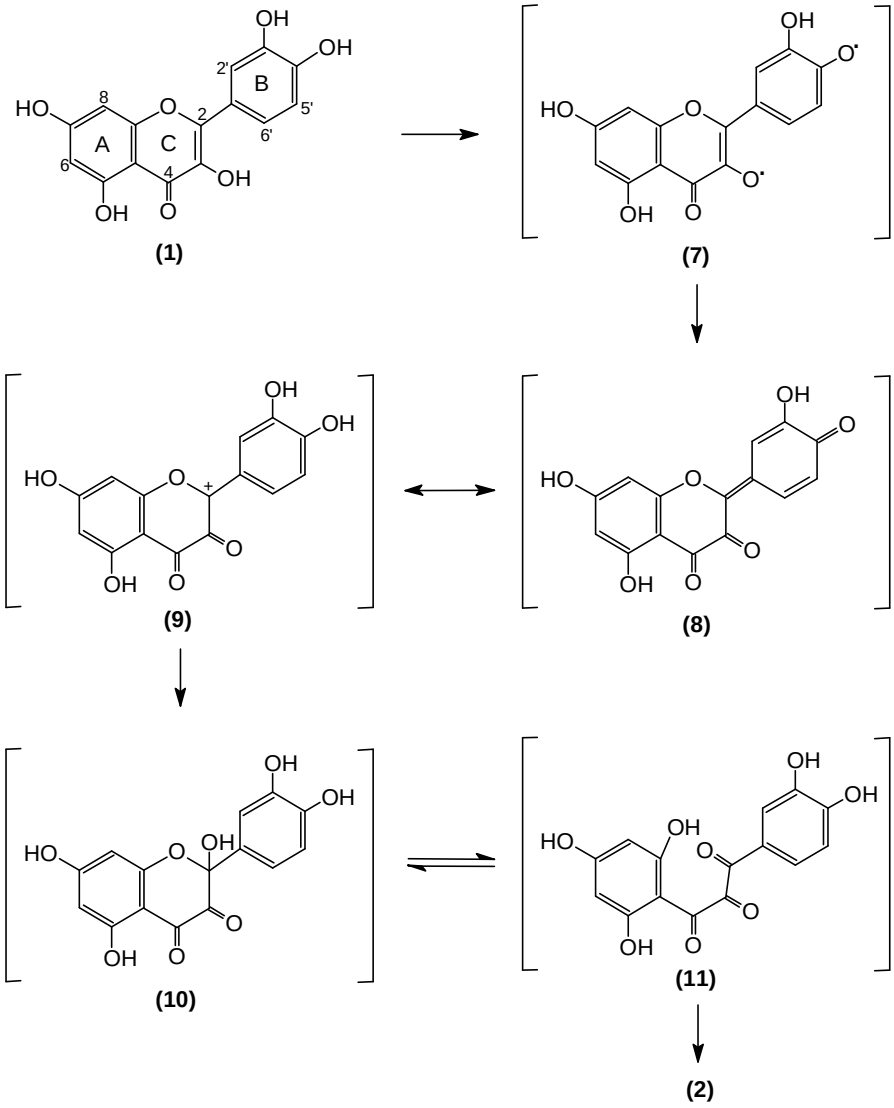

Figure 3.3 Proposed mechanism for the electrochemical oxidation of quercetin [20]. Structure **2** is given in Figure 3.2.

In the least-modified product generated from the reaction, the pyranone C-ring of quercetin was converted to a furanone-carbonyl derivative. This benzofuranone derivative (structure **2**, Figure 3.2) has been observed previously in a two-electron electrochemical [20] and a metal ion mediated oxidation [21] of quercetin. The other major product formed from the oxidation of quercetin

was a dimer that has been observed previously during the autoxidation of methyl linoleate solutions containing quercetin (structure **3** in Figure 3.2) [22]. The first indication of a cleaved C-ring (structure **4** Figure 3.2), generated from the oxidation of quercetin, was the absence of signals corresponding to the C2 and C3 carbons in the 13C NMR spectrum. This phenolic carboxylic acid ester, a depside, has been reported under different oxidation conditions such as singlet oxygen and superoxide anion radical [23-24], as well as in the enzyme system using quercetinase and its mimics [25-27]. The product methyl 3,4-dihydroxyphenylglyoxylate (structure **5** in Figure 3.2) had not been observed earlier. This may, at least in part, be due to its low abundance and close association with other polar reaction products [19].

The formation of depsides (structure **4** in Figure 3.2) and substituted 3(2*H*)benzofuranones (structure **2** in Figure 3.2) have been reported in several oxidation systems [20-21, 23-24]. For example, the electrochemical oxidation of quercetin and kaempferol is thought to proceed through a two-electron oxidation, first to yield a 3,4-flavandione (structure **10** in Figure 3.3) which rearranges to form a substituted 3(2*H*)benzofuranone through the chalcantrione ring chain tautomer (structure **11** in Figure 3.3) [20-21]. On the basis of reported pK_a values and the respective benzofuranone products observed, diradical (structure **7**) and quinone methide (structure **8**) intermediates have been proposed [20]. Although the participation of a flavylium ion (structure **9**) was suspected, no further studies to validate the mechanism have been reported [20].

3.3 Catalyst scope: Mechanism of MnTACN catalysis

Manganese complexes containing 1,4,7-trimethyl-1,4,7-triazacyclononane and related ligands were initially prepared as structural mimics for enzymes with dinuclear or polinuclear manganese active sites (see Section 2.1 in Chapter 2 and references therein). The aim was to provide better insight in the nature of these natural compounds. Nevertheless, during last decade these complexes have received a lot of attention for their catalytic properties in the oxidative processes. The MnTACN complex has shown considerable potential as a catalyst for oxidations with H_2O_2 in aqueous and organic solution [5, 28-34]. The mechanisms of many of these reactions remain unclear yet. Moreover, it is noteworthy that there have been no publications on the mechanism of MnTACN catalysis using O_2 as terminal oxidant.

Hage *et al*. reported on the use of MnTACN and related species in combination with hydrogen peroxide or hydrogen peroxide precursors as highly effective bleaching catalyst in detergents [5]. Hydrogen peroxide, i.e. the perhydroxyl ion (HOO^-), is generally rather unstable under alkaline conditions and easily undergoes decomposition in the presence of trace amounts of metal ions such as Mn(II), Cu(II), and Fe(II). However, owing to the high stability of the manganese complexes the decomposition of peroxide was low and the bleaching

activity was superior compared to trials performed in the presence of free manganese salts. Furthermore, the aqueous MnTACN system exhibited excellent catalytic activity in the epoxidation of 4-vinylbenzoic acid and styrene used for model oxidation studies [5]. Repeated additions of substrate to the oxidant system, did not result in loss of activity, which implies that the catalyst system was quite stable. The oxidation of catechol, used as a tea-stain mimic, gave an EPR (Electron Paramagnetic Resonance) spectrum with 16 peaks which is typical of a mixed-valence Mn(III)Mn(IV) complex. It was suggested that at pH < 9.5 mononuclear Mn(IV) species are operative in the bleaching cycle.

The work published by Gilbert ***et al.*** [32, 35-36] has significantly contributed to the understanding of the catalyst speciation in the oxidation of a range of phenolic substrates by a MnTACN/H_2O_2 aqueous system at pH 10.5. The authors found that for electron-rich substrates, the reaction proceeds via a rapid overall one-electron process from the phenolate ion to the Mn(IV)Mn(IV) species (MnTACN) to give initially, a Mn(III)Mn(IV) species detected via its characteristic 16-line EPR spectrum and the corresponding phenoxyl radical [35]. The dimeric Mn(III)Mn(IV) species is ultimately converted to monomeric Mn(II), whereas the addition of H_2O_2 regenerates active oxidant. Nevertheless, the nature of active oxidants in the catalytic system was not identified, although it was speculated that possible candidates were high-valent mono- or dinuclear MnTACN complexes, including their oxo, hydroperoxo or μ-peroxo derivatives. Indeed, Barton ***et al.*** [37] have suggested the formation of the O=Mn(V)Mn(IV) intermediate during the oxidation of 2,6-di-***tert***-butyl phenol with MnTACN and H_2O_2. In a following paper, Gilbert ***et al.*** [36] used ESI-MS (Electrospray Ionisation Mass Spectrometry) as a valuable tool for the investigation of charged metal complexes aiming to obtain more detailed evidence for intermediates other than EPR-detectable species. The authors confirmed that in a regeneration process, mononuclear Mn(II) is oxidised to O=Mn(V) species. Moreover, in several subsequent publications [32, 34, 38], O=Mn(V) species has been proposed as the active oxidant. Nevertheless, in the azo dye oxidation by MnTACN/H_2O_2, the ESI-MS study provided no evidence for the presence of O=Mn(V) species [40]. The reason for this, according to the authors, is that the species is too short-lived to be detected, whilst in the oxidation of electron-rich phenols with H_2O_2 catalysed by MnTACN the equivalent mononuclear O=Mn(V) species is sufficiently stabilised in a MnTACN-biphenolate mixed-ligand species for it to be detected by ESI-MS. It was suggested that the reaction of the azo dye anion, MnTACN and HOO^- leads to a breakdown of the dinuclear MnTACN to give reactive mononuclear manganese species. Whether these are Mn(III), Mn(IV) or Mn(V) remains unclear.

3.4 Experimental section

3.4.1 Chemicals

The catalyst MnTACN was provided by Unilever R&D (The Netherlands). Manganese chloride and manganese sulphate were obtained from Fluka. Hydrogen peroxide (30%), potassium superoxide, sodium hydroxide and sodium hydrogencarbonate were obtained from Merck. Flavonoids and benzendiols (Table 3.1) were purchased from Sigma (**a** and **e**), Aldrich (**b**-**d**), Acros Organics (**f** and **g**) and Sigma-Aldrich (**h**-**j**). 1,4,7-Trimethyl-1,4,7-triazacyclononane (TACN), lithium hydroxide and potassium hydroxide were obtained from Sigma-Aldrich. Acetonitrile received from Riedel-de Haën was HPLC grade, and other chemicals were reagent grade.

3.4.2 Homogeneous catalysis experiments

Homogeneous catalysis experiments included the following studies: the structure-reactivity relationship with a series of flavonoids and benezendiols (Table 3.1) at pH 10.2 and 25^{o}C; the stability of MnTACN at pH 10.2 and 25^{o}C; the effect of ligand TACN (pH 9.5, 25^{o}C); and the kinetic study over the temperature range of 20-60^{o}C at pH 9.5 and pH 10. The experiments were carried out using a UV-Vis spectrophotometer according to the procedure described in Chapter 2 (Section 2.5.3).

3.4.3 Reaction kinetics and activation parameters calculation

The flavonoids and benzendiols discolouration was monitored using a UV-Vis spectrophotometer by recording absorbance vs. time plots at the wavelength of maximum absorbance. The recording time was 20 minutes which assured a complete discolouration of morin. A “complete” discolouration is defined as a levelling of the discolouration curve. It should be noted that 100% discolouration of morin is impossible due to a non-zero absorbance at 410 nm resulting from a wide tailing of broad peak in the UV which overlap the 410 nm. The degree of discolouration i.e. the percentage decrease in the peak was determined according to Eq. 3.1 for 5 and 10 minutes reaction time.

$$\%\ \text{Discolouration} = \frac{\text{Abs}_0 - \text{Abs}_t}{\text{Abs}_0} \cdot 100 \qquad (3.1)$$

The first order rate constants k with respect morin and reaction rates of the reaction $\text{morin} \xrightarrow[O_2/\text{MnTACN}]{k} \text{product}$ were calculated for the different temperatures as explained in Chapter 2 (Section 2.5.5).

The activation energy E_a is calculated from the slope of the Arrhenius plot (ln k vs. 1/T), according to Eq. (3.2):

$$\ln k = -\frac{E_a}{RT} + \ln A \tag{3.2}$$

The Eyring plot of ln (k/T) vs. 1/T was used to calculate the activation enthalpy $\Delta H^{\#}$ and the activation entropy $\Delta S^{\#}$ for 298 K; the slope was used to calculate $\Delta H^{\#}$ and the y-intercept to calculate activation entropy $\Delta S^{\#}$ for 298 K according to Eq. 3.3, wherein k_B, h, and R are the Boltzmann's constant, the Plank constant and the gas constant, respectively).

$$\ln \frac{k}{T} = -\frac{\Delta H^{\#}}{R}\frac{1}{T} + \ln \frac{k_B}{h} + \frac{\Delta S^{\#}}{R} \tag{3.3}$$

Free activation enthalpy $\Delta G^{\#}$ for 298 K was calculated using Eq. 3.4:

$$\Delta G^{\#} = \Delta H^{\#} - T \cdot \Delta S^{\#} \tag{3.4}$$

3.4.4 ESI-MS analysis

Electrospray ionisation mass spectra (ESI-MS) were recorded on a Triple Quadrupole LC/MS/MS mass spectrometer API 3000 (Perkin-Elmer Sciex Instruments, USA). A sample (20 µl) was taken from the reaction mixture at the indicated times and was diluted in acetonitrile (1 ml) before injection in the mass spectrometer (via syringe pump). The mass spectrometer was operated in both positive and negative mode in the range of m/z 100-1500. The operating conditions in the mass spectrometer were as follows: ion-spray voltage: 5200 V, orifice: 15 V, ring: 150 V, Q0: -10 V.

3.4.5 NMR

^{1}H-NMR spectra of morin and its oxidation product were recorded at 25^{o}C in a DMSO-d_6 solution using a Mercury Plus NMR (Varian, USA) spectrometer operating at 400 MHz. Chemical shifts are denoted relative to the solvent residual peak ($CDCl_3$ 7.26 ppm; CD_3CN: 1.94 ppm).

A sample of the reaction product for NMR was prepared according to the following procedure. Morin (0.200 g in 2 L H_2O) was brought to pH 10.3 using KOH. 4 mg of MnTACN catalyst was added and the reaction was followed by UV-Vis spectroscopy. After near complete loss in absorbance at 410 nm, the

solution was neutralised with diluted H_2SO_4 (to pH 6.7) and extracted with ether. The extract was evaporated to dryness, yielding a red/brown powder.

3.5 Results and discussion

3.5.1 Structure-reactivity relationship study

Key to elucidation of the mechanism of oxidation of morin is the selection of a series of model compounds structurally related to morin and a systematic study of their oxidation. This approach is even more attractive bearing in mind that, apart from morin, there are also other flavonoids present in cotton fibre contributing to its natural yellowish colour such as, for example, hexahydroxyflavone gossypetin [41]. Hence, the degree of polyhydroxylation and the distribution of hydroxyl groups within flavonoid molecule, such as the presence or absence of hydroxyl group at C-3 position, are chosen as the main criteria for the selection of model flavonoids (Figure 3.4 and Table 3.1). The study is extended to the MnTACN catalysed oxidation of *o*-, *p*- and *m*-benzendiols since flavonoids are considered as catechol derivatives.

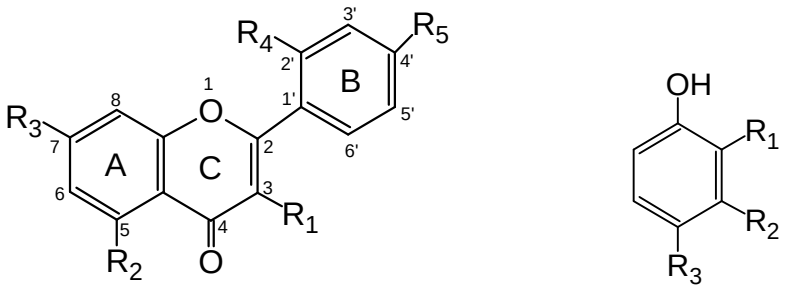

(a) (b)

Figure 3.4 Labelling scheme used in Table 3.1 for flavonoids (a) and benzendiols (b). Note: Structure (a) for R1 = R2 = R3 = R4 = R5 = H corresponds to the general structure of an unsubstituted flavone. Flavones belong to a subgroup of flavonoids.

Absorption spectra of flavones generally exhibit two distinctive bands. Band I in the 240-270 nm region is attributed to the benzoyl structure and Band II in the 300-400 nm region to the cinnamoyl structure [42], as it is confirmed in the absorption spectrum of morin (spectrum 0 in Figure 3.5). With regard to that, UV-Vis spectrometry was used as a suitable technique to follow oxidative degradation of flavones and, consequently, to measure the catalytic activity of MnTACN through the absorbance change in the region of these bands with time.

Table 3.1 Substitution patterns and percentage of discolouration of a series of flavonoids and benzendiols during oxidation catalysed by O_2/MnTACN. [(i)]

Label	Substrate	Substituents					% Discolouration at	
		R1	R2	R3	R4	R5	5 min	10 min
	Flavonoids							
a	3,5,7,2',4'-$(OH)_5$ flavone (Morin)	OH	OH	OH	OH	OH	75.50	98.96
b	3,5,7-$(OH)_3$ flavone (Galangin)	OH	OH	OH	H	H	60.76	89.63
c	3,7-$(OH)_2$ flavone	OH	H	OH	H	H	17.21	29.74
d	3-OH flavone (Flavonol)	OH	H	H	H	H	49.75	90.15
e	5-OH flavone	H	OH	H	H	H	0.00	2.94
f	7-OH flavone	H	H	OH	H	H	1.26	2.21
g	5,7-$(OH)_2$ flavone (Chrysin)	H	OH	OH	H	H	1.17	2.04
	Benzendiols							
h	1,2-Benzendiol (Catechol)	OH	H	H			1.00	1.41
i	1,3-Benzendiol (Resorcinol)	H	OH	H			0.81	1.84
j	1,4-Benzendiol (Hydroquinone)	H	H	OH			1.63	2.42

[(i)] [MnTACN], 2.5 μM; [flavonoid] or [benzendiol], 160 μM; 10 mM $NaHCO_3$ buffer at 25°C pH 10.2.

Morin and flavonoids selected are only slightly soluble in water, giving a pale yellow colour, which is difficult to quantify. However, in a $NaHCO_3$/NaOH buffer morin dissolves completely and gives an intense yellow owing to an intense peak at 410 nm. During the oxidation of morin, its colour fades which can be evidenced by an almost complete loss of the 410 nm peak as shown previously in Chapter 2. During the oxidation of morin as well as the other flavonoids containing a hydroxyl group in C-3 position (flavonoids **a-d** in Table 3.1), considerable changes in the spectral shape with time are observed (Figures 3.5 and 3.6). A rapid decrease in absorbance at 275 and 410 nm for morin (Bands I and III in Figure 3.5) is observed, with almost complete loss of absorbance at 410 nm. At the same time, an increase in absorbance at 325 nm is observed (Band II, Figure 3.5). Well defined isosbestic points are obtained at 289, 373 and 479 nm. This is the direct evidence that no long lived reaction intermediates are formed and that morin is converted to a single degradation product without any side reactions. It is noteworthy that the similar spectral changes were monitored for the reaction of morin with either H_2O_2/MnTACN or KO_2/MnTACN suggesting formation of the same reaction product.

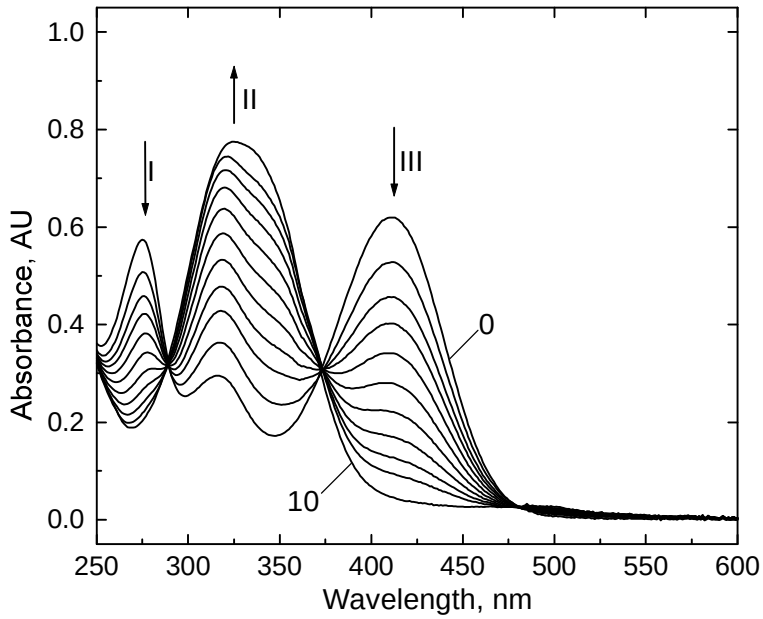

Figure 3.5 Oxidation of morin by O_2/MnTACN between 0 and 10 min monitored by UV-Vis spectroscopy. [MnTACN], 2.5 μM; [morin], 160 μM; 10 mM $NaHCO_3$ buffer, pH 10.2 at 25°C.

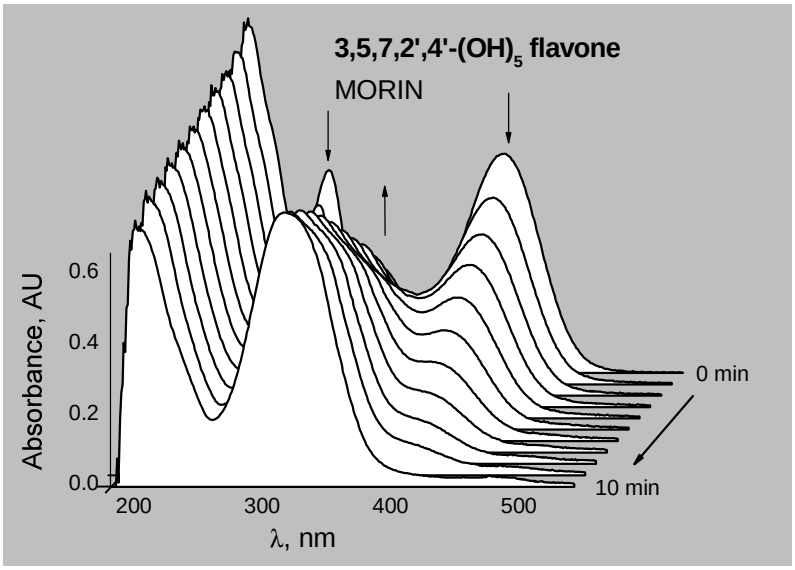

Figure 3.6 UV-Vis spectra of discolouration of morin (**a** in Table 3.1) obtained between 0 and 10 minutes of reaction time. [MnTACN], 2.5 μM; [morin], 160 μM; 10 mM $NaHCO_3$ buffer, pH 10.2 at 25°C.

Selected results for % discolouration of the flavonoids and benzendiols after 5 and 10 minutes reaction are shown in Table 3.1, whereas the 3D diagrams illustrating spectral changes within 10 minutes of reaction time are given in

Figures 3.6-3.10. In agreement with the previous research on structure-reactivity of flavonoids (see Section 3.2), C-3-hydroxyl flavonoids indeed prove to be reactive. For flavonoids labelled as **a**-**d** in Table 3.1, a rapid depletion in the absorbance within 10 minutes in the near UV region is observed (Figure 3.6-3.9). The effect of hydroxyl substitutents on rings A and B (see Figure 3.4) on the rate of oxidation catalysed by MnTACN is found to be quite modest, with the exception of flavonoid **c** (Table 3.1).

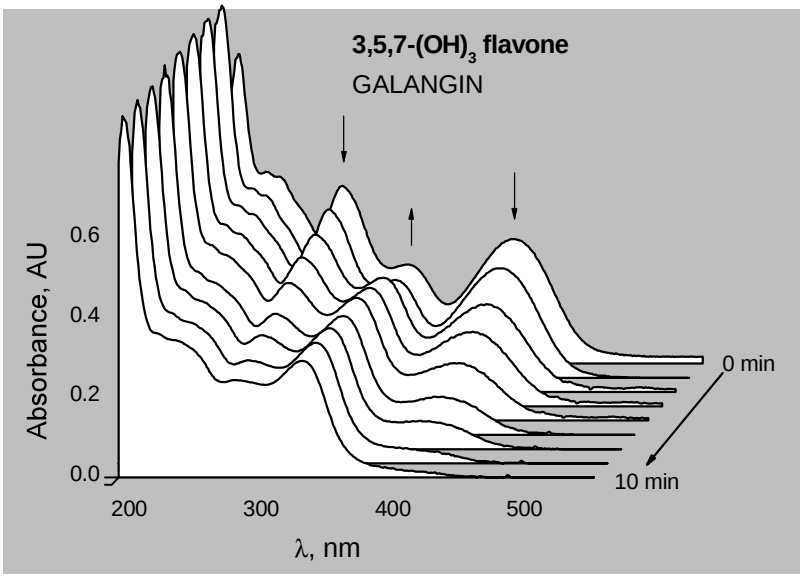

Figure 3.7 UV-Vis spectra of discolouration of galangin (**b** in Table 3.1) obtained between 0 and 10 minutes of reaction time. [MnTACN], 2.5 μM; [galangin], 160 μM; 10 mM $NaHCO_3$ buffer, pH 10.2 at 25°C.

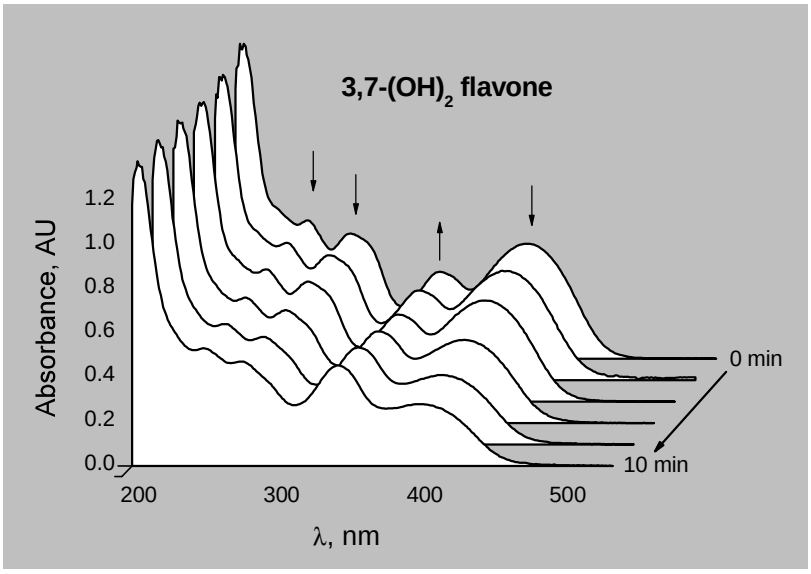

Figure 3.8 UV-Vis spectra of discolouration of 3,7-dihydroxyflavone (**c** in Table 3.1) obtained between 0 and 10 minutes of reaction time. [MnTACN], 2.5 μM; [3,7-$(OH)_2$ flavone], 160 μM; 10 mM $NaHCO_3$ buffer, pH 10.2 at 25°C.

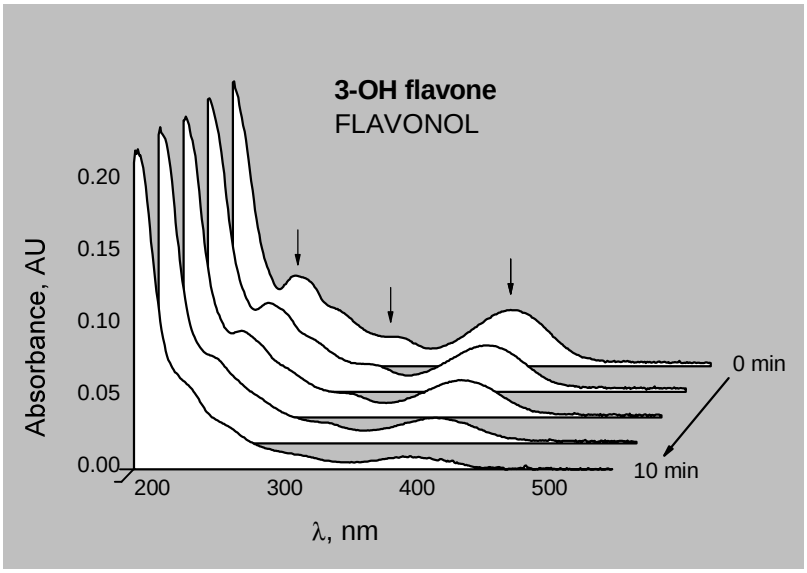

Figure 3.9 UV-Vis spectra of discolouration of flavonol (**d** in Table 3.1) obtained between 0 and 10 minutes of reaction time. [MnTACN], 2.5 μM; [flavonol], 160 μM; 10 mM $NaHCO_3$ buffer, pH 10.2 at 25°C.

Contrary to the results obtained for the flavonoids with the C-3 hydroxyl group, flavonoids **e**-**g** in Table 3.1 lacking this group, together with benzendiols (**h**-**j** in Table 3.1), show no reactivity, i.e. no change in UV-Vis spectra taken upon addition of MnTACN under the present reaction conditions (Figure 3.10 and Table 3.1). This suggests that the mechanism of the reaction is unrelated to catechol dioxygenation [43-44], but it requires flavonoid structure with the presence of C-3 hydroxyl group being essential to the activity of MnTACN.

These results suggest that the binding between the catalyst and the flavonoid involves interaction with the hydroxyl at C-3, the carbonyl at position C-4, and the manganese of the catalyst. The geometry of the orbital overlap between the manganese as constrained by the catalyst and the C-3 hydroxyl and C-4 carbonyl may be more favourable than that with the C-5 hydroxyl and C-4 carbonyl. This agrees with studies on metal-flavone complexes where chelates involving the C-3 hydroxyl are more stable than those involving the C-5 hydroxyl [45-46]. The dependence on the C-3 hydroxyl group implying binding of the flavone to the manganese complex occurs probably in a manner similar to that proposed for Cu(II) complexes ($[(N3)_2Cu_2^{II}(\mu\text{-}O)_2]$ and $[(N3)_2Cu_2^{II}(\mu\text{-}\eta^2\text{:}\eta^2\text{-}O)_2]$ where *N3* = N,N,N-trialkyl-1,4,7-triazacyclononane) [47]. These complexes form the corresponding stable flavonato complexes, which undergo non-catalytic ring scission at elevated temperatures in the presence of O_2, forming (O-benzoylsalicylato)copper(II) complexes and carbon monoxide [47].

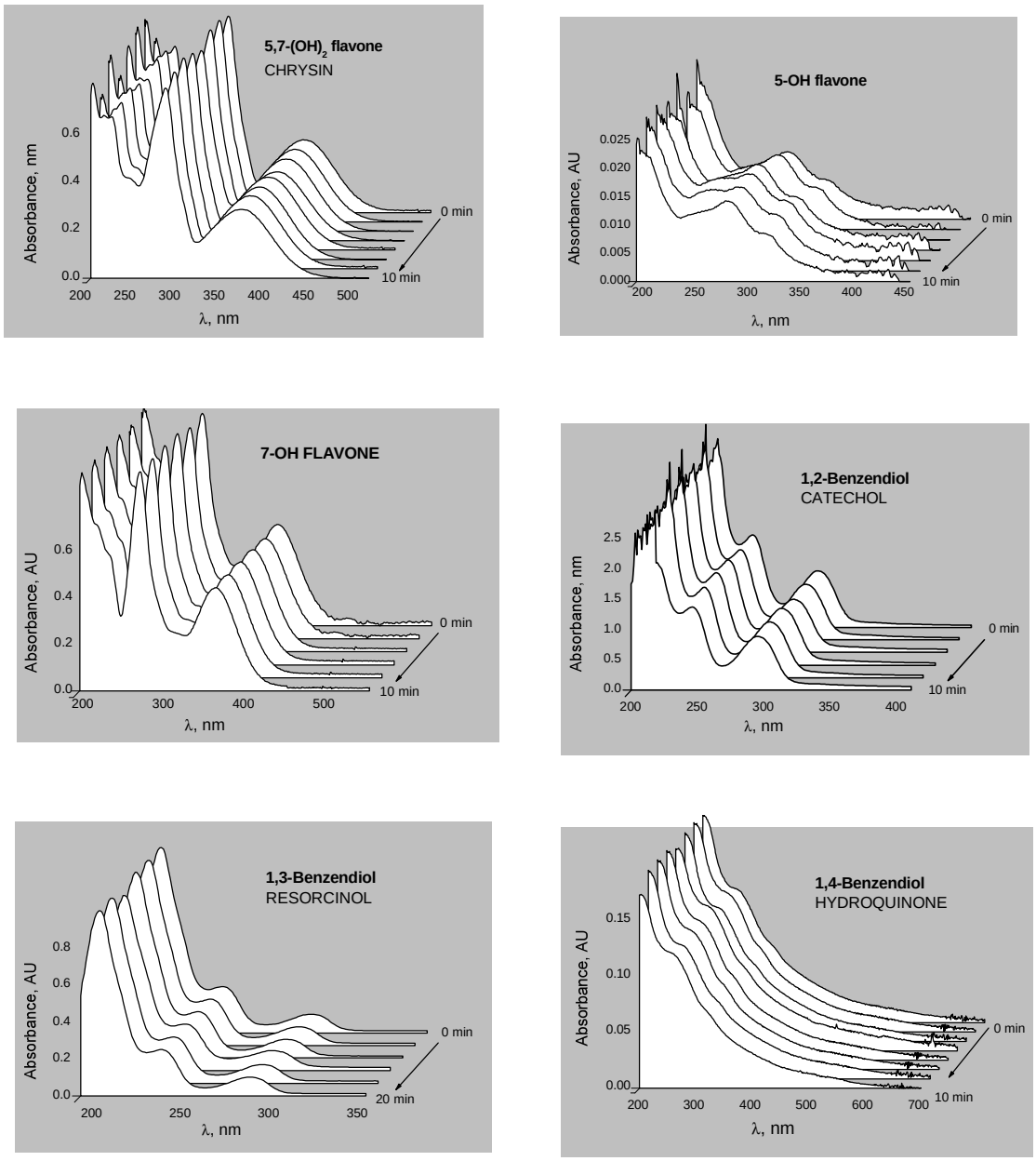

Figure 3.10 UV-Vis spectra of C-3 hydroxyl group lacking flavonoids and *o*-, *p*- and *m*-benzendiols (**e-g** and **h-j** in Table 3.1, respectively) obtained between 0 and 10 minutes of reaction time. [MnTACN], 2.5 μM; [flavonoid] or [benzendiol], 160 μM; 10 mM $NaHCO_3$ buffer, pH 10.2 at 25°C.

An alternative explanation for the structure-reactivity dependence may lie in the importance of the C-3 hydroxyl group in achieving planarity of rings A and B (Figure 3.4a) [48]. Until recently the structure-activity relationship of flavonoids has mainly been descriptive, not explanatory by means of a quantitative relationship. Usually conjugation effects are mentioned but this does not explain why flavonoids with a hydroxyl at C-3 are more active towards catalytic oxidation. In order to explain this phenomenon in a molecular way, van Acker ***et al.*** [48] calculated that the torsion angle of ring B with the rest of the flavonoid molecule was correlated with scavenging activity of the flavonoids. In quercetin

(structure **1** in Figure 3.2), the C-3 hydroxyl moiety anchored the position of ring B in the same plane as rings A and C (Figure 3.4) via hydrogen bonds, resulting in a torsion angle of ring B with the rest of the molecule close to 0° and thereby yielding increased coplanarity of ring B. Removal of the hydroxyl moiety at C-3 induced a torsion angle of approximately 20° of ring B with the rest of the molecule, causing a loss of coplanarity and decreasing the conjugation.

3.5.2 ESI-MS and proton NMR studies of morin and the reaction product

Electrospray ionisation-mass spectrometry (ESI-MS) analysis of morin and the oxidation product is performed in a negative mode using somewhat modified conditions when compared to those typical for the UV-Vis experiments. Thus the reactions studied by ESI-MS were performed in aqueous solutions of LiOH (pH 11.3) instead of using the $NaHCO_3$/NaOH buffer. This was to avoid the formation of sodium cluster ions in ESI-MS [49]. In the absence of the catalyst, the ESI-MS of morin shows characteristic peaks with *m*/*z* 301 (dominant peak) identified as a singly charged species of morin and *m*/*z* 603 (Figure 3.11a), which comes from singly charged species of a dimerised morin species. The ESI-MS spectra of reaction mixture of morin with MnTACN scanned at timed intervals (Figure 3.11b and 3.11c) show a new signal with *m*/*z* 317 apart from *m*/*z* 301. This peak, characteristic of the adduct, a singly charged species with one oxygen atom transferred to the molecule of morin, increases to a maximum at the expense of the ion of morin. In the final phase (Figure 3.11d), a peak attributable to the ion of morin *m*/*z* 301 disappears completely, whereas *m*/*z* 317 is the only clearly detected signal.

The ESI-MS spectra of morin and the oxidation product therefore suggest that the reaction proceeds predominantly via a monooxygenase mechanism (one O-atom incorporated into the molecule of morin).

The NMR spectrum of morin in DMSO-d_6 at 25^{o}C (partially shown in Figure 3.12) and chemical shifts of the five aromatic protons is consistent with its structure and the literature data [50]. The NMR spectra of the oxidised product and morin show a key similarity, that is 5 aromatic resonances for each spectrum (Figure 3.12). This agrees with the ESI-MS results providing an additional evidence that morin has not been oxidised and hydrolysed to the free benzoic acids. A unique structure validation based on the one-dimensional NMR data is however difficult [21].

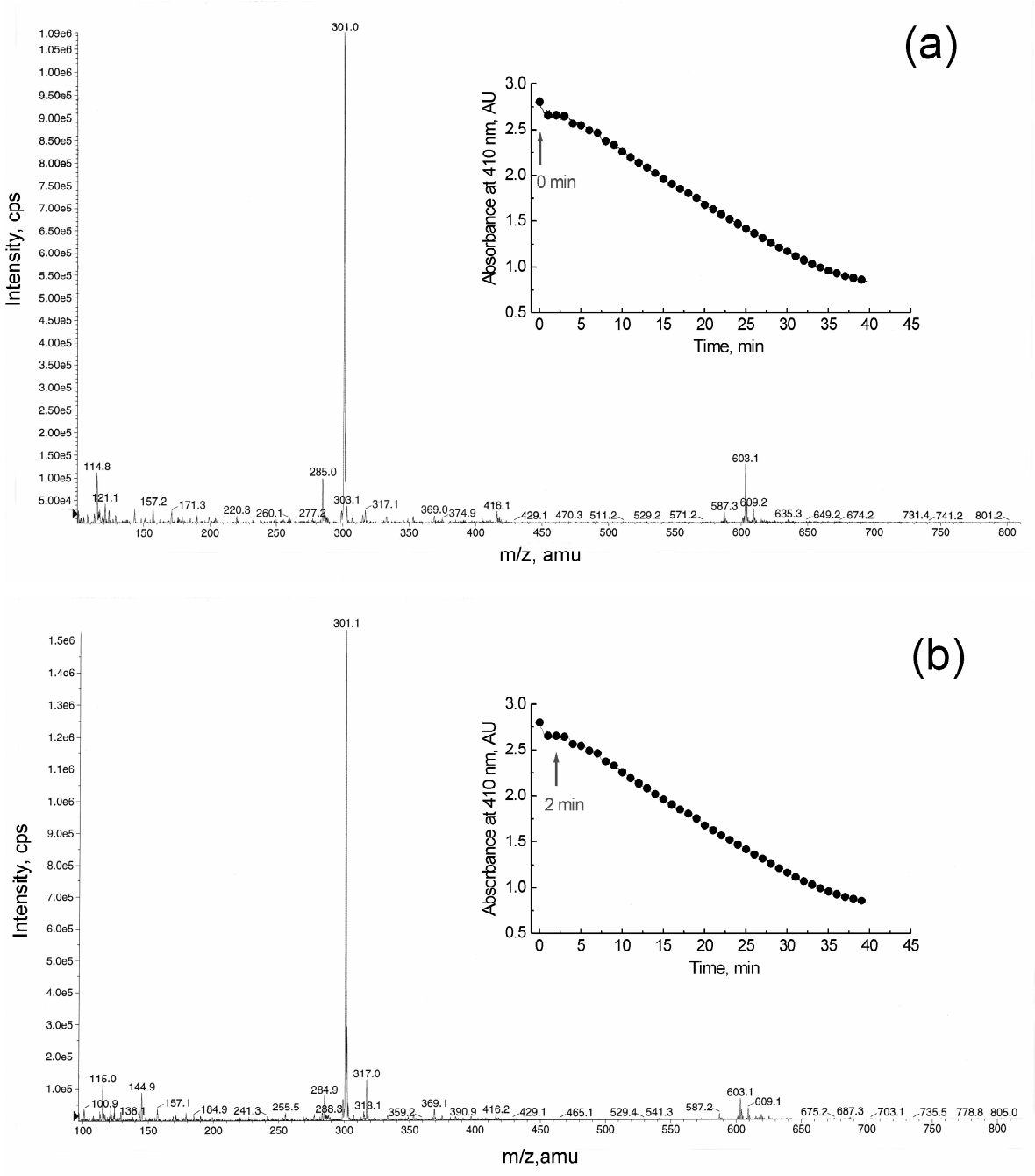

Figure 3.11 ESI-MS spectra of an aqueous solution of morin before (a) and after 2 min (b) of reaction with O_2/MnTACN (pH 11.3, 25°C) compared with the UV-Vis reaction profiles obtained under the same reaction conditions.

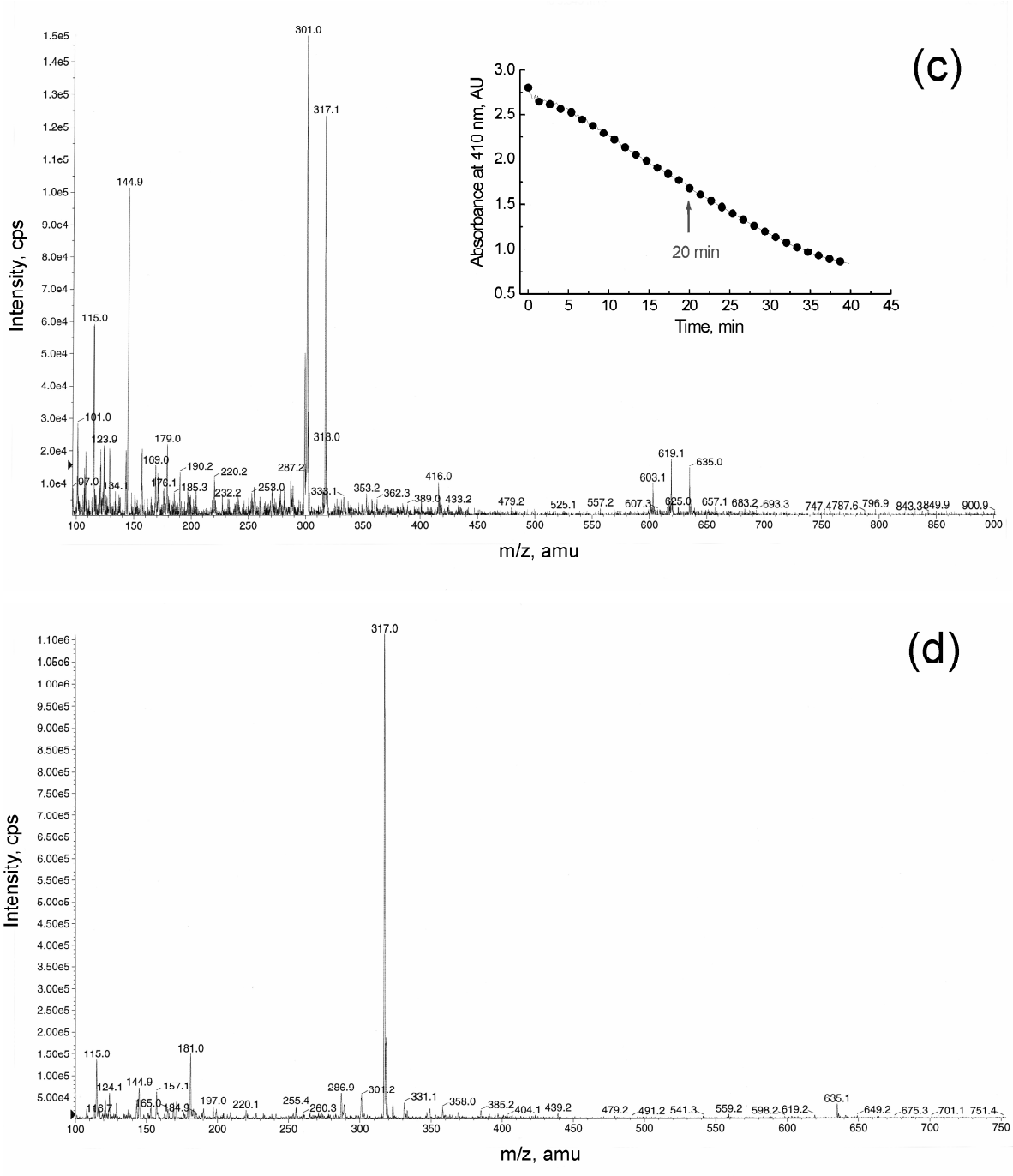

Figure 3.11 (*continued*) ESI-MS spectra of an aqueous solution of morin after 20 min (c) and 2 h (d) of reaction with O_2/MnTACN (pH 11.3, 25^{o}C) compared with the UV-Vis reaction profile obtained under the same reaction conditions.

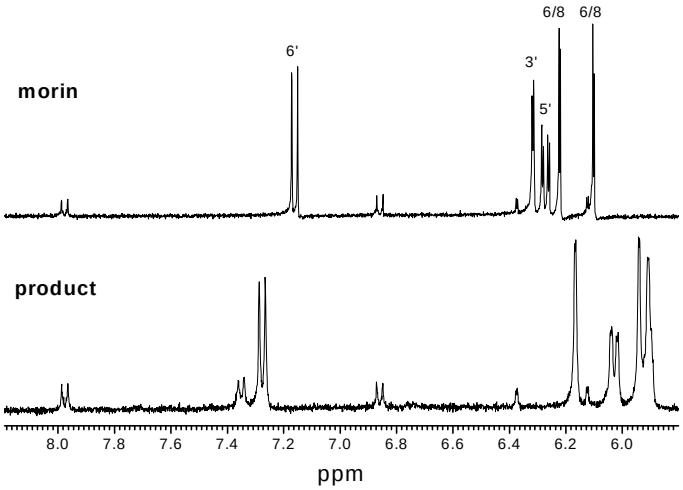

Figure 3.12 Proton NMR spectrum of morin and the reaction product.

An increased molecular weight of 16 g/mol of the oxidation product confirmed by ESI-MS with respect to its parent compound morin (*m/z* 317, the reaction product; *m/z* 301, morin) with unchanged substitution pattern in the A- and B-ring shown by ^{1}H NMR are in agreement with the data published earlier for the product of electrochemical, metal-catalysed, and peroxyl radical oxidation of C-3 hydroxyl flavonoids which are discussed in Section 3.2. The UV-Vis spectra change in the same manner [51] making it likely that a substituted benzo-furanone (2-(2,4-dihydroxybenzoyl)-2,4,6-trihydroxy-3(2*H*)-benzofuranone is formed converting the pyranone C-ring of morin to a furanone-carbonyl derivative as shown in Figure 3.13.

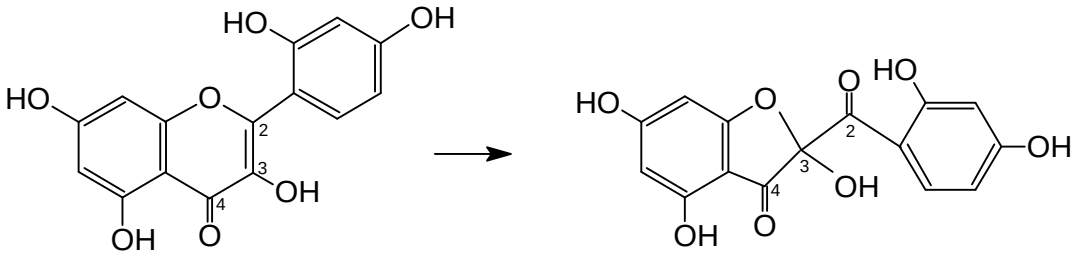

Figure 3.13 Product of the oxidation of morin proposed on the basis of comparison of experimental data (ESI-MS, proton NMR and UV-Vis) and the literature data. (Note: numbering of C-atoms does not follow IUPAC rules, but was adapted from the numbering used in the literature for comparison of NMR results).

3.5.3 ESI-MS study of MnTACN

ESI-MS experiments were carried out on aqueous solutions of MnTACN as well as mixtures of MnTACN with O_2 and/or morin operating the spectrometer in a negative mode under the same conditions explained in Section 3.5.2. The dominant peaks in the spectrum from MnTACN are at *m*/*z* 250 and *m*/*z* 645

(Figure 3.14a), consistent with dicationic $[L_2Mn(IV)_2(\mu\text{-}O)_3]^{2+}$ and the monocationic species $[L_2Mn(IV)_2(\mu\text{-}O)_3]^{2+}(PF_6)^{1-}$ respectively, where L is ligand TACN.

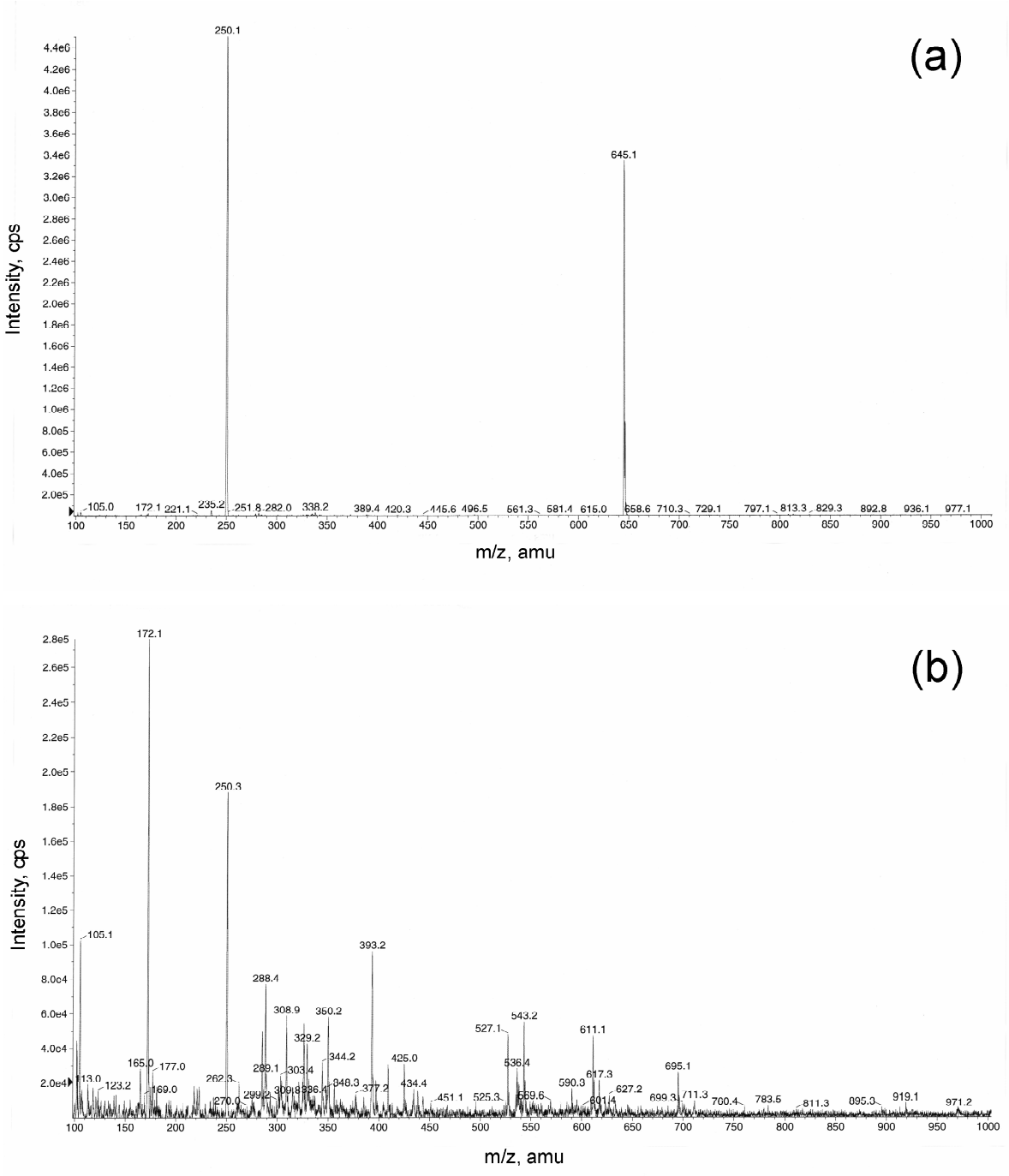

Figure 3.14 ESI-MS spectra of an aqueous solution (pH 11.3) of MnTACN before (a) and 5 minutes after addition of morin (b).

Addition of morin to MnTACN leads to detection of many new signals (Figure 3.14b), whereas the intensity of a peak at ***m/z*** 250 is still quite remarkable suggesting the existence of dinuclear $[L_2Mn(IV)_2(\mu\text{-}O)_3]^{2+}$ form of the catalyst

MnTACN in the reaction mixture after addition of morin. The ion with ***m/z*** 172 is assigned to the protonated free ligand TACN (LH^+). Some of the new species (e.g. ***m/z*** 329, 165) can perhaps be characterised as dinuclear species $[LMn(III)Mn(IV)(\mu\text{-}O)_3]^+$ and $[LMn(IV)_2(\mu\text{-}O)_3]^{2+}$ respectively, resulting from the ligand exchange (i.e. liberation of ligand L). Besides, it cannot be excluded that some of the new signals such as ***m/z*** 543 and ***m/z*** 527 originate from mononuclear Mn(IV) and Mn(II) complexes with morin: $[(morin^-)LMn(IV)=O]^+$ and $[(morin^-)LMn(II)]^+$.

The results from the ESI-MS experiments suggest that the dinuclear manganese species play an important role, whereas the ligand exchange can be the real situation. The ligand exchange rates in the manganese complexes are dependent on the oxidation state of manganese, i.e. they are dramatically faster in Mn(II) and Mn(III) than in Mn(IV) complexes [52]. Manganese triazacyclononane complexes, in which the manganese ions are chelated in a hexadentate fashion, are reported to be active only if at least one of the ligand arms in the complex becomes detached from the manganese ion to open up a free coordination site for an incoming peroxide or substrate molecule [53].

3.5.4 Effect of ligand TACN

We have shown in Chapter 2 that under identical reaction conditions Mn(II) salts ($MnCl_2$ or $MnSO_4$), although effective in the oxidation of morin, catalyse this reaction with a considerably lower maximum reaction rate than MnTACN at the different temperatures and pHs, which precludes the possibility of that the catalysis observed for MnTACN is due to ligand dissociation to produce free Mn(II).

Table 3.2 % Discolouration of morin in the reactions catalysed by MnTACN or Mn(II) as a function of the addition of ligand TACN [(i)].

Catalyst	% Discolouration at	
	5 min	10 min
MnTACN	31	57
MnTACN / 1 eq. of TACN	34	59
MnTACN / 10 eq. of TACN	32	56
MnTACN / 100 eq. of TACN	26	41
$MnCl_2$ ($MnSO_4$)	15 (12)	25 (21)
$MnCl_2$ / 1 eq. of TACN	17	37
$MnCl_2$ / 10 eq. of TACN	16	36
$MnCl_2$ / 100 eq. of TACN	15	27

[(i)] [MnTACN], 2.5 μM; [$MnCl_2$] or [$MnSO_4$], 5 μM; [morin], 160 μM; 10 mM $NaHCO_3$ buffer, pH 9.5; 25°C.

Indeed, *in situ* formation of Mn(II)-TACN species by addition of 1-10 equivalents of the ligand 1,4,7-trimethyl-1,4,7-triazacyclononane (TACN) to the reaction mixture of morin and $MnCl_2$ has no significant effect on the observed reaction kinetics (Table 3.2). Interestingly, the addition of 100 equivalents of the ligand TACN has an inhibitory effect on the reaction catalysed by either free Mn(II) or MnTACN. From the literature it is known that the TACN ligand can also be oxidised by MnTACN/H_2O_2 and if present in large amounts, the retardation of reaction with morin is perhaps a result of competition between morin and the ligand for the oxidant [40].

3.5.5 Stability of the catalyst

The stability of MnTACN under the reaction conditions was examined by repeated additions of morin to a solution of MnTACN at pH 10.2. These experiments reveal that no significant change in reaction kinetics is observed for the second and third addition, whilst subsequent additions of morin to the reaction mixture involving MnTACN lead to a gradual deceleration of the reaction (Figure 3.15).

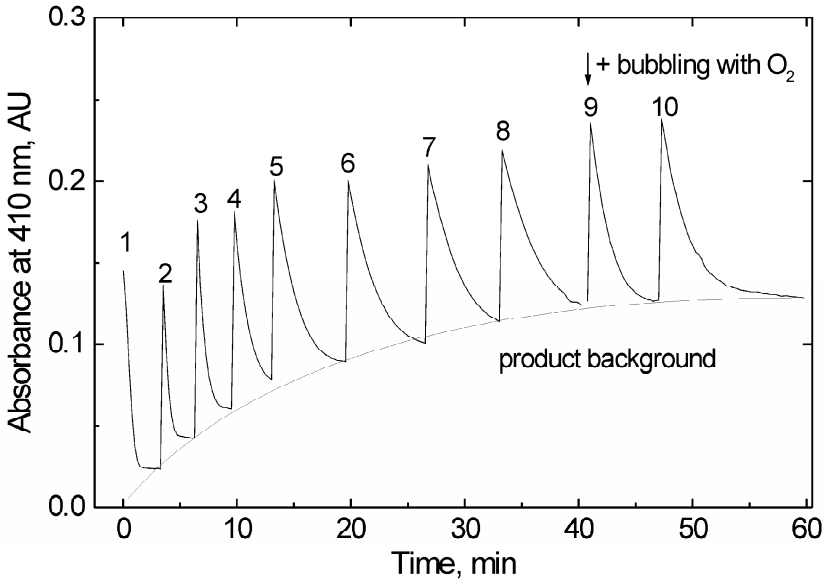

Figure 3.15 Time dependence of the reaction as a function of the repeated additions of morin. Reaction conditions: (**1**) 25 µL of a 0.1 mM stock solution of MnTACN was added to 1 mL of a 80 µM solution of morin in buffer; (**2-10**) 80 µL of a 1 mM stock solution of morin added to the reaction mixture; (**9**) gassed with O_2 prior to addition of morin.

Most importantly, it seems that the manganese complex is not destroyed after the second addition of morin. On the contrary, after approximately 320 turnovers it is still able to effectively catalyse oxidation of morin. The O_2 gassing of the reaction mixture prior to addition of a fresh aliquot of a stock solution of morin

(addition no. 9 in Figure 3.14) results in somewhat faster reaction rate. This signifies that the gradual deceleration of reaction after addition no. 4 of morin is not only because of decrease in the stability of MnTACN but also due to a decrease in the concentration of oxygen.

3.5.6 Effect of temperature: kinetics and activation parameters

The temperature dependence of the first-order rate constant k is studied at pH 9.5 and pH 10.0 over the temperature range 20-60°C. As a reference, the reaction kinetics of oxidation of morin in the absence of MnTACN (autooxidation of morin) is followed over the same temperature range at pH 10. As expected, the reaction rates increase gradually in all cases with rise in temperature (Table 3.3).

Table 3.3 Kinetic data for the oxidation of morin over a temperature range 20-60°C at pH 10 and pH 9.5. [(i)]

Temp. °C	pH 10.0			pH 9.5		
	$(-dC_M/dt)_{max} \times 10^6$ mol L^{-1} s^{-1}	$k \times 10^2$ s^{-1}	R [(ii)]	$(-dC_M/dt)_{max} \times 10^6$ mol L^{-1} s^{-1}	$k \times 10^2$ s^{-1}	R [(ii)]
20	0.18	0.28	0.999			
25	0.38 0.01 [(iii)]	0.36 0.00[(iii)]	0.999 0.999	0.02	0.10	0.997
30	0.56±0.01 0.01[(iii)]	0.56±0.11 0.01[(iii)]	0.999 0.999	0.03	0.17	0.999
35	0.84±0.00 0.01[(iii)]	0.95±0.03 0.01[(iii)]	0.998 0.996	0.06	0.30	0.998
40	1.34±0.04 0.02 [(iii)]	1.66±0.15 0.02 [(iii)]	0.999 0.997	0.07	0.40	0.999
45	1.72±0.00	2.20±0.04	0.998			
50	3.66±0.20 0.06 [(iii)]	3.78±0.06 0.06 [(iii)]	0.999 1.000	0.11	0.75	0.999
55	4.42±0.46	4.53±0.07	0.992			
60	6.11±0.69 0.19 [(iii)]	6.04±0.04 0.16 [(iii)]	0.996 1.000	0.18	1.42	0.999

[(i)] Reaction conditions: [MnTACN], 2.5 μM; [morin], 160 μM; 10 mM $NaHCO_3$ buffer, pH 10 at 25°C.
[(ii)] Correlation coefficients of least-squares regressions.
[(iii)] In the absence of the catalyst MnTACN (the autooxidation of morin).

Interestingly, the effect of pH is remarkable and a much faster catalysis is observed at pH 10 than at pH 9.5 regardless of reaction temperature (25-60^{o}C). For example, at 25^{o}C the rate constant icreases with a factor 3.6 when pH is raised from pH 9.5 to pH 10, whilst the rise in temperature from 25^{o}C to 40^{o}C at pH 9.5 leads to the similar increase (with a factor 4).

From literature [54-55] is known that most flavonoids are singly (or doubly) deprotonated at pH 10 in a fast pre-equilibrium to yield the flavonolate anion (Figure 3.16). In contrast to pH 9.5 where the deprotonation is not complete, at pH 10 the concentration of the initial flavonolate concentration is identical to the initial flavonoid concentration. The pH dependence of the reaction, as well as the electrophylic nature of the catalyst [35, 40], indicate that the morin anion is more susceptible to be attacked by the MnTACN catalytic system than a protonated morin species.

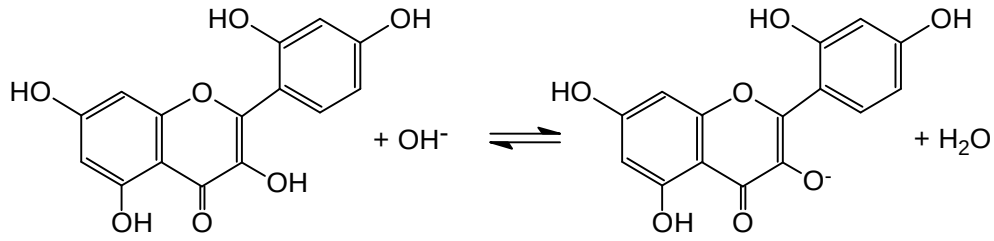

Figure 3.16 Deprotonation of morin in alkaline media.

In addition, oxidation is expected to be favoured at higher pH because the higher concentration of perhydroxyl anion (HOO^- is more nucleophilic than H_2O_2). The pK_a value of the deprotonation equilibrium between H_2O_2 and HOO^- at 25^{o}C is 11.65. However, it is known that at such high pH active Mn-species derived from MnTACN are not stable [5, 40]. Consequently, the pH where the maximum rate constant is obtained (see Figure 2.7 in Chapter 2) is most likely a result of the three effects, i.e. the ionisation of both morin and H_2O_2 as well as the stability of the catalyst active species.

The temperature dependence of the reaction rate of catalysed reactions at pH 9.5 and pH 10 is compared to that of the autoxidation of morin in the Arrhenius plot (Figure 3.17). In all cases, ln k vs. 1/T gives a straight line over the temperature range of 20-60^{o}C. Consequently, the Eyring plot of ln (k/T) vs. 1/T also results in a straight line and is used to calculate the other activation parameters shown in Table 3.4. The activation energy E_a given in Table 3.4 is calculated from the slope of the Arrhenius plot.

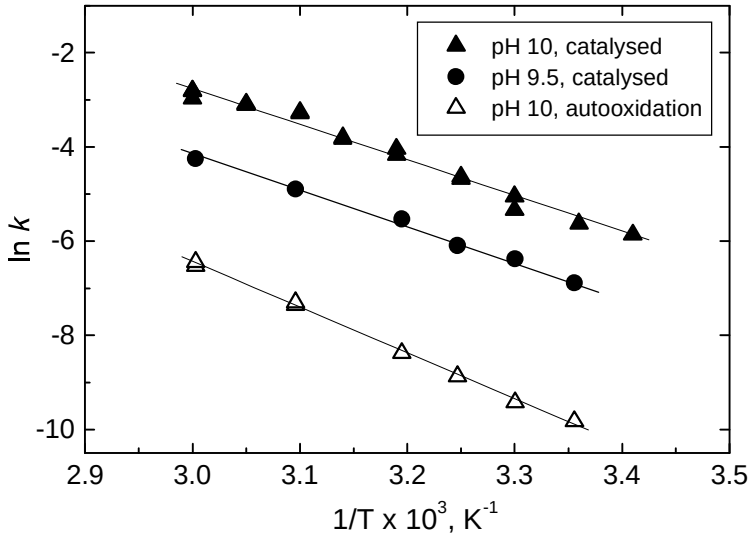

Figure 3.17 Arrhenius plot for the catalysed reactions at pH 9.5 and pH 10 as well as the autooxidation of morin at pH 10.

The other activation parameters shown in Table 3.4 are calculated using Eqs. 3.3 and 3.4. It may be seen that while there is no appreciable difference in the enthalpy of activation $\Delta H^{\#}$, the entropy of activation $\Delta S^{\#}$ is 12 eu more negative at pH 9.5. This large negative value suggests that the formation of the transition state is accompanied by a considerable loss of degrees of freedom, i.e. the reaction is entropy controlled, which is characteristic for an electron transfer mechanism [55-56]. As a further example, an order of magnitude difference in the rates of oxidation at pH 10 and pH 9.5 originates from the more negative $\Delta S^{\#}$ in the case of reaction at pH 9.5.

Table 3.4 Activation parameters of the MnTACN catalysed oxidation of morin determined at pH 9.5 and pH 10 and the autooxidation at pH 10 at 25°C.

pH	$-dC_M/dt$ mol L^{-1} s^{-1}	$\Delta H^{\#}$, kJ mol^{-1}	$\Delta S^{\#}$, kJ mol^{-1} K^{-1}	$\Delta G^{\#}$, kJ mol^{-1} K^{-1}	E_a, kJ mol^{-1}
		MnTACN catalysed oxidation			
10	3.8×10^{-5}	60.3 ± 0.8	-290 ± 2	149.4	63.0 ± 0.8
9.5	0.2×10^{-5}	61.3 ± 1.4	-302 ± 5	152.9	62.9 ± 0.8
		Autooxidation of morin			
10	0.0×10^{-5}	78.3 ± 1.9	-324 ± 6	177.4	80.9 ± 1.9

3.6 Mechanistic conclusions

On the basis of experimental data and the data available in the literature, suggestions can be made for the possible mechanism of the MnTACN catalysed oxygenation of morin. These are summarised in Figure 3.18 and Figure 3.19. According to the mechanistic pathway proposed in Figure 3.18, in the first step the mesomeric form **2** of the deprotonated morin (flavonolate ion **1**) complexes Mn(IV)Mn(IV) form of MnTACN followed with an electron transfer from the flavonolate ion to manganese(IV), resulting in the complex of catalytically active dimer Mn(III)Mn(IV) coordinated to the flavonoxy radical (structure **3**). This complex reacts with dioxygen in the rate-determining step to form a superoxide complex with the flavonoxy radical coordinated to the manganese ion (**4**).

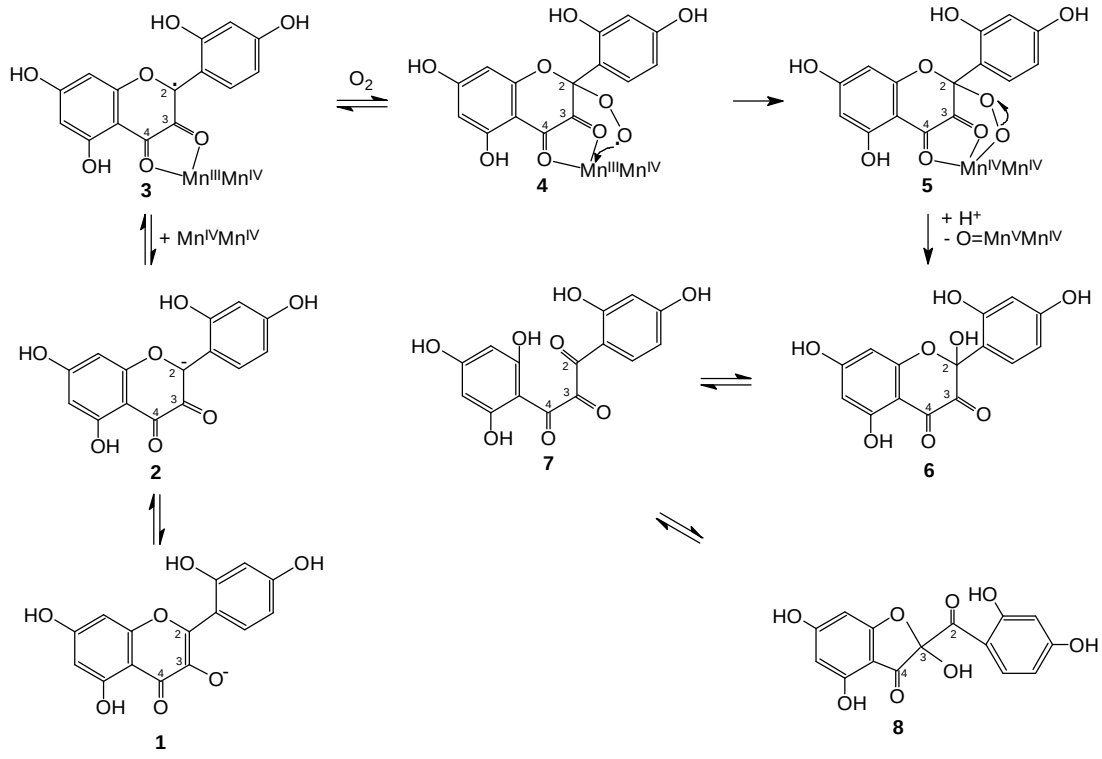

Figure 3.18 Overall mechanism suggested for the oxygenation of morin by O_2/MnTACN in aqueous alkaline media.

Further possible fast reaction steps of the complex **4** leading to the endproduct **6→8** are as shown in Figure 3.18. It is reasonable to assume an intramolecular attack of superoxide radical on manganese in which peroxide species **5** is formed. The cyclic peroxide **5** undergoes an asymmetric intramolecular decomposition first to yield a 3,4-flavandione **6**, 2-(1,3-dihydroxyphenyl)-2-hydroxybenzopyran-3,4-dione, which rearranges to form a substituted 3(2*H*) benzofuranone **8**, 2-(hydroxybenzoyl)-2-hydroxybenzofuran-3(2*H*)-one, through

the chalcan-trione ring-chain tautomer **7**. This is likely followed with the oxidation of manganese and the formation of O=Mn(V)Mn(IV) species which has been proposed as a catalytically active intermediate.

The mechanism outlined in Figure 3.18 gives a simplified picture in terms of the fate of MnTACN. It involves the cyclic regeneration of the catalyst reduced to Mn(III)Mn(IV) in a single-electron transfer through the subsequent oxidation by H_2O_2 into O=Mn(V)Mn(IV) species. Figure 3.19 summarises the other possibilities which also include the involvement of mononuclear catalyst species [57]. It is possible that reoxidation of the MnTACN reduced species by O_2, generates superoxide and/or hydrogen peroxide (Figure 3.19a). Both superoxide and H_2O_2 can in turn be activated by the catalyst to form active high-valent mono or dinuclear oxo- or peroxo-manganese species (Figure 3.19b).

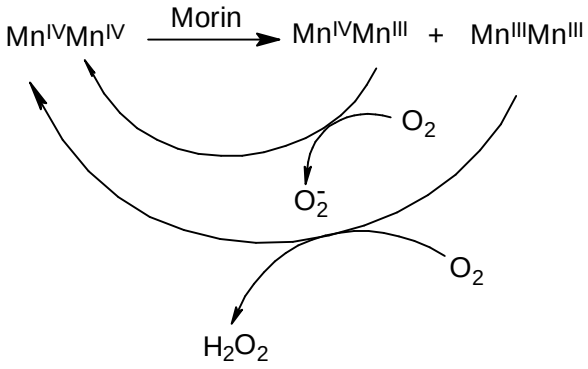

(a)

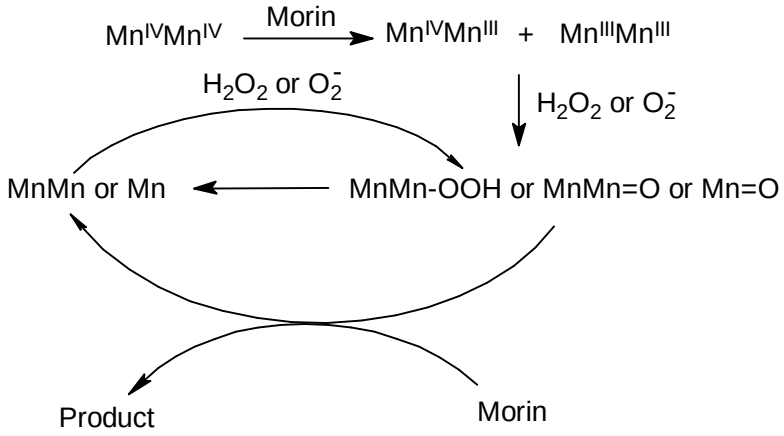

(b)

Figure 3.19 Mechanism of MnTACN catalysis [57].

The proposed mechanistic pathways correlate well with the experimental results obtained in Chapter 2 and Chapter 3. In general, this study sheds more light on the catalytic oxidation of cotton pigment morin as well as the modes of action of the catalyst MnTACN. It is expected that the knowledge generated on the mechanism of reaction under homogeneous conditions will contribute to a better understanding of the reaction in a real (heterogeneous system) that includes cotton substrate. The latter will be the subject of discussion in the following chapters. Besides, it is expected that organic chemists will be interested to find out whether this type of catalysed oxidation has synthetic uses too.

Literature cited

[1] Wieprecht, T., Xia J., Heinz, U., Dannacher, J., Schlingloff, G., Novel terpyridine-manganese(II) complexes and their potential to activate hydrogen peroxide, J. Mol. Catal. A: Chem., **203** (2003) 113-128.

[2] Thompson, K.M, Spiro, M., Griffith, W.P., Mechanism of bleaching by peroxides. Part 4: Kinetics of bleaching of malvin chloride by hydrogen peroxide at low pH and its catalysis by transition-metal salts, J. Chem. Soc., Faradey Trans., **92** (1996) 2535-2540.

[3] Ohura, R., Katayama, A. Takagishi, T., Decoloration of Natural Coloring matter with Sodium Percarbonate, Text. Res. J., **61** (1991) 242-246.

[4] Pulvirenti, A.L, Epoxidation and bleaching catalyses by homo- and heterogeneous manganese, cobalt, and iron azamacrocyclic complexes, PhD thesis, Purdue University, 2000.

[5] Hage, R., Iburg, J.E., Kerschner, J., Koek, J.H., Lempers, E.L.M., Martens, R.J., Racherla, U.S., Russell, S.W., Swarthoff, T., van Vliet, M.R.P., Warnaar, J. B., van der Wolf, L., Krijnen, L.B., Efficient manganese catalysts for low-temperature bleaching, Nature **369** (1994) 637-639.

[6] Bors, W., Heller, W., Michel, C., Saran, M., Flavonoids as antioxidants: Determination of radical-scavenging efficiencies, Methods Enzymol., **186** (1990) 343-355.

[7] Rice-Evans, C.A., Miller, N.J., Antioxidant activities of flavonoids as bioactive components of food, Biochem. Soc. Trans., **24** (1996) 790-795.

[8] Cook, N.C., Samman, S., Flavonoids - Chemistry, metabolism, cardioprotective effects, and dietary sources, J. Nutr. Biochem., **7** (1996) 66-76.

[9] van Acker, S.A.B.E., van den Berg, D.-J., Tromp, M.N.J.L., Griffioen, D.H., van Bennekom, W.P., van der Vijgh, W.J.F., Bast, A., Structural aspects of antioxidant activity of flavonoids, Free Radical Biol. Med., **20** (1996) 331-342.

[10] Makris, D.P., Rossiter, J.T., Hydroxyl free radical-mediated oxidative degradation of quercetin and morin: A preliminary investigation, J. Food Comp. Anal., **15** (2002) 103-113.

[11] Lippai, I., Speier, G., Quercetinase model studies. The oxygenation of flavonol catalyzed by a cationic 2,2'-bipyridine copper(II) flavonolate complex, J. Mol. Catal. A: Chem., **130** (1998) 139-148.

[12] Miller, E., Schreier, P., Studies on flavonol degradation by peroxidase (donor: H2O2-oxidoreductase, EC 1.11.1.7): Part 1 - kaempferol, Food Chem., **17** (1985) 143-154.

[13] Schreier, P., Miller, E., Studies on flavonol degradation by peroxidase (donor: H2O2-oxidoreductase, EC 1.11.1.7): Part 2 - quercetin, Food Chem., **18** (1985) 301-317.

[14] Jiménez, M., García-Carmona, F., Oxidation of the flavonol quercetin by polyphenol oxidase, J. Agric. Food Chem., **47** (1999) 56-60.

[15] Wedepohl, K., Schwedt, G., Analysis of copper/flavonoid complexes as element species

in vegetables, Anal. Chim. Acta, **203** (1987) 23-34.
[16] Miller, N.J., Castelluccio, C., Tijburg, L., Rice-Evans, C., The antioxidant properties of theaflavins and their gallate esters - Radical scavengers or metal chelators?, FEBS Lett., **392** (1996) 40-44.
[17] Marmolle, F., Leize, E., Mila, I., van Dorsselaer, A., Scalbert, A., Albrecht-Gary, A.M., Polyphenol metallic complexes: Characterization by electrospray mass spectrometric and spectrophotometric methods, Analysis, **25** (1997) M53-M55.
[18] Awad, H.M., Boersma, M.G., Vervoort, J., Rietjens, I.M.C.M., Peroxidase-catalyzed formation of quercetin quinone methide-glutathione adducts, Arch. Biochem. Biophys., **378** (2000) 224-233.
[19] Krishnamachari, V., Levine, L.H., Paré, P.W., Flavonoid oxidation by the radical generator AIBN: A unified mechanism for quercetin radical scavenging, J. Agric. Food Chem., **50** (2002) 4357-4363.
[20] Jørgensen, L.V., Cornett, C., Justesen, U., Skibsted, L.H., Dragsted, L.O., Two-electron electrochemical oxidation of quercetin and kaempferol changes only the flavonoid C-ring, Free Radical Res. Commun., **29** (1998) 339-350.
[21] Jungbluth, G., Rühling, I., Ternes, W., Oxidation of flavonols with Cu(II), Fe(II) and Fe(III) in aqueous media, J. Chem. Soc., Perkin Trans., **2** (2000) 1946-1952.
[22] Hirose, Y., Fujita, T., Nakayama, M., Structure of doubly-linked oxidative product of quercetin in lipid peroxidation, Chem. Lett. (1999) 775-776.
[23] Tournaire, C., Hocquaux, M., Beck, I., Oliveros, E., Maurette, M.-T., Anti-oxidant activity of flavonols: Reactivity with potassium superoxide in the heterogeneous phase, Tetrahedron, **50** (1994) 9303-9314.
[24] Kano, K., Mabuchi, T., Uno, B., Esaka, Y., Tanaka, T., Iinuma, M., Superoxide anion radical-induced dioxygenolysis of quercetin as a mimic of quercetinase, J. Chem. Soc., Chem. Commun. (1994) 593-594.
[25] Oka, T., Simpson, F.J., Krishnamurty, H.G., Degradation of rutin by Aspergillus flavus. Studies on specificity, inhibition, and possible reaction mechanism of quercetinase, Can. J. Microbiol., **18** (1972) 493-508.
[26] Brown, S.B., Rajananda, V., Holroyd, J.A., Evans, E.G., A study of the mechanism of quercetin oxygenation by ^{18}O labeling, Biochem. J., **205** (1982) 239-244.
[27] Balogh-Hergovich, E., Kaizer, J., Speier, G., Kinetics and mechanism of the Cu(I) and Cu(II) flavonolate-catalyzed oxygenation of flavonol. Functional quercetin 2,3-dioxygenase models, J. Mol. Catal. A: Chem., **159** (2000) 215-224.
[28] Lindsay Smith, J.R., Shul'pin, G.B., Efficient stereoselective oxygenation of alkanes by peroxyacetic acid or hydrogen peroxide and acetic acid catalysed by a manganese(IV) 1,4,7- trimethyl-1,4,7-triazacyclononane complex, Tetrahedron Lett., **39** (1998) 4909-4912.
[29] Brinksma, J., La Crois, R., Feringa, B.L., Donnoli, M.I., Rosini, C., New ligands for manganese catalysed selective oxidation of sulfides to sulfoxides with hydrogen peroxide, Tetrahedron Lett., **42** (2001) 4049-4052.
[30] Shul'pin, G.B., Süss-Fink, G., Shul'pina, L.S., Oxidations by the system "hydrogen peroxide-manganese(IV) complex-carboxylic acid" part 3. Oxygenation of ethane, higher alkanes, alcohols, olefins and sulfides, J. Mol. Catal. A: Chem., **170** (2001) 17-34.
[31] Bennur, T.H., Sabne, S., Deshpande, S.S., Srinivas, D., Sivasanker, S., Benzylic oxidation with HO catalyzed by Mn complexes of N,N′,N″-trimethyl-1,4,7-triazacyclononane: Spectroscopic investigations of the active Mn species, J. Mol. Catal. A: Chem., **185** (2002) 71-80.
[32] Gilbert, B.C., Lindsay Smith, J.R., Mairata Payeras, I.A., Oakes, J., Formation and reaction of $O=Mn^{V}$ species in the oxidation of phenolic substrates with H_2O_2 catalysed by the dinuclear manganese(IV) 1,4,7-trimethyl-1,4,7-triazacyclononane complex

$[Mn^{IV}_2(\mu\text{-}O)_3(TMTACN)_2](PF_6)_2$, Org. Biomol. Chem. (2004) 1176-1180.

[33] Barker, J.E., Ren, T., Facile oxygenation of organic sulfides with HO catalyzed by Mn-MeTACN compounds, Tetrahedron Lett., **45** (2004) 4681-4683.

[34] Smith, J.R.L., Murray, J., Walton, P.H., Lowdon, T.R., Organosulfur oxidation by hydrogen peroxide using a dinuclear Mn-1,4,7-trimethyl-1,4,7-triazacyclononane complex, Tetrahedron Lett., **47** (2006) 2005-2008.

[35] Gilbert, B.C., Kamp, N.W.J., Lindsay Smith, J.R., Oakes, J., EPR evidence for one-electron oxidation of phenols by a dimeric manganese(IV)/(IV) triazacyclononane complex in the presence and absence of hydrogen peroxide, J. Chem. Soc., Perkin Trans. (1997) 2161-2165.

[36] Gilbert, B.C., Kamp, N.W.J., Lindsay Smith, J.R., Oakes, J., Electrospray mass spectrometry evidence for an oxo-manganese(V) species generated during the reaction of manganese triazacyclononane complexes with H_2O_2 and 4-methoxyphenol in aqueous solution , J. Chem. Soc., Perkin Trans. (1998) 1841-1843.

[37] Barton, D.H.R., Choi, S.-Y., Hu, B., Smith, J.A., Evidence for a higher oxidation state of manganese in the reaction of dinuclear manganese complexes with oxidants. Comparison with iron based gif chemistry, Tetrahedron, **54** (14) 3367-3378.

[38] Gilbert, B.C., Lindsay Smith, J.R., Mairata I Payeras, A., Oakes, J., Pons I Prats, R., A mechanistic study of the epoxidation of cinnamic acid by hydrogen peroxide catalysed by manganese l,4,7-trimethyl-l,4,7-triazacyclononane complexes, J. Mol. Catal. A: Chem., **219** (2004) 265-272.

[39] Smith, J.R.L., Murray, J., Walton, P.H., Lowdon, T.R., Organosulfur oxidation by hydrogen peroxide using a dinuclear Mn-1,4,7-trimethyl-1,4,7-triazacyclononane complex, Tetrahedron Lett., **47** (2006) 2005-2008.

[40] Gilbert, B.C., Lindsay Smith, J.R., Newton, M.S., Oakes, J., Pons i Prats, R., Azo dye oxidation with hydrogen peroxide catalysed by manganese 1,4,7-triazacyclononane complexes in aqueous solution, Org. Biomol. Chem., **1** (2003) 1568-1577.

[41] Sadov, F., Korchagin, M., Matetsky, A., Natural admixtures of cotton fibre. In "Chemical technology of fibrous materials", Mir Publishers, Moscow (1973) pp. 45-56.

[42] Jurd, L., Spectral properties of flavonoid compounds. In: "Chemistry of flavonoid compounds", Ed. Geissman, T.A., Pergamon Press, New York (1962) pp. 107-155.

[43] Costas, M., Mehn, M.P., Jensen, M.P., Que, L. Jr., Dioxygen Activation at Mononuclear Nonheme Iron Active Sites: Enzymes, Models, and Intermediates, Chem. Rev., **104** (2004) 939-986.

[44] Reynolds, M.F., Costas, M., Ito, M., Jo, D.-H., Tipton, A.A., Whiting, A.K., Que, L.J., 4-Nitrocatechol as a probe of a Mn(II)-dependent extradiol-cleaving catechol dioxygenase (MndD): Comparison with relevant Fe(II) and Mn(II) model complexes, J. Biol. Inorg. Chem., **8** (2003) 263-272.

[45] Hörhammer, L., Hänsel, R., Hieber, W., Über die unterschiedliche Stabilität füng- und sechsgliedriger Chelate des Zr^{+4}-Ions mit Polyoxyflavonen, Naturwissenschaften, **41** (1954) 529.

[46] Hörhammer, L., Hänsel, R., Hieber, W., Spektrophotometrische Untersuchungen an Komplexen des Zirkonium (IV)-Ions mit Polyoxyflavonen. II. Die Systeme mit Flavonol und Myricetin. Fresenius' Z. Anal. Chem., **148** (1955) 251-259.

[47] Kaizer, J., Pap, J., Speier, G., Párkányi, L., The reaction of $\mu\text{-}\eta^2\text{:}\eta^2$-peroxo- and bis($\mu$-oxo)dicopper complexes with flavonol, Eur. J. Inorg. Chem., **11** (2004) 2253-2259.

[48] van Acker, S.A.B.E., de Groot, M.J., van Berg, D.-J.D., Tromp, M.N.J.L., Kelder, G.D.-O.D., van der Vijgh, W.J.F., Bast, A., A quantum chemical explanation of the antioxidant activity of flavonoids, Chem. Res. Toxicol., **9** (1996) 1305-1312.

[49] Zhou, S., Hamburger, M., Formation of Sodium Cluster Ions in Electrospray Mass Spectrometry, Rapid. Commun. Mass Spectrom., **10** (1996) 797-800.

[50] Wu, T.-W., Fung, K.-P., Zeng, L.-H., Wu, J., Hempel, A., Grey, A.A., Camerman, N.,

Molecular properties and myocardial salvage effects of morin hydrate, Biochem. Pharmacol., **49** (1995) 537-543.

[51] Jungbluth, G., Ternes, W., HPLC separation of flavonols, flavones and oxidized flavonols with UV-, DAD-, electrochemical and ESI-ion trap MS detection, Fresenius J. Anal. Chem., **367** (2000) 661-666.

[52] Pecoraro, V.L., Manganese redox enzymes, VCH, New York, 1992.

[53] de Vos, D.E., Bein, T., Highly selective olefin epoxidation with manganese triazacyclononane complexes: impact of ligand substitution, J. Organomet. Chem., **520** (1996) 195-200.

[54] Balogh-Hergovich, E., Speier, G., Kinetics and Mechanism of the Base-Catalyzed Oxygenation of Flavonol in DMSO-H_2O Solution, J. Org. Chem., **66** (2001) 7974-7978.

[55] Jovanovic, S.V., Steeden, S., Tosic, M., Marjanovic, B., Simic, M.G., Flavonoids as Antioxidants, J. Am. Chem. Soc., **116** (1994) 4846-4851.

[56] Jovanovic, S.V., Jankovic, I., Josimovic, L., Electron-transfer reactions of alkyl peroxy radicals, J. Am. Chem. Soc., **114** (1992) 9018-9021.

[57] Personal communication with Dr. R. Hage.

4

Catalytic bleaching of cotton

This chapter discusses the performance of the catalyst MnTACN in the bleaching of cotton with hydrogen peroxide. The most important bleaching parameters, pH and temperature, as well as the kinetics of hydrogen peroxide decomposition during the bleaching process, have been investigated. The results show that very small quantities of the catalyst MnTACN increase the reaction rates in hydrogen peroxide bleaching system. As a result, bleaching of cotton in the presence of the catalyst at temperature as low as 30^{o}C produces a satisfactory whiteness for the fabric used in this study within relatively short time.

4.1 Introduction

At the present, no catalytic bleaching process applied to textiles is carried out in industrial conditions. The aim of this chapter is to disclose some important facts with regard to a possible application of dinuclear manganese(IV) trimethyltriazacyclononane catalyst MnTACN for hydrogen peroxide based cotton bleaching. The study is encouraged with the promising results of the MnTACN catalysed bleaching of cotton pigment morin in a homogeneous model system presented in Chapter 2 and Chapter 3. Bleaching of cotton takes place in a heterogeneous system, which is naturally more complex than a homogeneous model system; so phenomena other than chemical reaction between active bleaching species and colouring matter present in fibres can also play an important role, which will be discussed in more detail in Chapter 6. Besides, raw cotton fibre, although made of cellulose (88.0-96.0%), contains impurities (up to 10% of fibre weight) such as pectins, wax, proteins ash and other organic products, which lead to its chemical heterogeneity. Although a considerable part of these impurities is removed in the processing steps preceding the bleaching process, the presence of non-removed impurities at the fibre surface cannot be neglected as will be shown in Chapter 5. In terms of quantity, coloured substances are of little significance (generally less than 0.5%) [1], but their optical effect is much greater and can impair the final appearance of the material.

The fact that a heterogeneous bleaching system is not as well defined as a homogeneous model system entails to probe the performance of catalytic bleach system that includes textile material. The use of this macroscopic approach will provide more insight into a possible application of the catalyst in the hydrogen peroxide based bleaching of cotton in practical conditions. As discussed in Chapter 1, the most important indicators of the acceptability of a (catalytic) bleaching process are the degree of whiteness produced and fibre damage. The fibre damage i.e. the decrease in degree of polymerisation of cellulose will be the subject of study in Chapter 5 together with other physicochemical changes on cotton fibre (or fabric) that result from catalytic bleaching. The main objective of the present study has been to quantify the bleaching effectiveness i.e. the degree of whiteness produced on cotton employing the system with the catalyst at low temperatures. Here we have studied the effect of most important parameters, such as pH and temperature, together with the performance of bleaching system with respect hydrogen peroxide decomposition kinetics. Besides, a kinetic study of bleaching at the different temperatures is included. The experiments carried out in the absence of the catalyst enable to distinguish the role of the catalyst.

4.2 Experimental section

4.2.1 Chemicals and materials

Chemicals. The catalyst MnTACN was provided by Unilever R&D (The Netherlands). Hydrogen peroxide Perhydrol® (30%), sodium hydroxide (extra pure), sodium hydrogencarbonate (99%), di-sodium tetraborate decahydrate (Borax) (extra pure), di-sodium hydrogen phosphate monohydrate (99%) and potassium chloride KCl (99.5%) were obtained from Merck. 0.25 N cerium(IV) sulphate solution in 1-4 *N* H_2SO_4 and hydrochloric acid (37%) were received from Aldrich. Ethylenediaminetetraacetic acid EDTA (99%) was purchased from Acros Organics.

Cotton fabric. Desized and double scoured, 100% cotton woven plain fabric with a weight per unit area of 105 g m^{-2} was used for bleaching experiments. The fabric was kindly supplied by Vlisco B.V. (The Netherlands). It had initial whiteness index of WI = 71.3. In each bleaching experiment 3 fabric strips with a total weight of 10 g were used.

Tea stains. Cotton tea stains STC EMPA 167 (Empa, Switzerland) were used to study the effect of a chelating agent (EDTA) on the bleaching performance in addition to the cotton fabric described above. These were standard artificially soiled test cloths with a specific weight of 200 g m^{-2}.

4.2.2 Bleaching experiments

Fabric bleaching experiments involved: variations of pH at a constant temperature (30^{o}C) and bleaching time (30 minutes); and variations of temperature and bleaching time keeping constant pH 10.2. The effect of pH was studied over a pH range of 8-11.5 using a $Na_2H_4B_4O_7$/NaOH buffer (pH $\leq$ 10.2); $NaHCO_3$/NaOH and Na_2HPO_4/NaOH buffer (10 < pH $\leq$ 11); and KCl/NaOH buffer (pH > 11). The effect of temperature on the bleaching was studied at 30, 40, 50 and 60^{o}C, running for different times (1-30 min).

The experiments were conducted in 300 mL wide neck Erlenmeyer flasks placed in a shaking water bath SW 21 (Julabo, Germany) controlled to ± 0.2^{o}C and with a shaking frequency of 150 rpm. Each flask was filled with a buffer solution and once the target temperature achieved, a cotton fabric sample (10 g) was introduced and required amounts of H_2O_2 (30%) and 1 mM stock solution of MnTACN added to make final concentrations 88 mM (9 mL/L) H_2O_2 and 10 μM MnTACN in 200 mL (total volume) of bleaching solution (liquor ratio 1:20). After bleaching, the samples were removed and rinsed thoroughly twice in hot water and once in cold water, and dried at ambient temperature over night.

The pH of the bleaching solution was measured before and after the treatment

using a Titroline Alpha pH meter (Schott, Germany). There were no significant deviations from the initial pH values.

4.2.3 Whiteness and reflectance measurements

The bleaching effectiveness was evaluated by measuring the whiteness index (WI) of the fabric samples with a spectrophotometer 968 (X-Rite, USA) using D_{65} illuminant and 10° observer. Each sample was folded twice to give an opaque sample with four plies and sixteen measurements were carried out on different locations of the sample. The colorimetric coordinates of the studied sample (*X*, *Y* and *Z*) were used to calculate WI applying the formula of Berger [2] (Eq. 4.1).

$$WI = Y + 3.448 \cdot Z - 3.904 \cdot X \tag{4.1}$$

In order to calculate the observed rate constants k^{obs}, the reflectance *R* of the same samples was read at 460 nm and converted to the Kubelka-Munk K/S value using Eq. 4.2.

$$\frac{K}{S} = \frac{(100 - R)^2}{2R} \tag{4.2}$$

As it can be seen from Eq. 4.2, the mathematical expression of Kubelka-Munk theory relates the absorption coefficient (*K*), scattering coefficient (*S*), and percentage reflectance (*R*). According to the optical theory which predicts the reflectance of surface colours that was first proposed by Kubelka and Munk in 1931, this function is directly proportional to the concentration of coloured matter. Based on that, K/S values are commonly used for a quantitative measure of the presence of coloured matter on the cotton fabric [3]. A detailed analysis of Kubelka-Munk theory is available in several basic books on colour science and optometry.

An 'unbleached', $\left(\frac{K}{S}\right)_0$, and a 'completely bleached', $\left(\frac{K}{S}\right)_\infty$, fabric sample were included in each set of experimentally bleached samples for time *t*, $\left(\frac{K}{S}\right)_t$, as standards. The 'completely bleached' sample was bleached at 60°C for 15 minutes with H_2O_2/MnTACN (*R* = 90.17). The dimensionless (relative) concentration of coloured matter available for bleaching before (C'_{CM0}) and after bleaching for time *t* (C'_{CM}) are given by Eq. 4.3 and Eq. 4.4, respectively:

$$C'_{CM0} = \left(\frac{K}{S}\right)_0 - \left(\frac{K}{S}\right)_\infty \qquad (4.3)$$

$$C'_{CM} = \left(\frac{K}{S}\right)_t - \left(\frac{K}{S}\right)_\infty \qquad (4.4)$$

4.2.4 Cerium(IV) titration reactions

The content of hydrogen peroxide remaining in a bleaching solution after different bleaching times and different temperatures was determined by cerium(IV) titration reactions following a previously described procedure [4]. The amount of H_2O_2 remaining, given in % of initial moles H_2O_2 was calculated on the basis that one mole H_2O_2 reacted with 2 moles Ce(IV) in acidic solution (Eq. 4.5). The method was calibrated with blank bleaching solutions of hydrogen peroxide (in the absence of cotton and MnTACN, at t = 0). Using this method, it was possible to remove 17 mL aliquots from a bleaching solution at timed intervals and to mix them with a solution of 1 mL concentrated hydrochloric acid added to 7.5 mL water, which was then titrated with a commercial solution of yellow 0.25 M $Ce(SO_4)_2$ in sulphuric acid to the first appearance of yellow, indication that Ce(IV) is no longer reduced.

$$2\ Ce(IV)(aq) + H_2O_2(aq) \longrightarrow 2\ Ce(III)(aq) + O_2(g) + 2\ H^+(aq) \qquad (4.5)$$

Reaction conditions: 1 mL of 1 mM stock solution of MnTACN and 0.9 mL of H_2O_2 (30%) were added to 98.1 mL of a $NaHCO_3$/NaOH buffer that contained 5.00 g of cotton fabric, so that 17 mL aliquot taken from the solution contained 1.5 mmol total H_2O_2 at t = 0.

4.2.5 UV-Vis experiments

A qualitative analysis of the kinetics of hydrogen peroxide decomposition catalysed by MnTACN was done employing UV-Vis spectrophotometry. The reaction conditions were chosen to mimic the conditions of the reaction of H_2O_2 with MnTACN in the absence of cotton described in Section 4.2.4: 0.5 mL of 1 mM stock solution of MnTACN and 0.45 mL of H_2O_2 (30%) were added to 0.5 mL 10 mM $NaHCO_3$/NaOH buffer pH 10.2 in a UV-Vis cuvette. Fluorimeter 17F type quartz cuvettes with quartz B24 joint neck (Chandos Intercontinental, UK) – lightpath 10 mm, were used in the experiments. The absorption spectra of the reaction mixture were measured at timed intervals during 30 minutes reaction time in a thermostated Carry 100 spectrophotometer (Varian, USA) at 30°C and 60°C.

4.3 Results and discussion

4.3.1 Effect of temperature on bleaching rate

The main aim of introducing the catalyst into bleaching process is to lower the temperature of the process. Hence, a satisfactory effectiveness of catalytic bleaching at lower temperatures, where a non-catalysed H_2O_2 process shows rather poor effectiveness, is the prerequisite to consider the acceptability of certain catalyst. The benchmark for bleaching effectiveness, i.e. the target value for whiteness index (WI 80) has been established on wide experience in industrial bleaching for fabrics destined for coloured white end-products as well those to be dyed pastel or very bright shades.

In order to compare the bleaching effectiveness of the catalyst based system (H_2O_2/MnTACN) to that of peroxide system (H_2O_2), we have studied bleaching rates at pH 10.2 over the temperature range of 30-60^{o}C. Above 60^{o}C hydrogen peroxide decomposition becomes dominant. Figure 4.1 shows that catalytic bleaching can be performed at lower temperature (30-40^{o}C) and WI 80 can be easily obtained within 15 minutes of bleaching time. When bleaching with hydrogen peroxide alone under unchanged conditions, the bleaching effectiveness is significantly lower (Figure 4.2), and the target value for WI is not achievable at temperatures below 60^{o}C for such a short bleaching times.

In all experiments the bleaching shows two distinct phases: a relatively fast initial phase followed with distinctly slower phase at longer times (Figure 4.1). This implies that most of bleaching occurs in first few minutes. Particularly high WI values within short-time bleaching are obtained as a result of catalytic bleaching at 60^{o}C. The WI 80 is obtained in less than 2.5 minutes, whereas for the bleaching in the absence of the catalyst keeping the other parameters constant, at least 10 minutes of bleaching is required to produce the similar result. Interestingly, comparable WI vs. bleaching time dependence is obtained for catalytic bleaching at 30^{o}C and the uncatalysed hydrogen peroxide bleaching at 60^{o}C (Figure 4.1 and Figure 4.2).

For bleaching over the temperature range studied, logarithmic plots of C'_{CM0}/C'_{CM} against bleaching time give straight lines, although not passing through the origin (i.e. for t = 0, $\ln(C'_{CM0}/C'_{CM}) \neq 0$). C'_{CM0} and C'_{CM} are the dimensionless concentrations of coloured matter on the unbleached fabric and fabric bleached for time t (see Section 4.2.3). This is likely to be the consequence of the presence of two distinct phases explained above. The observed rate constant k^{obs} (Table 4.1) is calculated as a slope of $\ln(C'_{CM0}/C'_{CM})$ vs. t plots on the basis of Eq. 4.6:

$$\ln \frac{C'_{CM0}}{C'_{CM}} = k^{obs} t \qquad (4.6)$$

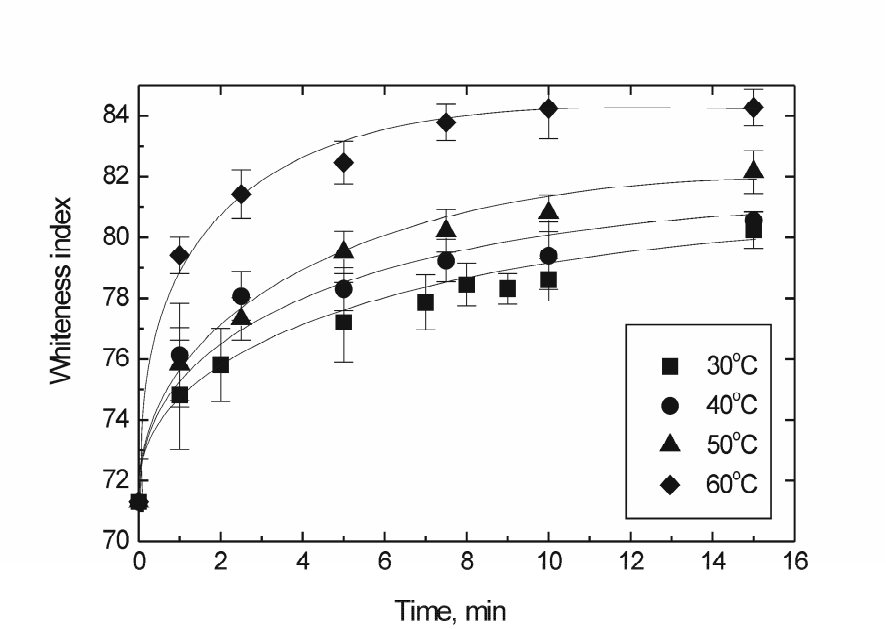

Figure 4.1 Plot of whiteness vs. bleaching time obtained for the MnTACN catalysed hydrogen peroxide bleaching at different temperatures. The bleaching solution contained 10 μM MnTACN, 88 mM H_2O_2 in 12.5 mM borate buffer at pH 10.2.

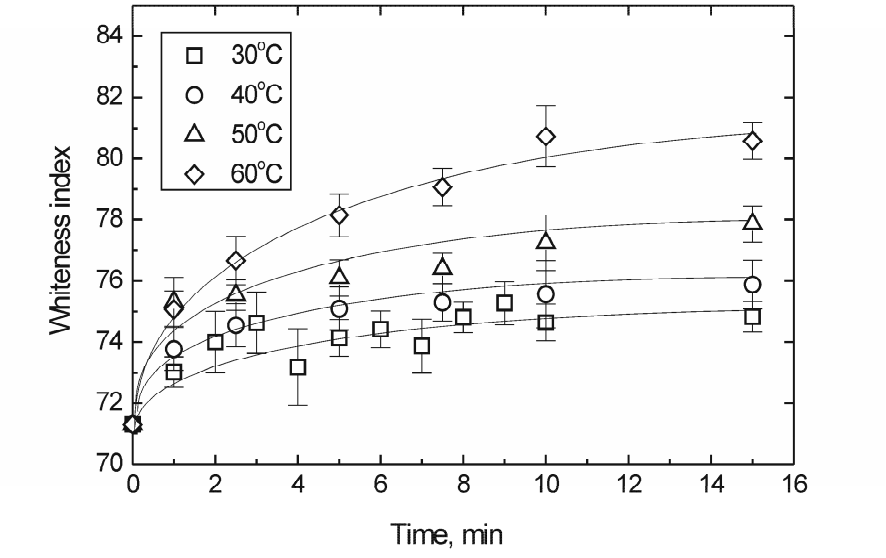

Figure 4.2 Plot of whiteness vs. bleaching time obtained for the (uncatalysed) hydrogen peroxide bleaching at different temperatures. The bleaching solution contained 88 mM H_2O_2 in 12.5 mM borate buffer at pH 10.2.

Table 4.1 Observed rate constant k^{obs} and apparent activation energy E_a of the catalysed and uncatalysed peroxide bleaching.

Bleaching system	Observed rate constant $k^{obs} \times 10^3$, s^{-1}				E_a, kJ mol^{-1}
	30°C	40°C	50°C	60°C	
H_2O_2/MnTACN	0.58	0.93	1.59	3.06	46.2
H_2O_2	0.08	0.20	0.28	0.77	61.8

The observed k^{obs} (s^{-1}) shows higher values for catalytic bleaching compared to corresponding values for bleaching with hydrogen peroxide alone. The resulting Arrhenius plot i.e. a logarithmic plot of the observed rate constants versus reciprocals of absolute temperature gives a straight line (Figure 4.3). According to the Arrhenius equation (Eq. 4.7), a slope of straight line fitted in the Arrhenius plot represents the negative quotient of activation energy E_a and the gas constant R:

$$k^{obs} = Ae^{-E_a/RT} \tag{4.7}$$

where A is the frequency factor. A lower slope ($-E_a/R$) obtained in case of catalytic bleaching confirms that the introduction of MnTACN into the bleaching reaction leads to a decrease in the activation energy of bleaching process compared to the non-catalytic process (Table 4.1).

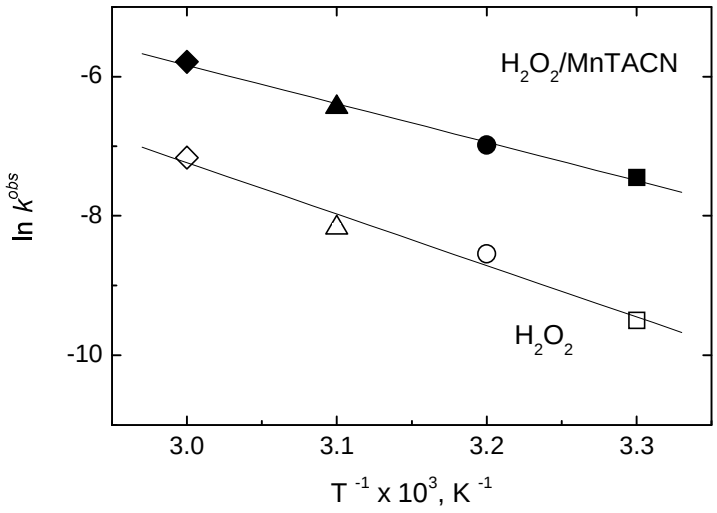

Figure 4.3 Arrhenius plot for bleaching of cotton in the presence and absence of MnTACN. The same symbols are used as in Figure 4.1 and Figure 4.2.

4.3.2 Hydrogen peroxide decomposition kinetics study

Under the conditions of high temperatures, bleaching competes with the decomposition of hydrogen peroxide. To quantify the competition between the use of hydrogen peroxide in oxidation of cotton pigments (and perhaps cellulose) and its decomposition, the amount of hydrogen peroxide in a bleaching solution was monitored as a function of time. Bleaching reactions were run as normal (with cotton). At regular time intervals, hydrogen peroxide was titrated with cerium(IV) to determine the amount of hydrogen peroxide remaining. Identical reactions, in the absence of cotton (without substrate), were run as controls.

As anticipated, the amount of peroxide remaining in bleaching solution decreases considerably with increasing temperature from 30°C to 60°C owing to peroxide decomposition (Figure 4.4 and Figure 4.5). This is especially apparent in the control reaction (carried out in the absence of cotton) where the bleaching solution, when heated to 60°C, loses peroxide rapidly, while the peroxide content of reaction at 30°C remains nearly unchanged during first 20 minutes. The latter shows that hydrogen peroxide is rather stable in the presence of MnTACN at 30°C, whereas a significant consumption of H_2O_2 is observed only after the introduction of substrate (cotton) into bleaching solution (Figure 4.4).

On the basis of the experimental results and simple kinetic calculation it has been concluded that the hydrogen peroxide consumption in the presence of MnTACN follows first order kinetics. The corresponding values for the rate constant k_{decomp} are obtained from the plots ln $[H_2O_2]$ vs. time and are given in Table 4.2. In case of reactions performed at 30°C, k_{decomp} of hydrogen peroxide consumption increases with a factor 6.6 in the presence of cotton, while at 60°C this factor is 2.3. These values illustrate an intensified competition between the decomposition of hydrogen peroxide and the bleaching of cotton substrate at 60°C.

Table 4.2 First order rate constant of H_2O_2 consumption in the catalysed bleaching reaction in the presence and absence of cotton at 30°C and 60°C.

Temperature	$k_{decomp} \times 10^{-3,}$ s^{-1}	
	with cotton	without cotton
30°C	0.46	0.07
60°C	2.53	1.12

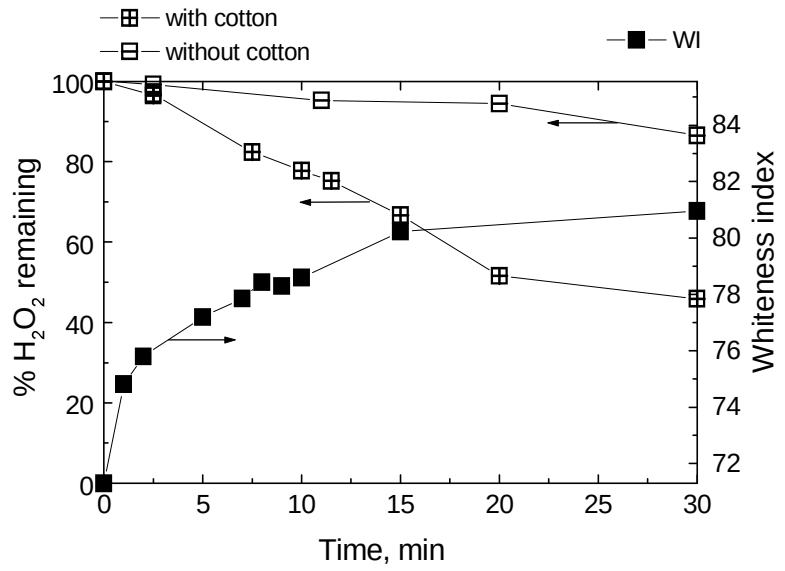

Figure 4.4 The amount of hydrogen peroxide remaining in a bleaching solution (H_2O_2/MnTACN) in the presence and absence of cotton at 30°C as a function of bleaching time. Results are compared to WI produced under the same conditions.

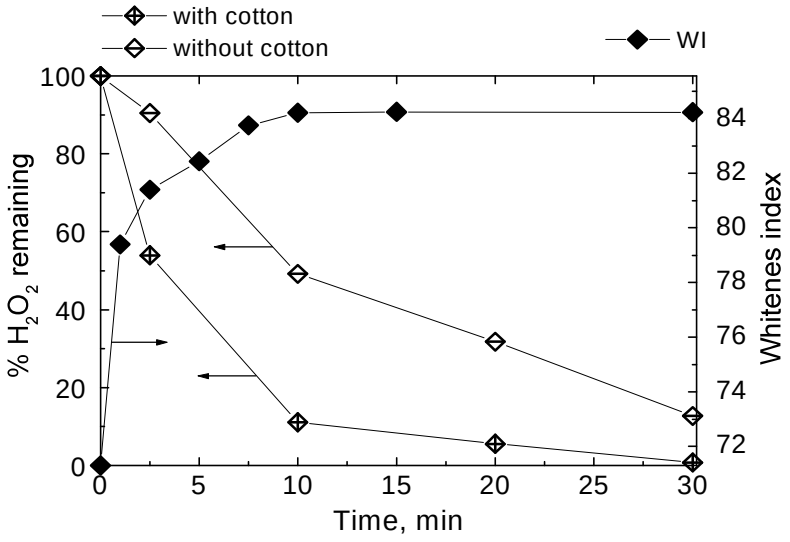

Figure 4.5 The amount of hydrogen peroxide remaining in a bleaching solution (H_2O_2/MnTACN) in the presence and absence of cotton at 60°C as a function of bleaching time. Results are compared to WI produced under the same conditions.

The results obtained for the control reactions based on cerium(IV) studies are in accordance with the change in UV-Vis spectra observed for the mixture of H_2O_2 and MnTACN under similar conditions. Figure 4.6 and Figure 4.7 give a qualitative illustration of the different kinetics of peroxide decomposition catalysed by MnTACN at 30°C and 60°C in the absence of cotton substrate. The peroxide to MnTACN ratio used in these experiments was the same as in the bleaching experiments, although higher initial concentrations (0.344 mM

MnTACN and 3.012 M H_2O_2) were chosen to obtain a satisfactory distribution of the UV-Vis spectra of reaction mixture within 30 minutes reaction times.

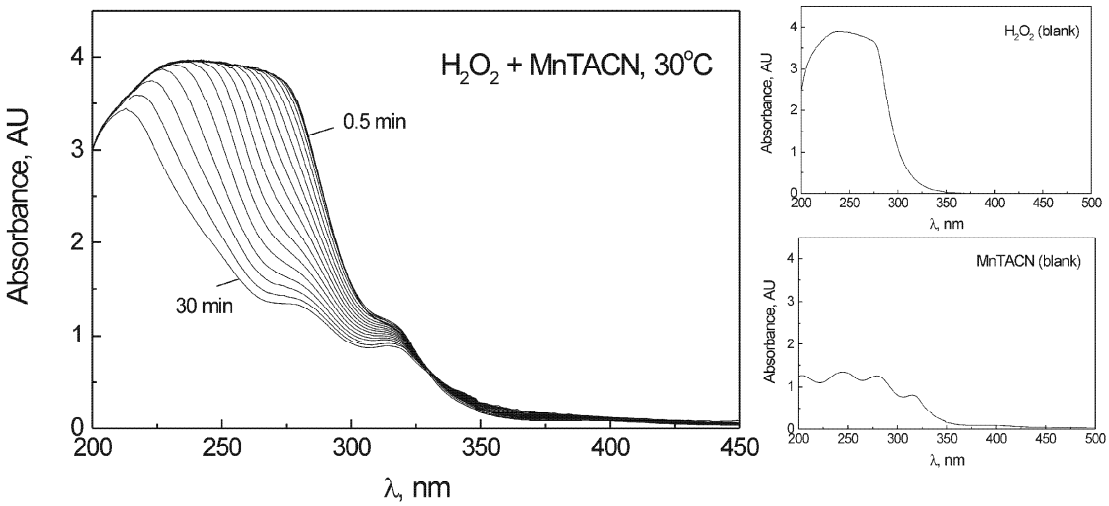

Figure 4.6 UV-Vis spectra of the hydrogen peroxide decomposition catalysed by MnTACN at 30°C monitored at intervals between 0.5 and 30 minutes (left). The spectra of the blank H_2O_2 and blank MnTACN at 30°C and t = 0 are given on the right. The blanks (H_2O_2 or MnTACN) are measured at the same concentrations as for the H_2O_2 decomposition measurement in the presence of MnTACN. Reaction conditions: 0.50 ml 1 mM MnTACN is mixed with 0.45 ml H_2O_2 (30%) in 0.5 ml 10 mM $NaHCO_3$ buffer pH 10.2.

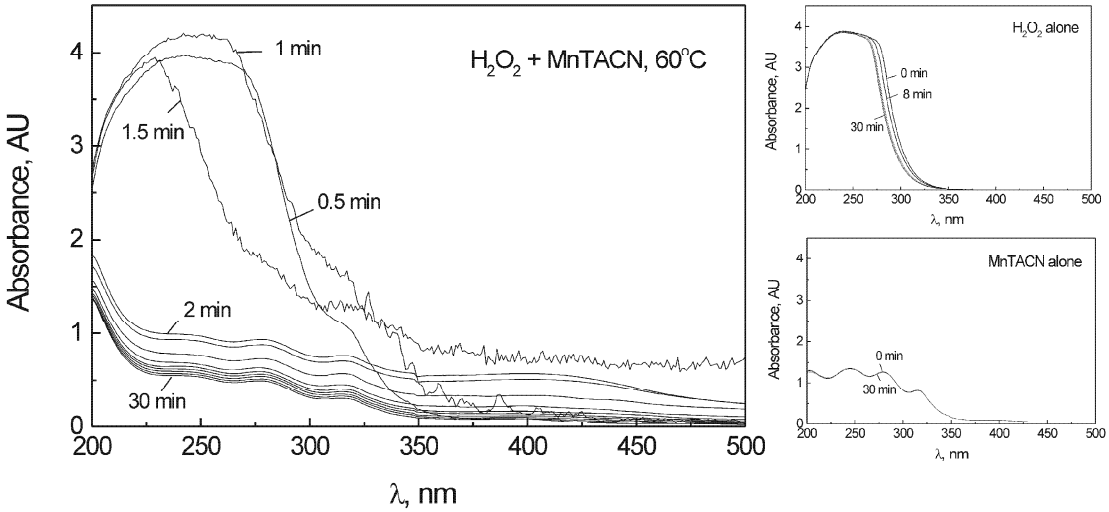

Figure 4.7 UV-Vis spectra of the hydrogen peroxide decomposition catalysed by MnTACN at 60°C monitored at intervals between 0.5 and 30 minutes (left). The spectra of the blank H_2O_2 (in the absence of MnTACN) and blank MnTACN (in the absence of H_2O_2) at 30°C during 30 minutes are given on the right. The blanks (H_2O_2 or MnTACN) are measured at the same concentrations as for the H_2O_2 decomposition measurement in the presence of MnTACN. Reaction conditions: 0.50 ml 1 mM MnTACN is mixed with 0.45 ml H_2O_2 (30%) in 0.5 ml 10 mM $NaHCO_3$ buffer pH 10.2.

Figure 4.6 shows relatively slow (especially at the beginning of the reaction) and gradual decomposition of hydrogen peroxide at 30°C. After 30 minutes reaction time there is still some peroxide left in the reaction mixture. At 60°C the total amount of peroxide is lost after only 1.5 minutes reaction time (Figure 4.7). The absorbance registered between 2 and 30 minutes is due to the catalyst. As it can be seen from figures on the right (Figure 4.7), the decomposition of peroxide alone under same conditions is negligible, while no change in the spectra of the catalyst alone are registered during the same time course.

As shown in previous section, and as will be shown later in Chapter 6, catalytic bleaching proceeds via a fast bleaching phase (less than 2.5 minutes) followed by a noticeably slower bleaching phase (Figure 4.1). It is interesting to compare the percentage of hydrogen peroxide remaining in a bleaching solution in the presence and absence of cotton substrate after the fast bleaching phase at different temperatures. The results presented in Figure 4.8 show that hydrogen peroxide remaining in the control reactions is higher than 90%, i.e. less than 10% of H_2O_2 is decomposed after 2.5 minutes of bleaching time, for all temperatures studied. Nevertheless, owing to the presence of cotton in a bleaching solution, the percentage of hydrogen peroxide remaining in a bleaching solution decreases appreciably with increasing temperature. This is especially evident at 60°C where nearly 50% of peroxide is consumed during first 2.5 minutes of the bleaching process (almost the half life time of H_2O_2 reached).

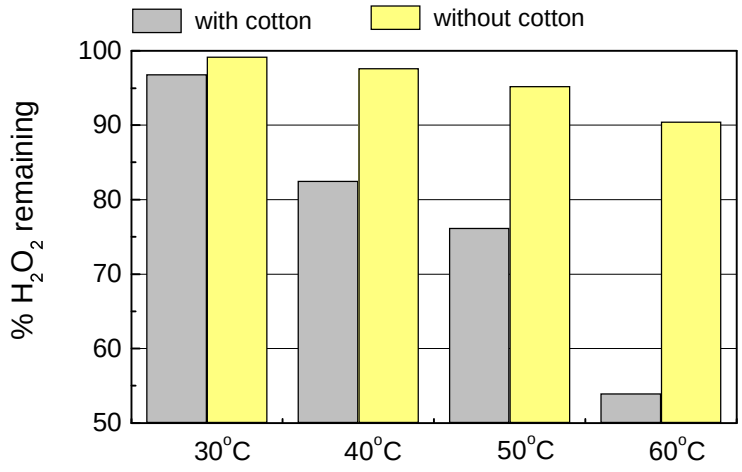

Figure 4.8 The amount of hydrogen peroxide remaining in a bleaching solution (H_2O_2/MnTACN) with or without cotton substrate after 2.5 minutes reaction time at different temperatures.

In an attempt to differentiate the use of hydrogen peroxide caused solely by the presence of cotton from the amount decomposed in the bleaching solution at any time of reaction, we have calculated the fraction of H_2O_2 consumed by the cotton substrate ($f_{S(t)}$) (Eq. 4.8). Here we assume that the total amount of H_2O_2

used during bleaching, n_B, equals the sum of the amount used exclusively by the cotton substrate, n_S, and the amount that has been decomposed in the bulk solution, n_C, i.e. $n_{B(t)} = n_{S(t)} + n_{C(t)}$. Based on that we can define the fraction consumed by the cotton substrate at the different bleaching times as:

$$f_{S(t)} = \frac{n_{B(t)} - n_{C(t)}}{n_{B(t)}} = \frac{n_{S(t)}}{n_{B(t)}} \qquad (4.8)$$

wherein $n_{B(t)}$ and $n_{C(t)}$ are experimentally determined in the bleaching experiments with cotton and the control reactions (without cotton), respectively. Hence, $n_{S(t)}$ reflects moles of H_2O_2 consumed due to the involvement of cotton in the reaction and not decomposition of H_2O_2 in the bleaching solution.

The corresponding results for reactions at 30°C and 60°C are compared in Figure 4.9. It can be seen that a large fraction of peroxide (~0.8) is consumed due to the presence of cotton substrate and not because of decomposition in the solution at any time during bleaching carried out at 30°C. This suggests that the active species formed during bleaching catalyses the oxidation of the cotton, and not decomposition of H_2O_2 in solution, showing that cotton bleaching is the major pathway under these conditions. The bleaching system is stable since peroxide is predominantly activated in the reaction with both the catalyst and the cotton. Like this, there is no need for peroxide stabilisation under present conditions.

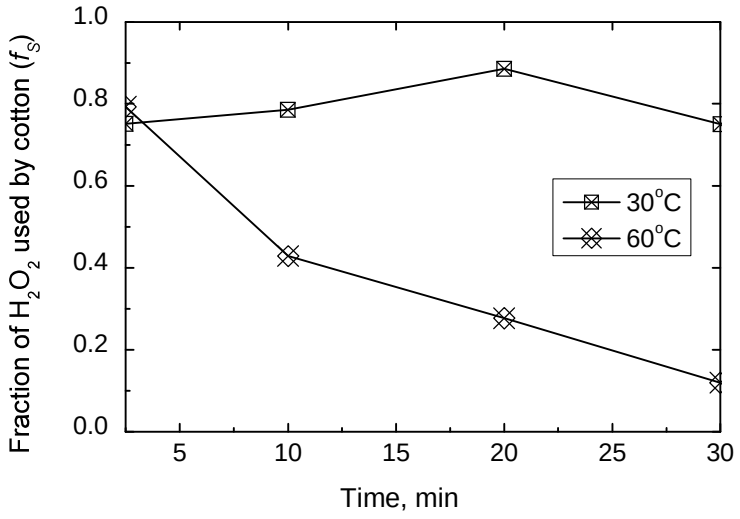

Figure 4.9 The fraction of hydrogen peroxide consumed due to the presence of cotton (f_S) as a function of bleaching time at 30°C and 60°C.

At 60°C, however, the fraction of H_2O_2 consumed due to the presence of cotton decreases appreciably with bleaching time. This indicates that the catalysed decomposition $H_2O_2 \rightarrow H_2O + 1/2\ O_2$ in the bleaching solution (catalase reaction) becomes the major pathway during the time course of bleaching. A higher WI produced under these conditions compared to the corresponding

results over the temperature range of 30-50^{o}C is likely to be a result of the double mechanism of bleaching under these conditions: the mechanism of MnTACN catalysed activation of hydrogen peroxide on the cotton substrate as well as the mechanism of decomposition of hydrogen peroxide in a bulk solution. This makes the system under these conditions unstable because of the uncontrolled decomposition and loss of hydrogen peroxide and, hence, it needs to be stabilised.

4.3.3 Effect of a chelating agent

The stabilisation of hydrogen peroxide in current (non-catalytic) industrial processes is easily achieved with the addition of different auxiliaries into the bleaching solution, as partially discussed in Chapter 1. Although our objective has not been to optimise the bleaching process based on the catalyst MnTACN, so neither to optimise the bleaching procedure, we find it important to underline principle differences between the catalytic and conventional bleaching process regarding the choice of stabiliser. This is especially related to agents that have chelating properties, and can possibly sequester active manganese species removing it from catalytic cycle. A typical example of a strong chelating agent that is commonly used in current bleaching processes is ethylenediaminetetraacetic acid (EDTA) (Figure 4.10a). EDTA is a ligand with a high affinity constant to form metal-EDTA complexes (Figure 4.10.b). It forms especially strong complexes with Mn, Cu, Fe(III), and Co(III) [5-7]. In the bleaching with hydrogen peroxide, these metals promote the formation of hydroxyl radical (HO$^{\cdot}$), which damages cellulose fibres and decomposes the bleaching agents. For this reason, we have tested the performance of the catalyst based bleaching system in the presence of this ligand. At the same time, we have used it to get an insight whether mononuclear manganese species are operative in the bleaching of cotton as pointed out for the reactions carried out under homogeneous conditions (Chapter 3).

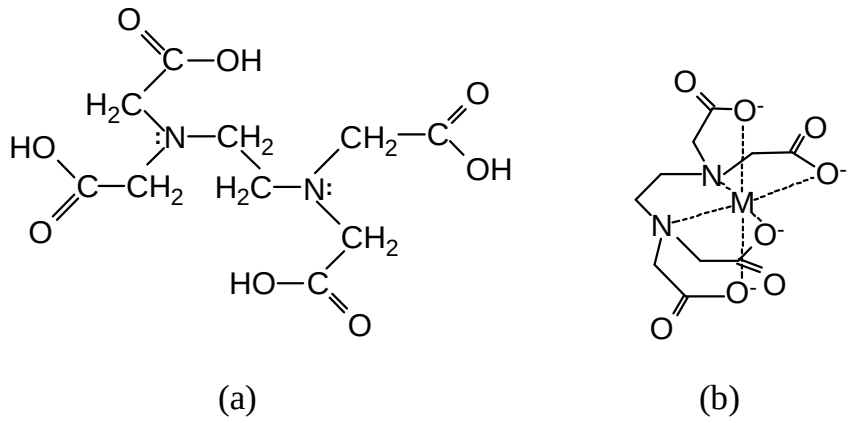

(a) (b)

Figure 4.10 Structural formula of EDTA (a) and a metal-EDTA chelate (b).

The kinetics of bleaching of cotton fabric in the presence of EDTA has been investigated under the standard conditions (30°C and pH 10.2). As it can be seen from Figure 4.11, the inclusion of EDTA at concentration of 1 g L^{-1} (5.2 mM) in the bleaching solution has a strong inhibitory effect on the cotton bleaching catalysed by MnTACN. The WI obtained after bleaching with H_2O_2/MnTACN in the presence of EDTA is significantly lower than in the absence of EDTA for all times investigated. Consequently, the difference in bleaching effectiveness of the system with and without the catalyst is diminished (Figure 4.11). The similar effect is observed in the catalytic bleaching of the standard cotton tea stains in the presence of EDTA (Figure 4.12), i.e. the better result in terms of WI produced is obtained by excluding EDTA from the bleaching solution.

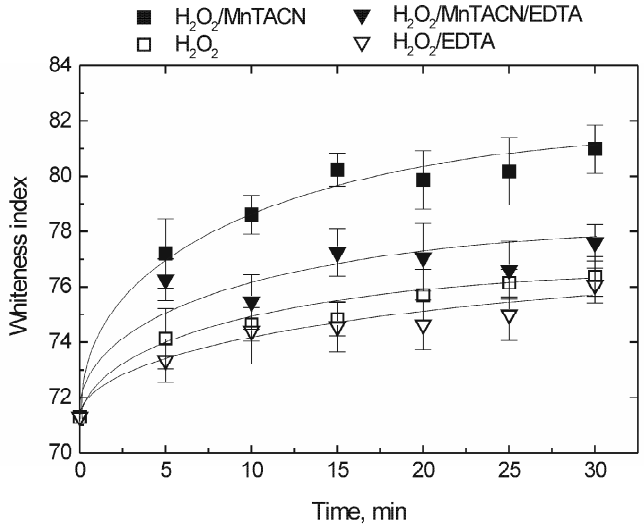

Figure 4.11 Kinetics of bleaching in the presence and absence of EDTA. The bleaching solution contained 10 µM MnTACN, 88 mM H_2O_2 and 5.2 mM EDTA, in 12.5 mM borate buffer at pH 10.2 and 30°C.

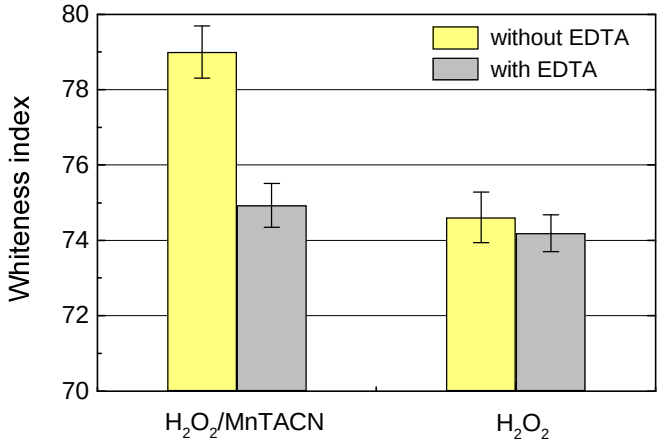

Figure 4.12 The influence of EDTA on bleaching effectiveness in the bleaching of tea stains. The bleaching solution contained 10 µM MnTACN, 88 mM H_2O_2 and 5.2 mM EDTA, in 12.5 mM borate buffer at pH 10.2 and 40°C.

This proves that EDTA complexes the manganese and effectively removes it from the catalytic cycle. Since EDTA does not react with MnTACN complex in the aqueous basic solution [8], we attribute the strong bleaching inhibitory effect of this ligand to its ability to remove manganese from one or more of the mononuclear manganese intermediates (Chapter 3) to give inactive Mn-EDTA chelate complexes.

4.3.4 pH dependence of bleaching effectiveness

The pH dependence of cotton bleaching effectiveness of catalyst based system (H_2O_2/MnTACN) has been studied through the macroscopic assessment of whiteness produced after 30 minutes by varying pH from pH 7.9 to pH 11.4 under low-temperature conditions (30^{o}C). The same experiments, in the absence of MnTACN, are also run as controls.

Figure 4.13 shows that maximum WI of cotton fabric is obtained by bleaching with H_2O_2 alone at *ca.* pH 11.5, which corresponds to the pK_a 11.6 of H_2O_2. This result is in accordance with the known fact that the rates of certain hydrogen peroxide and organic peracid reactions increase with pH until the maximum value obtained at pK_a, above which the reaction rate decreases [3, 9]. This behaviour has been interpreted as the evidence that the H_2O_2 bleaching occurs by the same mechanism as auto-decomposition, which is at its maximum at the pK_a value of H_2O_2.

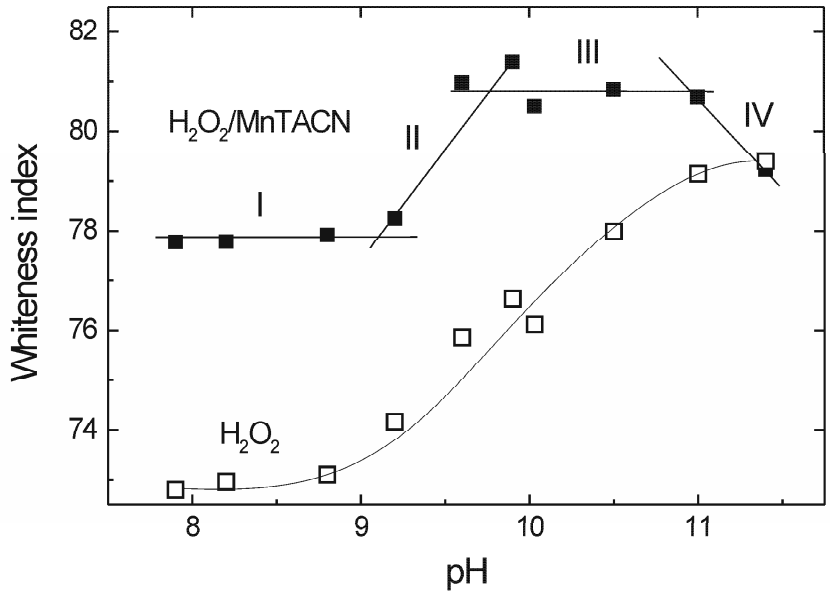

Figure 4.13 pH dependence of bleaching effectiveness of the catalytic (H_2O_2/MnTACN) and non-catalytic (H_2O_2) reaction systems. Bleaching conditions: [MnTACN], 10 μM; [H_2O_2], 88 mM; temperature, 30^{o}C; bleaching time, 30 min.

Bleaching with H_2O_2/MnTACN shows, however, a considerably different pattern of pH dependence represented by four separate trend lines in Figure 4.13, drawn between the points obtained experimentally. The trend lines denote four different pH ranges, each showing monotonous dependence of bleaching effectiveness (i.e. whiteness produced) on pH. There are two 'plateaus' where WI does not change significantly with pH increase. The first 'plateau' (line I) corresponds to the pH range (pH 8-9) with the lowest whiteness obtained. Nevertheless, this WI value is considerably higher (WI = 78) than the corresponding WI obtained for the fabric bleached with H_2O_2 alone (WI = 73), where almost no bleaching occurs within the same pH range. The second 'plateau' (line III) is placed within a relatively wide range of pH (pH 9.5-11) in which the maximum cotton whiteness is obtained. It is interesting to note that, as already observed in the case of bleaching of morin in a homogeneous model system (Figure 2.7a), maximum activity of the catalyst is achieved at a lower pH value than in case of bleaching with H_2O_2 alone. Line II in the Figure 4.13 corresponds to a narrow pH range (pH 9-9.5) with an abrupt change of WI. This correlates well with the results of the morin bleaching (Figure 2.7), where a significant increase of reaction rate occurs up to pH 10.2. Bleaching is expected to be favoured by higher pH because of the larger concentration of perhydroxyl anion (HOO^- is more nucleophilic than H_2O_2). A drop in the WI at higher pH (line IV) correlates well with previously observed decrease of the maximum reaction rate of morin at pH > 11 (Figure 2.7a). As in case of reaction of the MnTACN catalysed bleaching of morin under homogeneous conditions, this effect can be explained by the instability of active species derived from MnTACN at higher pH [8, 10]. Therefore, a wide maximum where the maximum catalytic activity is observed is perhaps the sum of the double effect: increased concentrations of perhydroxyl ion concentration on one side and on the other, a low stability of catalyst active species at higher pH.

A relatively wide pH range of the maximum catalyst activity in the bleaching of cotton obtained at lower pH than with bleaching with H_2O_2 alone is of particular importance when the application aspects are considered. This means that the process can be performed with a lower amount of NaOH while the pH does not need to be strictly controlled, e.g. small variations of pH inside the "safe" pH range represented by line III in Figure 4.13 will assure a high bleaching effectiveness of the catalytic system.

4.4 Conclusions

This chapter discloses important facts related to the performance of the catalyst MnTACN in the hydrogen peroxide based bleaching of cotton. The effects of pH, temperature, hydrogen peroxide decomposition as well as the presence of a chelating agent have been investigated.

The effect of temperature was studied over range 30-60^{o}C. It was shown that very small quantities of MnTACN increase the reaction rates by providing a new mechanism with lower activation energy of bleaching. Satisfactory bleaching results i.e. WI 80 could be easily achieved in a low-temperature bleaching (30-40^{o}C) within short time (15 minutes). Under the same conditions, considerably lower WI was obtained as a result of bleaching with hydrogen peroxide alone.

The kinetics of the H_2O_2 consumption from bleaching solution showed that under the condition of high temperatures bleaching competes with decomposition of hydrogen peroxide. This enabled to differentiate the fraction of peroxide consumed due to the involvement of cotton substrate, from the fraction of peroxide lost because of the decomposition unrelated to the presence of cotton. The results confirmed that a large fraction of hydrogen peroxide is consumed due to the presence of cotton and not because of decomposition in the solution at 30^{o}C, producing satisfactory whiteness and showing that cotton bleaching is the major pathway under the low-temperature catalytic conditions. At 60^{o}C, the fraction of H_2O_2 consumed due to the presence of cotton decreased appreciably with time, showing that the decomposition of H_2O_2 becomes the major pathway. Based on that, the double mechanism was postulated at 60^{o}C, the mechanism of MnTACN catalysed activation of hydrogen peroxide on the cotton substrate as well as the mechanism of decomposition of hydrogen peroxide in a bulk solution.

Lower bleaching effectiveness of H_2O_2/MnTACN system observed in the presence of a chelating agent was attributed to its ability to remove manganese from one or more of mononuclear manganese intermediates to give inactive Mn-EDTA chelate complexes. This is an important finding in further clarifying the mechanism of catalytic bleaching (Chapter 3).

The pH dependence of cotton bleaching with H_2O_2/MnTACN was studied under low-temperature conditions. The activity of catalyst based system in the cotton bleaching shows pH dependence similar to that of bleaching of cotton pigment under homogeneous conditions (Chapter 2). At pH 8-9, where no bleaching with hydrogen peroxide alone was observed, the bleaching effect in the presence of catalyst was evident. A maximum activity of bleaching catalysed with MnTACN was obtained within a relatively wide range of pH (pH 9.5-11), whereas maximum bleaching effectiveness for uncatalysed bleaching was observed at higher pH (pH 11.5). This is of particular importance for possible application of the process in the industrial conditions, since pH is not required to be strictly controlled. Operating within wider pH range gives the catalytic system an advantage over conventional peroxide bleaching since it allows for normal fluctuations in everyday plant operations without sacrificing quality and reproducibility.

Literature cited

[1] Bille, H.E., Correct pretreatment - the first step to quality in modern textile processing, J. Soc. Dyers Colour., **103** (1987) 427-434.
[2] Berger, A., Weissgradformeln und ihre praktische Bedeutung, Farbe, **8** (1959) 187-202.
[3] Brooks, R.E., Moore, S.B., Alkaline hydrogen peroxide bleaching of cellulose, Cellulose, **7** (2000) 263-286.
[4] Pulvirenti, A.L, Epoxidation and bleaching catalyses by homo- and heterogeneous manganese, cobalt, and iron azamacrocyclic complexes, PhD thesis, Purdue University, 2000.
[5] Boot, L.A., Kerkhoffs, M.H.J.V., van der Linden, B.Th., van Dillen, A.J., Geus, J.W., van Buren, F.R., Preparation, characterization and catalytic testing of cobalt oxide and manganese oxide catalysts supported on zirconia, Appl. Catal., A, **137** (1996) 69-86.
[6] Marina, M.L., Andres, P., Diez-Masa, J.C., Separation and quantitation of some metal ions by RP-HPLC using EDTA as complexing agent in mobile phase, Chromatographia, **35** (1993) 621-626.
[7] Räsänen, E., Kärkkäinen, L., Modelling of Complexation of Metal Ions in Pulp Suspensions, J. Pulp Pap. Sci., **29** (2003) 196-203.
[8] Gilbert, B.C., Lindsay Smith, J.R., Newton, M.S., Oakes, J., Pons i Prats, R., Azo dye oxidation with hydrogen peroxide catalysed by manganese 1,4,7-triazacyclononane complexes in aqueous solution, Org. Biomol. Chem., **1** (2003) 1568-1577.
[9] Thompson, K.M, Spiro, M., Griffith, W.P., Mechanism of bleaching by peroxides. Part 4: Kinetics of bleaching of malvin chloride by hydrogen peroxide at low pH and its catalysis by transition-metal salts, J. Chem. Soc., Faradey Trans., **92** (1996) 2535-2540.
[10] Hage, R., Iburg, J.E., Kerschner, J., Koek, J.H., Lempers, E.L.M., Martens, R.J. , Racherla, U.S., Russell, S.W., Swarthoff, T., van Vliet, M.R.P., Warnaar, J.B., van der Wolf, L., Krijnen, B., Efficient manganese catalysts for low-temperature bleaching, Nature, **369** (1994) 637-639.

5

Physicochemical changes on cotton fibre as affected by catalytic bleaching

Surface chemistry and wetting properties of cotton fibres as affected by catalytic bleaching have been investigated. Two types of cotton fabric have been analysed: the regular and a model cotton fabric. In the regular (double scoured) cotton fabric, cellulose was contaminated with both non-removable and removable impurities including different pigments. The model cotton fabric, previously freed of most removable impurities, was stained for the purpose of this study with one pigment only, i.e. morin, a component that is typically found in native cotton fibre. This approach has provided the tool to explore and to quantify the chemical and physical effects on cotton fibre after catalytic bleaching and to distinguish between the three types of catalytic action: pigment bleaching, removal of non-cellulosic compounds and oxidation of cellulose.

5.1 Introduction

Cotton fibres are composed of a secondary wall (typically 90% by weight) and an outer primary wall/cuticle (see Chapter 1 and references therein). Whilst the secondary wall is essentially cellulosic in nature, the primary wall/cuticle consists of approximately only 55% cellulose, the remainder attributed to proteins, pectins and wax. Due to these surface contaminants raw cotton is water repellent, exhibiting little water absorbency. Hence, to ensure uniform and rapid absorbency, acceptable dyeability and uniform colour it is important to pre-process the raw cotton fibres by a scouring and bleaching process. Scouring is mainly responsible for the removal of hydrophobic waxes and pectic substances. The fact that the purpose of bleaching is to improve cotton whiteness while preventing or at least minimising fibre damage probably explains why little attention has been given to study the effect of bleaching on other impurities incorporated in cotton fibres.

This chapter is aimed to get an integrated view of both chemical and physical changes that catalytic bleaching impart to cotton fibre. In that context, we have investigated the change in the degree of polymerisation of cotton cellulose (which reflects the change in fibre bulk properties), as well as the change in fibre surface chemistry. The latter has been investigated using X-ray photoelectron spectroscopy (XPS). In order to establish the interrelationship between the fibre chemical changes (bulk and/or surface) and expected changes in wetting properties, we have examined the contact angle and capillary constant of bleached cotton samples applying the Washburn method (i.e. capillary-rise method). The method is based on the well known determination of the weight gain due to liquid penetration into a porous structure. The results are compared to the bleaching effectiveness and the fibre damage as the most relevant bleaching parameters. Parallel analyses have been carried out on a model cotton fabric, “clean” cotton fabric stained with morin for the purpose of this study, in order to differentiate between pigment oxidation and other bleaching effects produced on the (regular) industrially scoured cotton fabric. At a more macroscopic level, pore volume distribution (PVD), e.g. change in pore structure of cotton fabric, is determined using the liquid porosimetry technique.

Prior to presentation of the results, a brief theoretical background of all aspects investigated in this chapter will be given in following sections.

5.2 Fibre chemical damage

Generally speaking, bleaching of a cotton fabric is a major process in the textile industry and is used to oxidise the impurities and colouring matter contained in fibres. On the fibre level, however, oxidative damage of cellulose may occur after bleaching and be reflected in a lower degree of polymerisation. Bearing in mind

this consideration, the question is to what degree it is actually necessary to oxidise the pigments present in fibre and to remove all non-cellulosic matter for satisfactory results. On the other hand, it is well documented in the literature that fibre damage is not reflected in a decrease in fibre tensile strength until considerable chain scissions have occurred [1].

5.2.1 Catalytic damage phenomenon

The phenomenon of "catalytic damage", which occurs during hydrogen peroxide bleaching of cotton fabrics contaminated with heavy metal ions; Fe(II) or Fe(III) ions in particular, is a well known serious problem in cotton finishing. The vigorous decomposition of the peroxide in contact with such catalytic ions causes catalytic damage tendering in places where the ions are deposited, which can range from very low degree of polymerisation (DP) to actual pin-holes (or razor) cuts in the textile materials. Hebeish ***et al.*** [2] have proposed that ceasing of the catalytic degradation of the cotton cellulose caused by the presence of Fe(II) and/or Fe(III) ions could be achieved by pretreatment of cotton fabric with oxalic acid. It has been reported that the extent of "catalytic damage" is, however, largely dependent on the type of heavy metal [3]. The metals can be either present in native cotton fibre (iron, calcium and magnesium forming complexes with pectin) [1] or introduced accidentally into the system through corroded equipment or rust abrasion. Marahusin ***et al.*** [4] demonstrated that fabric damage similar to that observed in practice can be produced by oxygen species generated at a Pt anode in contact with the cotton. Subsequent systematic studies [3, 5-7] using this approach have clarified some of the mechanistic aspects of fabric damage at the Pt electrode and have demonstrated the catalytic effects of some common metals on the damage.

For this reason, it may seem that the implementation of innovative catalyst based bleaching processes in industry is not preferred [8]. Nevertheless, inasmuch as bleaching and damage originate in various chemical species, there is no reason to believe that the so-called catalytic approach is bound to fail. To evaluate any bleaching catalyst properly it is therefore imperative that both its activity and its damage potential are determined.

5.2.3 Mechanism of oxidation of cellulose

Zeronian and Inglesby [9] have discussed the reactions of hydrogen peroxide bleaches and the catalytic effects of heavy metal ions with cotton cellulose. The DP of cellulose can be lowered by the reaction with hydrogen peroxide and it can be transformed into an oxycellulose. Lewin and Ettinger [10] made a comprehensive study of the reaction between hydrogen peroxide and cellulose in the form of purified cotton fibres. They differentiated between the hydrogen peroxide that was decomposed and the hydrogen peroxide that oxidised the cellulose. The purified cotton contained a small amount of iron. If the iron was

extracted from the purified cotton with HCl, the decomposition was relatively strong and the oxidation was relatively slow. Thus they suggested that the HOO^- ion is, by itself, not highly effective in oxidation, but the traces of iron normally found in cotton bring about a marked catalytic effect possibly by the formation of active complexes between iron and the HOO^- ion. The authors found that as the oxygen consumption increased the carboxyl, aldehyde and ketone content increased progressively, whereas the oxidation predominantly formed ketone groups. They proposed that in an alkaline solution it is the perhydroxyl radical $HOO^{\bullet}$ that oxidises cellulose in the following manner at either the C_2 or C_3 carbon atoms (Figure 5.1).

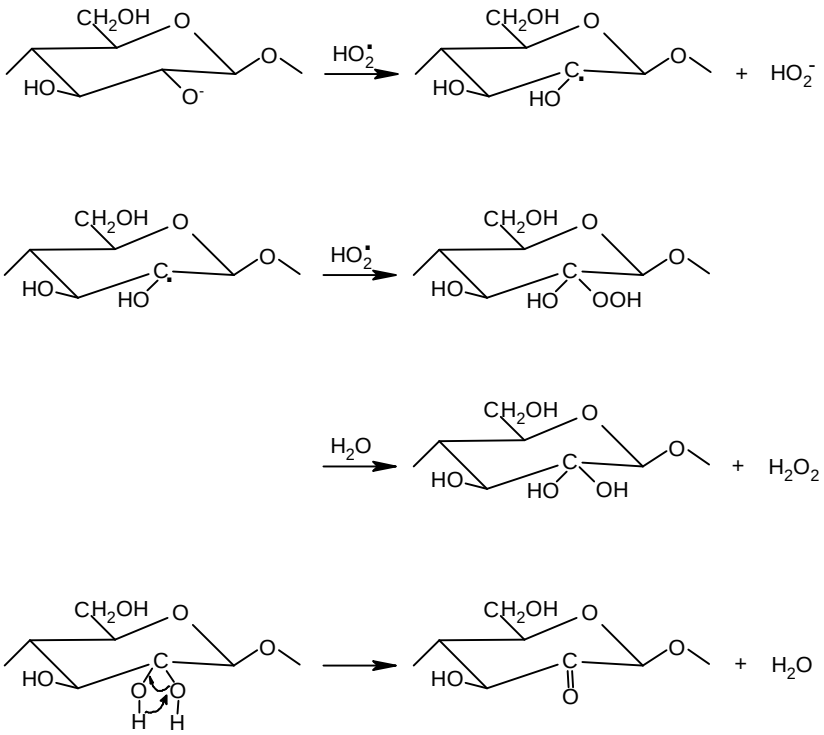

Figure 5.1 Mechanism of alkaline oxidation of cellulose with H_2O_2 [9].

Oxidised cellulose containing the electronegative aldehyde and ketone groups which are in position β to the glucosidic linkage, are susceptible, according to the β-alkoxyl elimination mechanism, to chain cleavage [11]. This can be seen in Figure 5.2 for cellulose containing a C_6 aldehyde or a C_2 and a C_3 ketone.

In case of a C_1 aldehyde group, (as in the case of hydrocellulose) which is in position γ to the glycoxyl group, a Lobry-de Bryun-van Eckenstam transformation takes place by which an enediol of C_1 and C_2 is formed, which is then converted to the C_2 ketose, being beta to the glycoxyl group, which enables the elimination of another monomeric double-bond containing monosaccharide (Figure 5.3). This depolymerisation process will continue until the whole length of the chain located sets in, in which metasaccharinic end groups are formed.

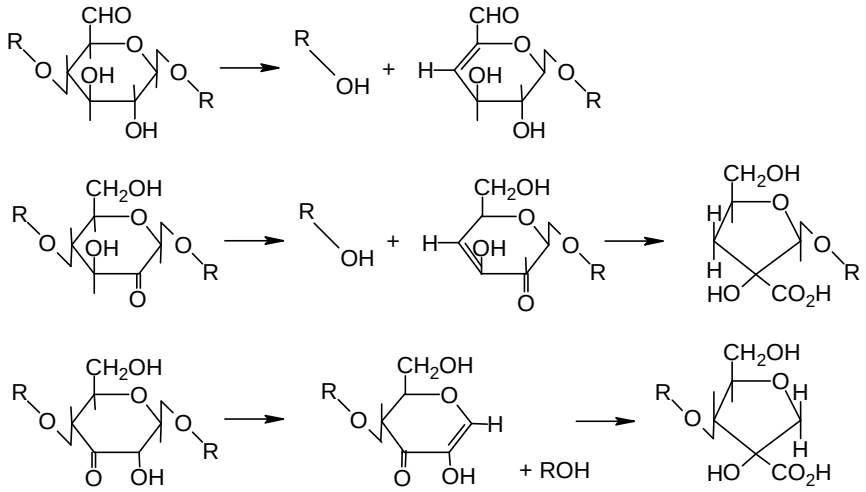

Figure 5.2 Alkaline degradation of cellulose containing C_6, C_2 and C_3 carbonyls [11].

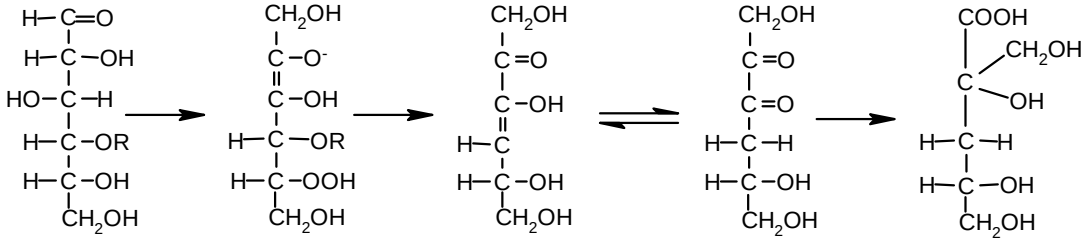

Figure 5.3 Mechanism of alkaline degradation of cellulose [11].

5.3 Surface chemistry of cotton fibre

The chemical composition of cotton fibres varies with plant variety and growth conditions. [12-13]. Each cotton fibre is composed of concentric layers. The cuticle layer on the fibre itself is separable from the fibre and consists of wax and pectin materials. The primary wall, the most peripheral layer of the fibre, is composed of cellulosic crystalline fibrils. The secondary wall of the fibre consists of three distinct layers. All three layers of the secondary wall include closely packed parallel fibrils with spiral winding of 25-35^o and represent the majority of cellulose within the fibre. The innermost part of cotton fibre- the lumen- is composed of the remains of the cell contents. Before boll opening, the lumen is filled with liquid containing the cell nucleus and protoplasm.

In general, cotton fibres are composed of mostly α-cellulose (88.0-96.5%) [12]. Non-cellulosic materials in the fibres include protein (1.0-1.9%), wax (0.4-1.2%), pectin (0.4-1.2%), inorganics (0.7-1.6%), and other (0.6-8.0%) substances. Most of the non-cellulosics are located in the outer layer of fibres. These non-cellulosic materials play an important role in cell growth and development, and they are

responsible for the nonwetting behaviour and colouring of native cotton.

The need to fundamentally understand changes in fibre surface chemistry after conventional processes such as scouring and bleaching and how it affects the properties of final textile products, has highlighted the interest in surface chemistry of cotton fibres. X-ray photoelectron spectroscopy (XPS also called ESCA) has shown to be a powerful tool for monitoring the changes in the surface chemistry of many materials together with textile fibres. The use of this technique to study the surface changes of chemically modified cotton fibres was pioneered by Soignet *et al.* [14]. Since then, XPS has been used in many investigations of surface chemistry of cellulosic fibres [15-18], including the surface composition of paper and wood fibres [19-21]. Mitchell *et al.* [22] have recently published the surface chemical analysis of raw, scoured and hydrogen peroxide bleached cotton material. They have successfully analysed the surface chemical composition of raw unscoured cotton by XPS and Time of Flight Secondary Ion Mass Spectrometry (ToF-SIMS). The presence of non-cellulosic material at the fibre surface has been established and determined to be a complex mixture of fatty acids, alcohols, alkanes, esters and glycerides. The effect of bleaching and especially scouring was to reduce the surface concentration of these materials, but even after these treatments some non-cellulosic material residue was still detected at the fibre surface.

5.4 Wetting properties

Raw cotton fibres contain hydrophobic non-cellulosic surface materials that make them nonwettable in water. For effective chemical processing (dyeing and finishing) and maintenance (cleaning) of cotton assemblies involving aqueous media, improved and uniform water wetting properties is essential because it facilitates the transport of active reagents among and into the fibres. Although it is commonly recognised that removing non-cellulosic materials improves water wetting and spreading on cotton assemblies, quantitative measurements of such a relationship have not been clearly established. Theoretical [23] and experimental [24-25] approaches for quantitative determinations of liquid wetting and retention in fibrous materials have been documented.

In case of textiles the interactions with liquids are very complex. They involve several physical phenomena, such as wetting of fibre surfaces, spontaneous flow of a liquid into an assembly of fibres driven by capillary forces (wicking), adsorption on the fibre surface and possible diffusion of the liquid into the interior of the fibres [26-27]. In general, fibre assembly/liquid interactions depend on the wettability of fibres, their surface geometry, the capillary geometry of fabric, the amount and the nature of test liquid, and external forces (such as applied pressure).

5.4.1 Contact angle

Contact angles on single natural fibres can be measured either directly [28-29] or indirectly, using the modified Wilhelmy technique [27]. However, in the case of natural fibres the Wilhelmy method is hardly applicable, due to wide variation in fibre perimeter and fibre shape [30]. Dimensional irregularities along the cotton-fibre axis and in cross-sectional shapes complicate the measurements and thus affect the single-fibre contact angles. Greater variations in the measured contact angle might also be due to the inhomogeneous character of the fibre surfaces and therefore varying fibre surface wettability. Hsieh *et al.* [25] compared the measured contact angles on a variety of fabrics (natural and man-made textile fibres) with the wetting properties of single fibres. They found [24] that contact angles derived from fabrics and single-fibre measurements were identical and that neither the existence nor the magnitude of liquid retention interfered with the contact-angle determination from fabrics. However, the error range was broader for contact angles measured on single fibres.

The modified Washburn or capillary rise-method enables the characterisation of porous solids and powders, but also of fibre bundles, fabrics and mats with regard to their wettability or at least their surface tension. Different experimental techniques are available for the characterisation of the wetting behaviour of those kinds of solids. In general, they are all based on measuring the weight gain due to liquid penetration as a function of time [31-33] or the penetration time needed for a liquid to rise to a certain height (known as the thin layer wicking technique) [34].

The evaluation of the measured data is based on modifications of the Washburn equation for a single capillary [35]:

$$\cos\theta = \frac{2}{A^2 r}\frac{\eta}{\sigma\rho^2}\frac{m^2}{t} \qquad (5.1)$$

which results from the combination of the expression for the Laplace pressure and the Hagen-Poiseuille equation for steady flow conditions [31, 33, 36-44], where σ, the liquid surface tension; θ, the solid/liquid contact angle; A, the cross-sectional area; r, the radius of the capillary; η, the liquid viscosity; ρ, the liquid density; m, the weight of the liquid that penetrates into the capillary, and t, the penetration time.

In case of fibre assemblies, the geometry of the capillary system is unknown and, therefore, the factor $[2/A^2r]$ is replaced by an unknown factor $1/c$, which leads to:

$$\cos\theta = \frac{1}{c}\frac{\eta}{\sigma\rho^2}\frac{m^2}{t} \qquad (5.2)$$

The factor $\eta/(\sigma\rho)^2$ reflects the properties of the test liquid, and m^2/t is to be measured. The constant c reflects the capillary geometry of the sample. This modified Washburn equation can be applied by making the following assumptions: (1) the liquid flow is predominantly laminar in the "pore" spaces; (2) gravity is negligible; and (3) the pore structure of the porous solid or fibre assemblies is constant [32].

5.4.2 Pore structure

Fast liquid spreading in fibrous materials is essential for efficient wet-treatments. It is facilitated with small uniformly distributed and interconnected pores, whereas high liquid retention can be achieved by having a large number of such pores or a high total pore volume [23]. In any fibrous structure of woven, nonwoven, or knitted fabrics, a distribution of pore sizes along any planar direction is expected. In a plain woven structure, such as the cotton fabric used in this study, a gradient of pore sizes across the thickness of the fabric is also expected. The changes in fibre properties when wet by the liquid can significantly affect liquid movement due to a change in pore structure [23].

Hsieh *et al.* [12] in their intention to quantify the effects of alkaline scouring, swelling, and bleaching of cotton assemblies, have found that scouring of cotton fabric, although improving water wettability and water retention, reduces the pore volume in the fabric. Bleaching, on the other hand, does not affect the fabric pore structure, while further improves the wettability and water retention. The authors explain the effect of bleaching by the cause of chemical changes only (i.e. oxidation) without affecting the pore structure of the fabrics. It is, in general, a quite firmly established opinion in both textile practice and scientific literature that most non-cellulosic materials can be made soluble and removed with alkaline scouring, whilst the bleaching is limited to the cotton fibre pigments oxidation.

Contrary to this, Volkov *et al.* [45] have recently published a brief communication on effect of the degree of purity of cotton fabric on its capillary parameters applying the modified Washburn method. Each of four wet-treatments, i.e. desizing, scouring, mercerizing or bleaching of cotton fabric not only leads to an increase in the hydrophilicity of the cotton fibre surface due to the partial removal of the contaminants and sizing preparation but also increases the dimensions of the interfibre capillaries (Table 5.1). The authors discuss that the additional increase in capillary size after bleaching is due to a modification of fibre occurring simultaneously with bleaching of unsaturated compounds giving a colour to cotton fibre.

Table 5.1 Capillary properties of the fabrics [45].

Fabric sample	$r \times 10^6$, m	cos θ	θ, deg
Raw	0.79	0.0007	89.9
Desized [(i)]	4.12	0.0290	88.4
Scoured [(ii)]	6.81	0.0658	86.2
Mercerized [(iii)]	7.91	0.0761	85.6
Bleached [(iv)]	9.17	0.1065	83.9

[(i)] at 70°C with NaOH (10 g/l) in the presence of potassium persulfate (2g/l);
[(ii)] at 95°C with NaOH (20 g/l);
[(iii)] at 20°C with NaOH (200 g/l), 30 s;
[(iv)] at 80°C and pH 11.7 with H_2O_2 and Na_2SiO_3 (8 g/l)

Of the few experimental methods for quantitative characterisation of porous solids, mercury porosimetry is among the most common [46-47]. However, application of mercury porosimetry to nonrigid fibrous materials is limited due to structural changes under high pressure required for these measurements. Liquid porosimetry, which employs a variety of wetting liquids [48], has the advantage of a much lowered pressure requirement, thus improving its applications for nonrigid structures such as, for example, textile fabrics.

Liquid porosimetry is a procedure for determining the pore volume distribution (PVD) within a porous solid matrix. The data obtained provide a direct picture of the absolute and relative contributions of each pore size to the total available free volume within a network. Each pore is sized according to its effective radius (R_{eff}), and the contribution of each size to the total free volume is the principal objective of the analysis. Woven fabrics typically give bimodal distributions [48-49], where the larger pore sizes are formed by the spaces between yarns (interyarn pores); the smaller (interfibre) pores reflect the intrayarn structure. Intrafibre pores are smallest and their distribution cannot be analysed due to the method limitations. The structure and dimensions of the inter- and intrayarn (interfibres) pores are strongly affected by the yarn structure and the density of yarns in the woven structure. These interyarn pores can be wide-ranging, with sizes similar to the fibres to larger than the yarns.

5.5 Experimental section

5.5.1 Bleaching procedure and sample preparation

Bleaching experiments with both regular (designated as the "as received") and model cotton fabric were carried out in 300 ml wide neck Erlenmeyer flasks that were placed in a shaking water bath SW 21 (Julabo, Germany) controlled to ±0.2^{o}C and with a shaking frequency of 150 rpm. Each flask was filled with a buffer solution and once the target temperature achieved, a cotton fabric sample was introduced and H_2O_2 and MnTACN added to make a final volume of 200 ml. In the experiments where H_2O_2 was replaced with O_2, the bleaching solution was purged with air throughout the bleaching experiments. In each bleaching experiment 3 fabric strips with a total weight of 10 g were used. The conditions were as follows: liquor ratio, 20:1; [MnTACN], 10 μM; [H_2O_2], 0.1 M; $NaHCO_3$/NaOH buffer pH 10.5, 30^{o}C. After 15 minutes of the treatment the samples were removed, rinsed thoroughly twice in hot water and once in cold water, and dried at room temperature over night.

For bleaching experiments, we used both the "as received" and model cotton fabric. The "as received" cotton fabric (100% cotton woven plain fabric with a weight of unit area 105 g·m^{-2}) was previously desized and double scoured in industrial conditions (sample **b**, Table 5.3). Its whiteness index (WI) was 71 Berger units. The "as received" cotton fabric, desized and scoured once (sample **a**, Table 5.3), served as a reference only. Both fabrics were kindly supplied by Vlisco B.V. (The Netherlands).

The main idea of producing the model fabric was to take sufficiently white cotton fabric (which has most of the impurities removed) and to stain it in a controlled way with a pigment (morin) that mimics the natural cotton coloured impurities. Accordingly prepared model fabric mimics raw (unbleached) cotton fabric. The "as received" double scoured cotton fabric (sample **b**, Table 5.3) was used to produce the model fabric. To remove the coloured matter thoroughly, bleaching procedure with H_2O_2 was undertaken under the conditions that are characteristic for the conventional hydrogen peroxide bleaching proces: liquor ratio, 20:1; [H_2O_2], 0.1 M; $NaHCO_3$/NaOH buffer pH 11; 70^{o}C, 30 min. The bleached cotton fabric sample (sample **g**, Table 5.3) was subsequently stained with morin (sample **h**, Table 5.3). The staining procedure was as follows: liquor ratio, 20:1; [morin], 0.6 g/l; [NaCl], 2.5 g/l; $NaHCO_3$/NaOH buffer pH 11; 30^{o}C; 60 min; 130 rpm. After staining, the samples were rinsed twice in cold water for 60 min at a liquor ratio of 160:1.

5.5.2 Bleaching effectiveness

Bleaching effectiveness was evaluated by measuring the whiteness index (WI) with a spectrophotometer 968 (X-Rite, USA) using D_{65} illuminant and observer 10°. Four measurements of WI per piece of fabric were carried out. The ***XYZ*** scale was used to determine the WI applying the formula of Berger (Eq. 5.3).

$$WI = Y + 3.448 \cdot Z - 3.904 \cdot X \tag{5.3}$$

5.5.3 Fibre damage

In order to establish the amount of fibre damage caused by the catalytic bleaching, the changes in the cotton fibre cuprammonium fluidity (*F*) were studied before and after different bleaching conditions. The fluidity measurements have been performed using cuprammonium hydroxide under standard conditions [50]. To express the amount of damage of the cotton samples the degree of polymerisation (DP) has been used applying the following equation [51-52].

$$DP = 2032\left(\log\frac{74.35 + F}{F}\right) - 573 \tag{5.4}$$

The fibre damage was also expressed as the damage factor (*S*) [51, 53] (also called Eisenhut's Tendering factor, T.F.) by using Eq. 5.5, originally proposed by Eisenhut, to determine the degree of damage in cotton after chemical treatment [54]:

$$S = \frac{1}{\log 2} \cdot \log\left(\frac{2000}{DP} - \frac{2000}{DP_0} + 1\right) \tag{5.5}$$

where, DP_0, DP before treatment; *DP*, DP after treatment. The damage factor relates damage to the change in DP (Table 5.2) by taking into account initial DP of undamaged cotton.

Table 5.2 Categorisation of the damage factor *S* according to the degree of damage [51].

S factor	Fibre damage
0.01-0.2	very good, undamaged
0.21-0.30	good - very carefully bleached
0.31-0.50	satisfactory
0.51-0.75	slightly damaged
> 0.75	seriously damaged

5.5.4 Surface chemical analysis

XPS analyses were performed to investigate the surface chemical changes of the cotton fibres using a PHI Quantera Scanning ESCA Microprobe spectrometer

(Physical Electronics, USA). Two different spots were analysed per sample. The samples were irradiated with monochromatic Al Kα X-rays (1486.6 eV) using a X-ray spot size with a diameter of 100 μm and a power of 25 W. The standard take-off angle used for analysis was 45°, producing a maximum analysis depth in the range of 3-5 nm. Survey spectra were recorded with a pass energy of 224 eV (stepsize 0.8 eV), from which the surface chemical compositions were determined. In addition, high-resolution carbon (1s) spectra were recorded with a pass energy of 26 eV (stepsize 0.1 eV), from which the carbon chemical states were determined. All binding energies values were calculated relative to the carbon (C 1s) photoelectron at 285 eV applying a linear background substraction method followed by C 1s curve deconvolution into three Gaussian's curves. Peak positions of these curves were fixed at 285.0 eV (C-C/C-H); 286.6 eV (C-O); and 288.1 eV (C=O/O-C-O) [55-56].

5.5.5 Wetting measurements

The wetting behaviour of the fibres was characterised, according to the capillary-rise method, using a Processor Tensiometer K12 (software version K121, Krüss, Germany). The structural contact angle was calculated using the modified Washburn equation [27] (Eq. 5.2 in Section 5.4.1) with the help of the measured capillary velocity (m^2/t):

A detailed experimental procedure is given elsewhere [27]. In our experiment *n*-decane was used as a total wetting liquid ($\cos\theta = 1$) to determine the capillary constant c [57]. Both the capillary constant c and the contact angle θ were determined as an average of 5 independent measurements performed always in the warp direction on the 2 cm × 2 cm square fabric pieces cut from different (randomly chosen) locations on the sample. For each measurement the initial slope m^2/t of the function $m^2 = f(t)$ was determined using a second-order polynomial fit. The error bars in the plot represent the standard deviation of the measured wetting rate m^2/t averaged over at least five single measurements.

5.5.6 Liquid porosity

An auto-porosimeter (TRI, USA) [48] was used to measure the inter- and intra-yarn pore size distribution in the fabric. The pore size is determined via its effective radius, and the contribution of each pore size to the total free volume. Miller [48] described the operating procedure for liquid porosimetry in detail, which requires quantitative monitoring of the movement of liquid into or out of a porous structure. The effective radius R_{eff} of a pore is defined by the Laplace equation:

$$R_{eff} = \frac{2\sigma\cos\theta}{\Delta P} \tag{5.6}$$

wherein: σ, surface tension of the liquid; θ, advancing or receding contact angle between the solid and the liquid; and ΔP, the Laplace pressure difference across

the liquid/air meniscus. The test liquid used was 0.1% solution of Triton X-100 in double distilled water. It was assumed that cos θ = 1 for the liquid used because of its low surface tension (30 mN m^{-1}).

The pore volume distribution (PVD) of each sample was measured in receding mode in the range of 1-800 μm whereas the PVD taken into consideration represented the curve obtained as a result of averaging of five independent PVD's. For that, the measurements were performed on five swatches of 2.5 × 3.5 cm cut randomly from a fabric sample. The PVD's of a fabric sample obtained in this way were further used to calculate the average effective pore radius as an average of five R_{eff}'s determined at a peak appearing in region of either inter- or intra-yarn pores.

5.6 Results and discussion

5.6.1 Bleaching effectiveness and fibre damage

In this section, special emphasis is given to the problem of chemical damage of cotton fibre, e.g. the decrease in DP of cellulose, caused by catalytic bleaching that is, apart from bleaching effectiveness, a very important indicator of the process acceptability (Section 5.2.1).

The results obtained for the WI, DP and *S* for the "as received" and model fabric after being subjected to the different bleaching treatments are compared in Table 5.3. When analysing the values obtained for DP and WI, it can be seen that the catalytic bleaching of the "as received" fabric (sample **b**, DP = 1978) does not cause significant damage (sample **f,** DP = 1905) whilst producing satisfactory WI (~81). Bleaching under the same conditions with H_2O_2 alone (sample **e**) does not reach the target value (above 80) for the WI, whereas producing slightly lower DP value. The samples treated by O_2/MnTACN (sample **d**) and in a buffer solution only (sample **c**) show negligible change in the WI with no change in DP (within a standard deviation of measurement).

Conventional bleaching (sample **g**) results in good whiteness, similar to the one obtained by catalytic bleaching, but with considerably higher fibre damage (DP = 1543). As this sample has been used to produce the model fabric, all DP values obtained for model fabric are considerably lower when compared to the "as received" fabric. Regarding whiteness (WI) of the untreated model fabric (sample **h**), staining with morin produces WI ~ 50, making it similar to raw unbleached cotton.

When the model fabric (sample **h**) is bleached in the same systems as the "as received" double scoured fabric, the DP decreases from 1361 till 1200 approximately (sample **j**, sample **k**, sample **l**). Therefore, we can conclude that,

although causing approximately the same (if not lower) fibre chemical damage, the H_2O_2/MnTACN bleaching is more effective in terms of WI produced for both fabrics tested, the "as received" and model fabric (~81, sample **f**; and ~80, sample **l**) than the bleaching with H_2O_2 alone (~ 78, sample **e**; and ~61, sample **k**). Moreover, this indicates that different species are operative in the pigment discolouration and fibre damage (i.e. oxidation of cellulose) when using the H_2O_2/MnTACN system instead of H_2O_2 alone.

Table 5.3 WI and DP values for the "as received" fabric and model fabric before and after bleaching at 30°C, pH 10.5 for 15 min.

Label	Sample	WI	DP	S [(iv)]
	"As received" fabric			
a	"as received" scoured once	46.00±0.56	-	-
b	"as received" scoured twice	71.30±0.66	1978	-
c [(i)]	"**b**" treated in buffer solution	74.50±0.33	2056	-
d	"**b**" bleached with O_2/MnTACN	73.33±0.42	2180	-
e	"**b**" bleached with H_2O_2	77.53±0.46	1844	0.16
f	"**b**" bleached with H_2O_2/MnTACN	80.93±0.08	1905	0.12
	Model fabric			
g [(ii)]	"**b**" bleached with H_2O_2 (at 70°C, pH 11)	81.92±0.29	1543	0.41
h	"**g**" stained with morin (model fabric)	50.39±1.10	1361	0.59
i [(iii)]	"**h**" treated in buffer solution	56.64±0.31	-	-
j	"**h**" bleached with O_2/MnTACN	59.08±0.37	1222	0.74
k	"**h**" bleached with H_2O_2	61.03±0.21	1203	0.76
l	"**h**" bleached with H_2O_2/MnTACN	79.70±0.35	1234	0.73

[(i)] blank for the "as received" fabric bleaching experiments
[(ii)] used for preparation of model fabric by staining it with morin
[(iii)] blank for the model fabric bleaching experiments
[(iv)] DP_0 = 2070 in Eq. 5.4, calculated as mean value of the DP for samples **b**, **c** and **d**.

The values obtained for the damage factor *S* show that both sample **e** and sample **f** can be categorised as "undamaged according to the degree of damage classification applied by Interox (1981) (Table 5.2). The sample **g** is categorised as "satisfactory", while all other samples are considered as "slightly damaged", except sample **k** that is categorised as "seriously damaged". This confirms that H_2O_2/MnTACN bleaching at 30°C (sample **f**) produces the same whiteness as conventional bleaching at 70°C (sample **g**), with much lower fibre damage.

5.6.2 Surface chemical analysis of cotton fibre

A low-resolution XPS scan is run to determine the percentages of the elements present at the cotton fibre surface before and after bleaching of both the "as received" cotton fabric and model cotton fabric (Figure 5.4). As expected, the main elements detected are carbon and oxygen. Using area sensitivity factors, an oxygen-to-carbon (O/C) atomic ratio was calculated as an initial indication of

surface oxidation. The O/C atomic ratio found for the "as received" fabric scoured once is 0.32 (sample **a**) and for the double scoured is 0.55 (sample **b**), while the value expected for pure cellulose is 0.83 (Table 5.4). The different bleaching treatments (H_2O_2/MnTACN; H_2O_2 or O_2/MnTACN) further increase the O/C atomic ratio where the highest value of 0.62 is obtained after the bleaching with the H_2O_2/MnTACN catalytic system and H_2O_2 alone (samples **f** and **e**, respectively). It is interesting to note that the treatment in a buffer solution (sample **c**) also leads to a significant increase in the O/C atomic ratio (0.60).

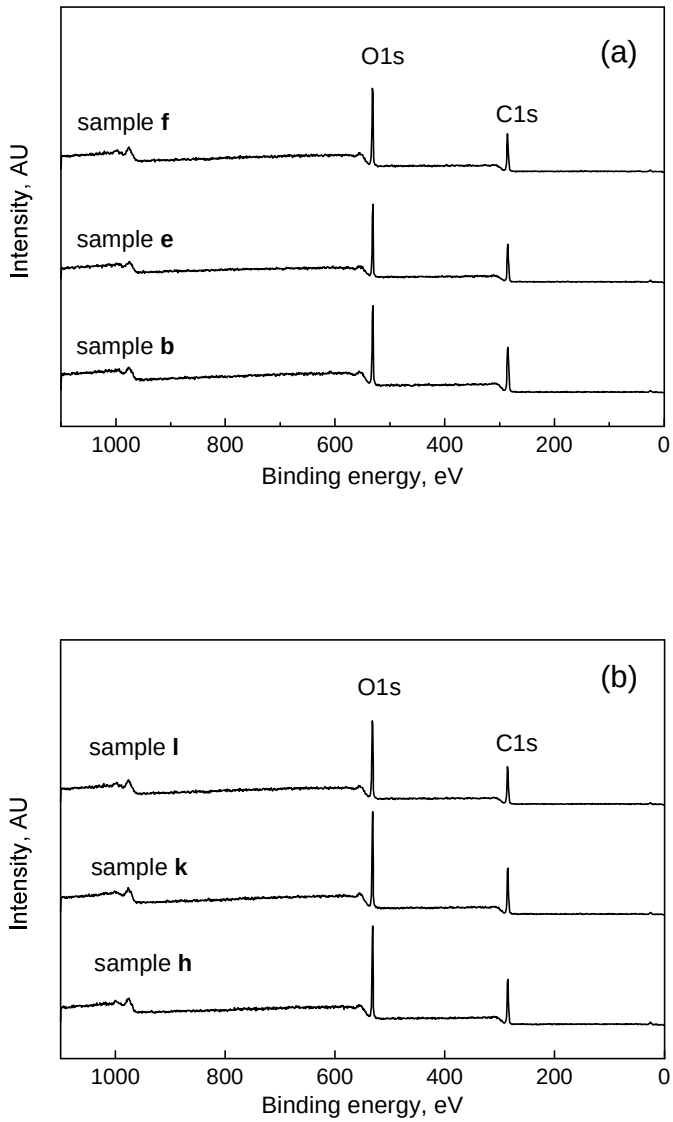

Figure 5.4 Some XPS survey spectra of the "as received" (a) and model (b) cotton fabric before and after bleaching. Labelling scheme used in Table 5.3.

When the "as received" fabric is replaced with the model fabric, the difference in the O/C atomic ratio after the bleaching with H_2O_2/MnTACN (0.76, sample **l)** and H_2O_2 alone (0.69, sample **k**) becomes noticeable. It is important to realise that the "as received" double scoured cotton fabric (sample **b**) is used to produce the model fabric by staining it with morin (sample **h**) after it has been pre-treated with H_2O_2 at 70^{o}C (sample **g**). Knowing that, it is not surprising that sample **g** has a comparable O/C atomic ratio value of 0.63 to that of samples **e** and **f**. Nevertheless, the O/C of sample **g** is not significantly affected after staining it with morin (0.62). This cannot be explained by the similarity in stoichiometry of cellulose (O/C = 0.83) and morin (O/C = 0.47), but lower proportion of morin compared to that of cellulose at the cotton fibre surface.

Table 5.4 XPS analysis of the "as received" and model fabric before and after bleaching.

Sample label [(i)]	O/C	Binding energy, eV		
		285.0	286.6	288.1
		C-C or C-H aliphatic	C-OH or C-O- alcohol, ether	O–C–O or C=O double ether, carbonyl
		C1, at.%	C2, at.%	C3, at.%
a	0.32±0.02	60±2	32±0	8 ±2
b	0.55±0.01	35±2	52±2	13±1
c	0.60±0.01	27±1	58±2	15±1
d	0.60±0.04	27±2	60±0	13±1
e	0.62±0.01	27±1	59±1	14±0
f	0.62±0.02	23±3	59±2	18±1
g	0.63±0.00	26±2	58±0	15±2
h	0.62±0.05	25±2	59±2	16±1
i	0.67±0.02	21±1	64±1	15±1
j	0.69±0.01	19±1	66±2	15±1
k	0.69±0.01	18±0	66±1	16±1
l	0.76±0.01	19±2	69±1	12±3
Cellulose (theor.)	0.83			
Morin (theor.)	0.47			

[(i)] Labelling scheme used in Table 5.3.

Similarly to the "as received" cotton fabric, the treatment of the model fabric in a buffer solution (sample **i**) contributes to approximately the same increase in the O/C atomic ratio as in case of bleaching with H_2O_2 and O_2/MnTACN. On the other hand, after the bleaching of model fabric with the H_2O_2/MnTACN system, the O/C atomic ratio is remarkably increased (up to 0.76) which is the highest value obtained and hence the most comparable to the theoretical value for cellulose (0.83). The observed increase in the O/C atomic ratio cannot be assigned to the oxidation of morin at the fibre surface, as it has been seen that staining with morin (sample **h**) had no impact on the O/C atomic ratio of the

original fabric (sample **g**). This indicates that more complex phenomena occur during bleaching, apart from oxidation of pigment present in cotton fibre.

As explained in Section 5.3, cotton fibre is mainly composed of cellulose with some non-cellulosic components surrounding the cellulose core. These non-cellulosic components are waxes, pectins, and proteins [17, 22, 58] and are mainly found in the cuticle layer and the primary wall which are the outermost layers of the cotton fibre. Scouring process of the cotton fabric removes these impurities for better bleaching and dyeing. It is generally accepted [59] that commonly used alkaline scouring removes waxes, pectins and other impurities from the cotton fabric by treating the fabric in hot sodium hydroxide solution (see Section 5.4.2). As it can be seen from the chemical structures of cellulose, pectin, and waxes (Figure 5.5), cellulose and pectins are carbohydrate polymers. Pectins in the cotton fabrics have been reported to have most of the carboxyl group methylated [58]. Waxes are mixtures of hydrocarbons, alcohols, esters and free acids which have long alkyl chains.

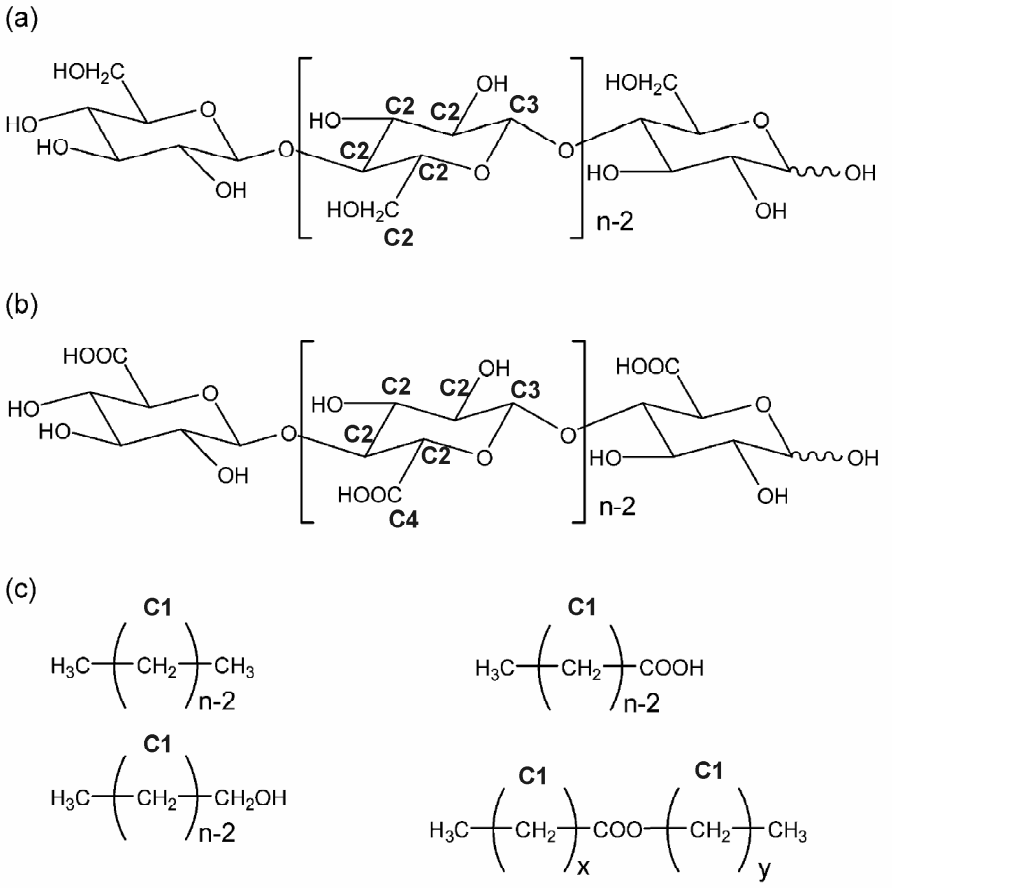

Figure 5.5 Chemical structures of (a) cellulose, (b) pectin, and (c) waxes. For the pectin and the carboxylic acid form of waxes, only free acids structures are drawn. In natural state, they exist as mixtures of carboxylates, free acids, and methyl esters. (C1) C-C/C-H, (C2) C-OR, (C3) C=O/O-C-O, (C4) COOR [58].

To obtain more detailed information on the cotton fibre surface chemical composition as affected by catalytic bleaching, a high-resolution scan is conducted on the C 1s region for all samples listed in Table 5.4 in order to determine the types and amounts of carbon-oxygen bonds present (Figures 5.6 and 5.7). The theoretical binding energies and corresponding bond types are given in Table 5.4. Cellulose is made up of a chain of glucopyranose units, joined at the 1 and 4 positions through elimination of water. Therefore, it is expected that pure cellulose exhibits a two-component C 1s XPS spectrum (C2 and C3 in Table 5.4), having the ratio of lower binding energy (E_B = 286.6 eV) to higher binding energy (E_B = 288.1 eV) components of 0.83 : 0.17 (or ~ 5 : 1). That is, the carbon bonded to two ether linkages appears at higher E_B while all other carbons, whether bonded to an ether or alcohol oxygen, appear at the lower E_B (C3 and C2, respectively, in Figure 5.5a.).

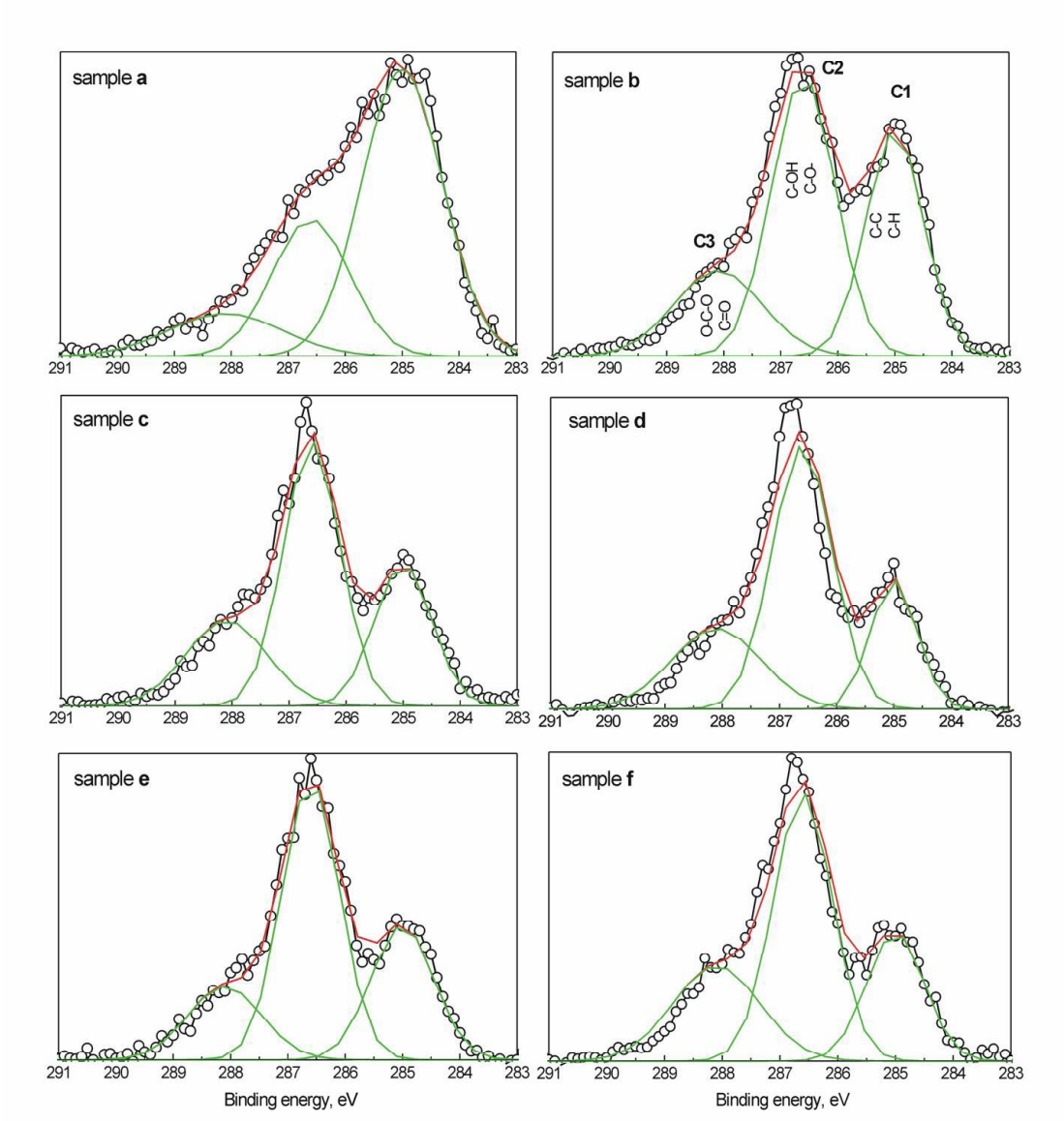

Figure 5.6 XPS scan of C 1s region of the "as received" cotton fabric before and after bleaching. Labelling scheme used in Table 5.3.

In practice, however, additional peaks are found because of the presence of these non-cellulosic impurities which, even though not considered to be covalently bound to the fibre, need to be removed. This is to achieve two main objectives: to convert the cotton fibre from its hydrophobic raw state to a commercially acceptable and 'clean' absorbent form and to visually improve the whiteness of cotton by destroying the yellowish cromophores. For this reason, cotton has to be pre-processed by scouring and bleaching, to remove a range of natural, non-cellulosic impurities, in order to allow effective, uniform dyeing, improve whiteness, fibre quality and impart water absorbency.

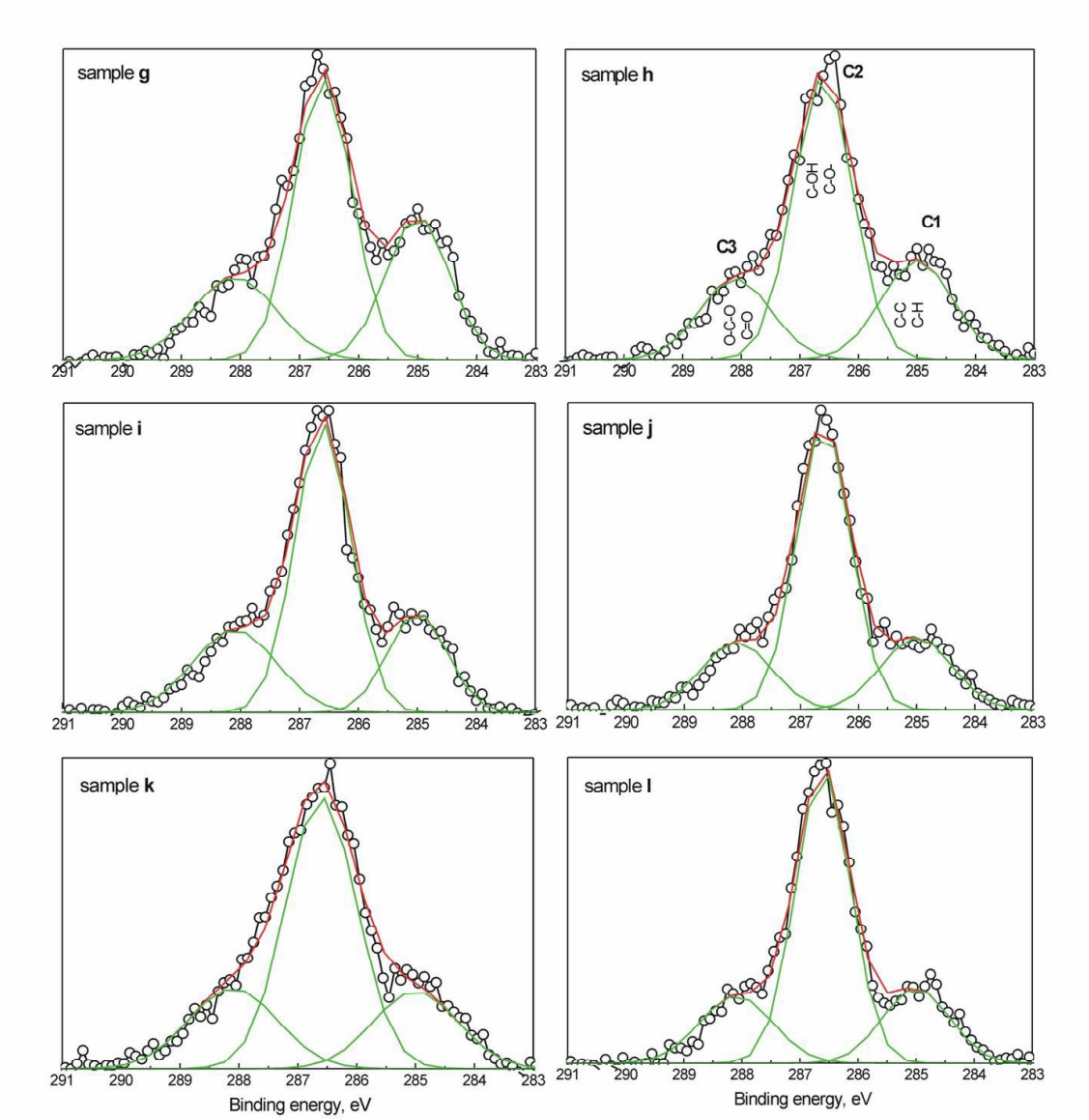

Figure 5.7 XPS scan of C 1s region of the model cotton fabric before and after bleaching. Labelling scheme used in Table 5.3.

The C 1s XPS spectra and deconvolution peaks of the "as received" and model fabrics before and after bleaching with H_2O_2/MnTACN and H_2O_2 are found in Figures 5.6 and 5.7, respectively. The C 1s peak is deconvoluted into three subpeaks, C1, C2, and C3. The C1 peak does not include a carbon–oxygen bond,

whereas C2 and C3 both include a carbon–oxygen bond. The experimentally determined ratios of the subpeaks for the "as received" cotton fabric scoured once and twice are C1 : C2 : C3 = 0.60 : 0.32 : 0.08 and C1 : C2 : C3 = 0.35 : 0.52 : 0.13, respectively (Figure 5.6, Table 5.4), as compared to the abovementioned theoretical values of C1 : C2 : C3 = 0 : 0.83 : 0.17. This shows that the major chemical oxidation state at cotton fibre surface occurs at binding energy of 285.0 eV after the first scouring process, attributed to aliphatic C-C, C-H bonding, indicating that it is of non-cellulosic origin. In addition, the second scouring produces a significant effect on the C 1s XPS spectrum, where a reduction in the spectral contribution of the C1 component from approximately 60 at.% to 35 at.% takes place. The C 1s XPS spectra of the H_2O_2 and O_2/MnTACN bleached fabric (sample **e** and sample **b**), together with the blank (sample **c**), show further and to the same extent, decrease in component C1 (27 at.%) (Table 5.4). After the H_2O_2/MnTACN bleaching, the minimum contribution of this component is reached (23 at.%), showing that this system has the greatest efficiency of removing non-cellulosic compounds.

The lack of any further reduction in component C1 after bleaching of model fabric with H_2O_2/MnTACN (19 at.%, sample **l**) as compared to that of model fabric bleached with H_2O_2 and O_2/MnTACN (18 at.% and 19 at.%, samples **k** and **j**, respectively) (Table 5.4) suggests strong substantivity and inertness of the bound organic material. This is perhaps not entirely unexpected since even with "pure" cellulose materials there is always spectral intensity at 285 eV, typically contributing 10-20 at.% of the C 1s XPS spectral intensity [13-17, 21] indicating either hydrocarbon contamination or polymer modification.

The magnitude of the C2 peak of the "as received" double scoured cotton fabric (52 at.%, sample **b**) is affected to approximately the same extent after bleaching with H_2O_2/MnTACN (59 at.%, sample **f**) as after bleaching with O_2/MnTACN and H_2O_2 (samples **d** and **e**, respectively) (Table 5.4), whereas the H_2O_2/MnTACN bleaching of the model fabric (sample **h**) leads to a larger increase of spectral contribution of the C2 component (69 at.%, sample **l**) than after the O_2/MnTACN and H_2O_2 bleaching (both 66 at.%, samples **j** and **k**, respectively).

Finally, it is shown in Table 5.4 that the H_2O_2/MnTACN bleaching of the "as received" fabric results in a greater increase of the spectral contribution of the C3 peak (from 13 at.% to 18 at.%, sample **b** and sample **f**) compared to the O_2/MnTACN (sample **d**) and H_2O_2 bleaching (sample **e**) due to the formation of surface carbonyl species, which in addition to the O-C-O spectral component, contributed to the observed spectral increase at the C 1s binding energy of 288.1 eV. On the contrary, after the bleaching of the model fabric (sample **g**) with H_2O_2/MnTACN (sample **l**), the contribution of the C3 component is reduced from 16 at.% to 12 at.% suggesting that two concomitant processes could be postulated to interpret the effect of the H_2O_2/MnTACN activity on the cellulose fibre surface:

oxidative degradation and removal of low-molecular-weight carbonyl-rich products into the bleaching solution.

5.6.3 Pore volume distribution

As explained in Section 5.4.2, woven fabrics typically give bimodal distributions [43], where the larger pore sizes are interyarn pores and the smaller reflect the intrayarn structure. The PVD prototype data output for a single incremental liquid extrusion run is shown in Figure 5.8. Starting from the right, as the pressure increased ($\Delta P \sim 1/R_{eff}$, Eq. 5.6), the cumulative curve represents the amount of liquid remaining in the pores. The first derivative of this curve as a function of pore size becomes the pore volume distribution plot, showing the fraction of the free volume of cotton fabric sample made up of pores of each indicated size (effective radius, R_{eff}) [48].

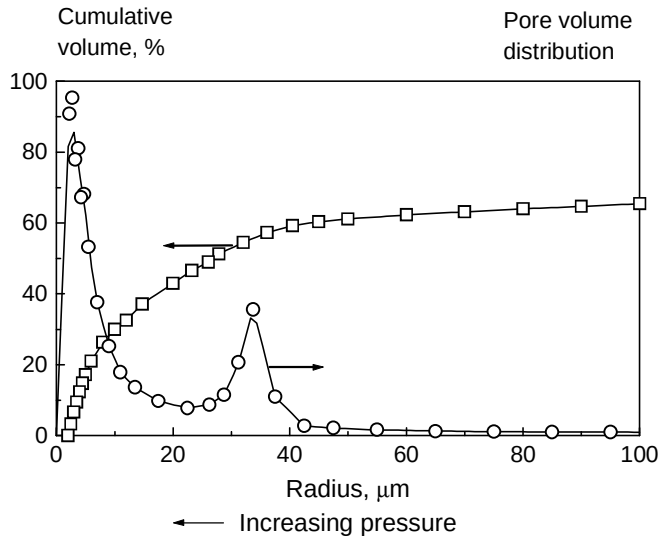

Figure 5.8 Prototype output for a liquid extrusion run: measured cumulative volume and first derivative (PVD).

The pore volume distribution (PVD) plots for the "as received" and model fabric before and after bleaching are presented in Figure 5.9. As it can be seen, the intrayarn pores range between 1 μm (lower limit of the instrument) and 22 μm, while interyarn pores range between 22 μm and 55 μm for both the "as received" and model fabric. The values for the average effective radius of intra- and interyarn pores for the two fabrics analysed are presented in Figure 5.10a-b.

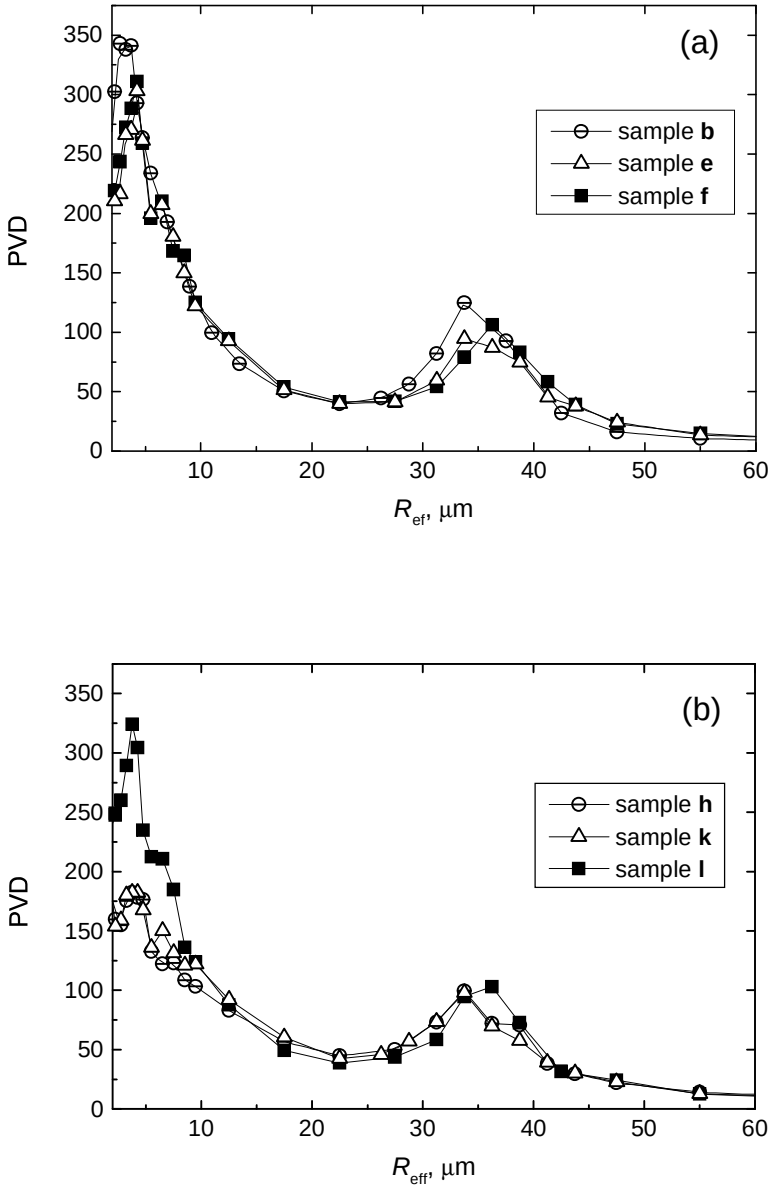

Figure 5.9 PVD results for of the "as received" double scoured (a) and model fabric (b) as a function of the bleaching with and without MnTACN catalyst. Labelling scheme used in Table 5.3.

Both smaller and larger pores remain distributed in the same range after bleaching in the presence and the absence of catalyst MnTACN (Figure 5.9). Nevertheless, the average R_{eff} represented by the peaks of the intra- and interyarn PVD's, shift to the right (towards higher values) after bleaching of both the "as received" and model fabric with the H_2O_2/MnTACN catalytic system (Figure 5.9). Figure 5.10 gives a quantitative observation of a change in the average R_{eff} after bleaching in the presence and absence of MnTACN. Apparently, the effective radius of the largest fraction of both intra- and interyarn pores is enlarged after bleaching with the H_2O_2/MnTACN system (samples **f** and **l**), whereas it stays

approximately unchanged after the bleaching with H_2O_2 alone (samples **e** and **k**). It is expected that the increase in pore size will facilitate fast liquid spreading in fabric which is essential for efficient subsequent wet-treatments such as dyeing and finishing.

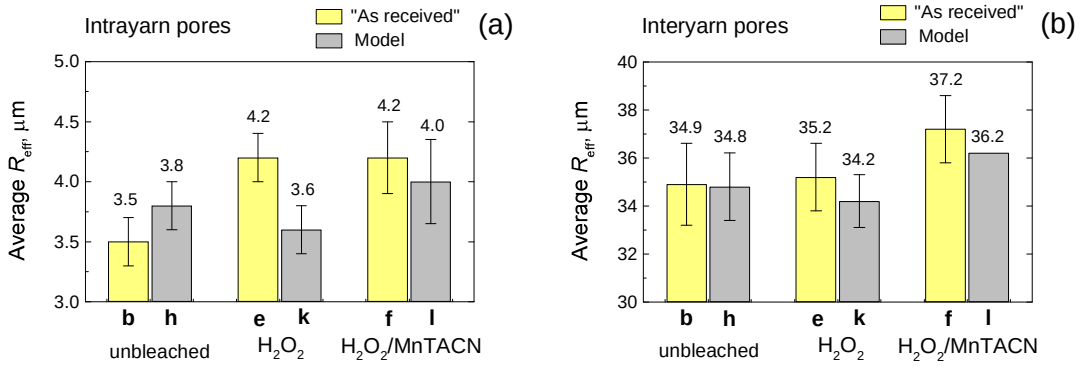

Figure 5.10 Average effective radius R_{eff} of intrayarn (a) and interyarn (b) pores in the "as received" and model fabric as a function of the bleaching in the presence and absence of the MnTACN catalyst. Labeling scheme used in Table 5.3.

5.6.4 Contact angle and capillary constant

Parallel to the PVD analysis, the water contact angles of the "as received" and model cotton fabric as a function of bleaching in the presence and absence of the catalyst MnTACN are determined. The same contact angle of *ca.* 50° is obtained for all bleached samples and the blanks listed in Table 5.3. This is probably not surprising when having in mind that the "as received" fabric is double scoured and therefore hydrophilic in nature. Similar results regarding the contact angle are obtained after bleaching of the model cotton fabric. The "as received" once scoured fabric (sample **a**) has, however, a contact angle above 90°. This can be related to the chemical composition of the fibre surface (Figure 5.6, Table 5.4), where it is possible to see that C1 component is predominant in the C 1s XPS spectrum of this sample (60 at.%). This is direct evidence that the surface of this fibre is to a very high extent covered with non-cellulosic compounds. After the second scouring process, the proportion of C1 component decreases from 60 at.% to 35 at.%, which certainly leads to a remarkable decrease in contact angle. In this case, the bleaching (or the treatment in a buffer solution only) is not critical to the contact angle. It is likely that the majority of cotton fibre impurities that can strongly affect the contact angle are removed by repeated scouring rather than by the bleaching process. On the contrary, even small differences between the different bleaching treatments can be observed by comparing the capillary constants *c* (Figure 5.11). Theoretically, the capillary constant for a porous solid is given by [27]:

$$c = \frac{1}{2}\pi^2 r^5 n^2 \qquad (5.7)$$

where: *r*, the average capillary radius within the porous solid; *n*, the number of capillaries in the sample. From the Washburn data alone, *r* and *n* cannot be calculated independently, whereas the *c* factor can be determined quite reproducibly. It can be seen in Figure 5.11 that the capillary constant *c* for the "as received" sample **b** (6.8×10^{-7} cm^5) increases to 8.5×10^{-7} cm^5 for the sample **f** bleached by H_2O_2/MnTACN. Interestingly, the treatment in a buffer solution (sample **c**) is of the same effect (8.2×10^{-7} cm^5) as bleaching with H_2O_2 (sample **e**) under the conditions applied. Bleaching of model fabric with H_2O_2/MnTACN (sample **l**) causes a remarkable increase in the capillary constant (up to 10.2×10^{-7} cm^5) when compared to that of the H_2O_2 bleached sample (9.0×10^{-7} cm^5, sample **k**). The increase in capillary constant *c*, i.e. in the average capillary radius (Eq. 5.7), is in agreement with the results published recently by Volkov *et al.* [45] (see also Table 5.1, Section 5.4.2) and indicate that bleaching is not limited to the chemical action (oxidation of pigments) as previously stated [12], but also affects the pore structure of the fabric.

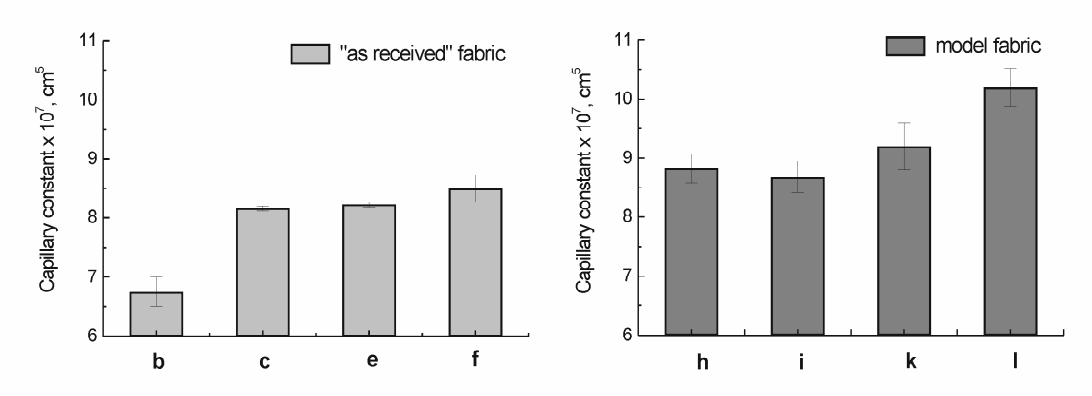

Figure 5.11 Capillary constant as a function of bleaching with and without the MnTACN catalyst. Labelling scheme used in Table 5.3.

5.6.5 Capillary constant vs. removal of the bleaching products

It is evident from Eq. (5.7) that the capillary constant *c* is very sensitive to a change in average capillary radius within the porous solid ($c \sim r^5$). An increase in the capillary constant of cotton fabric after the bleaching, i.e. an increase in the average capillary radius, can be explained by a lower concentration of component C1 (Figure 5.12a) assigned, as already discussed in Section 5.6.2, to a removal of non-cellulosic compounds. A decrease in component C1 is followed by an increase in component C2 (Table 5.4) that also correlates with an increase in the capillary constant (Figure 5.12a). Consequently, an increase in the O/C atomic ratio interrelates with an increase in the capillary constant (Figure 5.12b). As it can be seen in Figure 5.12a-b, the capillary constant changes exponentially with the percentage of C1 and C2 components and the O/C atomic ratio.

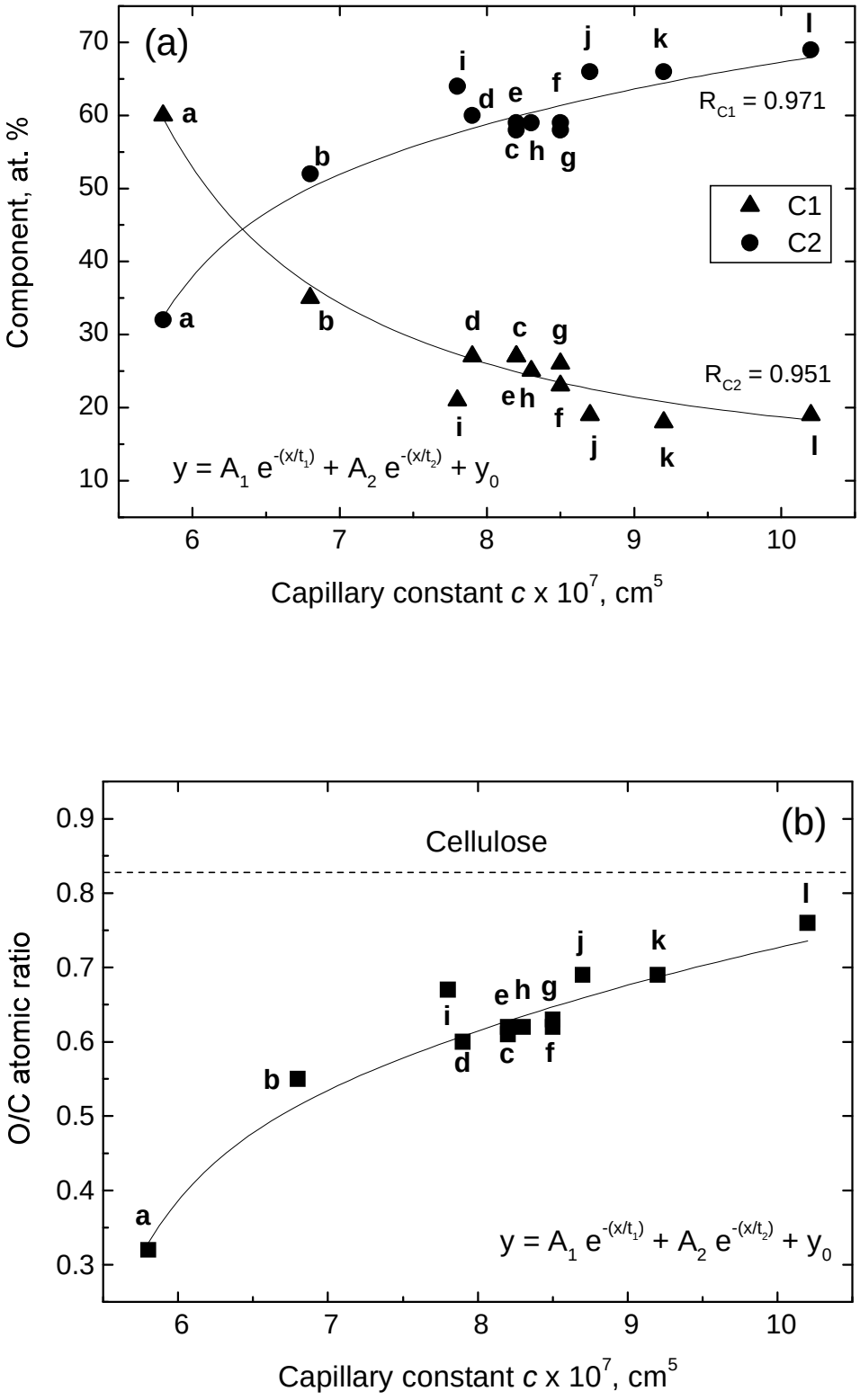

Figure 5.12 Effect of removal of non-cellulosic compounds represented by C1 component (a) and the O/C atomic ratio (b) on capillary constant. Labelling scheme used in Table 5.3.

It is interesting to note that although the proportion of component C1 slowly gets to 17-19 at.% (Figure 5.12a), which is attributed to the presence of non-removable impurities [22], the capillary constant continues with a considerable increase from 9.0×10^{-7} cm^5 to 10.2×10^{-7} cm^5. This means that a further increase in capillary constant *c*, when only non-removable impurities are present at the cotton fibre surface, can only be related to the removal of chain-shortened cellulose into the bleaching solution.

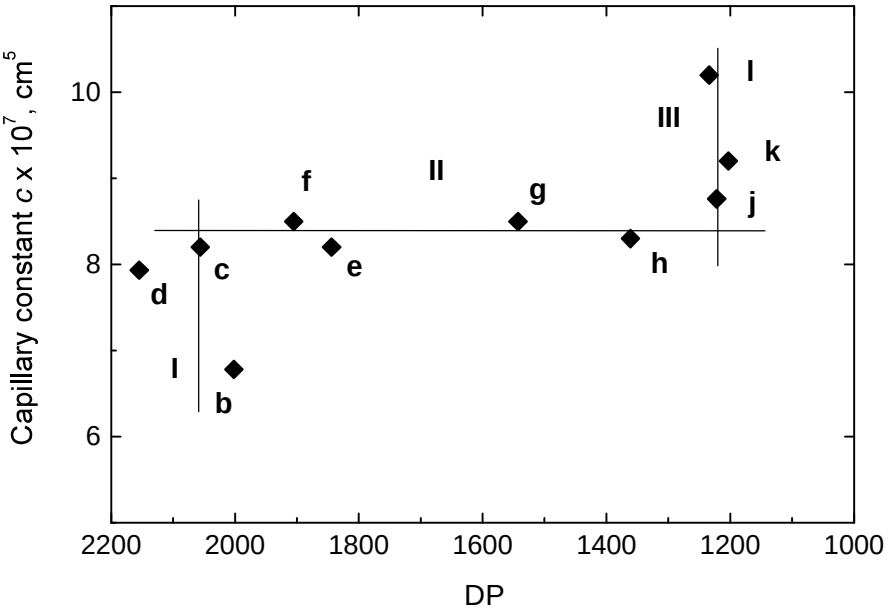

Figure 5.13 Capillary constant vs. DP. Labelling scheme used in Table 5.3.

It can be speculated that the capillary constant for samples **k** and **l** changes noticeably because of possible losses of chain-shortened 'hydrocellulose' during bleaching [9, 60], which we anticipate to be associated with the fibre damage. In an attempt to check this hypothesis, the values of capillary constant are plotted against DP for the samples investigated (Figure 5.13). The lines drawn between experimentally obtained results show that all samples can be set into three groups with respect appreciable changes in either DP or capillary constant. Despite a significant change in the capillary constant for the blank (sample **c**) with respect to the untreated sample **b**, the difference in DP between these two samples is negligible (line I). The samples with considerably different DP (from ~2000 to ~1500) and a similar capillary constant (~8.5×10^{-7} cm^5) are distributed along line II. These samples result from different treatments of the "as received" fabric (samples **c**, **d**, **e** and **f**) as well as from the treatments for obtaining model fabric (samples **g** and **h**). The DP critical to fibre damage (i.e. for $S > 0.5$) can be calculated using Eq. 5.5. Taking into account the DP of untreated sample **b**, the critical fibre damage is expected to occur at $DP \leq 1450$, as observed for model

fabric (sample **h**). Subsequent bleaching of sample **h** leads to a further, but to approximately the same extent, decrease in DP regardless the bleaching procedure applied (samples **j**, **k** and **l**). For these samples the different values for capillary constant are however observed (line III in Figure 5.13), with the maximum value of 10.2×10^{-7} cm^5 obtained after bleaching with H_2O_2/MnTACN (sample **l**). A stepwise change in the capillary constant after bleaching of model fabric, as distinguished from the "as received" fabric, is perhaps not entirely surprising considering the "weakened" cellulosic material in the model cotton fabric. Based on that, we may postulate that during the bleaching of model fabric, the lowering of DP is coupled with a removal of chain-shortened 'hydrocellulose' which results in appreciable increase in the capillary constant.

Hydrocellulose formation breaks glycosidic bonds and produces one reducing (aldehyde) and one non-reducing end group. This can be an explanation for the decrease in proportion of the C3 component at the fibre surface for the model fabric bleached with H_2O_2/MnTACN, whereas for the "as received" fabric this value increases (Table 5.4). The different result concerning the change in C3 component obtained after the H_2O_2/MnTACN bleaching of the "as received" and model fabric is in fact the consequence of the different chemical composition at the cotton fibre surface, whereas the presence of C1 component plays a very important role. In the presence of a significant amount of C1 component at the cotton fibre surface, non-cellulosic compounds represented by this component can be the target of catalytic action and therefore competitive with pigments and cellulose for the catalyst molecules. In the absence of the (removable) C1 impurities chain-breaking oxidative reactions are becoming predominant since more cellulose bonds are vulnerable on the "bare" surface.

5.7 Conclusions

The bleaching of cotton fabric with H_2O_2 catalysed by the dinuclear manganese(IV) catalyst MnTACN at temperature as low as 30°C shows satisfactory bleaching performance while causing limited fibre damage. It produces the same degree of whiteness as the conventional (non-catalytic) bleaching at 70°C, with considerably lower fibre damage. This confirms better selectivity of the catalyst based system in comparison with the less specific system with peroxide alone, indicating that different species are operative in the pigment discolouration and the cellulose oxidation when using the H_2O_2/MnTACN system.

The model fabric, obtained by staining with cotton pigment morin, provides the tool to differentiate between pigment discolouration and other phenomena by examining the chemical and physical effects on cotton fibre caused by catalytic bleaching. The surface changes are clearly observable by XPS analysis, particularly those induced by the H_2O_2/MnTACN bleaching. The decrease of the

relative amount of aliphatic bound carbon is assigned to the removal of non-cellulosic compounds. Cellulose then becomes more exposed on the cotton fibre surface, which is indicated by an increased O/C ratio. On the "bare" surface, more cellulose bonds are vulnerable to the oxidation and consequently the chain-scission of cellulose, i.e. lowering of the DP of cellulose, is more likely to occur.

The measuring of wetting properties indicated that bleaching with the H_2O_2/MnTACN system is not limited to the chemical action (discolouration of pigments and oxidation of cellulose), but also affects capillarity of cotton. The observed increase in capillary constant for regular fabric is explained by the removal of non-cellulosics. Contrary to this, in case of model fabric, the relative amount of non-cellulosic impurities remains constant after applying different bleaching procedures. Due to the considerable differences in DP of cellulose in model and regular fabric, the increase of the capillary constant of model sample after bleaching is likely to be due to removal of chain-shortened 'hydrocellulose'. The liquid porosimetry method indicates that also the fabric pore structure, i.e. the size of the pores in both the regular and model fabric, is affected after bleaching with the H_2O_2/MnTACN system. This is shown through the increase of the average effective radius of the largest fraction of intra- and interyarn pores.

In summary, the approach used in this study provided the tool to explore and to quantify the chemical and physical effects on cotton fibre after catalytic bleaching and to distinguish between the three types of catalytic action: pigment bleaching, removal of non-cellulosic compounds and oxidation of cellulose.

Literature cited

[1] Buschle-Diller, G., El Mogahzy, Y., Inglesby, M.K., Zeronian, S.H., Effects of scouring with enzymes, organic solvents, and caustic soda on the properties of hydrogen peroxide bleached cotton yarn, Text. Res. J., **68** (1998) 920-929.

[2] Hebeish, A., Hashem, M., Higazy, A., A New Method for Preventing Catalytic Degradation of Cotton Cellulose by Ferrous or Ferric Ions During Bleaching with Hydrogen Peroxide, Macromol. Chem. Phys., **202** (2001) 949-955.

[3] Marahusin, L., Kokot, S., Schweinsberg, D.P., Electrogeneration of oxygen at copper and iron electrodes and its interaction with cotton fabric, Corros. Sci., **34** (1993) 1007-1016.

[4] Marahusin, L.D., Kokot, S., Schweinsberg, D.P., Degradation of cotton fabric by electro-generated oxygen: Polarization behaviour of the Pt anode, Corros. Sci., **33** (1992) 1281-1293.

[5] Kokot, S., Marahusin, L., Schweinsberg, P., Morphological study of cotton fabric damage by electro-generated oxygen, Text. Res. J., **63** (1993) 313-319.

[6] Kokot, S., Marahusin, L., Schweinsberg, D.P., Characterizing oxidatively damaged cotton fabrics. II. A model for the catalytic damage phenomenon using electrogenerated oxygen, Text. Res. J., **64** (1994) 710-716.

[7] Kokot, S., Jermini, M., Characterizing oxidatively damaged cotton fabrics. I. A method for estimating relative fabric damage, Text. Res. J., **64** (1994) 100-105.

[8] Bachmann, F., Dannacher, J.J., Freiermuth, B., Studer, M., Kelemen, J., Vat dye

sensitised fibre damage and dye fading by catalytic and activated peroxide bleaching, J. Soc. Dyers Colour., **116** (2000) 108-115.
[9] Zeronian, S. H., Inglesby, M. K., Bleaching of cellulose by hydrogen peroxide, Cellulose, **2** (1995) 265-272.
[10] Lewin, M., Ettinger, A., Oxidation of cellulose by hydrogen peroxide, Cellul. Chem. Technol., **3** (1969) 9-20.
[11] Lewin, M., Oxidation and aging of cellulose, Macromol. Symp., **118** (1997) 715-724.
[12] Hsieh, Y.L., Thompson, J., Miller, A., Water wetting and retention of cotton assemblies as affected by alkaline and bleaching treatments, Text. Res. J., **66** (1996) 456-464.
[13] Duckett, K.E., Surface Properties of Cotton Fibers. In "Surface Characteristics of Fibers and Textiles", Ed. M.J. Schick, Fiber Science Series, Marcel Dekker, Inc. (1975) p. 67.
[14] Soignet, D.M., Berni, R.J., Benerito, R.R., ESCA - a tool for studying treated textiles, J. Appl. Polym. Sci., **20** (1976) 2483-2495.
[15] Ahmed, A., Adnot, A., Grandmaison, J.L., Kaliaguine, S., Douget J., ESCA analysis of cellulosic materials, Cellul. Chem. Technol., **21** (1987) 481-492.
[16] Belgacem, M.N., Czeremuszkin, G., Sapieha, S., Surface characterization of cellulose fibres by XPS and inverse gas chromatography, Cellulose, **2** (1995) 145-157.
[17] Buchert, J., Pere, J., Johansson, L.-S., Campbell, J.M., Analysis of the surface chemistry of linen and cotton fabrics, Text. Res. J., **71** (2001) 626-629.
[18] Johansson, L.-S., Campbell, J., Kolijonen, K., Kleen, M., Buchert, J., On surface distributions in natural cellulose fibre, Surf. Interface Anal., **36** (2004) 706-710.
[19] Dorris, G.M., Gray, D.G., The surface analysis of paper and wood fibres by ESCA (electron spectroscopy for chemical analysis). I. Application to cellulose and lignin, Cellul. Chem. Technol., **12** (1978) 9-23.
[20] Dorris, G.M., Gray, D.G., The surface analysis of paper and wood fibres by ESCA. II. Surface composition of mechanical pulps, Cellul. Chem. Technol., **12** (1978) 721-734.
[21] Laine, J., Stenius, P., Carlsson, G., Strum, G., Surface characterization of unbleached kraft pulps by means of ESCA, Cellulose, **1** (1994) 145-160.
[22] Mitchell, R., Carr, C.M., Parfitt, M., Vickerman, J.C., Jones, C., Surface chemical analysis of raw cotton fibres and associated materials, Cellulose, **12** (2005) 629-639.
[23] Hsieh, Y.L., Liquid transport in fabric structures, Text. Res. J., **65** (1995) 299-307.
[24] Hsieh, Y.L., Wetting contact angle derivations of cotton assemblies with varying perimeters, Text. Res. J., **64** (1994) 552-553.
[25] Hsieh, Y.L., Liquid wetting, transport, and retention properties of fibrous assemblies. I. Water wetting properties of woven fabrics and their constituent single fibers, Text. Res. J., **62** (1992) 677-685.
[26] Kissa, E., Wetting and wicking, Text. Res. J., **66** (1996) 660-668.
[27] Aranberri-Askargorta, I., Lampke, T., Bismarck, A., Wetting behavior of flax fibers as reinforcement for polypropylene, J. Colloid Interface Sci., **263** (2003) 580-589.
[28] Le, C.V., Ly, N.G., Stevens, M.G., Measuring the contact angles of liquid droplets on wool fibers and determining surface energy components, Text. Res. J., **66** (1996) 389-397.
[29] Silva, J.L.G., Al-Qureshi, H.A., Mechanics of wetting systems of natural fibres with polymeric resin, J. Mater. Process. Technol., **92-93** (1999) 124-128.
[30] van Hazendonk, J.M., van der Putten, J.C., Keurentjes, J.T.F., Prins, A., A simple experimental method for the measurement of the surface tension of cellulosic fibres and its relation with chemical composition, Colloids Surf., A, **81** (1993) 251-261.
[31] Grundke, K., Boerner, M., Jacobasch, H.-J., Characterization of fillers and fibres by wetting and electrokinetic measurements, Colloids Surf., **58** (1991) 47-59.
[32] Grundke, K., Bogumil, T., Gietzelt, T., Jacobasch, H.-J., Kwok, D.Y., Neumann, A.W., Wetting measurements on smooth, rough and porous solid surfaces, Prog. Colloid Polym. Sci., **101** (1996) 58-68.

[33] Tröger, J., Lunkwitz, K., Grundke, K, Bürger, W., Determination of the surface tension of microporous membranes using wetting kinetics measurements, Colloids Surf., A, **134** (1998) 299-304.
[34] Chibowski, E., Hołysz, L., Use of the Washburn equation for surface free energy determination, Langmuir, **8** (1992) 710-716.
[35] Washburn, E.W., The dynamics of capillary flow, Phys. Rev., 2nd Series, **27** (1921) 273-283.
[36] Szekely, J., Neumann, A.W., Chuang, Y. K., The Rate of Capillary Penetration and the Applicability of The Washburn Equation, J. Colloid Interface Sci., **35** (1971) 273-278.
[37] Dullien, F.A.L., El-Sayed, M.S., Batra, V.K., Rate of Capillary Rise in Porous Media with Nonuniform Pores, J. Colloid Interface Sci., **60** (1977) 497-506.
[38] Chibowski, E., Perea-Carpio, R., Problems of contact angle and solid surface free energy determination, Adv. Colloid Interface Sci., **98** (2002) 245-264.
[39] Holysz, L., Surface free energy interactions of a 'Thermisil' glass surface - A comparison of the thin layer wicking and contact angle techniques, Adsorpt. Sci. Technol., **14** (1996) 89-100.
[40] Siebold, A., Walliser, A., Nordin, M., Oppliger, M., Schultz, J., Capillary rise for thermodynamic characterization of solid particle surface, J. Colloid Interface Sci., **186** (1997) 60-70.
[41] Kilau, H.W., Pahlman, J.E., Coal wetting ability of surfactant solutions and the effect of multivalent anion additions, Colloids Surf., **26** (1987) 217-242.
[42] Varadaraj, R., Bock, J., Brons, N., Zushma, S., Influence of Surfactant Structure on Wettability Modification of Hydrophobic Granular Surfaces, J. Colloid Interface Sci., **167** (1994) 207-210.
[43] Labajos-Broncano, L., Gonzalez-Martin, M.L., Gonzalez-Garcia, C., Bruque, J.M., Comparison of the use of Washburn's equation in the distance-time and weight-time imbibition techniques, J. Colloid Interface Sci., **233** (2001) 356-360.
[44] Labajos-Broncano, L., Gonzalez-Martin, M.L., Gonzalez-Garcia, C., Bruque, J.M., Influence of the meniscus at the bottom of the solid plate on imbibition experiments, J. Colloid Interface Sci., **234** (2001) 79-83.
[45] Volkov, V.A., Bulushev, B.V., Ageev, A.A., Determination of the Capillary Size and Contact Angle of Fibers from the Kinetics of Liquid Rise along the Vertical Samples of Fabrics and Nonwoven Materials, Colloid J., **65** (2003) 523-525.
[46] Moscou, L., Lub, S., Practical use of mercury porosimetry in the study of porous solids, Powder Techn., **29** (1981) 45-52.
[47] van Brakel, J., Modry, S., Mercury porosimetry: State of the art, Powder Techn., **29** (1981) 1-12.
[48] Miller, B., Tyomkin, I., Liquid porosimetry: new methodology and applications, J. Colloid Interface Sci., **162** (1994) 163-170.
[49] Nierstrasz, V.A., Warmoeskerken, M.M.C.G., in "Textile Processing with Enzymes", Eds. A. Cavaco-Paulo and G.M. Gübitz, Woodhead Publishing Ltd., Cambridge (2003).
[50] DIN 54270, Teil 2, 1977.
[51] Interox, A Bleachers Handbook, Solvay Interox, Houston (1981) p.57.
[52] Malek, R.M.A., Holme, I., The effect of plasma treatment on some properties of cotton, Iranian Polym. J., **12** (2003) 271-280.
[53] Gürsoy, N.Ç., Lim, S.-H., Hinks, D., Hauser, P., Evaluating hydrogen peroxide bleaching with cationic bleach activators in a cold pad-batch process, Text. Res. J., **74** (2004) 970-976.
[54] Eisenhut, O., Zur Frage der Bestimmung des Schadigungswertes Von Fasern, Garnen Oder Geweben aus Zellulose und Von Zellstoffen, Melliand Textilber., **22** (1941) 424-429.

[55] Beamson, G., Briggs, D., “High Resolution XPS of Organic Polymers. The Scienta ESCA 300 Database”, Ed. Wiley, Chichester, UK (1992).
[56] Chastain, J., King, R.C., Jr. (Eds.), “PHI Handbook of X-ray Photoelectron Spectroscopy”, Physical Electronics, Eden Prarie, MN (1995).
[57] Krüss Users Manual, K121 Contact-Angle and Adsorption Measuring System, Version 2.1, 1996, Part C, p. 11.
[58] Chung, C., Lee, M., Kyung Choe, E., Characterization of cotton fabric scouring by FT-IR ATR, Carbohydr. Polym., **58** (2004) 417-420.
[59] Ellis, J., Scouring, enzymes, and softeners. In "Chemistry of the Textiles Industry", Ed. C.M. Carr, Chapman & Hall, London (1995) pp. 249-275.
[60] Cardamone, J.M., Marmer, W.N., in "Chemistry of the Textiles Industry", Ed. C.M. Carr, Chapman & Hall, London (1995) pp. 46-101.

6

Model of catalytic bleaching of cotton

In this chapter a kinetic model is established for a homogeneous model system and, based on that, an attempt is made to explain more complex kinetics of catalytic bleaching of cotton. A general strategy for the study of the mechanism and kinetics of catalytic bleaching is presented followed by the relevant theory to enable a discriminatory assessment of the experimental data obtained.

6.1 Introduction

In previous chapters, studies have been carried out to identify the kinetics of bleaching of both homogeneous model and real (fabric) systems independently, and to try to resolve the mechanistic issues of the bleaching reaction. The results show that both model and real systems were required to provide a comprehensive understanding of the catalytic bleaching of cotton. It has been essential to design a model system which allowed the sensitivity of monitoring pigment discolouration in a bulk solution. Nevertheless, the phenomena that occur in the system that includes textile material are more complex, so the results obtained from one system must therefore be treated with caution when applying them to another system. In this chapter, we make an attempt to evaluate the kinetics of catalytic bleaching of cotton using a kinetic model established for a homogeneous model system. Batch-type reactor is used in both systems, as it is typically used for testing new processes that have not yet been fully developed.

6.2 Model of catalytic bleaching in a homogeneous model system

In general, kinetic model equations for ideal reactor types are derived using mass (or rather molar) balance equations for each species involved. A molar balance on a species A at any instant in time *t*, yields the following general equation:

F_{A0}	+	$R_{v,A}V$	–	F_A	=	dn_A/dt	(6.1)
rate of flow of A into the reactor		rate of production of A by chemical reaction		rate of flow of A out of the reactor		rate of accumulation of A within the reactor	

where: F_{A0} and F_A are molar flow rates of A at reactor inlet and outlet, respectively (mol s^{-1}). $R_{v,A}$ is the production rate of A per unit of reaction volume (mol m^{-3} s^{-1}), V is the reaction volume (m_f^3), n_A is the amount of A (mol) and t is time (s).

In a catalysed reaction it is often more convenient to define the production rate per unit mass of catalyst, instead of the production per unit volume reaction mixture. Eq. 6.2 expresses the relation between these two rate definitions:

$$R_{v,A}V = R_{w,A}W \tag{6.2}$$

where: $R_{w,A}$ is the production rate per unit mass of catalyst (mol kg_{cat}^{-1} s^{-1}) and W is the mass of catalyst in reactor (kg_{cat}).

The mathematical description of bleaching in a homogeneous solution for an ideal batch reactor can be derived for isothermal conditions and the results will be compared to experimentally obtained values. During batch bleaching of cotton pigment of morin in a homogeneous model system, the concentrations of reactants and formed products change as a function of time. In the case of perfect mixing, i.e. in an ideal batch reactor, both temperature and composition (also the catalyst concentration) are uniform throughout the reactor. Since in a batch reactor there is no inflow or outflow of reactants and products during the reaction, a mass balance for morin only contains an accumulation term (left term in Eq. 6.3) and a production term (right term in Eq. 6.3):

$$\frac{dn_{\mathrm{M}}}{dt} = -R_{\mathrm{w,M}} \cdot W \tag{6.3}$$

where: n_{M} is the amount of morin in the reactor (mol), t is the time (s), $R_{\mathrm{w,M}}$ is the specific production rate of morin (mol kg_{cat}^{-1} s^{-1}) and W is the mass of the catalyst in the reactor (kg).

The degree of conversion of morin in the reaction is defined as:

$$X_{\mathrm{M}} = \frac{n_{\mathrm{M0}} - n_{\mathrm{M}}}{n_{\mathrm{M0}}} \tag{6.4}$$

with n_{M0}, the initial amount of morin. For a constant density system (V=constant) we can write:

$$X_{\mathrm{M}} = \frac{C_{\mathrm{M0}} - C_{\mathrm{M}}}{C_{\mathrm{M0}}} \tag{6.5}$$

where C stands for concentration (Chapter 3). Substitution of Eq. 6.4 into Eq. 6.3, with $n_{\mathrm{M0}} = C_{\mathrm{M0}} \cdot V$, leads to:

$$\frac{\mathrm{d}X_{\mathrm{M}}}{\mathrm{d}t} = \frac{W}{n_{\mathrm{M0}}} R_{\mathrm{w,M}} = \frac{1}{C_{\mathrm{M0}}} \frac{W}{V} R_{\mathrm{w,M}} \tag{6.6}$$

For a single reaction and known kinetics the balance for morin M can be integrated at a given temperature to yield a relation between the batch time and the degree of conversion:

$$\frac{1}{C_{\mathrm{M0}}} \frac{W}{V} t = \int_0^{X_{\mathrm{M}}} \frac{1}{R_{\mathrm{w,M}}} \cdot dX_{\mathrm{M}} \tag{6.7}$$

Since the experimental results showed that the bleaching of cotton pigment morin in a homogeneous system is a single irreversible first-order reaction (Chapter 3):

$$\text{Morin} \xrightarrow{k_{\mathrm{w}}} \text{Product}$$

we can write:

$$-R_{w,M} = -k_w C_M \tag{6.8}$$

where: k_w is the first-order rate constant for morin conversion ($m^3\ kg_{cat}^{-1}\ s^{-1}$).

Substitution of Eqs. 6.8 and 6.5 into Eq. 6.7 gives:

$$\frac{1}{C_{M0}}\frac{W}{V}t = \frac{1}{k_w C_{M0}}\int_0^{X_M}\frac{dX_M}{(1-X_M)} \tag{6.9}$$

and integration then yields:

$$X_M = 1 - \exp(-\tau_B k_w) \tag{6.10}$$

with:

$$\tau_B = t\frac{W}{V} \tag{6.11}$$

where τ_B is the batch space-time ($s^{-1}\ kg_{cat}\ m^{-3}$).

Figure 6.1 shows the experimentally obtained data of k_w as a function of the catalyst concentration C_{cat}.

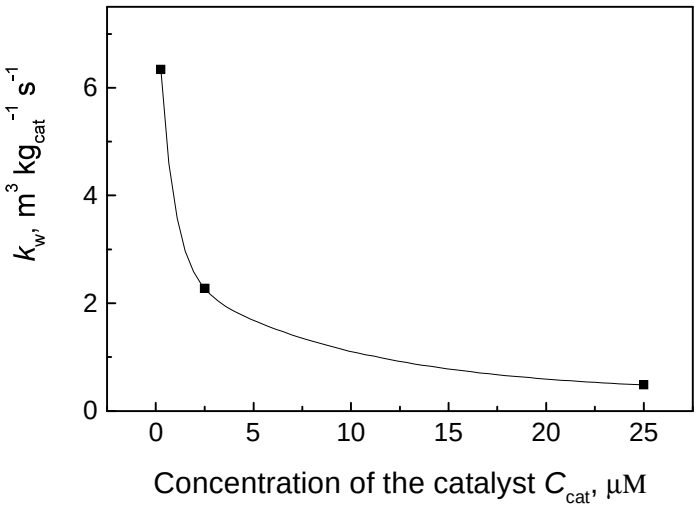

Figure 6.1 Plot of k_w vs. concentration of the catalyst at pH 10.2 and temperature 25°C.

It was possible to fit these data with a 2nd order exponential decay function:

$$k_w = y_0 + A_1 \cdot \exp\left(-\frac{C_{cat}}{B_1}\right) + A_2 \cdot \exp\left(-\frac{C_{cat}}{B_2}\right) \tag{6.12}$$

where: C_{cat} is concentration of the catalyst in the solution (μM). y_0, A_1, A_2, B_1 and B_2 are constants with the following values: 0.348; 5.380; 2.425; 0.636; and

8.717. Substitution of Eqs. 6.11 and 6.12 into Eq. 6.10 gives:

$$X_M = 1 - \exp\left\{-\tau_B\left[y_0 + A_1 \cdot \exp\left(-\frac{C_{cat}}{B_1}\right) + A_2 \cdot \exp\left(-\frac{C_{cat}}{B_2}\right)\right]\right\} \qquad (6.13)$$

Figure 6.2 shows the plots of X_M vs. time for both the calculated values of X_M (using Eq. 6.13) and X_M values obtained from the experimental data for the different concentrations of catalyst.

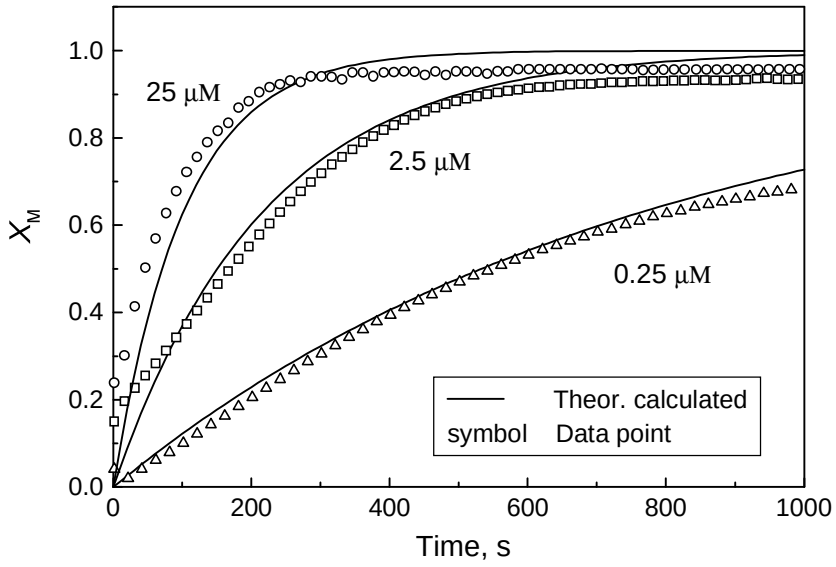

Figure 6.2 Experimental data for a variety of the catalyst concentrations at pH 10.2 and temperature 25°C plotted against model data calculated using Eq. 6.13.

The plots of X_M vs. time clearly show that there is a very good match between the experimental results and the theoretical data. So it can be concluded that the catalytic conversion of morin in a homogeneous system can be described by a first order rate constant in morin.

6.3 Model of catalytic bleaching of cotton

In a heterogeneous system, mass transfer from the fluid phase to the active sites of the porous solid takes place via transport through a stagnant fluid film surrounding the solid phase and via diffusion inside the solid. Transport resistances may lead to an under- or overestimation of the local conditions in the solid phase, and so deviating estimation of the reaction rate.

Based on the theoretical background and the results from Chapter 3 and Chapter 4, it is possible to distinguish seven different physical and chemical steps in a heterogeneous system containing textile material:

1. Transport of the catalyst and hydrogen peroxide from the fluid phase surrounding the cotton fabric (the so-called bulk fluid phase) to the external surface of the fabric.
2. Transport from the external surface of the fabric through the pores towards the CM (coloured matter) in the fibre.
3. Binding of the catalyst (*) on CM to form CM*.
4. Reaction of CM* with H_2O_2 into an intermediate P*.
5. Decomposition of P* (desorption of the reaction product P).
6. Transport of P through the pores towards the external fibre surface.
7. Transfer of P from the external fibre surface to the bulk fluid phase.

Steps 3 to 5 are strictly chemical and consecutive to each other as it can be seen from the chemical mechanism proposed in Chapter 3. In the transport limited situation, the supply of reactant and/or the removal of the reaction product will not be sufficiently fast to keep pace with the potential intrinsic rate, and the concentrations of the catalyst and H_2O_2 within the intra-yarn or intra-fibre pores will be different from the corresponding concentrations in the bulk of fluid phase.

The transport steps 1 and 7 are strictly physical and in series with steps 3 to 5: transfer occurs separately from the chemical reaction. The transport steps 2 and 6, however, cannot be separated from the chemical steps 3 to 5: the transport inside the pores occurs simultaneously with the chemical reaction. This generally points out to different phenomena, which may not exist in a homogeneous model system but can be critical to the bleaching mechanism functioning in a heterogeneous system. Hence, it is noteworthy to distinguish between the following different mechanisms that can occur during bleaching in a heterogeneous system:

1. Solution transport limited kinetics;
2. Intra-yarn and/or intra-fibre transport limited kinetics;
3. Reaction limited kinetics;
4. Coupled transport/reaction kinetics.

Solution transport limited kinetics. The bleaching reaction is transport limited if the reaction of the bleach (H_2O_2 and MnTACN) with the cotton substrate (i.e. fabric) is so fast that the kinetics is limited solely by the rate of mass transport of the bleach to the fibre surface.

Intra-yarn and/or intra-fibre transport limited kinetics. In this case the reaction of the bleach is controlled exclusively by the rate at which it diffuses into the cotton substrate (intra-yarn and/or intra-fibre). The concentration of the bleach at the substrate/water interface would thus be unchanged from that in bulk solution.

Reaction limited kinetics. The reaction is reaction limited if the bleaching is controlled solely by the slow reaction between the coloured molecules and the bleach. In this case, the concentration of bleach within the cotton substrate is uniform

$$[\text{bleach}]_{\text{substrate}} = \text{p}\,[\text{bleach}]_{\text{bulk}} \qquad (6.14)$$

where p is a partition coefficient. The bleaching reaction then follows simple first order kinetics:

$$\ln C_{\text{CM}} = \text{const} - kt \qquad (6.15)$$

provided that: $[\text{bleach}]_{\text{substrate}} >> C_{\text{CM}}$, where C_{CM} stands for concentration of coloured matter in cotton fibre.

Coupled transport/reaction kinetics. Another kinetic possibility is a combination of the above where both transport and diffusion control the bleaching process. For example, the reaction occurs near the surface of the cotton substrate so that diffusion within it may be neglected but the rate of the chemical reaction is comparable with mass transport in solution. In this case, the bleach concentration in solution adjacent to the cotton substrate becomes partly depleted and is described by the convective-diffusion equation [1]. The solution of this mathematical problem has been described using both analytical and numerical methods [2-3].

Assessment of the possible mechanisms

Our results show the linear Arrhenius plot in case of both bleaching in a homogeneous model system (Figure 3.17 in Chapter 3) and heterogeneous system (Figure 4.3 in Chapter 4), which excludes the possibility of the solution transport limited kinetics (external mass transfer from solution through the inter-yarn pores to the fibre surface). Figure 6.3 gives a qualitative illustration of the temperature dependence of observed rate constant which is determined by a physical resistance, τ_{T}, and by a chemical resistance τ_{R}:

$$k^{obs} = \left(\tau_{\text{T}} + \tau_{\text{R}}\right)^{-1} \qquad (6.16)$$

where: $\tau_{\text{T}} = 1/(k_f a)$ and $\tau_{\text{R}} = 1/k_r$; k_f is mass transfer coefficient; a is exterior surface area per unit volume and k_r is rate constant. Increasing the temperature always leads to the strongly transfer limited regime, as the mass transfer coefficient is almost independent of temperature [4]. Therefore, when a convex Arrhenius (or Eyring) plot is obtained it clearly implies that at least two different rate-limiting steps (external mass transfer and reaction rate) are involved [4-5] (Figure 6.3).

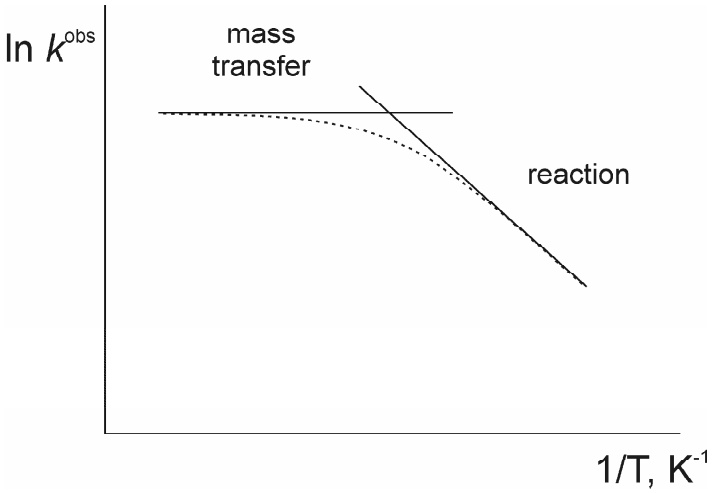

Figure 6.3 Observed rate constant as a function of temperature for transport and reaction in series: external mass transfer (first-order kinetics) [4].

In general, the resistance towards transport mainly originates from the collisions of the molecules, either with each other or with the pore walls. The latter dominate when the mean free path of the molecules is larger than the pore diameter. Usually both types of collision are totally random, i.e. the transport mechanism is of the diffusion type. The effective diffusivity with respect to cotton fabric has to take into account the fact that the diffusion does not occur in a homogeneous medium, but only through the intra-yarn or intra-fibre pores. This means that diffusion coefficient in porous systems is smaller than that in homogeneous systems since it depends on porosity, i.e. a fraction occupied by pore, ε. Besides, the orientation of pores deviates from the direction perpendicular to the external yarn surface, which results in a longer diffusion path through the pores, and thus, a smaller driving force. This effect can be described by tortuosity factor, β [6-8]. The expression for the effective diffusion coefficient D_e which includes the effects of both porosity and tortuosity is given by Eq. 6.17 [6]:

$$D_e = \frac{\varepsilon D}{\beta^2} \tag{6.17}$$

To describe the mass transport in the intra-yarn pores by diffusion, we assume that a textile fabric consists of infinite porous cylindrical yarns with diameter d. For a yarn of a porosity ε_y = 0.4 and tortuosity β_y = 2 [9], and the diffusion coefficient D = 10^{-9} m^2 s^{-1} for an aqueous (homogeneous) medium, Eq. 6.17 results in the effective diffusion coefficient of D_{ey} = 10^{-10} m^2 s^{-1}. Using the effective diffusion coefficient in a yarn D_{ey} and the effective diffusion coefficient in a fibre D_{ef} (D_{ef} = 10^{-14} m^2 s^{-1} [10-11]), the importance of the internal mass transfer limitations at both yarn and fibre level can now be discussed in terms of the degree of internal diffusion limitations given by the internal effectiveness factor (η_i) defined as:

$$\eta_i = \frac{\text{reaction rate with internal diffusion limitation}}{\text{reaction rate at external surface conditions}} \qquad (6.18)$$

The internal effectiveness factor η_i depends on the effective diffusivity D_e and kinetic parameters such as the rate constant k_r and shape of the solid substrate. In order to be able to quantify η_i the Thiele modulus ϕ is generally used [12]. The Thiele modulus ϕ is single dimensionless number given by the ratio of the "kinetic rate" and the "diffusion rate". A generalised equation for Thiele modulus can be found in literature [4, 12]. Without going into details (see for instance [12]), for an irreversible first order reaction, A $\rightarrow$ B, occurring in a solid with cylinder geometry, the generalised Thiele modulus becomes:

$$\phi = \frac{d}{4}\sqrt{\frac{k_r}{D_e}} \qquad (6.19)$$

where: d is the yarn or fibre diameter (d_y or d_f, respectively) (m) and k_r is reaction rate constant (s^{-1}). This allows us to calculate the Thiele modulus for the diffusion via intra-yarn pores (position of coloured matter on the fibre surface) and for the diffusion via intra-fibre pores (position of coloured matter inside the fibre), $\phi_y = 0.158$ and $\phi_f = 1.186$, respectively. ϕ_y and ϕ_f are calculated using Eq. 6.19 for the following the parameters: $d_y = 2 \times 10^{-4}$ m; $d_f = 1.5 \times 10^{-5}$ m [9], approximating a cylindrical shape for cotton fibre; and $k_r = 10^{-3}$ s^{-1}, determined experimentally using a homogeneous model system (Chapter 3).

Small values of ϕ correspond to a situation where internal diffusion limitations, and hence, internal concentration gradients, can be neglected, i.e. the observed rate agrees with the rate expected from intrinsic reaction kinetics. Large values of ϕ correspond to strong internal diffusion limitations. In the extreme case, the internal diffusion is so slow that the reactants do not penetrate the yarn or fibre interior at all. In this case the reaction is limited to the external surface of yarn or fibre. Large values of ϕ lead to an internal effectiveness factor η_i close to 0. The relation between ϕ and η_i is given by Eq. 6.20 [13].

$$\eta_i = \frac{\tanh\phi}{\phi} \qquad (6.20)$$

Figure 6.4 shows Eq. 6.20 on a double logarithmic scale. Two asymptotes can be distinguished:

$$\lim_{\phi \to 0} \eta_i = 1 \qquad (6.21)$$

$$\lim_{\phi \to \infty} \eta_i = \frac{1}{\phi} \qquad (6.22)$$

From Eqs. 6.22 and 6.19 it follows that for strong internal diffusion limitations, the effectiveness factor η_i is inversely proportional to the yarn/fibre diameter.

The internal effectiveness factor for a yarn and fibre can then be calculated substituting $\phi_y = 0.158$ and $\phi_f = 1.186$, respectively, into Eq. 6.20 (see also Figure 6.4). Based on the values obtained for the internal effectiveness factor ($\eta_{iy} = 0.99$ and $\eta_{if} = 0.70$), we can conclude that internal yarn diffusion limitations can be neglected ($\eta_{iy} \approx 1$), i.e. the observed rate agrees with the rate expected from intrinsic reaction kinetics (Eq. 6.18). Nevertheless, the fact that $\eta_{if} < 1$ points out that significant internal fibre diffusion limitations occur. Recently, Tzedakis *et al.* [14] have come to the similar conclusions for catalytic bleaching of kraft pulp (chemical pulp). Based on the results from a kinetic study, the authors found the limitation of the bleaching rate by the diffusion of the catalyst into the pulp fibres. This implies that the kinetic model established for a homogeneous model system cannot be simply applied to a heterogeneous system.

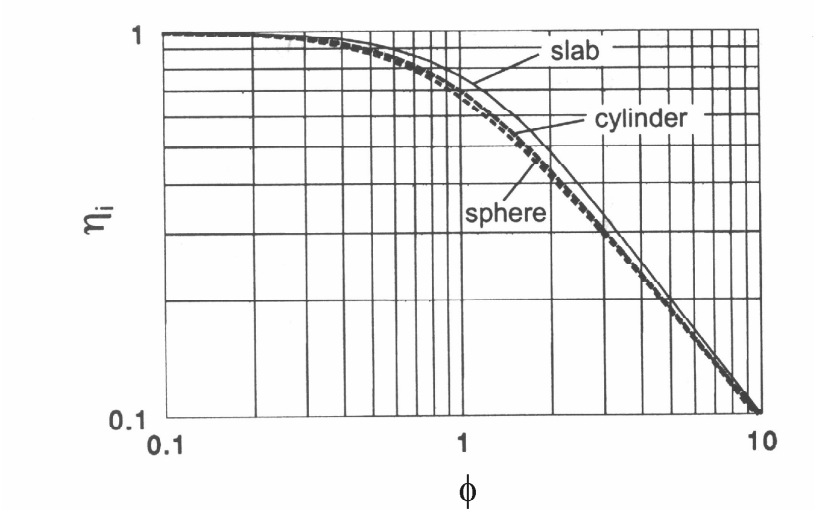

Figure 6.4 Effectiveness factor for slab, cylinder, and sphere geometry as function of the generalised Thiele modulus [4].

To be able to check the above statement and therefore to compare theoretically predicted kinetics on the basis of mathematical model established by Eq. 6.13 with experimental data for the kinetics in a heterogeneous system, it is first necessary to introduce the parameter X_{CM}, which represents the degree of 'removal' of colour from cotton fabric. It corresponds to the degree of conversion of morin in a homogeneous model system X_M in Eq. 6.10. The meaning of 'removal' of colour in this context does not necessarily mean a physical removal of the oxidised (colourless) molecules, but oxidation of coloured matter to colourless compounds. The quantitative measurement of the exact concentration of coloured matter on cotton samples as well as the concentration change after different bleaching time is not possible, since

coloured matter is present with less than 0.5% in an unbleached fibre (Chapter 4). Quantification of the bleaching effect can be done on the basis of the reflectance measurements of the bleached samples as discussed in Chapter 4. Brooks and Moore [15] used the Kubelka and Munk K/S values for a quantitative measure of the presence of coloured matter on the cotton fabric. The mathematical expression of Kubelka-Munk theory relates the absorption coefficient (*K*), scattering coefficient (*S*), and reflectance (*R*):

$$\frac{K}{S} = \frac{(100-R)^2}{2R} \tag{6.23}$$

where: *R* is the percentage reflectance of the sample at a particular wavelength. According to the optical theory which predicts the reflectance of surface colours that was first proposed by Kubelka and Munk, this function is directly proportional to the concentration of coloured matter. Therefore, for a quantitative measure of concentration of coloured matter the following equations can be used:

$A_0 = \left(\frac{K}{S}\right)_0$ = 'Unbleached' sample

$A_\infty = \left(\frac{K}{S}\right)_\infty$ = 'Completely bleached' sample

$A_t = \left(\frac{K}{S}\right)_t$ = 'Bleached' sample after time *t*

The 'completely bleached' sample was bleached at 60°C for 15 minutes with H_2O_2/MnTACN (*R* = 90.17). The dimensionless (relative) concentration of coloured matter available for bleaching before and after bleaching for time *t* are given by Eq. 6.24 and Eq. 6.25, respectively:

$$C'_{CM} = A_0 - A_\infty \tag{6.24}$$

$$C'_{CM} = A_t - A_\infty \tag{6.25}$$

Based on above equations, we define the degree of removal of coloured matter as:

$$X_{CM} = \frac{A_0 - A_t}{A_0 - A_\infty} \tag{6.26}$$

The experimentally obtained values for X_{CM} can now be compared to the theoretically calculated values for X_M (using Eq. 6.13) when the reaction in heterogeneous and homogeneous model systems performed under similar conditions pH, temperature and with the same concentration of the catalyst. The results obtained for the different temperatures are presented against bleaching time *t* in Figures 6.5-6.8. As expected on the basis of the Thiele modulus calculations presented above, the experimentally obtained values for X_{CM} vs. bleaching time curves show a significant deviation from the theoretically

calculated data at the different temperatures. A relatively fast kinetics at the beginning of the reaction is followed with a significantly slower kinetics at longer bleaching times. Bearing in mind the strong intra-fibre diffusion limitations, the bi-phasic nature of bleaching in a heterogeneous system (discussed also in Chapter 4) can be attributed to the fast bleaching of coloured matter present at the fibre surface and the slow bleaching of coloured matter present in the fibre bulk. Based on that, we may conclude that the initial bleaching is limited by the chemical reaction at the surface, whilst at longer times the intra-fibre diffusion plays a significant role in the bleaching kinetics. This can perhaps explain the discrepancy in the energy of activation E_a calculated for the bleaching in a homogeneous model system (63.0 kJ/mol, Chapter 3) and heterogeneous system (46.2 kJ/mol, Chapter 4), since not the intrinsic reaction constants are observed in a heterogeneous system.

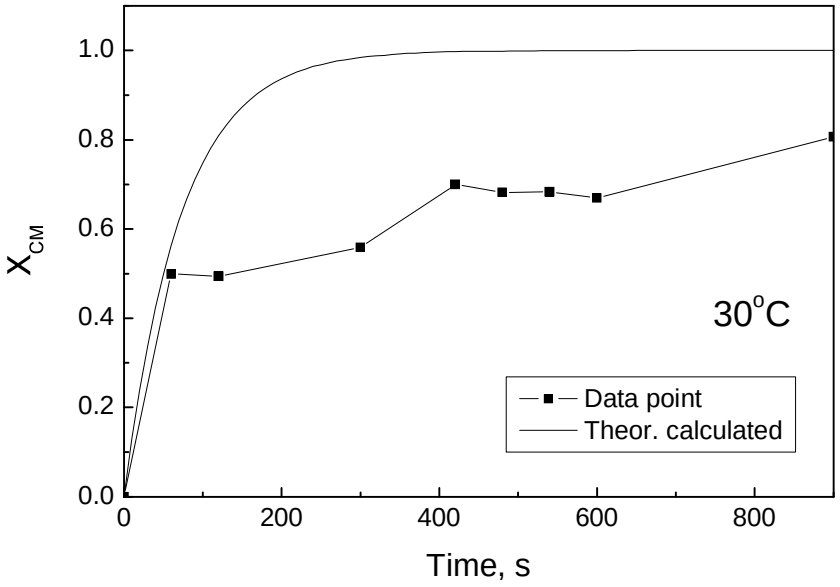

Figure 6.5 Theoretically calculated data (Eq. 6.13) for bleaching in a homogeneous model system plotted against experimental data for bleaching in a heterogeneous system at 30°C and pH 10.2 with 10 μM catalyst.

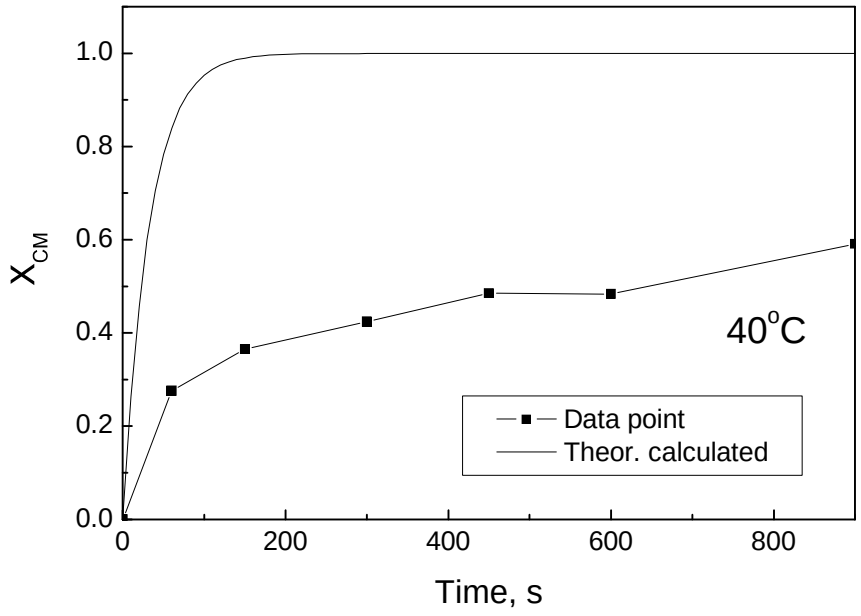

Figure 6.6 Theoretically calculated data (Eq. 6.13) for bleaching in a homogeneous model system plotted against experimental data for bleaching in a heterogeneous system at 40°C and pH 10.2 with 10 µM catalyst.

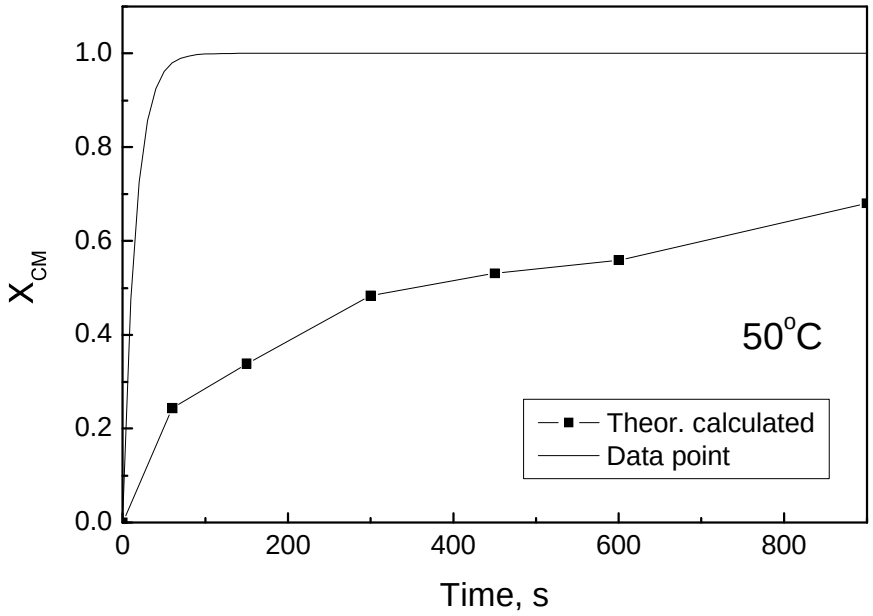

Figure 6.7 Theoretically calculated data (Eq. 6.13) for bleaching in a homogeneous model system plotted against experimental data for bleaching in a heterogeneous system at 50°C and pH 10.2 with 10 µM catalyst.

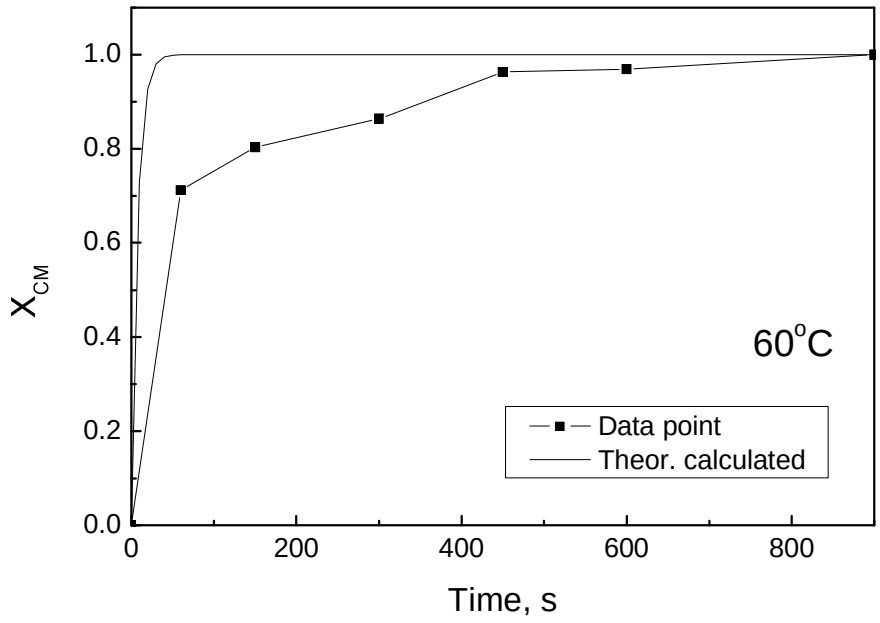

Figure 6.8 Theoretically calculated data (Eq. 6.13) for bleaching in a homogeneous model system plotted against experimental data for bleaching in a heterogeneous system at 60°C and pH 10.2 with 10 µM catalyst.

6.4 Conclusions

An understanding of the mechanism of the catalytic bleaching is essential in the design and optimisation of a new low-temperature process. In the work presented in this chapter, a kinetic model of bleaching of cotton pigment in a homogeneous system has been established. Nevertheless, the phenomena that occur in the system with textile material are more complex, so the results obtained from homogeneous system must therefore be treated with caution when applying them to heterogeneous system. It was shown on the basis of calculation of the Thiele modulus and internal effectiveness factor that the intra-yarn diffusion limitations can be neglected, whereas the significant intra-fibre diffusion limitations may occur during bleaching of cotton. This was in agreement with a significant deviation of the experimental results for the degree of removal of colour on cotton fibre (heterogeneous system) from the theoretical values for the degree of conversion of morin (homogeneous model system) plotted against time. It was concluded that the initial bleaching phase was limited by the chemical reaction at the surface, whereas the intra-fibre diffusion can play a significant role in the bleaching at longer times.

Literature cited

[1] Winkler, J., Smith, E.R., Compton, R.G., A Study of the Mechanism of Bleaching Cotton Using Peracids and Hydrogen Peroxide as Model Systems, J. Colloid Interface Sci., **195** (1997) 229-240.

[2] Gooding, J.J., Compton, R.G., Brennan, C.M., Atherton, J.H., The dyeing of nylon and cotton cloth with azo dyes: Kinetics and mechanism, J. Colloid Interface Sci., **180** (1996) 605-613.

[3] Compton, R.C., Winkler, J., Riley, D.J., Bearpark, S.D., Spectrofluorimetric Hydrodynamic Voltammetry: Investigation of Reactions at Solid/Liquid Interfaces, J. Phys. Chem., **98** (1994) 6818-6825.

[4] van Santen, R.A., van Leeuwen, P.W.N.M., Moulijn, J.A., Averill, B.A., Eds., Catalysis: An Integrated Approach, Elsevier, Amsterdam, 1999.

[5] James, A.P., Mackirdy, I.S., Chemistry of peroxygen bleaching, Chem. Ind., **12** (1990) 641-645.

[6] Rietema, K., Fysische transport- en overdrachtsverschijnselen, Het Spectrum, Utrecht, 1976.

[7] Nierstrasz, V.A., Warmoeskerken, M.M.C.G., Process engineering and industrial enzyme applications. In: Textile processing with enzymes, A. Cavaco-Paulo and G.M. Gübitz Eds., Woodhead Publishing Ltd, Cambridge, 2003, pp. 120-157.

[8] Warmoeskerken, M.M.C.G., van der Vlist, P., Moholkar, V.S., Nierstrasz, V.A., Laundry process intensification by ultrasound, Colloids Surf., A, **210** (2002) 277-285.

[9] van den Brekel, L.D.M., Hydrodynamics and mass transfer in domestic drum-type fabric washing machines, PhD thesis, Technical University of Delft (1987).

[10] Chrastil, J., Adsorption of direct dyes on cotton. Kinetics of dyeing from finite baths based on new information, Text. Res. J., **60** (1990) 441-446.

[11] Chrastil, J., Reinhardt, R.M., Blanchard, E.J., Influence of mercerization and crosslinking of cotton fabrics on dyeing kinetics of direct dyes from finite baths, Text. Res. J., **60** (1990) 413-416.

[12] van ‘t Riet, K., Tramper, J., Basic Bioreactor Design, Marcel Dekker, Inc., New York, 1991.

[13] Levenspiel, O., Chemical Reaction Engineering, John Wiley & Sons, Inc., New York, 1972.

[14] Tzedakis T., Benzada Y., Comtat, M., Kinetic Study of Binuclear Manganese-Tris(2-methyl pyridyl)amine Complex Used as a Catalyst for Wood Pulp Bleaching, Ind. Eng. Chem. Res., **40** (2001) 3435-3444.

[15] Brooks, R.E., Moore, S.B., Alkaline hydrogen peroxide bleaching of cellulose, Cellulose, **7** (2000) 263-286.

List of symbols

A	frequency factor (Arrhenius equation)
A	cross-sectional area (Washburn equation), m^2
A	concentration of coloured matter
a	exterior surface area per unit volume, m^{-1}
A_1, A_2	constants (Eq. 6.13)
Abs	absorbance
+b	yellowness
B_1, B_2	constants (Eq. 6.13)
c	capillary constant (Washburn equation), cm^5
C_{cat}	catalyst concentration, µM
C'_{CM}	dimensionless (relative) concentration of coloured matter available for bleaching
C_M	concentration of morin, $mol \cdot L^{-1}$
D	diffusion coefficient, $m^2 \cdot s^{-1}$
d	diameter, m
D_e	effective diffusion coefficient, $m^2 \cdot s^{-1}$
DP	degree of polymerisation
E_a	activation energy, $kJ \cdot mol^{-1}$
F	cuprammonium fluidity
F_A	molar flow rate (mass balance equation), $mol \cdot s^{-1}$
f_S	fraction of H_2O_2 consumed by the cotton substrate
$\Delta G^{\#}$	free activation enthalpy, $kJ \cdot mol^{-1} \cdot K^{-1}$
h	Plank constant [$6.626 \cdot 10^{-34}$ J·s]
$\Delta H^{\#}$	activation enthalpy, $kJ \cdot mol^{-1}$
K	absorption coefficient (Kubelka-Munk)
k	rate constant, s^{-1}
k_B	Boltzmann's constant [$1.381 \cdot 10^{-23}$ $J \cdot K^{-1}$]
k_{decomp}	rate constant of hydrogen peroxide consumption, s^{-1}
k_f	mass transfer coefficient, $m \cdot s^{-1}$
k^{obs}	observed rate constant, s^{-1}
k_r	reaction rate constant, s^{-1}
k_w	first-order rate constant for morin conversion, $m^3 \cdot kg_{cat}^{-1} \cdot s^{-1}$
K/S	Kubelka-Munk value
m	weight of the liquid that penetrates into the capillary (Washburn equation), kg
n	number of capillaries in the sample (Washburn equation)
n_A	amount of species A (mass balance equation), mol
n_B	total amount of H_2O_2 used during bleaching, mol
n_C	amount of H_2O_2 decomposed in the bulk solution, mol
n_M	amount of morin in the reactor, mol
n_S	amount of H_2O_2 used exclusively by the substrate, mol

ΔP	Laplace pressure difference across the liquid/air meniscus (Laplace equation), $N \cdot m^{-2}$
R	gas constant [8.314 $J\ K^{-1} \cdot mol^{-1}$]
R	percentage reflectance
R	correlation coefficients of least-squares regressions
r	average radius of the capillary within the porous solid, m
Rd	degree of reflectance
R_{eff}	effective radius of the pores (Laplace equation), μm
$R_{v,A}$	the production rate of A per unit of reaction volume (mass balance equation), $mol \cdot m^{-3} \cdot s^{-1}$
$R_{w,A}$	production rate per unit mass of catalyst, mol $kg_{cat}^{-1} \cdot s^{-1}$
$R_{w,M}$	specific production rate of morin, mol $kg_{cat}^{-1} \cdot s^{-1}$
S	damage factor (Eisenhut's Tendering factor, T.F.)
S	scattering coefficient (Kubelka-Munk)
$\Delta S^{\#}$	activation entropy, $kJ \cdot mol^{-1} \cdot K^{-1}$
T	temperature, K
t	time, s
t	penetration time (Washburn equation), s
V	reaction volume (mass balance equation), m_f^3
W	mass of catalyst in reactor, kg_{cat}
WI	whiteness index
X	colorimetric coordinate
X_{CM}	degree of 'removal' of colour from cotton fabric
X_M	degree of conversion of morin
Y	colorimetric coordinate
y_0	constant (Eq. 6.13)
Z	colorimetric coordinate

Greek symbols

β	tortuosity factor
ε	fraction occupied by pore; porosity (Eq. 6.17)
ϕ	Thiele modulus
η	liquid viscosity, Pa·s
η_i	internal effectiveness factor
σ	liquid surface tension, $N \cdot m^{-1}$
ρ	liquid density, $kg \cdot m^{-3}$
τ_B	batch space-time, $s^{-1} \cdot kg_{cat} \cdot m^{-3}$
τ_R	chemical resistance (Eq. 6.16)
τ_T	physical resistance (Eq. 6.16)
θ	solid/liquid contact angle, deg

List of abbreviations

AOX	absorbable organic halogens
AOX	alcohol oxidase
ATP	adenosine triphosphate
CIE	International Commission on Illumination
CM	cotton fibre coloured matter
DMSO	dimethyl sulphoxide
DP	degree of polymerisation
EDTA	ethylenediaminotetraacetic acid
EPR	Electron Paramagnetic Resonance
ESI-MS	Electrospray Ionisation Mass Spectrometry
HT	high temperature
HVI	High Volume Instrument
MnTACN	dinuclear tri-μ-oxo bridged manganese(IV) complex of the ligand 1,4,7-trimethyl-1,4,7-triazacyclononane
NMR	Nuclear Magnetic Resonance
NOBS	nonanoyloxybenzene sulfonate
OEC	oxygen evolving centre
PVD	pore volume distribution
RR	ribonucleotide reductase
SOD	superoxide dismutase
TACN	1,4,7-trimethyl-1,4,7-triazacyclononane ligand
TAED	tetraacetylethylenediamine
WI	whiteness index
XOD	xanthine oxidase
XPS	X-ray photoelectron spectroscopy

SUMMARY

The scope of this thesis was to investigate the possibility of low-temperature cotton bleaching employing dinuclear tri-μ-oxo bridged manganese(IV) complex of the ligand 1,4,7-trimethyl-1,4,7-triazacyclononane (MnTACN) as the catalyst in the system with hydrogen peroxide. With this objective in mind, the fundamental aspects of catalytic bleaching were studied both at molecular and macroscopic level.

In Chapter 1, an introduction to various aspects of cotton bleaching was given. After a brief overview of the importance of obtaining white textile material, the structural features of cotton were briefly discussed with the focus on the origin of its natural colour. A short introduction to the current hydrogen peroxide bleaching processes was presented and currently available possibilities for catalytic bleaching were reviewed. The application of catalytic oxidation in laundry bleaching is discussed with special emphasis on manganese complexes with 1,4,7-trimethyl-1,4,7-triazacyclononane ligands (TACN).

An unprecedented ability of the MnTACN catalyst to activate molecular oxygen via stepwise formation of hydrogen peroxide towards the oxidation of flavonoids at ambient temperatures in alkaline aqueous solution was reported in Chapter 2. A detailed investigation of the MnTACN catalysed dioxygen activation in the oxidation of morin, a typical representative of flavonoids giving colour to native cotton fibre, was described in this chapter. The involvement of superoxide O_2^- and/or H_2O_2 was investigated through the use of a novel method based on the enzymes: superoxide dismutase, catalase, xanthine oxidase and alcohol oxidase. Superoxide dismutase and catalase were used as inhibitory enzymes (superoxide dismutase catalyses dismutation of O_2^- anion into O_2 and H_2O_2; catalase catalyses decomposition of H_2O_2 into O_2 and H_2O). Xanthine oxidase and alcohol oxidase were used as acceleratory enzymes (xanthine oxidase catalyses reduction of O_2 to O_2^-; alcohol oxidase catalyses reduction of O_2 to H_2O_2). A combination of the inhibitory and acceleratory experiments was used to prove the nature of active species derived from dioxygen that are responsible for the oxidation of cotton pigment morin.

The primary focus of Chapter 3 was to reveal the kinetic and mechanistic details of catalytic bleaching under homogeneous conditions. To this end, both the substrate scope (coloured matter) and the catalyst scope (activation) were studied. The structure-reactivity relationship study involved a series of model compounds structurally related to morin and a systematic study of their oxidation by UV-Vis spectroscopy. These results suggested that binding between the catalyst and the flavonoid involves interaction with the hydroxyl at C-3, the carbonyl at position C-4, and the manganese centre of the catalyst. Electrospray ionisation-mass spectrometry (ESI-MS) analysis of morin and the oxidation product suggested that the reaction proceeds predominantly via a monooxygenase mechanism (one O-atom incorporated into the molecule of morin). These findings were confirmed by recording NMR spectra of the oxidised product and morin, thus providing an additional evidence that morin has not been oxidised and hydrolysed to the free benzoic acids. The results from the ESI-MS experiments on aqueous solutions of MnTACN as well as mixtures of MnTACN with O_2 and/or morin suggest that the dinuclear manganese species play an important role, whereas the ligand exchange can be the real situation. Reaction kinetics and activation parameters were calculated. The temperature dependence of the first-order rate constant k was studied at pH 9.5 and pH 10.0 over the temperature range 20-60^{o}C. The energy of activation E_a, the enthalpy of activation $\Delta H^{\#}$ and the entropy of activation $\Delta S^{\#}$ were calculated using the Arrhenius plot and the Eyring plot. The Chapter ended with a mechantic proposal that resulted from the approach used in Chapter 2 and Chapter 3.

The performance of the catalyst MnTACN in the bleaching of cotton with hydrogen peroxide was studied in Chapter 4. The most important bleaching parameters, pH and temperature, as well as kinetics of hydrogen peroxide decomposition during bleaching process, were investigated. Catalytic bleaching proceeds via fast bleaching phase (less than 2.5 minutes) followed by a noticeably slower bleaching phase. A qualitative analysis of the kinetics of hydrogen peroxide decomposition catalysed by MnTACN was done employing UV-Vis spectrophotometry. The content of hydrogen peroxide remaining in a bleaching solution after different bleaching times and different temperatures was determined by cerium(IV) titration reactions. The results showed that very small quantities of the catalyst MnTACN (10 μM) increased the reaction rates in hydrogen peroxide bleaching system. Decomposition kinetics study revealed that hydrogen peroxide consumption follows first order kinetics. The calculation of the fraction of hydrogen peroxide consumed due to the presence of substrate suggests that the active species formed during bleaching at 30^{o}C catalyses the oxidation of the substrate, and not decomposition of H_2O_2 in solution, showing that substrate bleaching is the major pathway under these conditions. The results show that bleaching of cotton in the presence of the catalyst at temperature as low as 30^{o}C produces a satisfactory whiteness within relatively short time. A maximum activity of bleaching catalysed with MnTACN was obtained within a

relatively wide range of pH (pH 9.5-11), whereas maximum bleaching effectiveness for uncatalysed bleaching was observed at higher pH (pH 11.5). Operating within wider pH range gives the catalytic system an advantage over conventional peroxide bleaching since it allows for normal fluctuations in everyday plant operations without sacrificing quality and reproducibility.

Chapter 5 reported on physicochemical changes on cotton fibre as affected by catalytic bleaching. The study involved, apart from the regular cotton fabric, the model cotton fabric prepared by staining with morin. This approach has provided the tool to explore and to quantify the chemical and physical effects on cotton fibre after catalytic bleaching and to distinguish between the three types of catalytic action: pigment bleaching, removal of non-cellulosic compounds and oxidation of cellulose. Surface chemistry and wetting properties of cotton fibres as affected by catalytic bleaching have been investigated by X-ray photoelectron spectroscopy (XPS) and contact angle measurement. The capillary constant of the cotton fabric changed after bleaching, whereas the highest values were obtained using the H_2O_2/MnTACN catalytic system. An auto-porosimeter was used to measure the inter- and intra-yarn pore size distribution in the fabric. The average effective radii of interyarn and intrayarn pores shifted towards higher values after bleaching with H_2O_2/MnTACN. The XPS spectra and the deconvolution peaks show that in the presence of a significant amount of C1 component (C-C or C-H, aliphatic) at the cotton fibre surface, non-cellulosic compounds represented by this component can be the target of catalytic action and therefore competitive with pigments and cellulose for the catalyst molecules. In the absence of the (removable) C1 impurities chain-breaking oxidative reactions are becoming predominant since more cellulose bonds are vulnerable on the “bare” surface. Finally, the increase in capillary constant was interrelated with the removal of bleaching products (low-molecular-weight products characterised by the C1 component in C 1s XPS spectrum) as well as chain-shortened cellulose (as assumed on the basis of critical drop in degree of polymerisation DP) into solution during bleaching and subsequent rinsing operations. The results obtained show an important interrelationship between the removal of non-cellulosic compounds and an increase in the capillary constant of the bleached cotton fabric. This detailed investigation confirmed that the bleaching efficiency of the H_2O_2/MnTACN system is superior to that of non-catalytic H_2O_2 system while causing the same (if not lower) fibre chemical damage.

A model for catalytic bleaching of cotton was proposed in Chapter 6. In the first part of the chapter, a general strategy for the study of the mechanism and kinetics of catalytic bleaching was presented followed by the relevant theory to enable a discriminatory assessment of the experimental data obtained. In the second part of the chapter, a kinetic model was established for a homogeneous model system and, based on that, an attempt was made to explain a more

complex kinetics of catalytic bleaching of cotton. It was shown on the basis of calculation of the Thiele modulus and internal effectiveness factor that the intra-yarn diffusion limitations can be neglected, whereas the significant intra-fibre diffusion limitations may occured during bleaching of cotton. This was in agreement with a significant deviation of the experimental results of the degree of removal of colour on cotton fibre (heterogeneous system) from the theoretical values of the degree of conversion of morin (homogeneous model system) plotted against time. It was concluded that the initial bleaching phase was limited by the chemical reaction at the surface, whereas the intra-fibre diffusion limitation occured in the bleaching at longer times.

The results discussed in the present thesis show that H_2O_2/MnTACN bleaching system can be used successfully for cotton bleaching at low temperature. An integrated approach considering both molecular and macroscopic aspects developed in this study, resulted in a multilateral understanding of the complex physicochemical phenomena occurring during bleaching in the system in which the catalyst was present.

SAMENVATTING

In dit proefschrift wordt de mogelijkheid van het bleken van katoen bij lage temperatuur met behulp van de katalysator dinulclear tri-μ-oxo gebrugde manganese(IV) complex van het ligand 1,4,7-trimethyl-1,4,7-triazacyclononane (MnTACN) in het systeem met waterstofperoxide beschreven. Hiertoe werden de fundamentele aspecten van katalytisch bleken op zowel moleculair als op macroscopisch niveau onderzocht.

In hoofdstuk 1 wordt een introductie gegeven van de verschillende aspecten van het bleken van katoen. Na een kort overzicht van het belang van het verkrijgen van wit textielmateriaal, worden de structuureigenschappen van katoen kort besproken met een focus op de oorsprong van de natuurlijke kleur. Een korte introductie van het huidige waterstofperoxide bleekproces wordt gepresenteerd en de huidige mogelijkheden voor katalytisch bleken passeren de revue. De toepassing van katalytische oxidatie in het bleken van was wordt besproken met speciale nadruk op manganese complexen met triazacyclononane liganden (TACN).

Omdat flavonoids de kleur aan de oorspronkelijke katoenvezel geven, wordt een gedetailleerd onderzoek naar de dioxygen activatie in de oxidatie van morin gekatalyseerd met MnTACN in hoofdstuk 2 beschreven. Een ongekende katalytische activatie van moleculair zuurstof met de MnTACN via stapsgewijze vorming van waterstofperoxide naar de oxidatie van flavonoids bij lage temperaturen in alkalische waterige oplossing wordt gerapporteerd. Deze vondst is een nieuwe reactie, niet alleen op het gebied van textielchemie, maar ook in het bredere veld van de chemie. De rol van superoxide O_2^- en/of H_2O_2 werd onderzocht met behulp van de enzymen: superoxide dismutase, catalase, xanthine oxidase and alcohol oxidase. Superoxide dismutase en catalase werden gebruikt als inhibitor enzymen (superoxide dismutase katalyseert dismutatie van O_2^- anion naar O_2 en H_2O_2; catalase katalyseert decompositie van H_2O_2 naar O_2 en H_2O). Xanthine oxidase en alcohol oxidase werden gebruikt als accelerator enzymen (xanthine oxidase katalyseert reductie van O_2 naar O_2^-; alcohol oxidase katalyseert reductie van O_2 naar H_2O_2). Een combinatie van inhibitor en accelerator experimenten werd gebruikt om de aard van de actieve verbindingen die uit dioxygen voortkomen en verantwoordelijk zijn voor de oxidatie van katoen pigment morin vast te stellen.

In hoofdstuk 3 worden de details van de kinetiek en het mechanisme van katalytisch bleken onder homogene condities besproken. Hiertoe werden het substraat (kleur materiaal) en de katalyse (activering) onderzocht. Het onderzoek naar de relatie tussen structuur en reactiviteit had betrekking op een serie modelverbindingen die qua structuur gerelateerd zijn aan morin en een systematische studie met gebruik van UV-Vis spectroscopie naar hun oxidatie. De resultaten suggereren dat de katalysator en flavonoid worden verbonden via hydroxyl op C-3, de carbonyl op positie C-4 en de manganese van de katalysator. Electrospray ionisatie-massa spectrometrie (ESI-MS) analyse van morin en het oxidatie-product suggereren dat de reactie voornamelijk via een monooxygenase mechanisme (één O-atoom bindt aan het morin-molecuul) verloopt. Deze vondst werd bevestigd door NMR spectra van het geoxideerde product en morin, waarmee nog eens werd aangetoond dat morin niet wordt geoxideerd en gehydrolyseerd naar de vrije benzoëzuren. De resultaten van de ESI-MS experimenten met waterige oplossingen van MnTACN en mengsels van MnTACN met O_2 en/of morin suggereren dat de dinuclear manganese verbindingen een belangrijke rol spelen, terwijl uitwisseling van ligand de echte situatie kan zijn. De reactiekinetiek en activeringsparameters zijn uitgerekend. De invloed van de temperatuur in de range van 20 ^{o}C tot 60 ^{o}C op de eerste-orde snelheidsconstante k werd bestudeerd bij pH 9,5 en pH 10. De activeringsenergie E_a, the activeringsenthalpie $\Delta H^{\#}$ en de activeringsentropie $\Delta S^{\#}$ werden berekend met Arrhenius en Eyring grafieken. Het hoofdstuk eindigt met een mechanistisch voorstel dat voortkomt uit de aanpak in hoofdstukken 2 en 3.

De performance van de katalysator MnTACN in het bleken van katoen met waterstofperoxide wordt in hoofdstuk 4 beschreven. De belangrijkste bleekparameters, pH en temperatuur, en de decompositiekinetiek van waterstofperoxide gedurende het bleekproces werden onderzocht. Katalytisch bleken verloopt via een snelle bleekfase (minder dan 2,5 minuten) gevolgd door een merkbaar langzamere bleekfase. Met UV-Vis spectrofotometrie werd de decompositiekinetiek van waterstofperoxide gekatalyseerd met MnTACN kwalitatief geanalyseerd. Met cerium(IV) titratiereacties werd het gehalte aan waterstofperoxide in de bleekoplossing na verschillende bleektijden en verschillende temperaturen bepaald. De resultaten laten zien dat zeer kleine hoeveelheden van de katalysator MnTACN de reactiesnelheden in het waterstofperoxide bleeksysteem vergroten. Uit onderzoek naar de decompositiekinetiek bleek dat het verbruik van waterstofperoxide een eerste-orde verloop volgt. De berekening van de verbruikte fractie waterstofperoxide als gevolg van het aanwezige substraat suggereert dat de actieve verbindingen, die worden gevormd tijdens het bleken bij 30^{o}C, de oxidatie van het substraat katalyseren, en niet de decompositie van H_2O_2 in oplossing. Dit laat zien dat onder deze condities vooral het substraat wordt gebleekt. De resultaten laten zien dat met bleken van katoen in de aanwezigheid van de katalysator bij een

temperatuur van slechts 30^{o}C een voldoende witheid kan worden bereikt in een relatief korte tijd. Een maximale bleekactiviteit gekatalyseerd met MnTACN wordt verkregen binnen een relatief brede pH-range (pH 9,5-11), terwijl de maximale bleekeffectiviteit voor niet-gekatalyseerd bleken bij een hogere pH van 11,5 wordt bereikt. De bredere pH-range van het katalytische systeem is gunstiger dan het conventionele waterstofperoxide bleken, omdat het de normale fluctuaties in de alledaagse praktijk van de fabriek toestaat zonder dat dit ten koste gaat van de kwaliteit en reproduceerbaarheid.

In hoofdstuk 5 worden de fysisch-chemische veranderingen aan de katoenvezel als gevolg van katalytisch bleken behandeld. Het onderzoek had naast het normale katoenen doek betrekking op katoenen modeldoek geïmpregneerd met morin. Door deze aanpak konden de chemische en fysische effecten op de katoenvezel na katalytisch bleken onderzocht en gekwantificeerd worden en konden drie soorten katalytische activiteit onderscheiden worden: bleken van pigment, verwijderen van niet-cellulose verbindingen en oxidatie van cellulose. De oppervlakte chemie en bevochtigingseigenschappen van katoenvezels na katalytisch bleken werden onderzocht met behulp van X-straling fotoelectronenspectroscopie (XPS) en contacthoekmeting. De capillairconstante van de katoenvezel verandert na het bleken, terwijl de hoogste waarden werden verkregen door het H_2O_2/MnTACN katalytisch systeem. Met een auto-porosimeter werd de distributie van de inter- en intra-draad poriegrootte in het doek gemeten. De maximale effectieve radii van de inter- en intra-draad poriën verschuiven naar hogere waarden na bleken met H_2O_2/MnTACN. De XPS spectra en de deconvolutie pieken laten zien dat in de aanwezigheid van een significante hoeveelheid C1 component (C-C of C-H, alifatisch) aan het katoenvezeloppervlak niet-cellulosische verbindingen die door deze component worden gerepresenteerd het doel kunnen zijn van katalytische activiteit en daardoor competitief zijn met pigmenten en cellulose voor de katalysator moleculen. Anderzijds worden in de afwezigheid van de (verwijderbare) C1 verontreinigingen ketting-brekende oxidatieve reacties belangrijk, omdat meer cellulose bindingen kwetsbaar zijn aan het “naakte” oppervlak. Tot slot werd de stijging van de capillairconstante gerelateerd aan de verwijdering van bleekproducten (laag-moleculair-gewicht producten gekarakteriseerd door de C1 component in C 1s XPS spectrum) en aan ketting-verkortende cellulose (aangenomen op basis van kritische druppel in polymerisatiegraad DP) in oplossing gedurende bleken en de opvolgende spoelstappen. De verkregen resultaten laten een belangrijke relatie zien tussen het verwijderen van niet-cellulosische verbindingen en een stijging van de capillairconstante van het gebleekte katoenen doek. Dit gedetailleerde onderzoek bevestigt dat de bleekefficiëntie van het H_2O_2/MnTACN systeem superieur is aan dat van het niet-gekatalyseerde systeem, terwijl het dezelfde (of zelfs minder) chemische vezelschade veroorzaakt.

Een model voor het katalytisch bleken van katoen wordt in hoofdstuk 6 voorgesteld. In het eerste deel van het hoofdstuk wordt een algemene strategie voor de studie van het mechanisme en de kinetiek van katalytisch bleken gepresenteerd gevolgd door relevante theorie waarmee experimentele data kunnen worden geëvalueerd. In het tweede deel van het hoofdstuk wordt een kinetisch model voor een homogeen model systeem uitgewerkt. Gebaseerd op dit model wordt een poging ondernomen om een complexere kinetiek van katalytisch bleken van katoen te verklaren. Op basis van de berekening van de Thiele modulus en de interne effectiviteitsfactor wordt aangetoond dat diffusielimitering in de draden kan worden verwaarloosd, terwijl significante diffusielimitering in de vezels kan optreden tijdens het bleken van katoen. Dit is in overeenstemming met een significante deviatie van de experimentele resultaten van de graad van kleursverwijdering van de katoenvezel (heterogeen systeem) met de theoretische waarden van de conversiegraad van morin (homogeen modelsysteem) uitgezet tegen de tijd. Er wordt geconcludeerd dat de initiële bleekfase gelimiteerd wordt door de chemische reactie aan het oppervlak, terwijl intra-vezel-diffusielimitering plaatsvindt bij langere bleektijden.

De besproken resultaten in dit proefschrift laten zien dat het H_2O_2/MnTACN bleeksysteem succesvol kan worden toegepast in het bleken van katoen bij lage temperaturen. Een geïntegreerde aanpak met de onderzochte moleculaire en de macroscopische aspecten resulteerde in een multilateraal begrip van de complexe fysisch-chemische verschijnselen die plaatsvinden tijdens bleken in het systeem waarbij een katalysator werd gebruikt.

SAŽETAK

Ova teza je posvećena istraživanju mogućnosti nisko-temperaturnog beljenja pamuka uz upotrebu kompleksa dinuklearnog tri-μ-okso premošćenog mangana(IV) sa ligandom 1,4,7-trimetil-1,4,7-triazaciklononanom (MnTACN) kao katalizatora u sistemu sa vodonik peroksidom. U skladu sa ovim ciljem su proučavani fundamentalni aspekti katalitičkog beljenja na molekulskom i makroskopskom nivou.

U poglavlju 1 je dat uvod u različite aspekte beljenja pamuka. Posle kratkog pregleda značaja dobijanja belog tekstilnog materijala, ukratko su diskutovana strukturna svojstva pamuka sa posebnim osvrtom na poreklo prirodnog obojenja pamuka. Dat je kratak osvrt na savremene postupke beljenja vodonik peroksidom i napravljen pregled trenutno mogućih rešenja za katalitičko beljenje. Diskutovana je primena katalitičke oksidacije radi beljenja prilikom pranja rublja sa posebnim osvrtom na komplekse mangana sa triazociklononan ligandima (TACN).

Pošto je prirodno obojenje pamuka uglavnom posledica prisustva flavonoida, u poglavlju 2 je detaljno opisano proučavanje aktivacije molekulskog kiseonika prilikom oksidacije morina koja je katalizovana sa MnTACN. Pokazana je reakcija katalitičke aktivacije molekulskog kiseonika sa MnTACN preko postupnog formiranja vodonik peroksida, za oksidaciju flavonoida na sobnoj temperaturi i u alkalnom vodenom sistemu. Ovo je nova reakcija, ne samo u oblasti tekstilne hemije, već uopšte u hemiji. Uloga superoksidnog jona O_2^- i/ili H_2O_2 je proučavana novom metodom na bazi enzima: superoksid dismutaza, katalaza, ksantin oksidaza i alkohol oksidaza. Superoksid dismutaza i katalaza su korišćeni kao enzimi inhibitori (superoksid dismutaza katalizuje dismutaciju O_2^- anjona u O_2 i H_2O_2; katalaza katalizuje razlaganje H_2O_2 na O_2 i H_2O). Ksantin oksidaza i alkohol oksidaza su korišćeni kao enzimi akceleratori (ksantin oksidaza katalizuje redukciju O_2 do O_2^-; alkohol oksidaza katalizuje redukciju O_2 do H_2O). Kombinacija eksperimenata inhibicije i akceleracije je korišćena za utvrđivanje prirode aktivnih komponenata koje nastaju iz molekulskog kiseonika i koje su odgovorne za oksidaciju morina, pigmenta prisutnog u pamuku.

Poglavlje 3 je posvećeno rasvetljavanju kinetičkih i mehanističkih detalja katalitičkog beljenja u homogenom sistemu. U tom cilju su proučavanja vršena kako sa aspekta supstrata (obojena materija), tako i sa aspekta kalizatora (aktivacija). Proučavanje korelacije između strukture i reaktivnosti je obuhvatilo sistematsko praćenje oksidacije serije model-jedinjenja, po strukturi sličnih morinu, putem UV-Vis spektroskopije. Dobijeni rezultati su ukazali da stvaranje veze između katalizatora i flavonoida uključuje interakciju C-3 hidroksilne grupe i C-4 karbonilne grupe sa manganom iz katalizatora. Analiza morina i proizvoda oksidacije putem elektro-sprej jonizujuće masene spektrometrije (ESI-MS) je ukazala da se reakcija odvija uglavnom preko mehanizma monooksigenacije (jedan atom kiseonika se inkorporira u molekul morina). Ovi rezulati su potvrđeni putem NMR spektara proizvoda oksidacije i morina, što je dalo dodatnu potvrdu da morin nije oksidisan i hidrolizovan do slobodnih benzoevih kiselina. Rezultati ESI-MS eksperimenata na vodenim rastvorima MnTACN i na sistemima MnTACN sa O_2 i/ili morinom, ukazuju da dinuklearni oblik mangana ima važnu ulogu, i da izmena liganda može biti realna situacija. Urađen je proračun kinetike reakcije i određeni su parametri aktivacije. Proučavana je temperaturna zavisnost konstante brzine reakcije prvog reda k na pH 9,5 i pH 10, u oblasti temperature 20-60^{o}C. Izračunate su entalpija $\Delta H^{\#}$ i entropija $\Delta S^{\#}$ aktivacije korišćenjem Arenijusovog i Ejringovog metoda. Poglavlje se završava predlogom mehanizma koji je rezultat istraživačkog pristupa primenjenog u poglavlju 2 i poglavlju 3.

U poglavlju 4 je proučavano ponašanje katalizatora MnTACN prilikom beljenja pamuka vodonik peroksidom. Razmatran je uticaj najvažnijih parametara beljenja (pH i temperatura) i praćena kinetika razlaganja vodonik peroksida tokom procesa beljenja. Utvrđeno je da se katalitičko beljenje odvija u dve faze: brza početna faza beljenja (kraća od 2,5 minuta) i znatno sporija kasnija faza beljenja. Kvalitativna analiza kinetike razlaganja vodonik peroksida u prisustvu katalizatora MnTACN je urađena korišćenjem UV-Vis spektrometrije. Putem reakcija titracije sa cerijumom(IV) je kvantitativno određen sadržaj vodonik peroksida u rastvoru za beljenje posle različitih vremena beljenja i za različite temperature. Rezultati su pokazali da vrlo male količine katalizatora (10 μM) znatno povećavaju brzinu reakcije u sistemu za beljenje sa vodonik peroksidom, kao i da je kinetika razlaganja vodonik peroksida prvog reda u odnosu na H_2O_2. Proračun udela vodonik peroksida koji se troši na reakciju sa supstratom (pamuk) ukazuje da aktivni međuprodukti koji se formiraju tokom beljenja na 30^{o}C katalizuju oksidaciju supstrata, a ne razlaganje H_2O_2 u rastvoru, što pokazuje da je osnovni tok reakcije pod tim uslovima beljenje supstrata. Rezultati pokazuju da se beljenjem pamuka u prisustvu katalizatora već na temperaturi od 30^{o}C i za relativno kratko vreme obrade može postići zadovoljavajući stepen beline. Maksimalna efikasnost beljenja u prisustvu katalizatora MnTACN je postignuta u relativno širokoj oblasti pH (pH 9.5-11), dok je kod beljenja bez katalizatora potrebna viša vrednost pH (pH 11.5).

Prednost katalitičkog sistema u odnosu na konvencionalno beljenje vodonik peroksidom je mogućnost rada u okviru šire oblasti pH, čime se obezbeđuje mogućnost postizanja visokog kvaliteta i reproduktivnosti nezavisno od varijacija pH koje uobičajeno nastaju u industrijskim uslovima.

Poglavlje 5 daje pregled fizičko-hemijskih promena pamučnog vlakna koje su posledica katalitičkog beljenja. Proučavanje je obuhvatalo, pored regularne pamučne tkanine, i model pamučnu tkaninu koja je pripremljena zaprljanjem sa morinom. Ovaj pristup je obezbedio metodu kojom mogu da se proučavaju i kvantifikuju hemijski i fizički efekti na pamučnom vlaknu koji su posledica katalitičkog beljenja, kao i da se napravi razlika između tri tipa katalitičkog dejstva: obezbojavanje pigmenta, uklanjanje necelulozних materija i oksidacija celuloze. Putem fotoelektronske spektroskopije X-zraka (XPS) i merenja ugla kvašenja, proučavane su hemijske promene na površini i svojstva kvašenja pamučnih vlakana kao posledica katalitičkog beljenja. Konstanta kapilarnosti pamučne tkanine se menja posle beljenja i najveće vrednosti ovog parametra su dobijene upotrebom H_2O_2/MnTACN katalitičkog sistema. Raspodela veličina pora (unutar prediva i među predivom) je merena kod tkanine pomoću auto-porozimetra. Srednje vrednosti efektivnog prečnika pora (unutar prediva i među predivom) su pomereni ka višim vrednostima posle beljenja sa H_2O_2/MnTACN. XPS spektri i pikovi dobijeni dekonvolucijom pokazuju da u prisustvu određene količine C1 komponente (C-C ili C-H, alifatična) na površini pamučnog vlakna necelulozne materije mogu biti primarni objekat katalitičkog dejstva, te na taj način konkurišu pigmentima i celulozi kod dejstva katalizatora. Sa druge strane, u odsustvu C1 primesa (koje se inače lako mogu ukloniti) reakcije oksidativnog raskidanja lanaca makromolekula mogu postati dominantne kao posledica činjenice da je onda veliki broj celuloznih veza lako dostupan na "ogoljenoj" površini vlakna. Na kraju poglavlja je urađena korelacija između povećanja konstante kapilarnosti i uklanjanja produkata beljenja (niskomolekulski produkti koji su okarakterisani C1 komponentom u C 1s XPS spektru), kao i skraćenih celuloznih lanaca (na bazi kritičnog pada stepena polimerizovanja, DP) u rastvor tokom beljenja i naknadnih postupaka ispiranja. Dobijeni rezultati ukazuju na suštinsku međusobnu povezanost između uklanjanja necelulozних materija i povećanja konstante kapilarnosti beljene pamučne tkanine. Ovo detaljno proučavanje je potvrdilo ne samo da je efikasnost beljenja sistemom H_2O_2/MnTACN superiorna u odnosu na nekatalizovan H_2O_2 sistem, već i da prouzrokuje isto (ako ne i manje) hemijsko oštećenje vlakna.

U poglavlju 6 je predložen model katalitičkog beljenja pamuka. U prvom delu poglavlja je prikazana opšta strategija za proučavanje mehanizma i kinetike katalitičkog beljenja, što je praćeno odgovarajućim teorijskim razmatranjima koja su imala za cilj da obezbede bazu za vrednovanje dobijenih eksperimentalnih rezultata. U drugom delu poglavlja je uspostavljen kinetički model za homogeni model sistem i, na bazi toga, učinjen je pokušaj da se

objasni kompleksna kinetika katalitičkog beljenja pamuka. Na bazi proračuna Thiele-modula i unutrašnjeg faktora efektivnosti, pokazano je da se kod beljenja pamuka otpor difuziji unutar pređe može zanemariti, a da unutar vlakna igra bitnu ulogu. Ovo je u skladu sa znatnim odstupanjem eksperimentalno dobijenih rezultata za stepen uklanjanja obojenja sa pamučnog vlakna (heterogeni sistem) u odnosu na teorijski dobijene vrednosti stepena konverzije morina (homogeni model sistem) kod dijagrama zavisnosti ovih parametara od vremena. Zaključeno je da je u početnoj fazi beljenje kontrolisano hemijskom reakcijom na površini vlakna, a da je u kasnijoj fazi brzina beljenja kontrolisana difuzijom unutar vlakna.

Rezultati diskutovani u ovoj tezi pokazuju da H_2O_2/MnTACN sistem za beljenje može biti uspešno korišćen za nisko-temperaturno beljenje pamuka. Razvijen je sveobuhvatni pristup koji uzima u obzir kako molekulske, tako i makroskopske aspekte. Ovakav pristup je doprineo razumevanju kompleksnih fizičko-hemijskih fenomena koji nastaju prilikom beljenja u sistemu sa katalizatorom.

Acknowledgements

Writing these very last lines of this book makes me looking back at an almost four years long period of getting this PhD thesis (1456 days exactly!), and trying to call to my mind all the people who made this work possible, less complicated or, maybe most importantly, more enjoyable… I write this part with the greatest joy, as I have finally got the chance to thank those who helped me to make my dream reality. Now, when it is all done I can say with all my heart that I did enjoy every single moment of being involved in this project. Even at the most difficult moments, I knew that it could have been just more difficult working on something that I did not like as much as I loved the topic of the work presented in this book. So, many times I thought of how lucky I must have been that Prof.Dr.ir. Marijn Warmoeskerken placed his trust in me offering me to do PhD thesis in this project.

I feel short of words to express my gratitude for the scientific guidance I have had from Marijn during my PhD study as well as for the enthusiasm and the excitement for the project he was able to transfer to me. I have never felt being short of his confidence in me, or not having enough freedom and independence when the new ideas were explored. Thanks to his optimism, encouragement and curiosity, together with the ideal research environment Marijn has built in the group, I feel myself privileged having him for my *promotor*.

I would also like to thank to my daily supervisor, Dr.ir. Vincent Nierstrasz, for his assistance and advice during research. I especially appreciate the comments received from Vincent on the presentations for conferences, scientific papers and, finally, on this thesis, which led to a significant improvement in readability and scientific quality. The part I will probably miss the most from now on is his unique sense of humour that helped me to understand a true Dutch spirit.

My interest in the research was mostly induced by Prof. Dr. Dragan Jocić from the University of Belgrade. I have no other word but *precious* for Dragan's contribution and help, which became essential in the final stage of writing this thesis. His support, help, advices, comments, patience, availability and openness, especially for the questions in the field of textile engineering, had a significant impact on the scientific as well as visual look of my thesis. At the same time, Dragan was one of the most truthful critics of my work, tirelessly longing for the highest quality of work, but always with the unwavering support in all my endeavours. It is simply not possible to name all kinds of help and support I received from him, but I am sure that without him being present in my personal and professional life the things would definitely not be the same as they look today.

A very important part is the collaboration and interaction with researches and experts from different fields that opened my eyes to new research possibilities which lay outside of my primary expertise.

The part on chemistry and catalysis in this thesis would certainly not look the same if I did not have an *external* supervisor - Dr. Ronald Hage (Unilever R&D), who was actively contributing to my thesis work from the very beginning till the end. I was indeed fortunate to have Ronald available at any time for the questions, doubts or ideas I had. The fruitful discussions, quick and detailed answers, suggestions and comments I have received from him resulted in a much faster progress of my work. The detailed comments received from Ronald on the draft thesis contributed greatly to a final look and quality of the thesis.

I am very grateful to Prof. B.L. Feringa at the Univeristy of Groningen for his willingness to allow me access to the facilities and chemical expertise of his group. I had fruitful conversations and received much assistance from the members of this group: Dr. Wesley Browne with ^{1}H NMR and UV-Vis spectrophotometry, and Hans de Boer with ESI-MS.

I would like to thank Prof. Antonio Navarro for giving me access to laboratory instruments and surface characterisation expertise of his group at the UPC, Terassa (Spain). I am very thankful to Lorenzo Bautista who generously shared with me his expertise and experience in the analysis of XPS spectra and the contact angle method. I also thank Dr. Manuel-Jose Lis and Dr. Tzanko Tzanov from Chemical Engineering Department at the UPC for providing useful information on some particular items in relation with their expertise.

I appreciate very much the help of Anton Tijhuis with arranging the DP analysis at Vlisco Helmond B.V. as well as for his interest in the progress of my work.

I would like to thank Dr. Ted Slaghek and Dr. Johan Timmermans from TNO Kwaliteit van Leven for the very productive discussions on the chemical mechanism and for sharing with me their organic chemistry expertise.

Regular contacts and project meetings with the members of the EET project "Bleekkracht" and WTT (Werkgroep Textieltechnologie) ensured that research stays in constant touch with industry, and I would like to acknowledge them for their support and useful suggestions as well as for the help they offered me in various ways. I thank especially: Anton Luiken (TNO Textiel), Bert Heesink (UT/Ten Cate), Jan Jetten (TNO Kwaliteit van Leven), Henri Aal (Ten Cate), Dan Ravensbergen (TNO Textiel), Herman Lenting, (TNO Textiel), Ronald Holweg, Harry van de Ven (Sympatex) and Henk Gooijer.

To all committee members I would like to express my gratitude for the comments and input, which have improved the quality of the thesis.

Special thanks must go out to my colleagues, present and past members of Textile Technology Group: Pramod and Huib (officially they are my ***paranimfen***, but I prefer to call them my bodyguards!), Marloes (and Sander!), Monica (and Marco!), Vijay, Edward and Micky. Although they were not directly involved in this research, they all contributed with their comments and suggestions, but above all for being great colleagues. I thank Huib for translating the thesis summary in Dutch. Most thanks must go out to Pramod (and Vishakha!) for showing goodwill to help me with the organisational tasks in the final stage of the thesis work (cutting my stress into half!).

With all my heart I thank Bartie, our group secretary, for the administrative help she has done for me, for bringing good spirits and fun to all of us in the group, but most of all to her and her husband Hans, for being my sincere friends since my very first day in the Netherlands.

I am very grateful to Benno Knaken who has always been in a good mood for troubleshooting of various instruments that was necessary for the completion of this work. Very special thanks to Henny Bevers for lending laboratory auxiliaries at rush hours.

I appreciate the help of Sandra, the only M.Sc. student involved in my project.

Living in the Netherlands was a valuable experience not only for my professional but also for personal life. I had chance to make friendship with people from the Netherlands, as well as people coming from different parts of the World. Amongst them, one the biggest group of friends of mine are people I met in Schiermonnikoog during the catalysis course: Tehila, Francesca, Kazu, Susanna, Hans, Pedro, and many others. Apart from studying various aspects of this fascinating discipline, we had a wonderful time, which continued throughout all these years.

For feeling being at home while living abroad, I have to thank all my Serbian friends I met in the Netherlands: Jelena and Boris, Nataša, Raša, Darja, Dragan, Maja, Vojkan and Sofka, Tijana and Žika, Biljana and Goran, Marko, Dule, Jelena M., and many others.

Many thanks to my friends from Belgrade: Maja and Dejan, Nataša, Milan, for their continuous interest in my new life as well as for a good time I had with them during the holidays I spent in Belgrade. Not least, I would like to thank to all my former colleagues at the University of Belgrade, who did not forget me in spite of the distance.

The strength, belief and love I have had from my family all my life, and especially for last four years when being far away from them, made me feel secure, but also strong and determined to hold out to the end of this work. My brothers, Veran and Dejan, were always there for me whenever I needed somebody to put me in a good mood, or give me support. My deepest love and respect is owed to my mother: *Mama, beskrajno hvala za sve sto si mi pružila. Srećna sam jer sam imala tvoju ljubav, strpljenje i podršku svih ovih godina.*

Tatjana Topalović

List of publications from PhD thesis

Journal papers

T.Topalović, V.Nierstrasz, L.Bautista, D.Jocić, A.Navarro, M.M.C.G.Warmoeskerken, XPS and contact angle study of cotton surface oxidation by catalytic bleaching, *Colloids and Surfaces A: Physicochemical and Engineering Aspects* (accepted for publication) (2006) doi:10.1016/j.colsurfa.2006.09.026

T.Topalović, V.Nierstrasz, R.Hage, W.R.Browne, B.L.Feringa, M.M.C.G. Warmoeskerken, Model system for mechanistic study of catalytic bleaching of cotton, *Dyes and Pigments* (in print) (2007).

T.Topalović, V.Nierstrasz, L.Bautista, D.Jocić, A.Navarro, M.M.C.G.Warmoeskerken, Analysis of the effects of catalytic bleaching on cotton, *Cellulose* (submitted) (2006).

Conference papers (oral presentations)

T.Topalovic, L.Bautista, V.A.Nierstrasz, D.Jocic, A.Navarro, M.M.C.G.Warmoeskerken, An integrated approach to catalytic bleaching of cotton – molecular and macroscopic aspects, *AUTEX 2006 Conference, Working together... Academia, Industry and Government, June 11-14, 2006, Raleigh, NC (USA,* Conference Proceedings CD-ROM, Paper 184, p.1-12 (2006).

T.Topalovic, V.A.Nierstrasz, R.Hage, W.R.Browne, B.L.Feringa, M.M.C.G.Warmoeskerken, Oxygen Activation by $[Mn_2O_3(tmtacn)_2]^{2+}$ in the Catalysed Flavonoids Oxidation Under Ambient Conditions, *VII Netherlands' Catalysis and Chemistry Conference (NCCC VII), March 6-8, 2006, Noordwijkerhout, The Netherlands*, Paper O-75, p.139 (2006).

T.Topalovic, V.A. Nierstrasz, M.M.C.G.Warmoeskerken, Efficient bleaching of cotton with hydrogen peroxide using a new $[Mn_2O_3(tmtacn)_2]^{2+}$ catalyst reaction system, *1st South East European Congress of Chemical Engineering (SEECChE 1), Belgrade, Serbia and Montenegro, September 25-28, 2005*, Book of abstracts (ISBN 86-905111-0-5), p.22 (2005).

T.Topalovic, V.A.Nierstrasz, R.Hage, W.R.Browne, B.L.Feringa, M.M.C.G.Warmoeskerken, Model system for mechanistic study of catalytic bleaching of cotton, *5th AUTEX Conference, Portorož, Slovenia, 27-29 June, 2005*, Proceedings, 916-923 (2005).

T.Topalovic, V.A.Nierstrasz, M.M.C.G.Warmoeskerken, The assesment of kinetics of cotton catalytic bleaching, *4th AUTEX Conference, World Textile Conference, 22-24 June 2004, ENSAIT Roubaix, France*, Proceedings CD-ROM (ISBN 2-9522440-0-6), Paper O-COL11, 7 pages (2004).

Conference papers (poster presentations)

T.Topalovic, V.A.Nierstrasz, M.M.C.G.Warmoeskerken, Catalytic bleaching, *3rd AUTEX Conference, Gdansk, Poland, 25-27 June 2003*, Proceedings, Book II, 80-82 (2003).

About the author

Tatjana Topalović was born on March 23, 1972 in Sjenica, Serbia. After finishing High school in Sjenica, in 1990 she enrolled the undergraduate study program at the Faculty of Technology and Metallurgy (TMF), University of Belgrade, Serbia. In October 1996 she graduated at the Textile Engineering Department with the final graduation project titled "The assessment of the electrophysical characteristics of textile materials".

Since March 1998 until February 2003 she was employed as Research Assistant at the TMF, University of Belgrade. During this period she participated in the different research projects, working as well as part-time Teaching Assistant for the subjects "General and Inorganic Chemistry" and "Textile Dyeing".

In October 1998 she enrolled the postgraduate study program (M.Sc.) at the Textile Engineering Department (TMF), University of Belgrade. In November 2002 she obtained M.Sc. degree (Master in technical science) after completing and defending the thesis titled "The influence of surface modification on dyeability of wool". As the special recognition for the quality of thesis, it was published in 2004 by Zadužbina Andrejević (Belgrade) as a book titled: "The dyeing of modified wool".

From September 2000 till February 2001 she stayed at the University of Twente (Textile Technology Group) as the IASTE trainee, where she participated in the project "Dynamic wetting of textile materials".

In February 2003 she joined the Textile Technology Group at the University of Twente where she started the Ph.D. project titled "Catalytic bleaching of cotton: Molecular and macroscopic aspects". The results of her research are presented in this thesis.

So far she has published 7 research papers and has made several oral presentations at international conferences.

ISBN 90-365-2454-7